Analysis of Timber Joints With Punched Metal Plate Fasteners

With Focus on Knee Joints

Ellegaard, Peter

Publication date:
2002

Document Version
Publisher's PDF, also known as Version of record

Acknowledgements

The present Ph.D. thesis, “Analysis of Timber Joints with Punched Metal Plate Fasteners – with Focus on Knee Joints” has been carried out in the period from August 1998 to November 2001 at the Department of Building Technology and Structural Engineering, Aalborg University, Denmark.

The project has been financed by the Danish Forest and Nature Agency. Some of the nail plates have kindly been delivered by Gang-Nail Systems AB, MiTek Industries, Inc., Sweden, and some of the timber material has been delivered by the The Association of Manufacturers of Roof Trusses in Denmark. Most of the test specimens have kindly been produced by Multi Spær A/S.

I would like to thank Jørn Ipsen, BMF, Bent Moseby, Pre-Træ, Gert Nordingsgaard, Palsgaard Træ A/S and Mogens Pedersen, Multi Spær A/S for valuable meetings and discussions. Furthermore, the discussions with Professor Hans Blaß and Professor Jürgen Ehlbeck, University of Karlsruhe, Germany have been fruitful.

The guidance by my supervisors N. Lambert Mortensen, Jacob Nielsen and Arne Rathkjen and the invaluable help from the technical staff at the laboratory are highly appreciated. The work performed by Martin Nørgaard and Klaus Thomsen as part of their B.Sc.-thesis has been very valuable.

The proof-reading has been performed by Mrs. Kirsten Aakjær. Her careful and professional work is appreciated.

I would also like to thank Frank Lam, University of British Columbia, Canada who made it possible for me to stay at University of British Columbia for four months.

Aalborg University, November 2001.

Peter Ellegaard

The Ph.D. – thesis was defended publicly at Aalborg University on 5th February 2002. The members of the assessment committee were L. Pilegaard Hansen, Reader, Aalborg University, Professor Sven Thelandersson, Lund University, Sweden and Professor Hans Blaß, Karlsruhe University, Germany.

Aalborg University, July 2002.

Peter Ellegaard

Contents

Notation

Roman

A	:	local node
A	:	anchorage area
A	:	cross-sectional area
$\tilde{A}$	:	modified cross-sectional area
b	:	width
B	:	local node
$\mathbf{B}$	:	strain distribution matrix
$\mathbf{D}$	:	multiplication factor
e	:	eccentricity
E	:	modulus of elasticity
f	:	distributed load
$\mathbf{f}$	:	force vector
g	:	gap
G	:	shear modulus
h	:	height
I	:	moment of inertia
$\tilde{I}$	:	modified moment of inertia
k	:	nail stiffness parameter
k	:	constant
kk	:	nail stiffness parameter
l	:	length of joint line
L	:	length
M	:	moment
n	:	arbitrary number
n	:	number of beams
N	:	axial force
$\mathbf{N}$	:	displacement distribution matrix
p	:	load
$\mathbf{p}$	:	load vector
P	:	load
p_0	:	nail stiffness parameter

$\mathbf{q}$	:	vector
r	:	distance
R	:	strength
$\mathbf{R}$	:	transformation matrix
s	:	standard deviation
$\tilde{S}$	:	modified static moment
t	:	thickness
$\mathbf{T}$	:	transformation matrix
u	:	displacement
$\mathbf{u}$	:	displacement vector
v	:	displacement
V	:	shear force
w	:	displacement
W	:	rotational section modulus
x	:	plate main direction
$\bar{y}$	:	mean value
y	:	direction perpendicular to plate main direction

Greek

α	:	constant
α	:	rotation
α	:	angle between main plate direction and force direction
β	:	angle between force direction and grain direction
γ	:	angle between plate main direction and joint line
δ	:	increment
Δ	:	displacement
$\mathbf{\Delta}$	:	displacement vector
ε	:	strain
ζ	:	nail density
θ	:	angle between global direction and plate main direction
κ	:	curvature
λ	:	load scale factor
ν	:	poisson ratio
σ	:	axial stress
τ	:	shear stress
ϑ	:	angle between grain direction and force direction
φ	:	angle between global direction and local direction
Φ	:	shear deformation
X	:	multiplication factor
ψ	:	angle between global direction and force direction
ω	:	angle between global direction and grain direction
$\Im$	:	multiplication factor

Superscripts

e	:	external
elem	:	element
int	:	internal
T	:	transpose of a matrix

Subscripts

1	:	direction
1	:	local node number
2	:	direction
2	:	local node number
A	:	local node
b	:	beam
B	:	local node
c	:	contact
c	:	compression
d	:	design
ef	:	effective
est	:	estimated
F	:	force
g	:	global
i	:	nail number
j	:	component number
k	:	characteristic
l	:	local
m	:	bending
max	:	maximum
M	:	moment
p	:	plastic
p	:	plate
par	:	parallel
perp	:	perpendicular
S	:	secant
t	:	tension
T	:	tangent
u	:	ultimate
v	:	shear
x	:	direction
y	:	direction
y	:	yield

1 Introduction

Prefabricated timber trusses are widely used as load-bearing structures in roof construction - not only in Denmark but world wide.

Most of the timber trusses are manufactured with joints with prefabricated punched metal plate fasteners. The punched metal plate fasteners are produced from thin steel plates (1-3 mm) in which a large number of nails are stamped, see figure 1.1 where a MiTek GNA20S nail plate is shown. In this thesis the word *nail plate* is used for these punched metal plate fasteners. The main direction of a nail plate corresponds to the stronger of the two directions when the nail plate is subjected to pure tension. The joints of a truss are made by pressing one nail plate on both sides of the truss into the timber members.

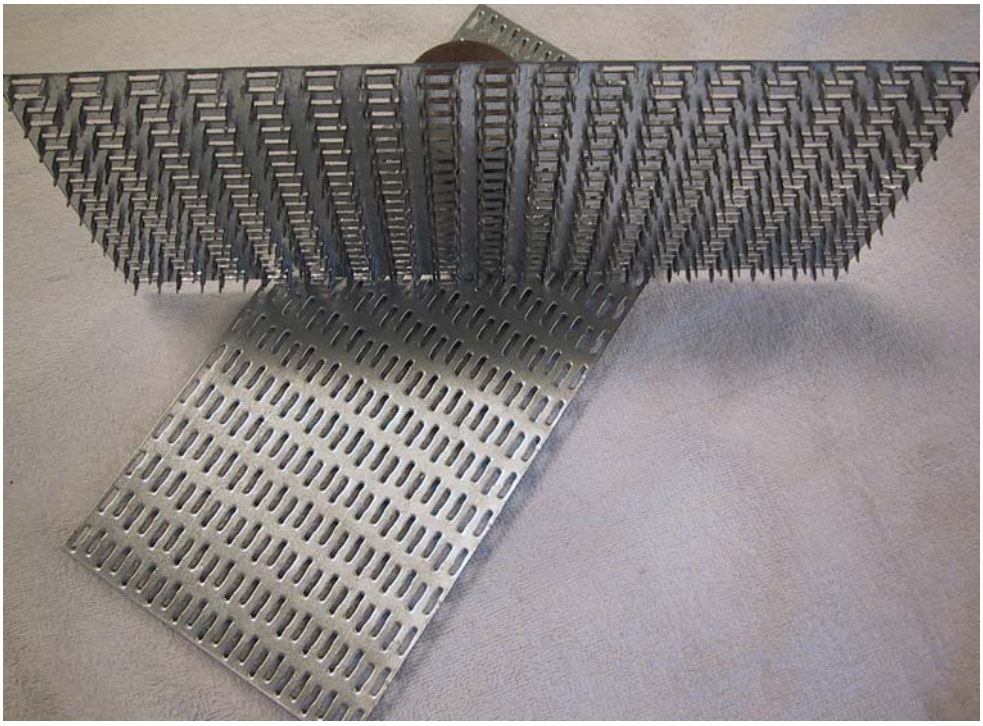

Figure 1.1. GNA20S nail plate.

Within recent years a new type of truss – the frame truss - has become more frequently used in Denmark. The frame truss is an alternative to the attic truss, see figure 1.2.

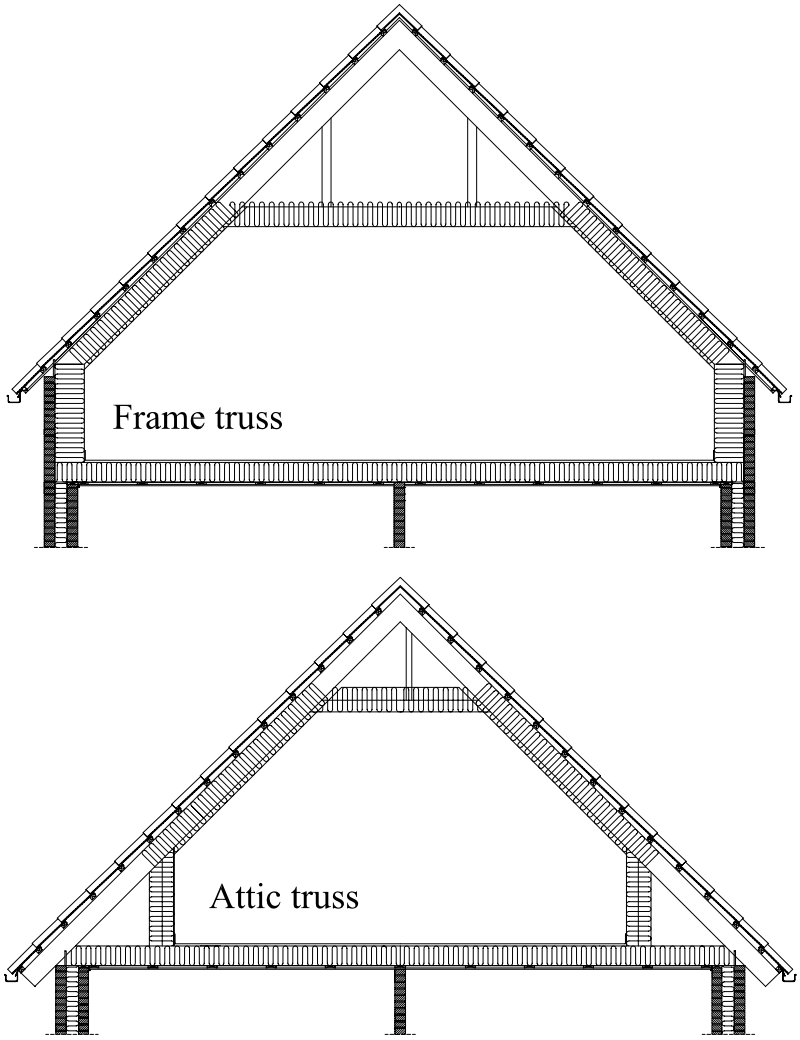

Figure 1.2. Frame truss versus attic truss.

The advantage of the frame truss is that it allows a better utilization of the upper floor and many architects find that use of the frame truss leads to more attractive buildings.

The strength and stiffness of the knee joints (joint between the rafter and the leg) is, however, of vital importance to the performance and therefore also the practicability of the frame truss. It is important that the stiffness of the knee joint is high enough to ensure that the neighbouring building parts (often a brick wall on the outside of the frame truss) is not subjected to large deflections.

More information about these knee joints is needed to expand the use of frame trusses and to produce frame trusses with larger spans.

During the last 10 years different projects at Aalborg University have analysed the frame truss and the knee joint as a part of the frame truss. The results from two of these projects are presented in the following section.

1.1 Results of Previous Research on Frame Trusses

In 1990 a series of full-scale tests with frame trusses was performed at Aalborg University. A brief summary of these test results is given in this section – for further details see *Hansen, F. T., Mortensen, N. L. & Hansen, L. P. (1990)*. The span of the frame trusses was 7 m and static loads were applied in the first stage of testing, and in the second stage dynamic loads were applied. The testing was stopped prior to failure in the first stage.

Three different types of frame trusses were tested (with three test specimens of each type). The only difference between the three test series was the design of the knee joint, see figure 1.3.

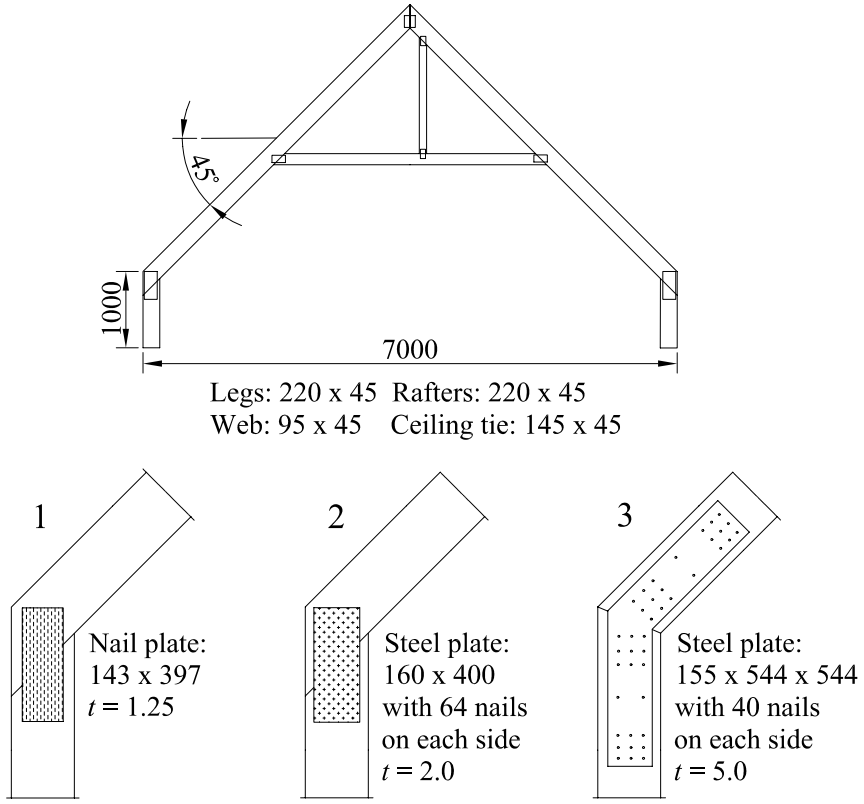

Figure 1.3. Full-scale frame trusses subjected to static and dynamic loads. Dimensions in mm. Timber quality K24. t: thickness.

In test series 1 the knee joint is produced with nail plates, in test series 2 the joint is made with steel plates perforated with holes (BMF nail plate) in which separate nails are used, and in test series 3 a specially produced steel plate with separate nails is used. All three types of knee joints have been used as parts of frame trusses in real buildings.

The static load corresponds to dead load + characteristic wind load. From the static tests it was concluded that the stiffness of test series 1 and 3 is almost identical and that the stiffness of test series 2 is 37% smaller. Comparing the manufacturing costs of test series 1 and 3, it seems that the solution with nail plates is preferable.

The results from the dynamic tests show, however, that test series 1 failed while test series 2 and 3 did not fail. The failures of test series 1 were often due to cracks in/splitting of the timber beams. In the rafter the cracks developed at the end of the rafter parallel to the grain direction. In the leg the cracks were observed in the middle of the beam parallel to the grain direction. One way to avoid these cracks could be to produce the frame truss with overhang and to produce the leg of two beams jointed with nail plates. Before testing these cracks were observed as shrinkage cracks.

In 1992 six different knee joint sections of a frame truss were tested at Aalborg University, see figure 1.4. For a detailed description see the test report *Mortensen, N. L. & Kloch, S. (1992).*

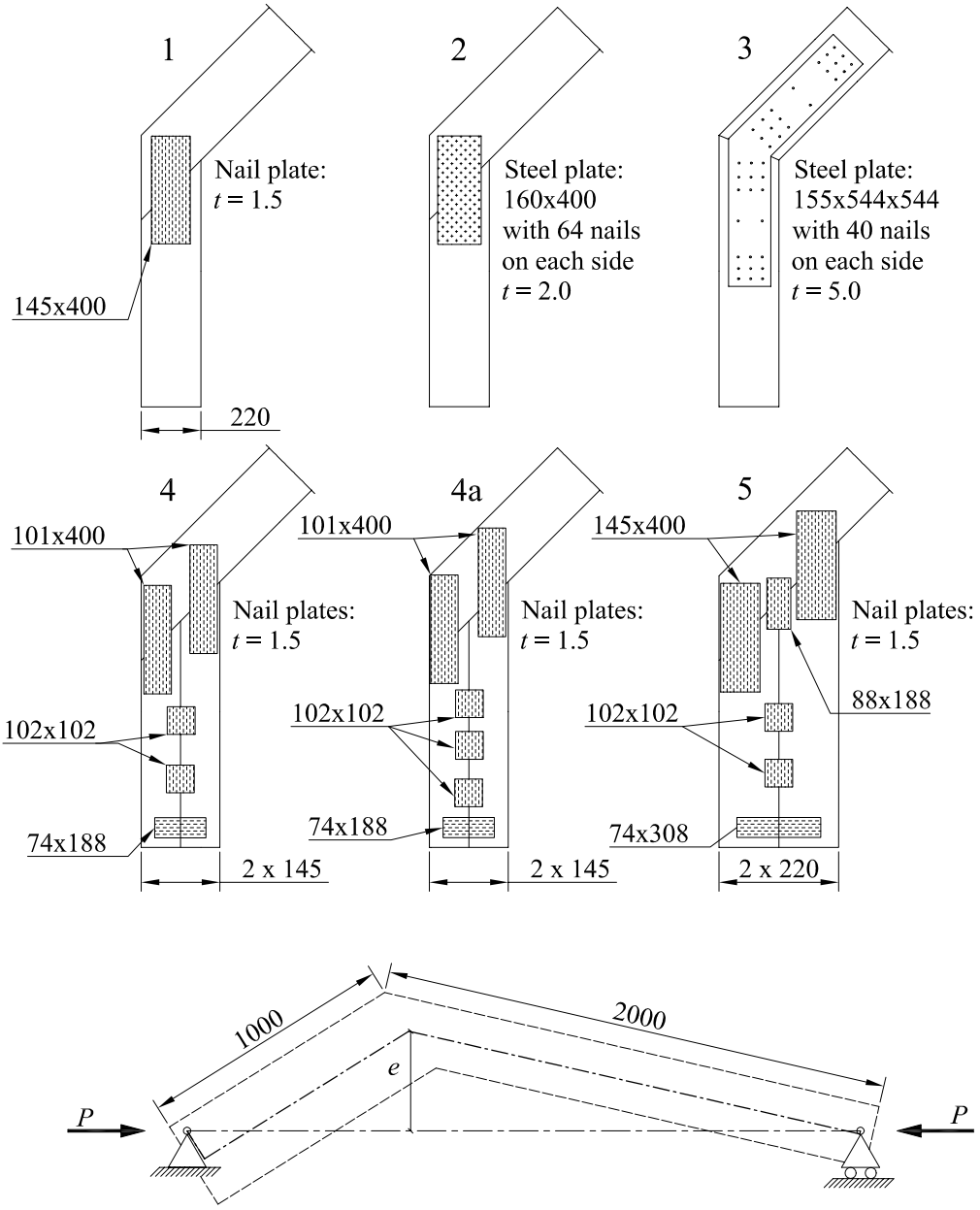

Figure 1.4. Tests series with knee joints performed in 1992. Dimensions in mm.

The test series 2 and 3 are similar to those of the full-scale tests shown in figure 1.3. The test series 4, 4a and 5 are manufactured in order to improve the knee joint type with nail plates. There were three test specimens in each test series.

The load is applied as illustrated in figure 1.4 and the average values of the failure moments ($P_{max} \cdot e$) for each test series are listed in table 1.1.

Test series	1	2	3	4	4a	5
Average failure moment [kNm]	4.7	4.8	9.7	5.8	8.3	11.6

Table 1.1. Failure moments for the test series.

During testing it was found that it is important to locate the nail plates as closely to the top of the rafter as possible to avoid splitting in the rafter, consider test series 4a versus test series 4.

The stiffness of test series 1 and 2 is almost identical, whereas the stiffness is doubled in test series 3 and 4. A further increase of 25% in the stiffness is observed for test series 4a and 5.

1.2 Different Methods of Truss Modelling

Besides the testing of the knee joints it is important that the stiffness and the load capacities of the knee joints can be predicted by e.g. a finite element program or by analytical calculations. However, to get a detailed description of the behaviour of knee joints, which is a relatively complex joint, calculations with finite element programs are considered to lead to the most accurate results.

In general the finite element models for timber trusses are based on plane frame models where the timber beams are modelled by beam elements. The main differences between the models are found in the joint modelling.

In this section four of the different methods of truss modelling are presented.

Model 1: In this model the joints can be either pinned or rigid. To take the deformations of the joints into account, a reduced modulus of elasticity is used for the webs of a truss, see figure 1.5.

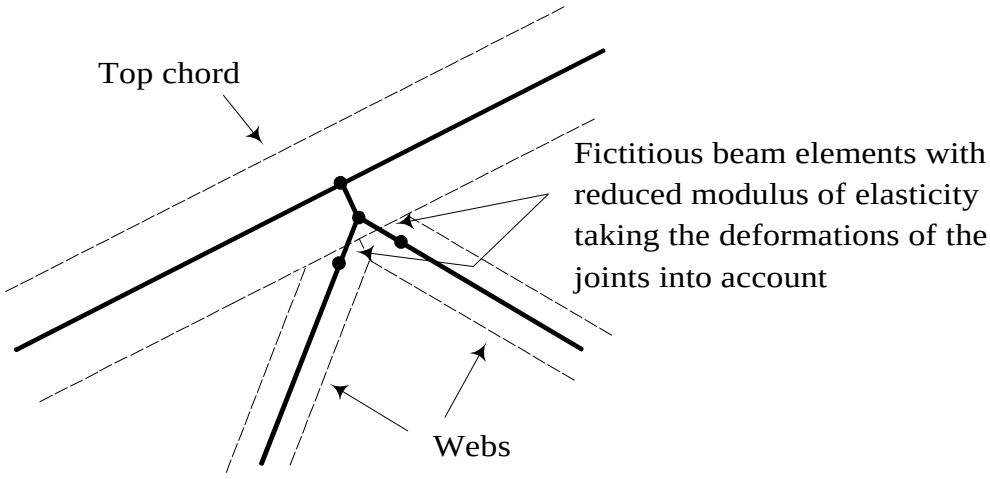

Figure 1.5. Model 1 for joint modelling – joint between rafter and two webs.

The model is implemented in the program Purdue Plane Structures Analyser II that is described in *Suddarth, S. K. & Wolfe, R. W. (1983).*

Model 2: In Denmark the most frequently used finite element models for design of timber trusses are based on models with fictitious elements. The joints can be either pinned or rigid and to add some kind of semi-rigidity a fictitious bar element is added, see figure 1.6.

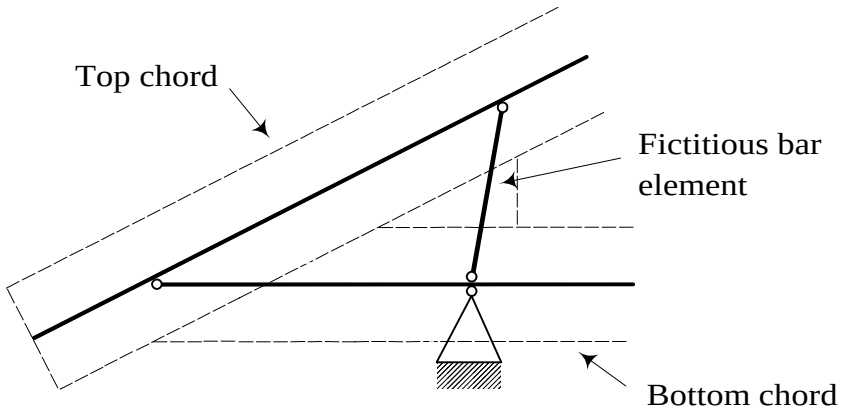

Figure 1.6. Model 2 used for joint modelling – heel joint.

The properties of the fictitious elements have to be estimated and also the location must be determined. A description of how fictitious elements can be used is given in, *Riberholt, H. (1982)* and *Riberholt, H. (1989).*

Model 3: The stiffness of the joints is taken into account by two translation springs and one rotation spring. The springs behave as mutual independent and the size of the nail plate is included in the stiffness values of the springs, see *Maraghechi, K. & Itani, R. Y. (1984).* An example of a spring model is shown in figure 1.7.

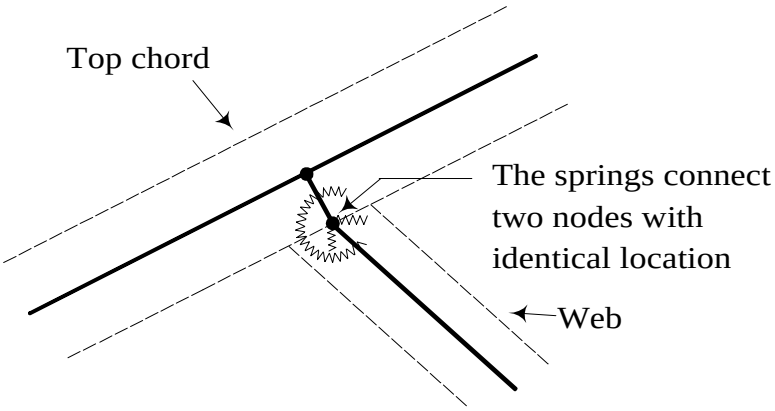

Figure 1.7. Model 3 used for joint modelling – joint between rafter and web.

In e.g. *Olsson, A. & Rosenqvist, F. (1996)* this model has been further developed by assuming that each of the nail groups is modelled by three springs.

Normally the springs act as linear elastic, but expressions for semi-rigidity of the nail groups are given in *Kevarinmäki, Ari (2000).*

Model 4: In 1977 Foschi presented a model for joints with nail plates, see *Foschi, R. O. (1977)*. The model is based on special elements used to take the deformations of the joints into account. Nail elements are used to model the stiffness of nail groups and a plate element is used to describe the stiffness and deformation of the nail plate over the joint line, see figure 1.8. The plate element connects the two nail elements. Furthermore, a contact element is used to transfer possible contact forces between timber members.

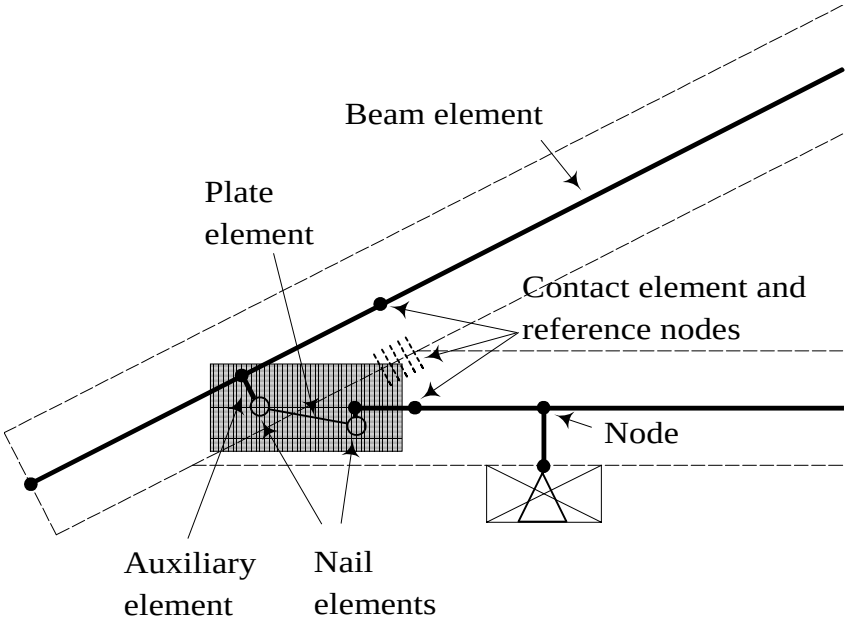

Figure 1.8. Model 4 used for joint modelling – heel joint.

Both the nail element and the plate element are based on nonlinear material properties.

The Foschi model has been implemented in the finite element program called SAT (Structural Analysis of Trusses) and a modified version is given in *Nielsen, J. (1996)*. In the modified version by Nielsen the use of the special nail, plate and contact elements is unchanged, but some changes are made to the elements.

1.2.1 Requirements for the Model - Choice of Model

Since the stiffness of the knee joint is of vital importance for the behaviour of the frame truss it is considered that the finite element model must take the stiffness of the joints into account. To do this in the most accurate way it is decided that the joints must have nonlinear material properties.

Furthermore, semi-rigid behaviour of the joints may lead to more economical structures, see *Larsen, H. J. & Jensen, J. L. (2000)*. The importance of semi-rigid joints is also described in *Kevarinmäki, Ari (2000)* and *Triche, M. H. (1993)*.

Due to the complex types of knee joints, where two or more legs are connected with several nail plates, it is also considered that the model must take the size and location of all nail plates into account. The model should also deal with contact forces, since large contact forces may be transferred in a knee joint.

Considering the requirements for the model it seems that the Foschi model forms the best basis for development of the knee joint as a part of the frame truss. In addition to the advantages of the Foschi model it predicts the sectional forces in all the nail plates directly.

1.3 Scope of the Thesis

The scopes of this thesis are:

- **Further development of the Foschi model to predict the stiffness and strength of timber joints/trusses with nail plates.**
- **To increase the knowledge of knee joints further and to compare the model with results from tests with knee joints.**

The basis for the model is given in *Foschi, R. O. (1977)* and in *Nielsen, J. (1996)* and the further developments have been made in the following areas:

- Plate element: A method to determine the geometry and the properties of the plate element is given. This has led to a modified plate element that consists of two types of steel beams, whereas only one beam type is considered in the models by Foschi and Nielsen.
- Nail element: A method to determine the stiffness of nail groups with arbitrary linear lines as boundaries is implemented in the model.

- Contact element: The contact element is modified to predict a probable increase of the contact area in the contact zone. The material properties of the contact element are changed from being linear elastic to being bilinear elastic.

Before testing the rather complex knee joints it is considered important that the model predicts the stiffness and strength of "simple" tension, shear and compression tests relatively accurately. Therefore, 234 tests with one type of nail plate have been performed and compared with the modified model. The modified model is named TRUSSLAB (the name emerges from TRUSSes and matLAB – the finite element program is set up as a package under MATLAB).

24 different types of knee joints (60 test specimens) have been tested in order to find a stiff and strong type of knee joint and in order to verify the TRUSSLAB model. The tests are performed with a fixed roof slope of 45º. The height of the leg in the tests is 1000 mm and the length of the rafter is 2000 mm. It is further assumed that the frame truss is supported at the outer corner of the leg on a fixed support and that the truss is produced without overhang (which is considered to be on the safe side due to the increased risk of splitting in the rafter).

This thesis concentrates on the behaviour of the nail plate and contact between timber members. The properties of and the failure modes in the timber are given less priority. Only two types of nail plates are considered – the GNA20S and the GNT150S from MiTek – and the timber used in the tests is spruce.

Some simple calculations by hand for the most promising types of the knee joints are also set up. The calculations are performed with sectional forces determined by a "simple" finite element model that only uses beam elements (the calculations are made for practical use by the truss manufacturers).

1.4 Reader's Guide

In chapter 2 the theory behind the finite element model TRUSSLAB is given.

In chapter 3 and chapter 4 the properties of the nail and plate elements are determined for the MiTek GNA20S and MiTek GNT150S nail plate, respectively. Furthermore, the stiffness and strength of the GNA20S nail plate attained from additional tests are compared with predictions given by TRUSSLAB. A test description for these tests is given in appendix A and some pictures from the tests are shown in appendix B.

In chapter 5 the knee joint is analysed – via tests and via numerical models in TRUSSLAB. A test description for these tests is given in appendix C together with detailed drawings of the test specimens.

The most promising type of knee joint, found in chapter 5, is used in the analysis of a frame truss in chapter 6. The behaviour of the frame truss is analysed considering both the displacements of the truss and the strength.

To show some of the applications that can be achieved by a model as TRUSSLAB the influence of chord splices in two types of trusses is analysed in chapter 7.

Chapter 8 contains the conclusions of the thesis and in chapter 9 a summary is given in Danish.

The references are listed in chapter 10 and the calculations of the knee joints aimed for the truss manufacturers are given in appendix D.

2 The Finite Element Model TRUSSLAB

The idea and the theory behind the finite element model TRUSSLAB are described in this chapter. The solution techniques used to solve the equations are also presented.

The finite element model is made as a package under the programme MATLAB – The Language of Technical Computing. TRUSSLAB can be used for analysis of timber structures with joints of punched metal plate fasteners (nail plates).

The theory behind TRUSSLAB is in general based on the ideas of joint modelling proposed by R. O. Foschi, see *Foschi, R. O. (1977)* and *Foschi, R. O. (1979)*. J. Nielsen developed some of the elements further and presented the work in the Ph.D.-thesis, *Nielsen, J. (1996)*. These improvements also form the basic of the TRUSSLAB model where additional modifications have been implemented.

A heel joint of a timber truss is used to describe the different special elements that are used in the joint modelling. The heel joint is shown in figure 2.1. The outer boundaries for the top chord and the bottom chord are shown as dashed lines.

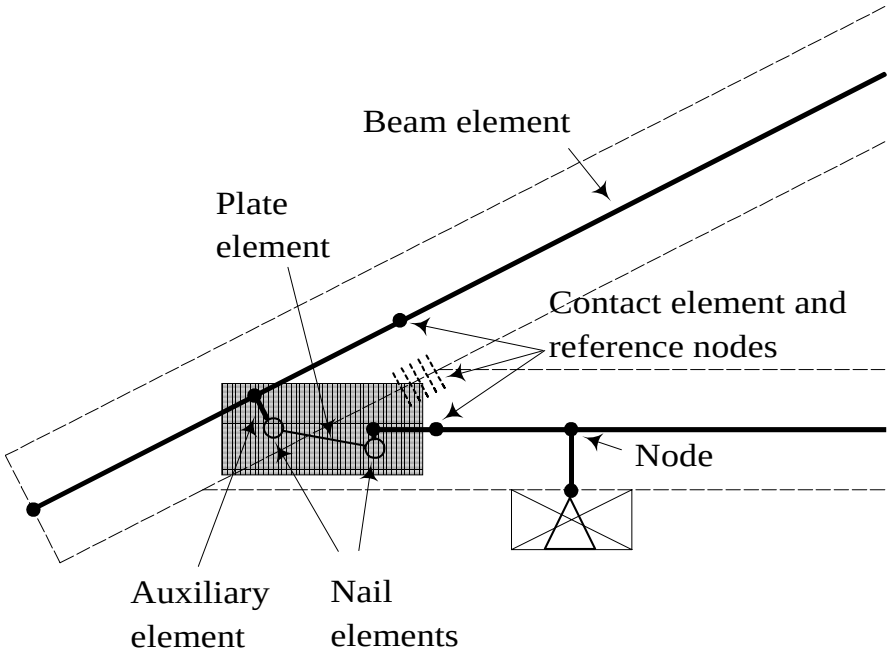

Figure 2.1. Heel joint used to explain the use of elements in TRUSSLAB.

Beam elements are used to model the timber members. The elements are located in the system line. Beam elements are also used as auxiliary elements. These auxiliary elements are used to transfer forces from nail groups to the system lines.

The stiffness of nail groups is taken into account via special nail elements. The nail elements connect beam elements with plate elements.

The behaviour of the nail plate over the joint line is modelled by a plate element. A plate element connects two nail elements. The nodes of a plate element and the corresponding nail elements are located at the centre of the respective nail groups.

Contact between timber members is modelled by a contact element. If there is an initial gap between the timber members the contact element is not activated until this gap is closed. The contact element refers to two nodes.

TRUSSLAB is a plane frame finite element programme with three degrees of freedom for each node: two displacements and one rotation.

2.1 Beam Element

Consider the beam element in figure 2.2. The global axes are given by x_g and y_g and the local axes by x_l and y_l (x_l is parallel to the beam direction). The angle between global and local is noted by φ and the beam element direction is from node 1 to node 2.

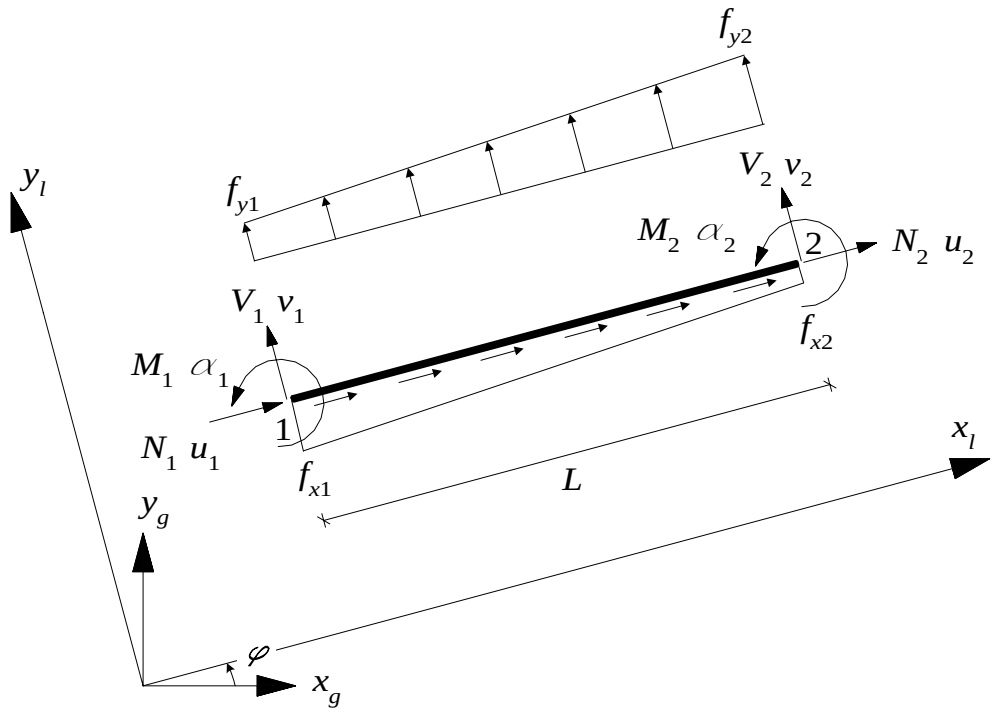

Figure 2.2. Beam element with notation of node forces and node displacements. The beam element is subjected to the distributed loads f_x and f_y.

The local element forces and the local displacements at the ends of the beam element are assembled in the vectors $\mathbf{f}$ and $\mathbf{u}$:

$$\mathbf{f} = \left[N_1 \; V_1 \; M_1 \; N_2 \; V_2 \; M_2 \right]^T \tag{2.1}$$

$$\mathbf{u} = \left[u_1 \; v_1 \; \alpha_1 \; u_2 \; v_2 \; \alpha_2 \right]^T \tag{2.2}$$

Considering Timoshenko beam theory the distributed loads f_x and f_y result in forces at the beam ends given by:

$$\mathbf{f}^{\mathbf{elem}} = \frac{L}{120\,(1+\Phi)} \begin{bmatrix} -120\,(1+\Phi)\left(\frac{f_{x1}}{3} + \frac{f_{x2}}{6}\right) \\ -f_{y1}(42+40\Phi) - f_{y2}(18+20\Phi) \\ -f_{y1}(6+5\Phi)L - f_{y2}(4+5\Phi)L \\ -120\,(1+\Phi)\left(\frac{f_{x1}}{6} + \frac{f_{x2}}{3}\right) \\ -f_{y1}(18+20\Phi) - f_{y2}(42+40\Phi) \\ f_{y1}(4+5\Phi)L + f_{y2}(6+5\Phi)L \end{bmatrix} \tag{2.3}$$

where Φ, for a rectangular cross section, is determined as:

$$\Phi = \frac{12EI}{\frac{5}{6}GAL^2} \tag{2.4}$$

E is the modulus of elasticity of the beam material and *I* is the moment of inertia. *A* is the cross-sectional area and *G* is the shear modulus. Formula (2.3) is derived when considering a small beam section and setting up the kinematic conditions, the constitutive relations and the equilibrium conditions.

The local relation between the element forces and the displacements is given by:

$$\mathbf{f} = \mathbf{f}^{\mathbf{elem}} + \mathbf{K}\mathbf{u} \tag{2.5}$$

$\mathbf{K}$ is the local stiffness matrix for the beam element. For a Timoshenko beam $\mathbf{K}$ is given by:

$$\mathbf{K} = \begin{bmatrix} \frac{EA}{L} & & & & & \\ 0 & 12\frac{EI}{(1+\Phi)L^3} & & & \textit{sym.} & \\ 0 & 6\frac{EI}{(1+\Phi)L^2} & \frac{4+\Phi}{1+\Phi}\frac{EI}{L} & & & \\ -\frac{EA}{L} & 0 & 0 & \frac{EA}{L} & & \\ 0 & -12\frac{EI}{(1+\Phi)L^3} & -6\frac{EI}{(1+\Phi)L^2} & 0 & 12\frac{EI}{(1+\Phi)L^3} & \\ 0 & 6\frac{EI}{(1+\Phi)L^2} & \frac{2-\Phi}{1+\Phi}\frac{EI}{L} & 0 & -6\frac{EI}{(1+\Phi)L^2} & \frac{4+\Phi}{1+\Phi}\frac{EI}{L} \end{bmatrix} \tag{2.6}$$

With the expressions in formula (2.6) the properties of the beam is assumed to be linear elastic. With $\Phi = 0$ the theory of a Bernoulli beam is attained.

As input in TRUSSLAB the following parameters are needed for each beam element: *E*, *I*, *A*, *G*, *L*.

2.1.1 Failure Conditions for Beam Elements

For the timber beams in TRUSSLAB the following failure conditions are implemented according to *Eurocode 5 (2001)* and *DS 413 (1998)*:

Tension:	$\sigma_t < f_t$
Compression:	$\sigma_c < f_c$
Bending:	$\sigma_m < f_m$
Bending and tension:	$\frac{\sigma_m}{f_m} + \frac{\sigma_t}{f_t} < 1.0$
Bending and compression:	$\frac{\sigma_m}{f_m} + \frac{\sigma_c}{f_c} < 1.0$
Shear:	$\tau < f_v$

where σ_t, σ_c, σ_m and τ are, respectively, the tension, compression, bending and shear stresses, determined by elasticity theory and the values of f_t, f_c, f_m and f_v are the corresponding strength values.

The failure check is performed after each load step and at *n*+2 points along each beam element where *n* is an arbitrary number given for input into TRUSSLAB.

Failure conditions with respect to instability are not included in TRUSSLAB.

2.2 Nail Element

Consider the nail plate area ABCD in figure 2.3. The nail plate area is located on a beam.

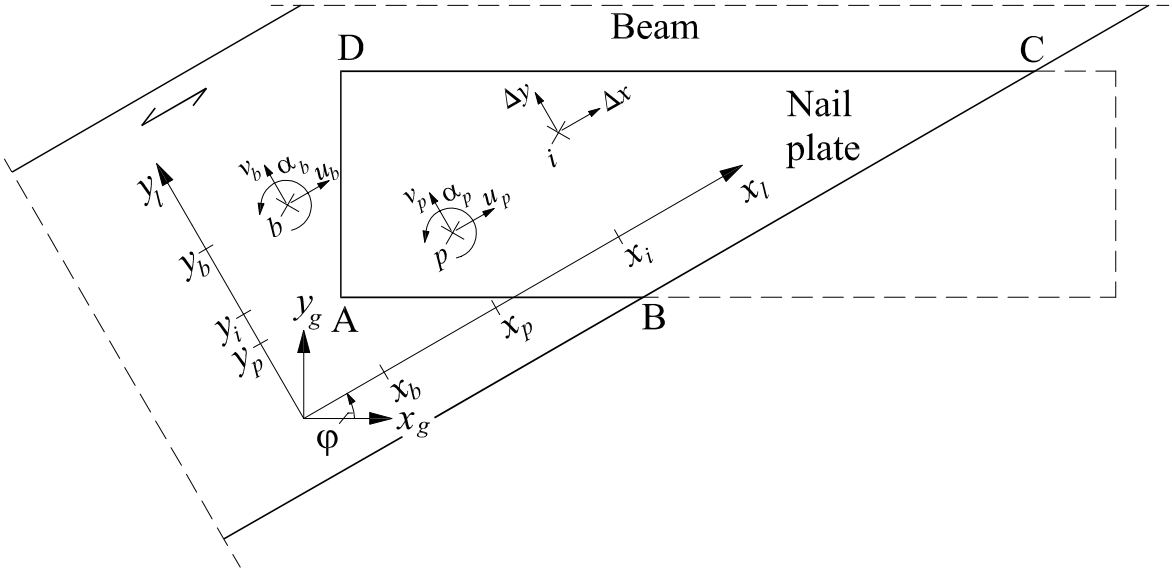

Figure 2.3. Plate area ABCD on a beam.

A local coordinate system x_l, y_l follows the grain direction and is rotated the angle φ from the global system given by x_g and y_g.

The displacements of the nail plate are given by u_p, v_p and α_p at location p (x_p, y_p) and the displacements of the beam are given by u_b, v_b and α_b at location b (x_b, y_b).

A nail at point i (x_i, y_i) is considered. It is assumed that the beam and the nail plate perform stiff-body motions and that the rotations α_b and α_p are small. The relative displacements of the nail at point i are given by (differences between the displacements of the beam and the nail plate at point *i*):

$$\Delta x = \mathbf{q}_\mathbf{x}^T \mathbf{u} \tag{2.7}$$

$$\Delta y = \mathbf{q}_\mathbf{y}^T \mathbf{u} \tag{2.8}$$

where:

$$\mathbf{q}_\mathbf{x} = \begin{bmatrix} 1 & 0 & -(y_i - y_p) & -1 & 0 & (y_i - y_b) \end{bmatrix}^T \tag{2.9}$$

$$\mathbf{q}_\mathbf{y} = \begin{bmatrix} 0 & 1 & (x_i - x_p) & 0 & -1 & -(x_i - x_b) \end{bmatrix}^T \tag{2.10}$$

$$\mathbf{u} = \begin{bmatrix} u_p & v_p & \alpha_p & u_b & v_b & \alpha_b \end{bmatrix}^T \tag{2.11}$$

The absolute displacement Δ of nail *i* is given by:

$$\Delta = \sqrt{\Delta x^2 + \Delta y^2} \tag{2.12}$$

The force p on nail i is assumed to be a function of the displacement Δ and is determined by, see also *Foschi, R. O. (1977)*:

$$p(\Delta) = (p_0 + k \cdot \Delta)\left(1 - \exp\left(\frac{-kk \cdot \Delta}{p_0}\right)\right) \tag{2.13}$$

The stiffness parameters k, kk and p_0 are defined in figure 2.4.

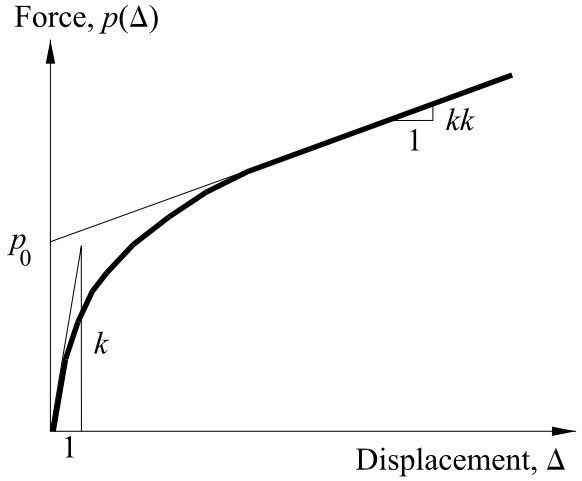

Figure 2.4. The nail force as a function of the displacement of the nail.

Besides the nail plate type the stiffness parameters are dependent on the angles between the grain direction, the main direction of the nail plate and the force direction. This dependence is described later in this section. The load-displacement curve shown in figure 2.4 is identical both during loading and during unloading, if any. However, this is only true if the load level is still on the elastic part of the load-displacement curve. Unloading may be possible in cases where contact is established.

The principle of virtual work is used to determine the contributions from the nail plate area ABCD to the stiffness. Consider figure 2.5.

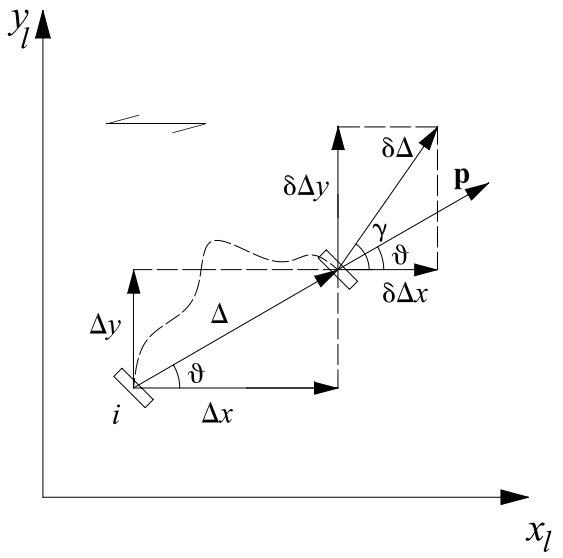

Figure 2.5. Force and virtual displacement of nail i.

The nail at location i was displaced the distance $\boldsymbol{\Delta}$ in the direction that forms an angle ϑ with the x_l-axis. The force required to perform this displacement is denoted $\mathbf{p}$. It is assumed that $\mathbf{p}$ is parallel to $\boldsymbol{\Delta}$, which is only true for an isotropic material. However, in *Nielsen, J. (1996)* and in *Jensen, J. L. (1994)* it is found that this assumption is good as the angle between $\mathbf{p}$ and $\boldsymbol{\Delta}$ is small.

A virtual displacement $\delta\boldsymbol{\Delta}$ of nail i is caused by a small variation in one of the displacement components of the displacement vector $\mathbf{u}$. The internal work δW^{int} done by nail i is given by:

$$\delta W^{\text{int}} = \mathbf{p} \cdot \delta\boldsymbol{\Delta} = p(\Delta) \cdot \delta\Delta \cdot \cos(\gamma - \vartheta) \tag{2.14}$$

The internal work performed over the nail plate area ABCD is found by summation over the n nails in this area:

$$\delta W^{\text{int}} = \sum_{i=1}^{n} p_i(\Delta_i) \cdot \delta\Delta_i \cdot \cos(\gamma_i - \vartheta_i) \tag{2.15}$$

When the nail density (number of nails/area) is denoted ζ and the area of nail plate ABCD is A, this summation can also be written as:

$$\delta W^{\text{int}} = \int_A \zeta \cdot p(\Delta) \cdot \delta\Delta \cdot \cos(\gamma - \vartheta)\, dA \tag{2.16}$$

$$\delta W^{\text{int}} = \int_A \zeta \cdot p(\Delta)\big(\cos(\vartheta)\, \delta\Delta x + \sin(\vartheta)\, \delta\Delta y\big)\, dA \tag{2.17}$$

$$\delta W^{\text{int}} = \int_A \zeta \cdot p(\Delta)\left(\frac{\Delta x}{\Delta}\delta\Delta x + \frac{\Delta y}{\Delta}\delta\Delta y\right) dA \tag{2.18}$$

When inserting $\mathbf{q_x}$ and $\mathbf{q_y}$ from formulas (2.7) and (2.8) into formula (2.18) a small variation in one of the six displacement components of $\mathbf{u}$ leads to:

$$\delta W_j^{\text{int}} = \int_A \zeta \frac{p(\Delta)}{\Delta} \left(\mathbf{q_x^T u}\ q_{x,j}\ \delta u_j + \mathbf{q_y^T u}\ q_{y,j}\ \delta u_j \right) dA \quad j = 1,...,6 \qquad (2.19)$$

$$\delta W_j^{\text{int}} = \left(\int_A \zeta \frac{p(\Delta)}{\Delta} \left(\mathbf{q_x^T u}\ q_{x,j} + \mathbf{q_y^T u}\ q_{y,j} \right) dA \right) \delta u_j \quad j = 1,...,6 \qquad (2.20)$$

The external work δW^e for a virtual displacement in one of the displacement components is given by:

$$\delta W_j^e = f_j \cdot \delta u_j \qquad j = 1,...,6 \qquad (2.21)$$

where f_j is the component j of $\mathbf{f}$. The size of the internal and the external work must be equal:

$$\delta W_j^{\text{int}} - \delta W_j^e = 0 \quad j = 1,...,6 \qquad (2.22)$$

and formula (2.20) and (2.21) then lead to:

$$\left(\int_A \zeta \frac{p(\Delta)}{\Delta} \left(\mathbf{q_x^T u}\ q_{x,j} + \mathbf{q_y^T u}\ q_{y,j} \right) dA - f_j \right) \delta u_j = 0 \quad j = 1,...,6 \qquad (2.23)$$

$$\int_A \zeta \frac{p(\Delta)}{\Delta} \left(\mathbf{q_x^T u}\ q_{x,j} + \mathbf{q_y^T u}\ q_{y,j} \right) dA - f_j = 0 \quad j = 1,...,6 \qquad (2.24)$$

$$\left(\int_A \zeta \frac{p(\Delta)}{\Delta} \left(\mathbf{q_x q_x^T} + \mathbf{q_y q_y^T} \right) dA \right) \mathbf{u} = \mathbf{f} \qquad (2.25)$$

$$\mathbf{Ku} = \mathbf{f} \qquad (2.26)$$

$\mathbf{K}$ is the local stiffness matrix for the nail element given by:

$$\mathbf{K} = \int_A \zeta \frac{p(\Delta)}{\Delta} \left(\mathbf{q_x q_x^T} + \mathbf{q_y q_y^T} \right) dA \qquad (2.27)$$

A nail group is bounded by 3,4,5,…,*n* edges. The integration in formula (2.27) is performed by splitting the nail group area into triangles and by using Gauss integration over each triangle. An example of this is shown in figure 2.6, where the method is illustrated on a peak joint.

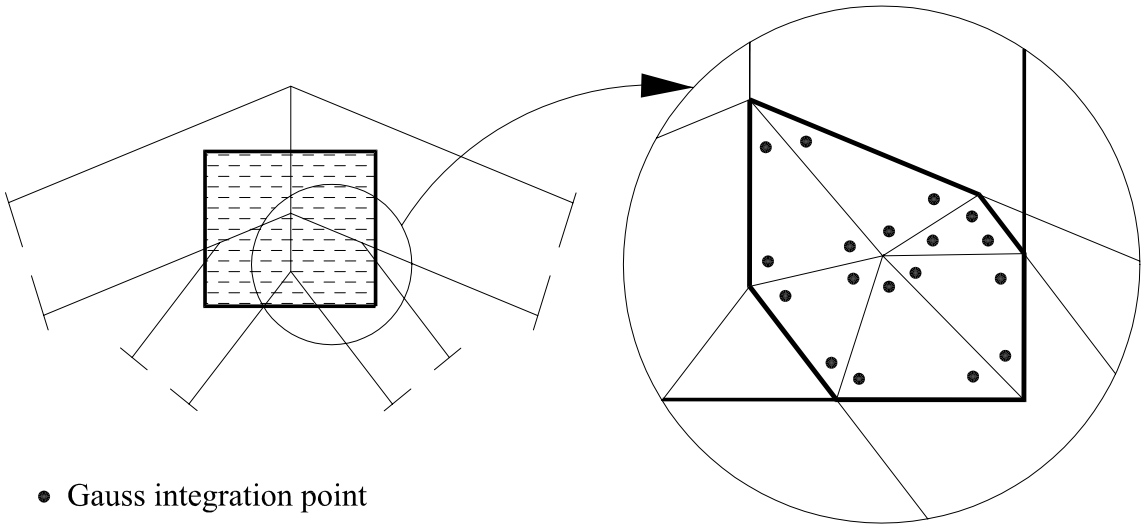

Figure 2.6. Illustration of splitting a nail group with a six-sided polygon into triangles. The integration points are shown by dots.

The integration can be performed with 3 or 6 integration points in each triangle, but numerical tests have shown that 3 integration points in each triangle are sufficient.

As mentioned above the load-displacement curve for a nail depends on the grain direction, the main direction of the nail plate and the force direction. Four test configurations (mentioned basic anchorage tests) where the nail plate and the timber are rotated in steps of 90º are used to determine the basic load-displacement curves. In figure 2.7 these four test configurations are shown with the index notation of the stiffness parameters. The first index of the stiffness parameter denotes the angle between the force direction and the main direction of the plate (α) and the second index denotes the angle between the force direction and the grain direction (β).

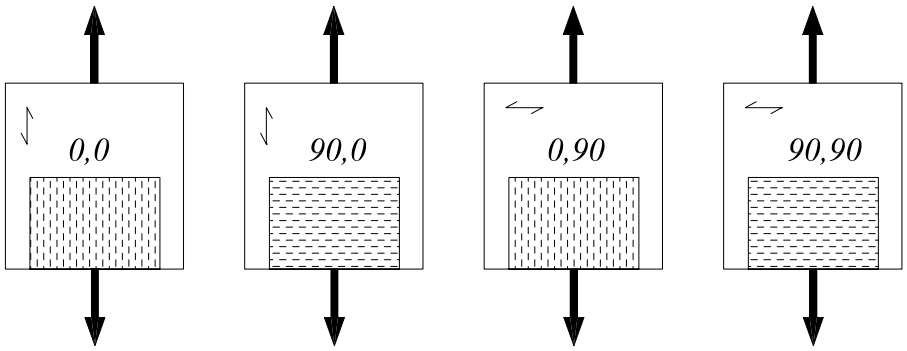

Figure 2.7. Basic anchorage tests and index notation for the stiffness parameters for each of the four test configurations.

Hankinson's formula is used for determination of the stiffness parameters k, kk and p_0 for other than the four basic cases. In the following it is shown how a stiffness value of k is determined. Similar calculations are used to determine values of kk and p_0. Consider figure 2.8.

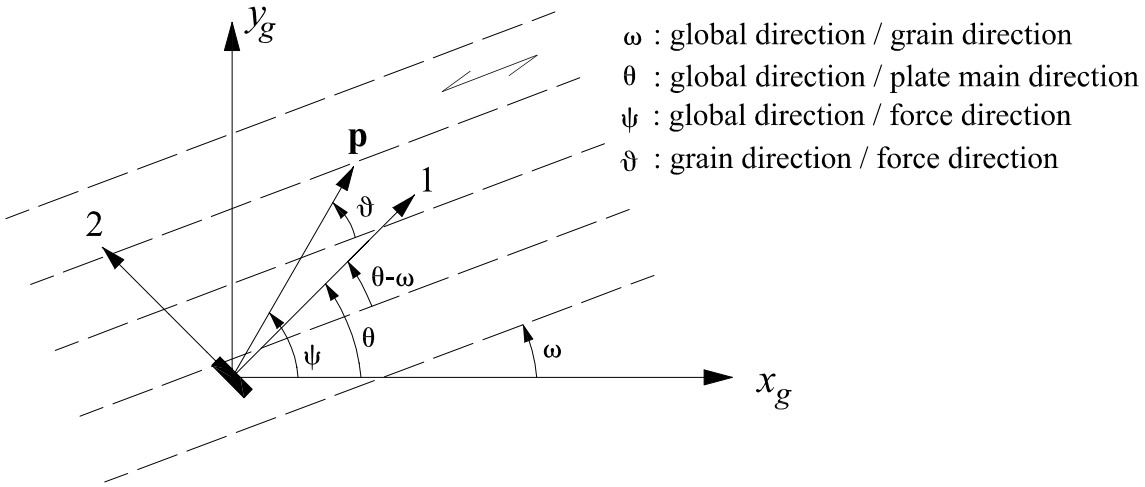

Figure 2.8. Definition of angles.

A value of k_1 in the main direction of the plate (direction 1) and a value of k_2 perpendicular to the main direction (direction 2) are determined by:

$$k_1 = \frac{k_{0,0} \cdot k_{0,90}}{k_{0,0} \cdot \sin^2(\theta - \omega) + k_{0,90} \cdot \cos^2(\theta - \omega)}$$
$$k_2 = \frac{k_{90,90} \cdot k_{90,0}}{k_{90,90} \cdot \sin^2(\theta - \omega) + k_{90,0} \cdot \cos^2(\theta - \omega)} \qquad (2.28)$$

A value of the stiffness k_x in the global *x*-direction and a value of the stiffness k_y in the global *y*-direction are given by:

$$k_x = \frac{k_1 \cdot k_2}{k_1 \cdot \sin^2(\theta) + k_2 \cdot \cos^2(\theta)}$$
$$k_y = \frac{k_1 \cdot k_2}{k_2 \cdot \sin^2(\theta) + k_1 \cdot \cos^2(\theta)} \qquad (2.29)$$

Finally, a stiffness *k* in the direction of the applied force **p** is given by:

$$k = \frac{k_x \cdot k_y}{k_x \cdot \sin^2(\psi) + k_y \cdot \cos^2(\psi)} \qquad (2.30)$$

The use of Hankinson's formula is one way to determine stiffness parameters for different angles between the force, grain and plate directions. Hankinson's formula is often used in timber engineering to represent the dependence of mechanical properties on grain direction, see *Foschi, R. O. (1979).*

The location of the two nodes in the nail element might be chosen arbitrarily due to the assumptions of stiff-body motions of the nail plate and of the beam. In general

the centroid of the nail groups is chosen as the location of both nodes of the nail element.

As input in TRUSSLAB for the nail element the following data are needed: Boundaries of the nail group area, angle between grain direction and main direction of the nail plate, angle between global direction and grain direction, nail density, stiffness parameters *k*, *kk* and p_0 for each of the four basic cases.

The failure conditions given in *Eurocode 5 (2001)* are implemented in TRUSSLAB, see section 3.5.3.

2.3 Plate Element

A plate element connects two nail elements. The plate element reflects the behaviour of the nail plate in the joint line and is made up of a two types of small steel beams. One type has the same direction as the main direction of the nail plate (four beams shown by solid hatch in figure 2.9) and the direction of the other type is perpendicular to the main direction of the nail plate (three beams), see figure 2.9.

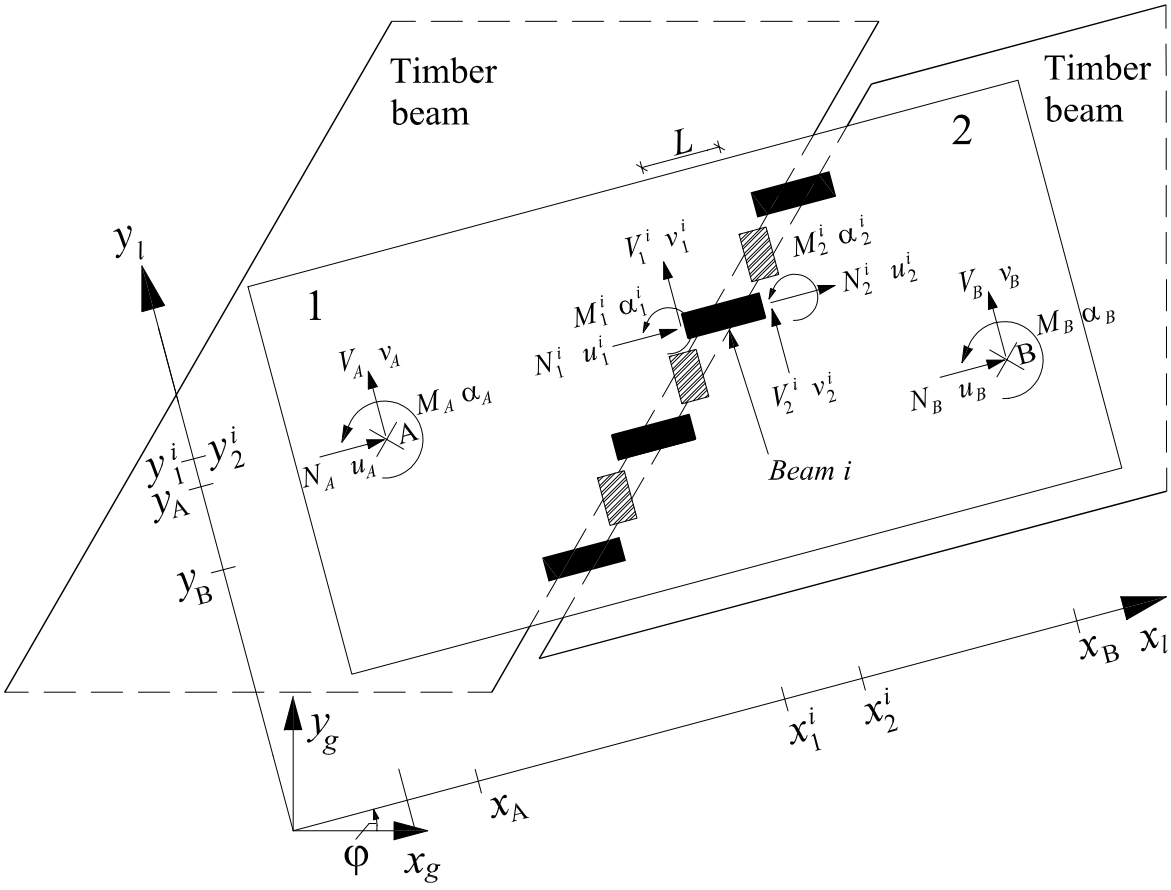

Figure 2.9. Plate element.

The nodes of the plate elements are given by point A and point B and the location of A and B can be chosen arbitrarily. The two plate regions 1 and 2 on the timber

beams (nail groups) are assumed to perform stiff-body movements. The small steel beams connect these two stiff regions.

In this section only the beams in the main direction of the nail plate are considered – in particular beam number *i*. The described method is repeated for the beams perpendicular to the main direction of the nail plate.

The local coordinate system x_l, y_l coincides with the direction of the considered beam *i*. The local system is rotated the angle φ from the global system x_g, y_g and the local system always coincides with the direction of the considered beam.

The beam has the length L. The displacements of the plate region (nail group) on the left-hand side are given by u_A, v_A and α_A at point A (x_A, y_A), and the displacements of the plate region on the right hand side are given by u_B, v_B and α_B at point B (x_B, y_B).

If small rotations are assumed the displacements $\mathbf{u^i}$ at the ends of beam *i* are given by:

$$\mathbf{u^i} = \mathbf{T^i u} \tag{2.31}$$

where:

$$\mathbf{u^i} = \begin{bmatrix} u_1^i & v_1^i & \alpha_1^i & u_2^i & v_2^i & \alpha_2^i \end{bmatrix}^T \tag{2.32}$$

$$\mathbf{T^i} = \begin{bmatrix} 1 & 0 & \left(y_A - y_1^i\right) & 0 & 0 & 0 \\ 0 & 1 & \left(x_1^i - x_A\right) & 0 & 0 & 0 \\ 0 & 0 & 1 & 0 & 0 & 0 \\ 0 & 0 & 0 & 1 & 0 & \left(y_B - y_2^i\right) \\ 0 & 0 & 0 & 0 & 1 & \left(x_2^i - x_B\right) \\ 0 & 0 & 0 & 0 & 0 & 1 \end{bmatrix} \tag{2.33}$$

$$\mathbf{u} = \begin{bmatrix} u_A & v_A & \alpha_A & u_B & v_B & \alpha_B \end{bmatrix}^T \tag{2.34}$$

Consider figure 2.10.

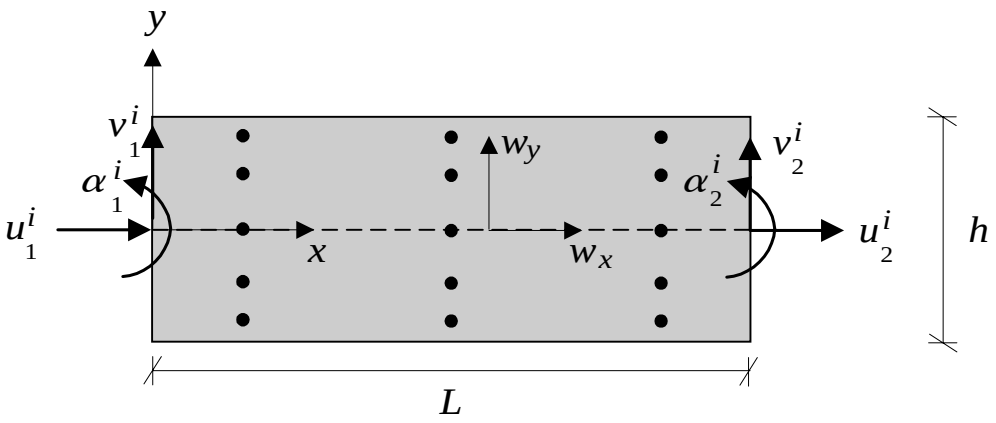

Figure 2.10. Beam i. The 15 Gauss integration points are shown with dots.

The displacements $\mathbf{w}$ at the system line of the beam as a function of x are determined using the displacement interpolation matrix $\mathbf{N}$ and the displacements at the ends of the beam:

$$\mathbf{w} = \mathbf{N}\mathbf{u}^{\mathbf{i}} \tag{2.35}$$

where:

$$\mathbf{N} = \begin{bmatrix} N_1 & 0 & 0 & N_4 & 0 & 0 \\ 0 & N_2 & N_3 & 0 & N_5 & N_6 \end{bmatrix}$$

$$\begin{aligned} N_1 &= 1 - \tfrac{x}{L} & N_2 &= 1 - 3\tfrac{x^2}{L^2} + 2\tfrac{x^3}{L^3} \\ N_3 &= x\left(1 - 2\tfrac{x}{L} + \tfrac{x^2}{L^2}\right) & N_4 &= \tfrac{x}{L} \\ N_5 &= \tfrac{x^2}{L^2}\left(3 - 2\tfrac{x}{L}\right) & N_6 &= \tfrac{x^2}{L}\left(\tfrac{x}{L} - 1\right) \end{aligned} \tag{2.36}$$

$$\mathbf{w} = \begin{bmatrix} w_x \\ w_y \end{bmatrix} \tag{2.37}$$

The axial strain ε at the system line and the curvature κ as a function of x are determined by:

$$\begin{bmatrix} \varepsilon \\ \kappa \end{bmatrix} = \mathbf{B}\mathbf{u}^{\mathbf{i}} \tag{2.38}$$

where $\mathbf{B}$ (strain distribution matrix) is the second derivative of $\mathbf{N}$ with respect to x.

The stresses in the beam are determined by the fibre strain $\varepsilon_{fibre}(x, y) = \varepsilon(x) - \kappa(x) \cdot y$ and by the constitutive relation given by:

$$\sigma = \left(\sigma_{y,t} + E_p\,\varepsilon_{fibre}\right)\cdot\left(1-\exp\left(\frac{-E\varepsilon_{fibre}}{\sigma_{y,t}}\right)\right) \quad \text{for } \varepsilon_{fibre} \geq 0$$
$$\sigma = \left(\sigma_{y,c} + E_p\,\varepsilon_{fibre}\right)\cdot\left(1-\exp\left(\frac{-E\varepsilon_{fibre}}{\sigma_{y,c}}\right)\right) \quad \text{for } \varepsilon_{fibre} < 0 \tag{2.39}$$

where the parameters are defined in figure 2.11.

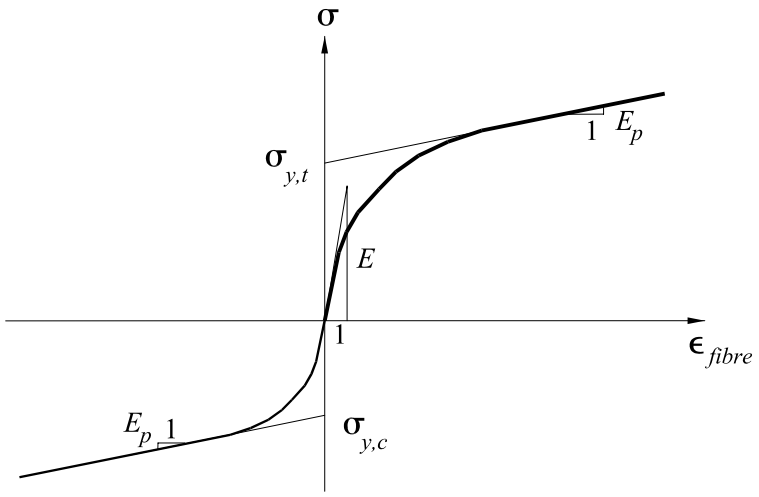

Figure 2.11. Definition of parameters in the constitutive relation.

To determine the forces at the beam ends it is convenient to introduce some "modified cross-sectional properties" $\tilde{A}$, $\tilde{S}$ and $\tilde{I}$ defined by, see *Byskov, E. (1982)*:

$$\tilde{A} = \int_A \tilde{E}dA \tag{2.40}$$

$$\tilde{S} = \int_A y\tilde{E}dA \tag{2.41}$$

$$\tilde{I} = \int_A y^2\tilde{E}dA \tag{2.42}$$

where A is the cross-sectional area and $\tilde{E}$ is defined as the secant modulus of elasticity E_S divided by the initial modulus of elasticity E, see figure 2.12.

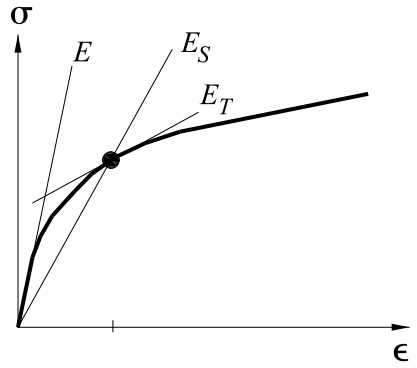

Figure 2.12. Secant modulus of elasticity and tangent modulus of elasticity at a given strain.

The local secant stiffness matrix $\mathbf{K_S^i}$ for beam *i* is given by:

$$\mathbf{K_S^i} = t\int_0^L \int_0^h \mathbf{B}^T \mathbf{D}\mathbf{B}\, dh\, dL \tag{2.43}$$

where *t* is the thickness of the beam and $\mathbf{D}$ denotes the secant material stiffness matrix given by:

$$\mathbf{D} = \begin{bmatrix} E\tilde{A} & -E\tilde{S} \\ -E\tilde{S} & E\tilde{I} \end{bmatrix} \tag{2.44}$$

The forces at the beam ends $\mathbf{f^i}$ are then given by:

$$\mathbf{f^i} = \mathbf{K_S^i}\,\mathbf{u^i} \tag{2.45}$$

where:

$$\mathbf{f^i} = \begin{bmatrix} N_1^i & V_1^i & M_1^i & N_2^i & V_2^i & M_2^i \end{bmatrix}^T \tag{2.46}$$

The forces $\mathbf{f}$ at points A and B from the *n* beams in the main direction of the nail plate are determined by:

$$\mathbf{f} = \sum_{i=1}^{n} \left(\left(\mathbf{T^i} \right)^T \mathbf{f^i} \right) \tag{2.47}$$

where

$$\mathbf{f} = \begin{bmatrix} N_A & V_A & M_A & N_B & V_B & M_B \end{bmatrix}^T \tag{2.48}$$

By inserting (2.31) and (2.45) into (2.47) the local finite element equation for the plate element is given by:

$$\mathbf{f} = \sum_{i=1}^{n} \left(\left(\mathbf{T^i} \right)^T \mathbf{K_S^i} \, \mathbf{u^i} \right) \tag{2.49}$$

$$\mathbf{f} = \sum_{i=1}^{n} \left(\left(\mathbf{T^i} \right)^T \mathbf{K_S^i} \, \mathbf{T^i} \right) \mathbf{u} \tag{2.50}$$

$$\mathbf{f} = \mathbf{K_S} \, \mathbf{u} \tag{2.51}$$

where $\mathbf{K_S}$ is the local secant stiffness matrix for the plate element given by:

$$\mathbf{K_S} = \sum_{i=1}^{n} \left(\left(\mathbf{T^i} \right)^T \mathbf{K_S^i} \, \mathbf{T^i} \right) \tag{2.52}$$

The integrations in formulas (2.40), (2.41), (2.42) and (2.43) are performed by Gauss integration. Each beam is divided into 3 Gauss points along the *x*-axis and 5 Gauss points along the *y*-axis, see e.g. the previous figure 2.10. It is again noted that only the beams in the main direction of the nail plate have been considered – the method described above is repeated for the beams in the direction perpendicular to the main direction.

To obtain a local tangent stiffness element matrix for the plate element, the formulas (2.41) to (2.47) are repeated, but with $\tilde{E}$ defined as the tangent modulus of elasticity E_T divided by the initial modulus of elasticity E, see figure 2.12.

When the joint line is either parallel or perpendicular to the main direction of the nail plate only one type of beam is activated, and it is rather easy to determine the number of beams in a plate element. However, in many joint types the joint line passes both types of beams and the beams may also "share" the same steel areas – see figure 2.13. This means that some kind of interaction between the two beam types should be implemented since the stresses in the two types of beams interact with each other.

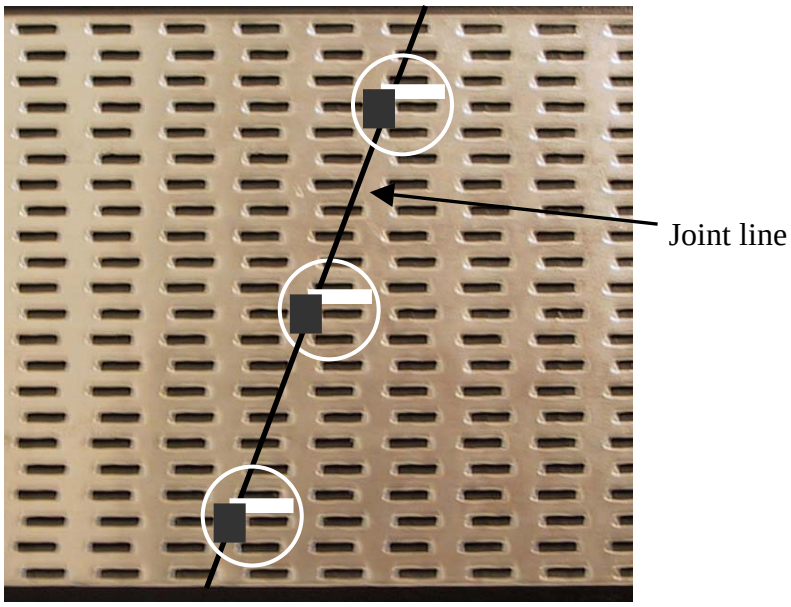

Figure 2.13. Joint where the two types of beams interact with each other.

In the figure the ends of the two types of beams cover the same piece of steel plate. The beams in the main direction of the plate are shown by white rectangles and the beams in the direction perpendicular to the main direction are shown by black rectangles.

Furthermore, the number of beams in the plate main direction decreases from maximum for $\gamma = 90^{\circ}$ to zero for $\gamma = 0^{\circ}$, but for the beams in the direction perpendicular to the main direction of the nail plate the opposite is seen – see figure 2.14. Only the beams in the plate main direction are considered in the figure. γ is the angle between the plate main direction and the joint line.

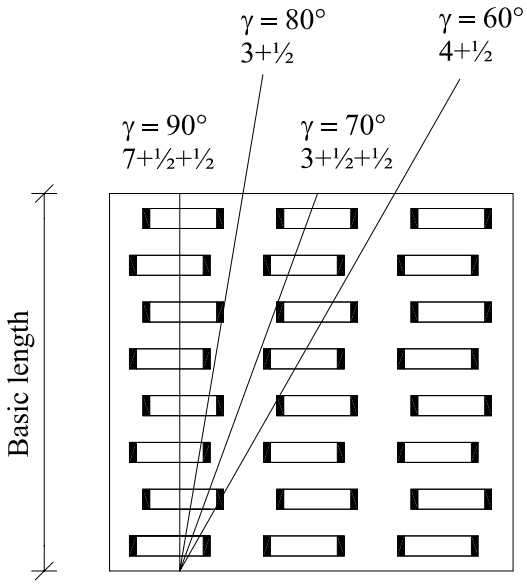

Figure 2.14. Example of number of beams dependent on the angle between the joint line and the nail plate.

For two nail plate types (MiTek GNA20S and MiTek GNT150S) the number of beams have been determined for different angles of γ, see table 2.1. The number of beams is determined for a given basic length, see figure 2.14 for a definition of the basic length when the beams in the plate main direction are considered (if the basic length is doubled the number of beams is doubled).

	GNA20S		GNT150S	
Basic length	83 mm	80 mm	70 mm	80 mm
γ	Beams in main direction	Beams perp. to main direction	Beams in main direction	Beams perp. to main direction
90˚	12	0	10	0
80˚	7-8	4	5-6	4
70˚	7-9	4	4-6	3-4
60˚	7-8	4	5	3-4
50˚	5-7	4	4-6	3-4
40˚	6-7	4	4-6	3-4
30˚	6-7	4	4-7	3-4
20˚	4-11	4	5-7	3-4
10˚	5-10	4	6-9	3-4
0˚	0	4	0	4

Table 2.1. Number of beams for different angles of γ.

As can be seen from the table, it is difficult to determine the number of beams when $\gamma \neq 0^{\circ},90^{\circ}$, since the number of beams may be different if the nail plate is moved just a few mm. Furthermore, tests show that the deformations and the failure line do not always follow the joint line – see chapter 3.

It is chosen to take both the change in the number of beams and the interaction between the two beam types into account by adjusting the number of beams (determined by $\gamma = 90^{\circ}$ and $\gamma = 0^{\circ}$, respectively). This adjustment is performed by a multiplication factor $\Im$. The factor is in the range between 0 and 1. It is multiplied by the number of beams determined directly from the mutual distance between the beams where $\gamma = 90^{\circ}$ for the beams in the main direction of the nail plate, and where $\gamma = 0^{\circ}$ for the beams perpendicular to the main direction. To illustrate this, see figure 2.15.

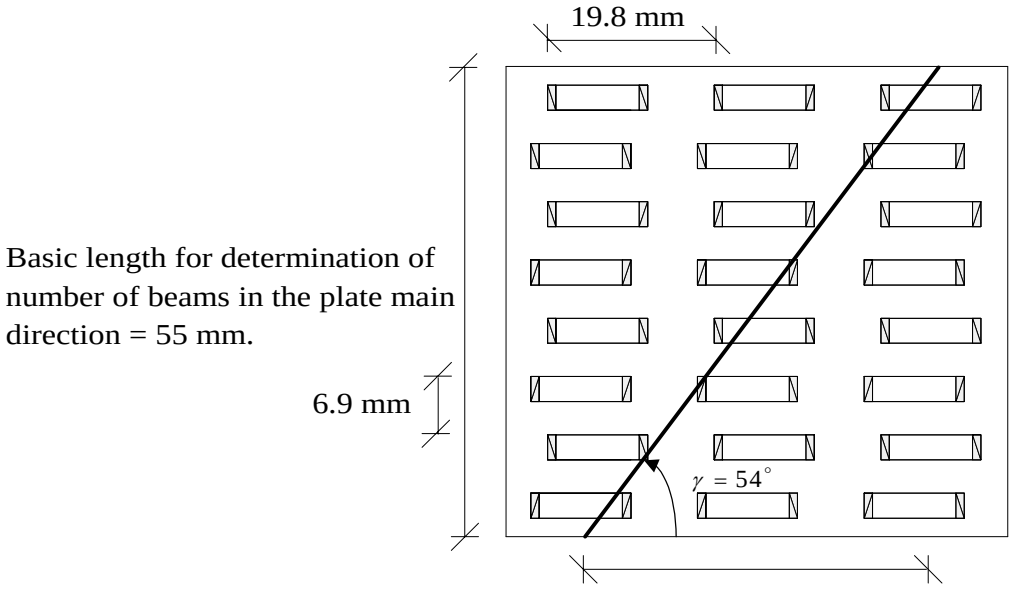

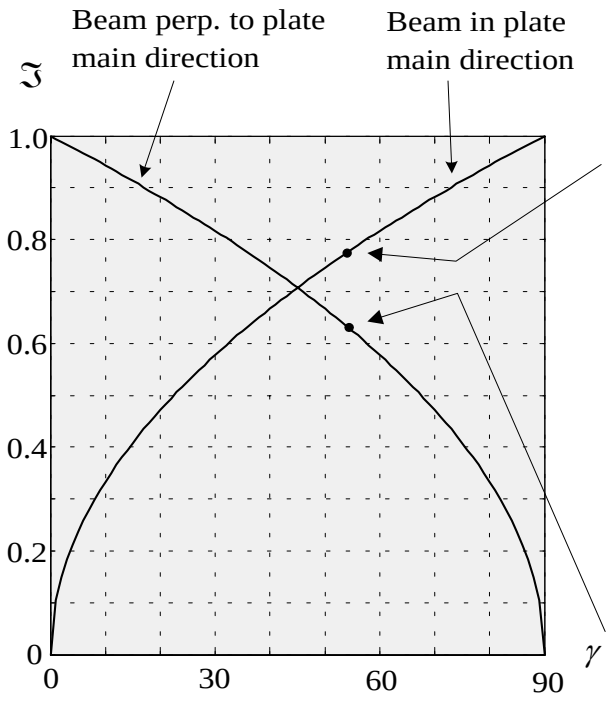

MAIN DIRECTION:
Number of beams in the plate main direction with $\gamma = 90^{\circ}$:
55 mm/6.9 = 8.0 beams.

Multiplication factor: 0.77

Actual number of beams in the plate main direction:
8.0 beams · 0.77 ≈ 6 beams

PERP. TO MAIN DIRECTION:
Number of beams perpendicular to the plate main direction with $\gamma = 0^{\circ}$:
40 mm/19.8 = 2.0 beams.

Multiplication factor: 0.63

Actual number of beams in the plate main direction:
2.0 beams · 0.63 ≈ 1 beam

Figure 2.15. Illustration of use of multiplication factor to determine the number of beams in the plate main direction and perpendicular to the plate main direction.

The formulas for the factor $\Im$ are given by:

$$\Im = \sqrt{\gamma / 90^\circ} \quad \text{for the beams in the main direction}$$
$$\Im = \sqrt{\left(90^\circ - \gamma\right) / 90^\circ} \quad \text{for the beams perpendicular to the main direction} \tag{2.53}$$

The formulas are determined empirically considering the number of beams. It may, however, be discussed if the expressions are too "complicated" and if they should simply be changed to linear ones.

The theory of the plate element has been applied to the MiTek nail plates GNA20S and GNT150S. As can be seen later in the thesis, results from tests with GNA20S are in close agreement with predictions given by TRUSSLAB. Only a few tests have been performed with the nail plate type GNT150S and it can therefore not be concluded if the theory of the plate element also predicts test results well for this type of plate. It is assumed, however, that the theory can be used for a wide range of nail plate types. The nail plates should have a geometry where it is possible to determine two types of beams – one type following the main direction of the nail plate and one type following the direction perpendicular to the main direction. For a description of the determination of the geometry of the beams, see section 3.1.

As input data the following parameters are needed for each type of beam: L, h, E, E_p, t, distance between the beams, $\sigma_{y,t}$, $\sigma_{y,c}$, angle between global direction and the beams in the main direction of the nail plate and the angle between global direction and the beams perpendicular to the main direction of the nail plate. For a detailed description of determination of these parameters, see section 3.1.

For a description of the failure conditions for the plate element, see section 3.2.3.

2.4 Contact Element

The contact element is used to transfer contact forces between timber members. An example of a contact element in a heel joint is shown in figure 2.16.

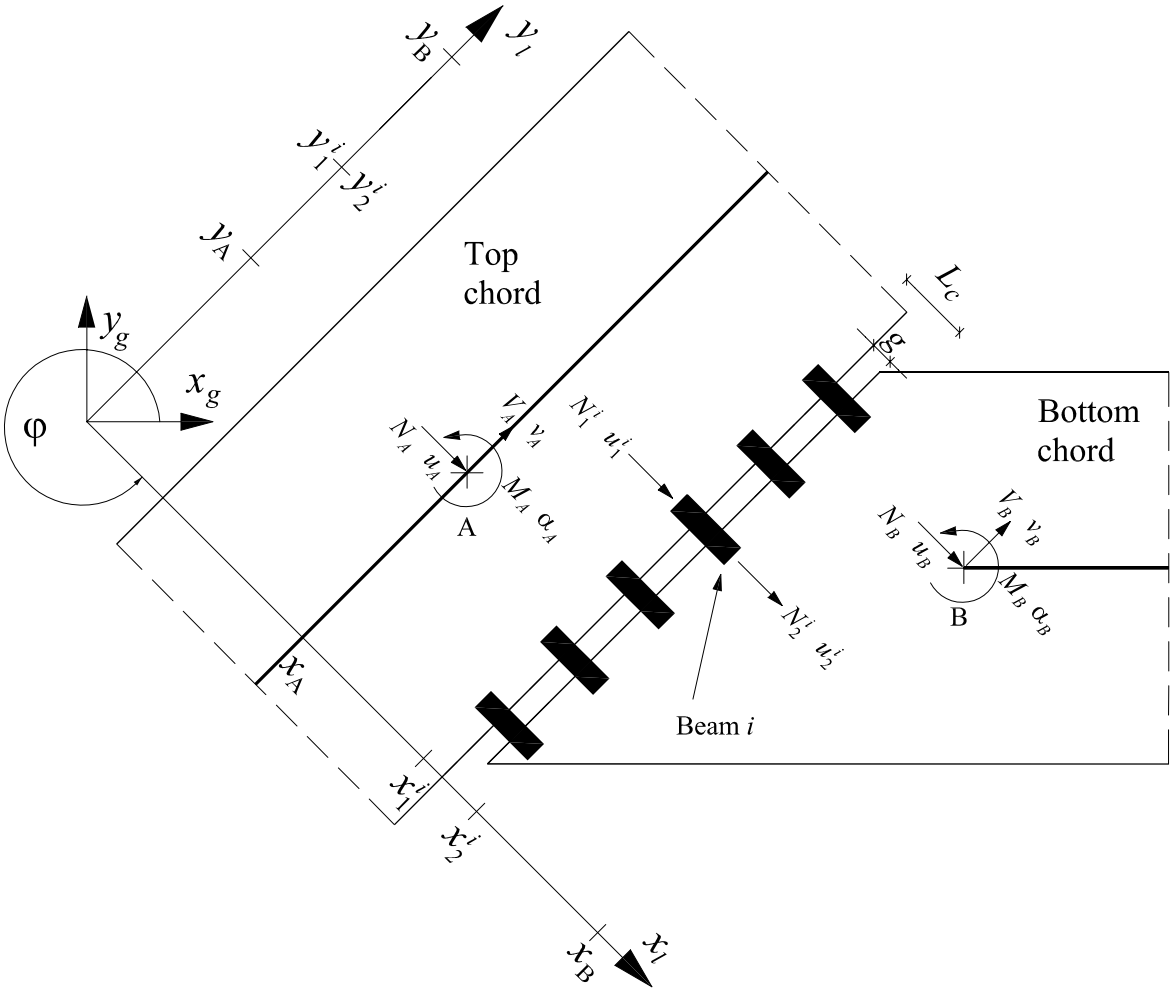

Figure 2.16. Contact element with notation of forces and displacements.

The contact element consists of a series of small beam elements and they are only activated if the initial gap *g* between the timber members is closed. The number of contact beams is a variable parameter in TRUSSLAB and the number of contact beams is chosen considering the length of the joint line – normally one beam per 20 mm of joint line. It is assumed that each of the beams of the contact element only transfers an axial compression force (they act as bars). The element refers to two nodes – in figure 2.16 node A on the top chord and node B on the bottom chord.

The *x*-axis of the local coordinate system follows the direction of the beams in the contact element. The local system is rotated the angle φ from the global system.

Consider beam *i* in figure 2.16. The length of the beams L_c has to be estimated, but as shown in the parameter analysis in section 5.2.2 the influence of the parameter is small. The displacements $\mathbf{u^i}$ at the ends of the beam are determined from the displacements at nodes A and B in the same way as for the plate element – see formulas (2.31) to (2.34).

The gap *g* is closed if:

$$u_2^i - u_1^i \le g \tag{2.54}$$

The load-displacement curve for the contact beams is assumed to be bilinear elastic as shown in figure 2.17.

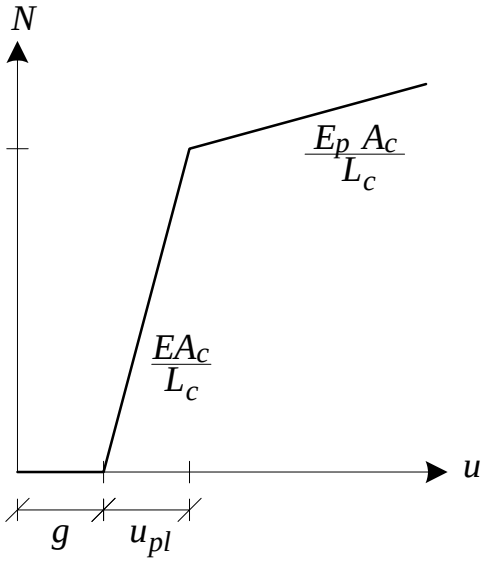

Figure 2.17. Load-displacement curve for the contact beams. A_c is the cross sectional area of one beam.

If the gap is not closed, the forces at the ends of beam *i* are equal to zero ($N_1^i = N_2^i = 0$). If the gap is closed and the axial force in the contact beam is still on the first part of the load-displacement curve the forces are given by:

$$\begin{aligned} N_1^i &= \frac{E \cdot A_c}{L_c}\left(u_1^i - u_2^i - g\right) \\ N_2^i &= -N_1^i \end{aligned} \tag{2.55}$$

If the gap is closed and the axial force in the contact beam is on the second part of the load-displacement curve the forces are given by:

$$\begin{aligned} N_1^i &= \frac{E_p \cdot A_c}{L_c}\left(u_1^i - u_2^i - g - u_{pl}\right) \\ N_2^i &= -N_1^i \end{aligned} \tag{2.56}$$

The forces at the nodes A and B are determined by a summation of the forces in the *n* beams:

$$\mathbf{f} = \sum_{i=1}^{n}\left(\left(\mathbf{T^i}\right)^T \mathbf{f^i}\right) \tag{2.57}$$

where $\mathbf{T^i}$ is given by formula (2.33) and $\mathbf{f^i}$ by:

$$\mathbf{f^i} = \begin{bmatrix} N_1^i & 0 & 0 & N_2^i & 0 & 0 \end{bmatrix}^T \tag{2.58}$$

The local stiffness matrix for beam *i* is given by:

$$\mathbf{K^i} = \begin{bmatrix} \frac{EA_c}{L_c} & & & & & \\ 0 & 0 & & & \textit{sym.} & \\ 0 & 0 & 0 & & & \\ -\frac{EA_c}{L_c} & 0 & 0 & \frac{EA_c}{L_c} & & \\ 0 & 0 & 0 & 0 & 0 & \\ 0 & 0 & 0 & 0 & 0 & 0 \end{bmatrix} \tag{2.59}$$

where E is the actual modulus of elasticity for beam *i* at the given load level (E or E_p). The local stiffness matrix for the *n* beams is given by the summation:

$$\mathbf{K} = \sum_{i=1}^{n} \left(\left(\mathbf{T^i} \right)^T \mathbf{K^i}\, \mathbf{T^i} \right) \tag{2.60}$$

As input in TRUSSLAB for the contact element the following are needed: Number of contact beams and location of joint line, L_c, E, E_p, g, stress level at which the contact beams starts acting “plastic” and angle between global and the contact beams.

2.5 Transformation between Local and Global System

The formulations above for the beam, nail, plate and contact elements are given in local coordinates. The local system is rotated the angle φ from the global system. The relation between the local and global systems are given by:

$$\mathbf{f_l} = \mathbf{R}\, \mathbf{f_g} \tag{2.61}$$

$$\mathbf{u_l} = \mathbf{R}\, \mathbf{u_g} \tag{2.62}$$

where index *l* refers to local and index *g* to global. The transformation matrix $\mathbf{R}$ is given by:

$$\mathbf{R} = \begin{bmatrix} \cos(\varphi) & \sin(\varphi) & 0 & 0 & 0 & 0 \\ -\sin(\varphi) & \cos(\varphi) & 0 & 0 & 0 & 0 \\ 0 & 0 & 1 & 0 & 0 & 0 \\ 0 & 0 & 0 & \cos(\varphi) & \sin(\varphi) & 0 \\ 0 & 0 & 0 & -\sin(\varphi) & \cos(\varphi) & 0 \\ 0 & 0 & 0 & 0 & 0 & 1 \end{bmatrix} \tag{2.63}$$

$\mathbf{R}$ is an orthogonal matrix ($\mathbf{R}^{-1} = \mathbf{R}^{T}$). The stiffness matrices and the forces given in local directions are transformed to global direction by formulas (2.66) and (2.67):

$$\mathbf{f_l} = \mathbf{K_l}\,\mathbf{u_l} \tag{2.64}$$

$$\mathbf{R}\,\mathbf{f_g} = \mathbf{K_l}\,\mathbf{R}\,\mathbf{u_g} \tag{2.65}$$

$$\mathbf{f_g} = \mathbf{K_g}\,\mathbf{u_g} \tag{2.66}$$

where the global stiffness matrix is given by:

$$\mathbf{K_g} = \mathbf{R}^{T}\,\mathbf{K_l}\,\mathbf{R} \tag{2.67}$$

2.6 Solution Technique For the Nonlinear Equations

To solve the system of nonlinear equations, several solution techniques have been used. Many of these techniques have difficulties in tracing the equilibrium path when the stiffness increases. This stiffness increase can be due to a gap between two timber members that is closed so contact forces between the members are transferred. This makes the stiffness increase. A typical load-displacement curve with these characteristics is shown in figure 2.18.

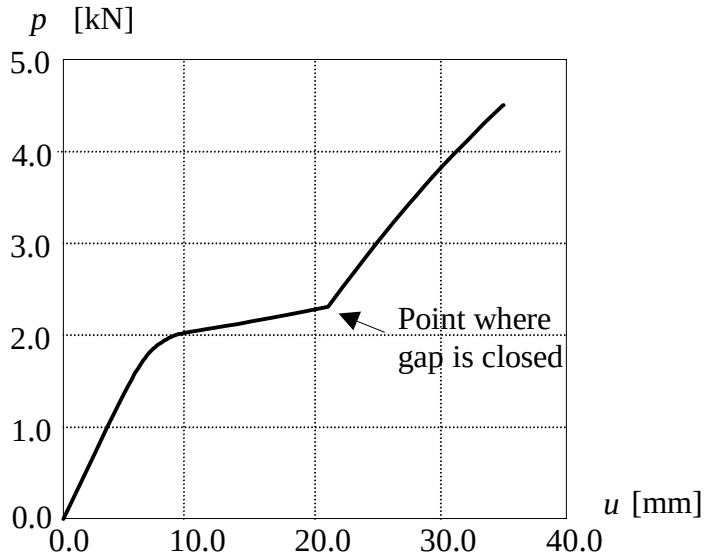

Figure 2.18. Typical load-displacement curve. The sudden change in stiffness is caused by contact between timber members.

One way to find the equilibrium path is to use one of the arc-length methods. The arc-length methods are intended to enable solution algorithms to pass limit points, e.g. where the load decreases. With some modifications one of the methods is found to be efficient and reliable to trace the equilibrium path for problems like the

one mentioned above. The way the arc-length method is used in TRUSSLAB as solution algorithm is presented in the following section.

2.6.1 Arc-Length Method

A linear form of the arc-length method is used. The arc-length method is described via an example with one degree of freedom u. A more detailed description of the arc-length method can be found in e.g. *Crisfield, M. A. (1997)*. From a given point of equilibrium $(u_0, \lambda_0 p)$ the iterations are started. The progress of the arc-length method is shown in figure 2.19. Special for the arc-length method is that not only the displacements but also the load changes.

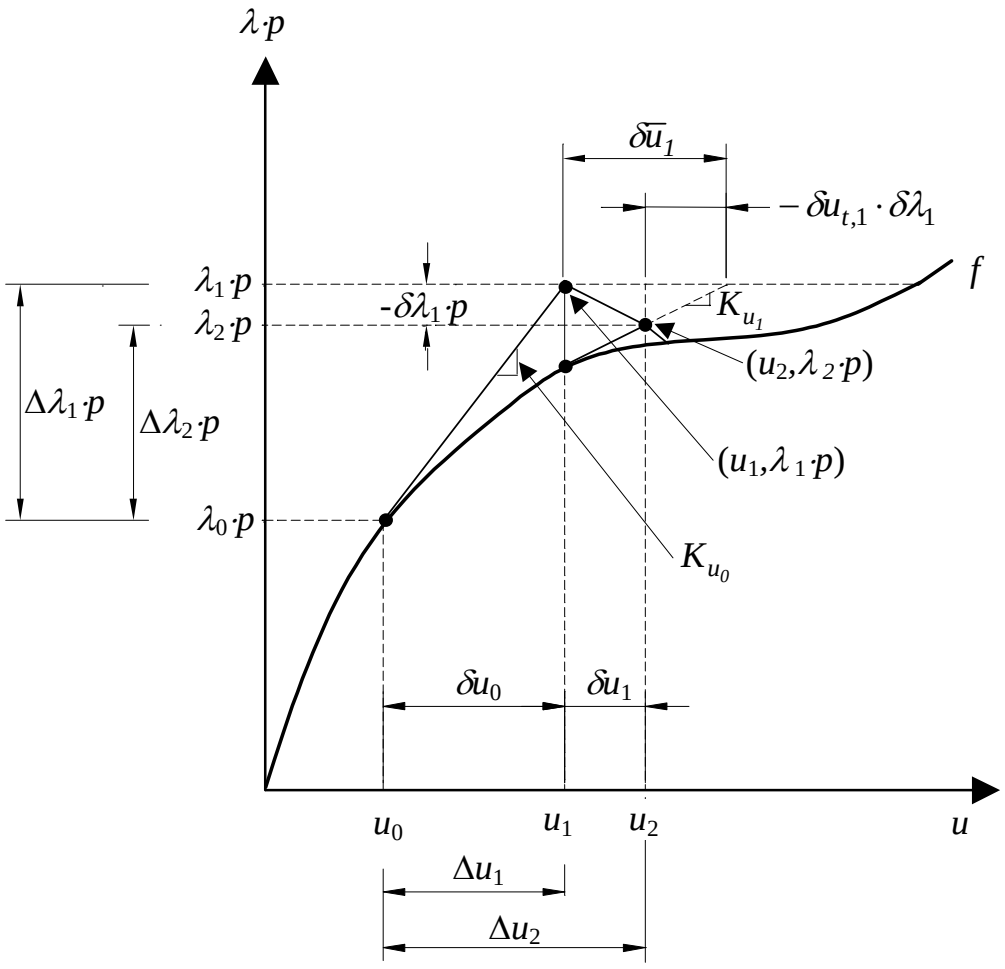

Figure 2.19. Illustration of arc-length method.

λ is a variable scale factor for the load. Δ is used for an increment and relates back to the last converged equilibrium state whereas, δ denotes a change within the iteration before a new point in equilibrium is found.

1) $\Delta\lambda_1$ is chosen in the interval [0;1] all dependent on the desired value of the load step in the current iteration.

2) The initial tangent stiffness K_{u_0} is calculated.

3) The first increment in the displacement is found as $\Delta u_1 = K_{u_0}^{-1} \cdot \Delta\lambda_1 \cdot p$.

4) The coordinates for the first iteration guess are $u_1 = u_0 + \Delta u_1$ and $\lambda_1 p = \lambda_0 p + \Delta\lambda_1 p$.

5) The tangent stiffness K_{u_1} at $u = u_1$ is determined.

6) $\delta\overline{u}_1 = -K_{u_1}^{-1} \cdot \left(f(u_1) - \lambda_1 p\right)$ is determined.

7) $\delta u_{t,1} = K_{u_1}^{-1} \cdot p$ is determined.

8) The change in the load scaling factor can be given by $\delta\lambda_1 = -\dfrac{\delta u_{t,1} \cdot \delta\overline{u}_1}{\delta u_{t,1} \cdot \delta u_{t,1} + 1}$, see *Crisfield, M. A. (1997)*.

9) The change in the displacement is given by $\delta u_1 = \delta\overline{u}_1 + \delta\lambda_1 \delta u_{t,1}$.

10) The new increments in displacement and load scale factor are given by $\Delta u_2 = \Delta u_1 + \delta u_1$ and $\Delta\lambda_2 = \Delta\lambda_1 + \delta\lambda_1$.

11) With the values of $u_2 = u_0 + \Delta u_2$ and $\lambda_2 = \lambda_0 + \Delta\lambda_2$ used as u_1 and λ_1 the iteration is repeated from point 5) to point 11) until the residual $f_{u_i} - \lambda_i p$ is sufficient small.

2.6.2 Modifications to the Arc-Length Method

If the value of the change in the load scaling factor at point 8) is set lower (e.g. by making the divisor bigger) the search line changes, see figure 2.20. In case A the divisor is increased and the search line forms an angle with the tangent stiffness that is smaller compared to case B. The chosen value for the change in load factor results in a search line like case A in figure 2.20. It is found that this gives a relatively quick and consistent way to follow the equilibrium path for the given problems.

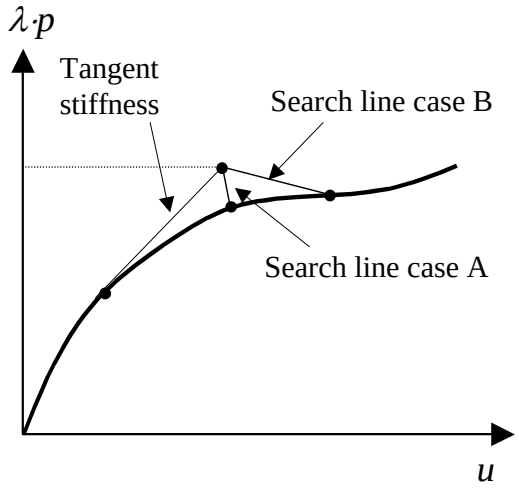

Figure 2.20. Illustration of influence of change to load factor.

As mentioned above, not only the displacements, but also the load is changed during the iterations. In order to reach a specific load level some modifications are made to the factor $\Delta\lambda$, so that λ ends up being equal to 1. Therefore, if λ is bigger than 1.001 the iteration is restarted from the last equilibrium point with half the value of $\Delta\lambda$. This makes λ converge to 1.000.

Furthermore, if the calculated value of $\Delta\lambda$ (point 10) is too big compared to the desired value of the load step $\Delta\lambda_1$ given at point 1) the iteration is restarted with a decreased value of $\Delta\lambda$. This is done to ensure that the load-displacement curve is traced with relative small steps.

For a few special load-displacement curves the arc-length method is not able to follow the equilibrium path without restarting the iteration with a smaller value of $\Delta\lambda$. A situation where the iterations proceed very slowly or do not converge at all is shown in figure 2.21 to the left.

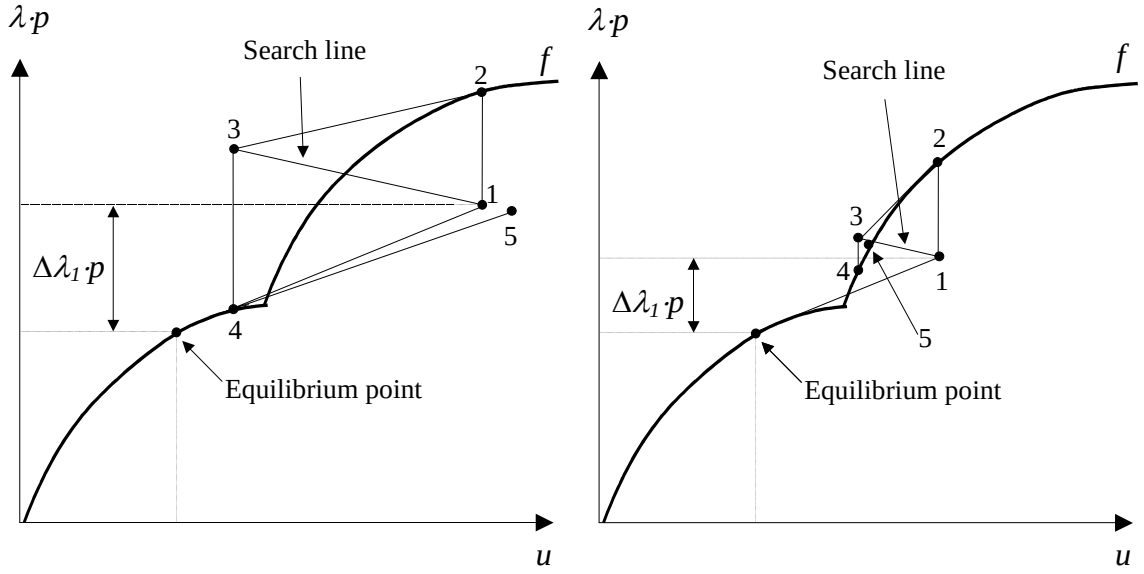

Figure 2.21. To the left an example, where the arc-length method proceeds very slowly or does not converge. To the right the same example is shown again but with smaller iteration steps, which makes the iterations converge.

Consider figure 2.21 to the left. From the equilibrium point a first guess (point 1) is determined. Point 3 is determined with the residual load between points 1 and 2, the updated tangential stiffness and with the direction of the search line. Similar from the residual load between points 3 and 4 a new guess is made (point 5). Dependent on the tangent stiffness calculated at points 2 and 4 the iterations proceed very slowly or even go round in circles (1-2-3-4-1-2-3…) if the values of the tangent stiffness at points 2 and 4 are identical.

To avoid this the iteration is restarted from the equilibrium point with half the value of $\Delta\lambda_1$. This makes the iterations proceed as shown in figure 2.21 to the right. The problem mentioned above is caused by a contact element that is activated. As an indicator of whether the problem will arise or not, a function in TRUSSLAB checks if the iterations switches several times between two stages, where the contact element is active or inactive. Furthermore, the iterations are restarted with a smaller step length if the number of iterations within a load step exceeds 35.

2.7 Conclusions

The theory behind the beam, nail, plate and contact elements is given in this chapter and a solution technique to find equilibrium of the nonlinear element equations is presented.

Compared with the theories for the models presented by *Foschi, R. O. (1977)* and *Nielsen, J. (1996)* the TRUSSLAB model has been modified in the following fields:

Beam element: In TRUSSLAB it is possible to apply distributed trapezoidal loads.

Nail element: In TRUSSLAB Hankinson's formula is used to predict the stiffness for situations other than the four basic cases (as in the model by Foschi). Nielsen developed a special formula based on tests. The input data for the nail element are based on 4 basic tests and the geometry of the nail plate, see chapter 3.1.1. In TRUSSLAB the failure conditions from *Eurocode 5 (2001)* have been implemented, see section 3.5.3.

Plate element: In TRUSSLAB the plate element consists of two types of beams. Each type of beam is modelled with nonlinear elastic material properties. As shown in section 3.1.1, the input data needed are based on the geometry of the nail plate and 6 basic tests. In the theories given by Foschi and Nielsen the plate element consists of one beam type. Only axial and shear forces are assumed to be transferred in each of the beams in the theory by Foschi (no bending moments can be transferred). Special failure conditions have been implemented in TRUSSLAB, see section 3.2.3.

Contact element: In TRUSSLAB the joint line is divided into a number of contact beams allowing the contact zone to develop. Furthermore, the contact element in TRUSSLAB has bilinear elastic material properties. In the theories by Foschi and Nielsen the contact element is set up as a single contact beam with linear elastic material properties.

For all four elements a possible unloading situation follows the loading path (e.g. in a splice joint where contact is established). This is only true when every part of the structure is still in the elastic state. It is assumed that unloading is only present in very few situations; however, this has not been investigated further. When considering this, it is clear why e.g. the words *plastic modulus of elasticity* are often written as *"plastic" modulus of elasticity* in the following.

Using a finite element model as TRUSSLAB with the special nail, plate and contact elements, the geometry of the model is based on the geometry of the analysed structure and no fictitious elements are needed. Except for the location of the reference nodes of the contact elements and the location of possible auxiliary elements, the geometry is given directly. Furthermore, the deformations of the joint lines and the nail groups are included in the model. Also possible gaps between timber members are included.

The specific values for the different elements (e.g. strength values, stiffness values, geometry of nail plates) needed as input in TRUSSLAB are mentioned in the chapters where they are needed.

The use of MATLAB as a base for TRUSSLAB has probably made TRUSSLAB relatively slow. If TRUSSLAB is translated to e.g. C++ it could reduce the calculation time by approximately a factor 10 to 20. The calculation time in

TRUSSLAB is dependent on the number of load steps. By choosing a small number of load steps the calculation time decreases, however, the load-displacement curve becomes rougher.

3 Analysis of Nail Plate Type MiTek GNA20S

The parameters needed as input in TRUSSLAB for the nail and plate elements for the nail plate type MiTek GNA20S are determined in this chapter. These parameters are determined from some basic tests performed on the nail plate. Additional tests are used to verify the theory behind the nail and plate elements. In these tests the main axis of the nail plate, the fibre direction, the direction of the joint line and the force direction are rotated in steps of 30° so every possible combination is covered. 114 tests have been performed to determine the parameters and verify the theory for the plate element, and 120 tests have been performed to find the parameters and verify the theory for the nail element. The results from the tests are shown in this chapter. For a test description and the test arrangements, see appendix A. Some typical pictures of the failure modes are shown in appendix B.

The tests are not performed as some kind of approval for the nail plates, but in order to determine certain parameters needed as input in TRUSSLAB and to verify the TRUSSLAB model. It is the aim to make the TRUSSLAB model predict the average of the load-displacement curves from each of the individual test series. Therefore, some modifications of the test methods described in *EN 1075 (1999)* have been made. The effective anchorage area has for example been treated differently. The modifications are mentioned in the text when they appear.

The test results are compared with results from TRUSSLAB and with the expressions given in Eurocode 5.

The geometry of the tested nail plate MiTek GNA20S is shown in figure 3.1.

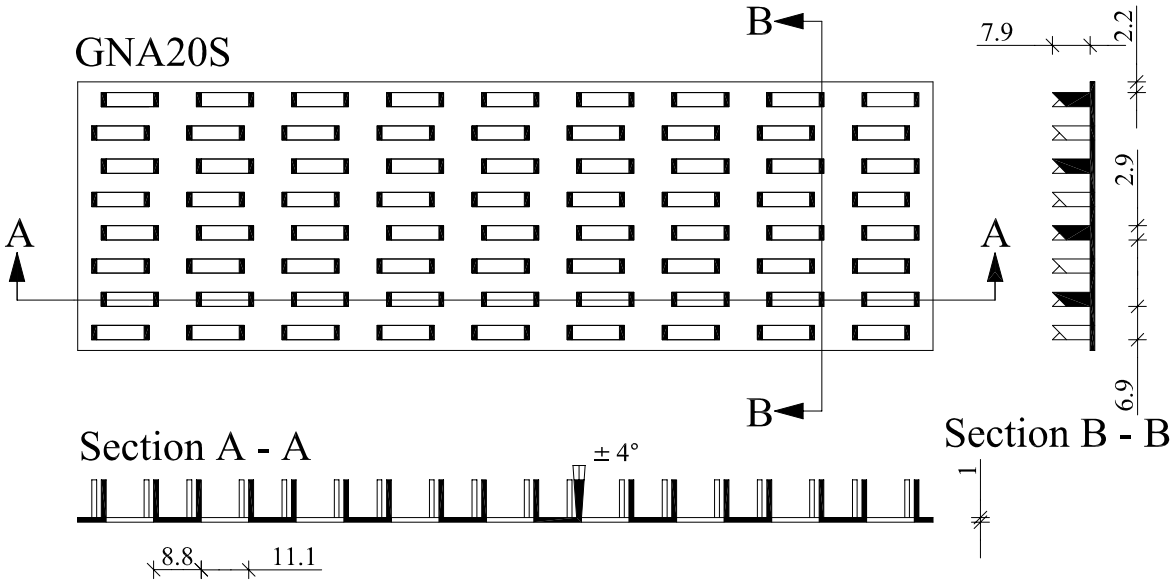

Figure 3.1. Geometry of the MITEK GNA20S nail plate. Dimensions in mm.

The nail density is 0.0147 nails/mm^2. The nail plates are galvanized and are produced by punching from a 1 mm thick steel plate.

In an earlier project, the properties of the steel used for production of the nail plates, have been determined as, see *Jensen, H. & Rasmussen, H. (1993)*:

- Modulus of elasticity, E = 188000 N/mm^2
- Yield stress, σ_y = 344 N/mm^2
- Yield strain, ε_y = 0.18%
- Ultimate stress, σ_u = 417 N/mm^2
- Ultimate strain, ε_u = 24.4%
- Poisson ratio ν = 0.30

The values are average values. It should be noted that the tested nail plates might have different material properties, because they are made of steel from different coils.

3.1 Properties for the Plate Element in TRUSSLAB

The plate element is composed by a number of small Bernoulli beams connecting two nail elements. Two different types of beams are considered – one type has the same orientation as the main axis of the nail plate and the other type has a direction perpendicular to the main axis. As input for the plate element the length, the height and the thickness of these two types of beams are needed. Furthermore, the stress-strain curve for the beams in both tension and compression has to be determined. For a detailed description of the plate element, see section 2.3.

As mentioned above, the test results were compared with results from calculations with TRUSSLAB. It should be noted that in some of the tensile test specimens the

failures were brittle. This destroyed one displacement transducer, and after this event the tests were stopped and the displacement transducers were dismounted after the plates became plastic, but before the ultimate load was reached. Some of the tests were continued after the transducers were dismounted to observe the failure mode, but the loads were not registered. Therefore, in 2/3 of the load-displacement curves shown, the tension tests were stopped before the ultimate load was reached but after the plates had become plastic. None of the compression tests were stopped before the ultimate load level was reached.

3.1.1 Basic Tests used to Determine the Properties of the Plate Element

For each type of the beams three basic test series were used to determine the properties, see figure 3.2. The three test series shown at the top of the figure were used to determine the properties of the beams that follow the main direction of the nail plate. The three other series were used to find the properties of the beams perpendicular to the plate main axis. The sizes of the nail plates were chosen so that failure in the joint line was achieved.

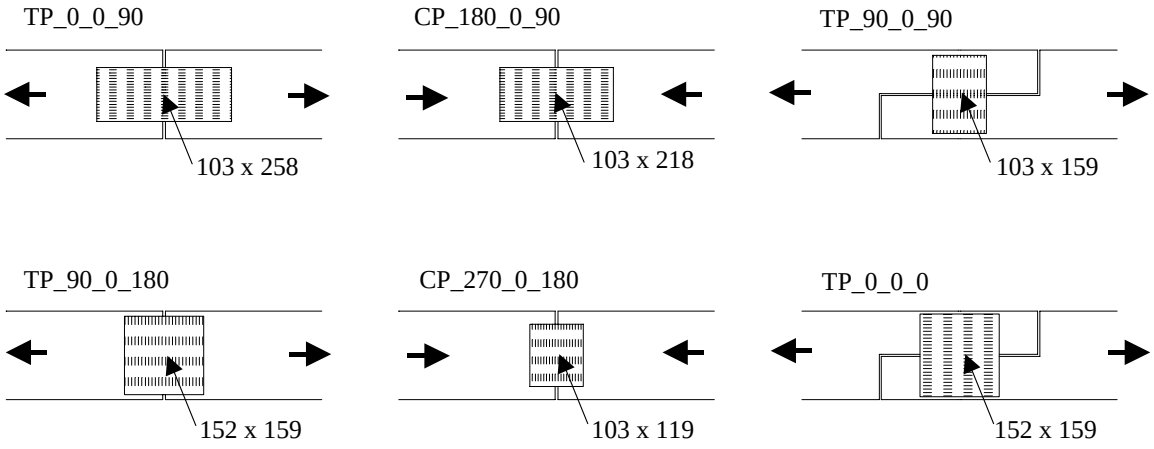

Figure 3.2. Test series used to determine the properties of the plate element. Dimensions in mm.

The gap between the timber members is 5 mm, the height of the beams is 170 mm and their thickness is 45 mm.

The notation of the specimens is TP_α_β_γ (Tension test arrangement Plate values) and CP_α_β_γ (Compression test arrangement Plate values) where:

- α is the angle between the plate main direction and the force $[0^\circ : 360^\circ]$
- β is the angle between the force and the grain direction $[0^\circ : 90^\circ]$
- γ is the angle between the plate main direction and the joint line $[0^\circ : 180^\circ]$.

The angles and their positive directions are defined in figure 3.3.

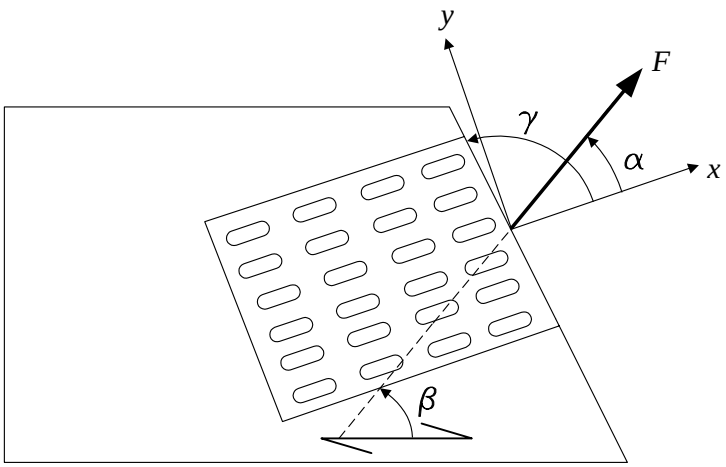

Figure 3.3. Definition of angles used to define the test specimens.

The load-displacement curves for the six basic test series are shown in figure 3.4. The curves illustrate the behaviour of one beam and the force is measured in N along the vertical axis while the deformation on the horizontal axis is measured in mm. The way the deformation of the plate is measured is described in appendix A.

For each of the six test series three identical test specimens have been tested. Due to either timber or anchorage failure, not all three specimens are shown for the series TP_0_0_90 and TP_0_0_0. For the series CP_180_0_90 one of the data files was destroyed.

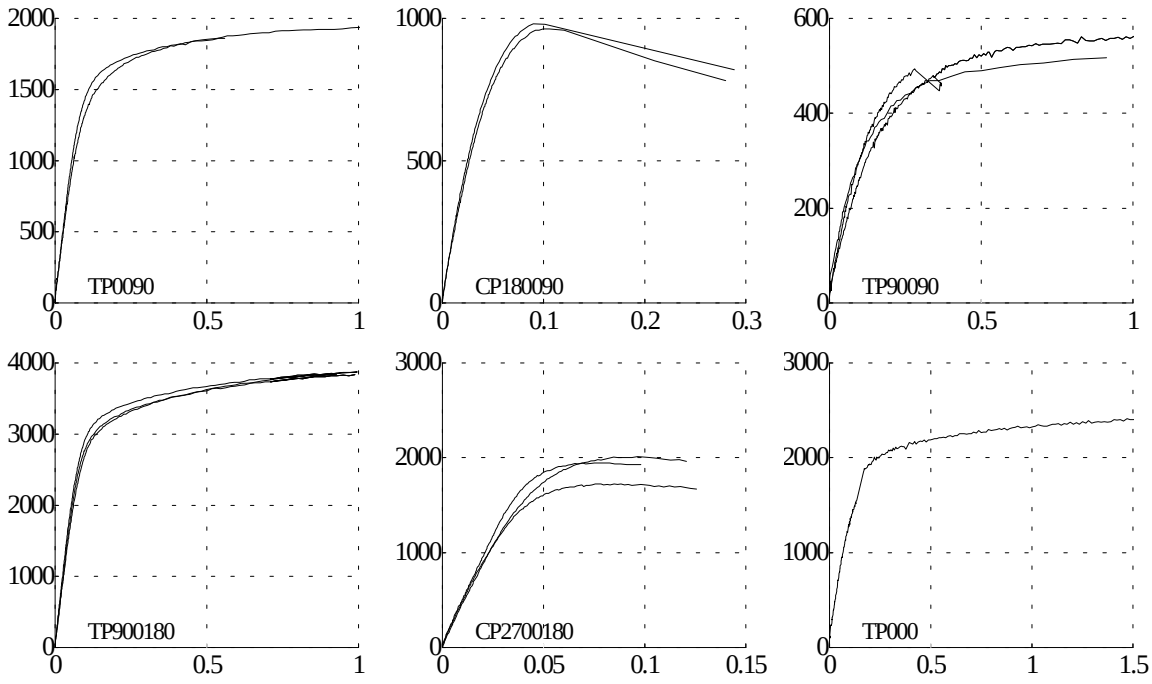

Figure 3.4. Load-displacement curves for the six basic test series used to determine the properties of the plate element. The load is converted to one beam. The force is shown on the vertical axis [N] and the deformation is shown on the horizontal axis [mm].

For each of the two types of beams the parameters are determined as described below – see also figure 3.6.

The thickness *t* of the beam is given directly from the geometry of the nail plate. The yield force in tension $N_{y,t}$ and the deformation $\Delta_{y,t}$ are determined/estimated from the results of the test where the beam is subjected to tension (TP_0_0_90 for the beams in the main direction and TP_90_0_180 for the beams in the direction perpendicular to the main direction). $N_{y,t}$ and $\Delta_{y,t}$ are defined on figure 3.5 where $N_{y,t}$ is determined as 1800 N/beam and $\Delta_{y,t}$ is determined as 0.08 mm for the test series TP_0_0_90.

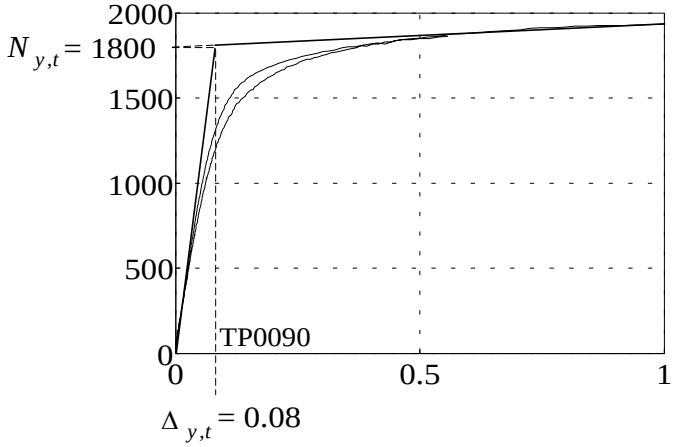

Figure 3.5. Definition of $N_{y,t}$ and $\Delta_{y,t}$. The load is converted to one beam. The force is shown on the vertical axis [N] and the deformation is shown on the horizontal axis [mm].

The yield stress in tension $\sigma_{y,t}$ and the corresponding yield strain $\varepsilon_{y,t}$ are calculated when the values of the length *L* and the height *h* of the beam have been determined (the way *L* and *h* are determined is explained later in this section):

$$\sigma_{y,t} = \frac{N_{y,t}}{h \cdot t} \tag{3.1}$$

$$\varepsilon_{y,t} = \frac{\Delta_{y,t}}{L} \tag{3.2}$$

The initial modulus of elasticity, *E*, is calculated afterwards:

$$E = \frac{\sigma_{y,t}}{\varepsilon_{y,t}} \tag{3.3}$$

The yield strain $\varepsilon_{y,c}$ in compression is calculated from the value of the yield stress in compression $\sigma_{y,c}$ and from the value of *E*:

$$\varepsilon_{y,c} = \frac{\sigma_{y,c}}{E} \tag{3.4}$$

The yield stress in compression (stress when buckling) is found from the test results and includes the buckling effect of the beams.

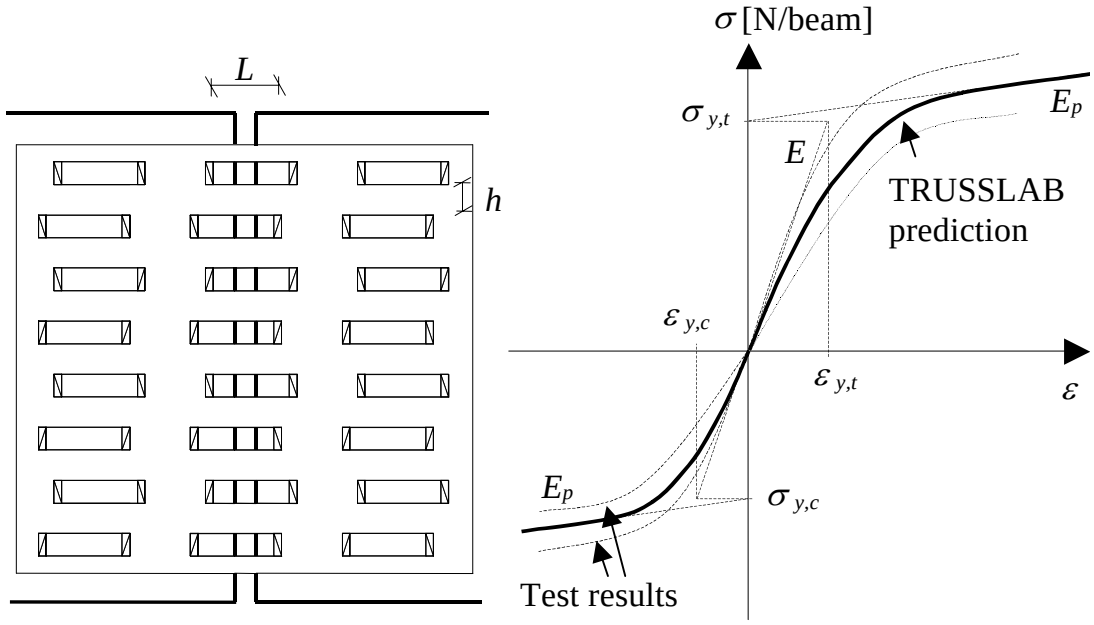

Figure 3.6. Definition of parameters for the beams in the plate element. L and h are only illustrated for the beams in the main direction of the plate.

For different pairs of the length *L* and the height *h* of the beam, TRUSSLAB may predict the results of both the tension and compression tests. In order to decide which pair of *L* and *h* should be used, the basic test where the beam is subjected to both bending and shear is considered (the test series shown to the right in figure 3.2). When a similar model for this basic test series is set up in TRUSSLAB it is found that one pair of the parameters *L* and *h* will make TRUSSLAB predict the test results in the best way. The load level where the beam starts buckling is considered more important than the initial stiffness when the values of *L* and *h* are chosen.

The value of the "plastic" modulus of elasticity E_p is taken as an average value so that it reflects the plastic behaviour of the beams both in tension, shear and compression.

In some cases the height of the beam is given directly from the geometry of the nail plate. For example, *h* is given as 4 mm for the beams that follow the main direction of the nail plate GNA20S. In those cases *L* is the only variable parameter. Anyhow, when considering the height of the beams perpendicular to the plate main axis it is more difficult to determine an appropriate value of *h*, and the method described above for determination of the parameters is used.

When following the above-mentioned procedure to determine the properties of the plate element, the parameters listed in table 3.1 are found.

	Beams in plate main direction	Beams perpendicular to plate main direction
$\sigma_{y,t}$ [N/mm^2]	450	430
$\varepsilon_{y,t}$	0.0100	0.0075
$\sigma_{y,c}$ [N/mm^2]	240	240
$\varepsilon_{y,c}$	0.0053	0.0042
L [mm]	8.0	8.0
h [mm]	4.0	8.0
t [mm]	1.0	1.0
E [N/mm^2]	45000	57300
E_p [N/mm^2]	300	300

Table 3.1. Parameters for the plate element for the MiTek GNA20S nail plate.

The distance between the beams in the main direction of the nail plate is 6.9 mm and the distance between the beams perpendicular to the main direction of the nail plate is 19.8 mm.

An illustration of the geometry of the beams for the GNA20S nail plate is shown in figure 3.7.

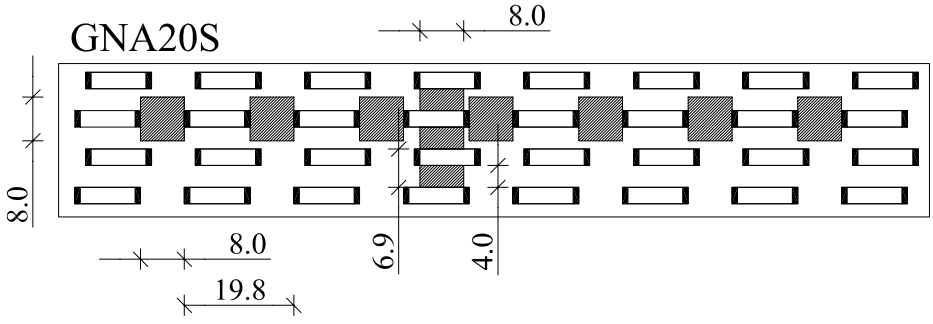

Figure 3.7. Geometry of the beams in the plate element for the GNA20S nail plate. Dimensions in mm.

A comparison between the basic test results and results from TRUSSLAB calculations is shown in figure 3.8. The force transformed to N per mm of plate along the joint line is shown vertically, and the displacement in mm is shown horizontally. The results from TRUSSLAB are shown by a dashed line and the dots

indicate the load level where TRUSSLAB predicts failure. The way plate failure is predicted by TRUSSLAB is described on page 59 and onwards. After the ultimate load level has been reached in TRUSSLAB the calculations are continued without any changes (e.g. no changes are made in the number of beams if some of the plate beams fail in tension).

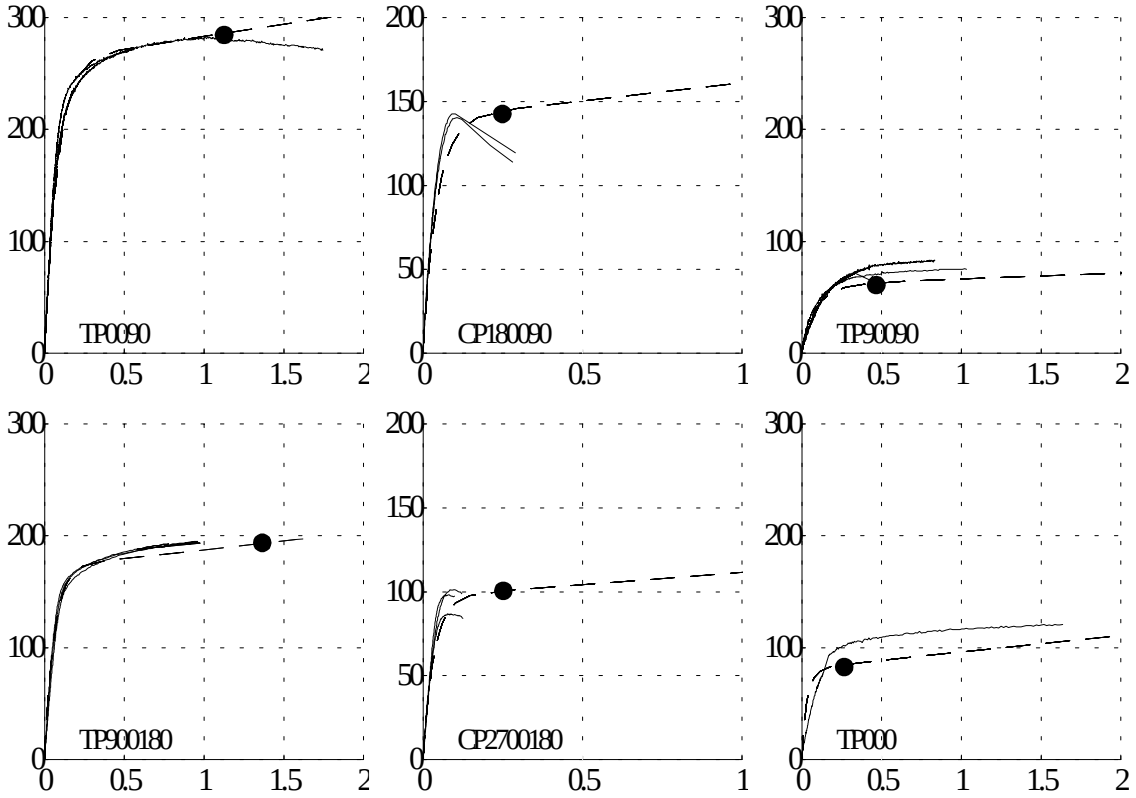

Figure 3.8. Comparison between TRUSSLAB calculations and results from the six basic tests for the GNA20S nail plate.

TRUSSLAB predicts the behaviour of the joints quite well. However, for the two series TP_90_0_90 and TP_0_0_0 where the beams are subjected to shear and bending, TRUSSLAB underestimates the load level where the beams start yielding.

Furthermore, TRUSSLAB is able to predict the load level of plate failure quite well but for the two series TP_90_0_90 and TP_0_0_0, TRUSSLAB underestimates the load level of failure. It should be noted that the test series TP_0_0_90, CP_180_0_90 and CP_270_0_180 are not stopped before the ultimate load is reached.

3.2 Comparison of Plate Test Results with TRUSSLAB Calculations and Eurocode 5

Besides the six basic tests, 32 test series with three identically specimens in each series have been produced and tested to verify the theory of the plate element.

Comparisons between the test results and results and predictions given by TRUSSLAB and Eurocode 5 are shown.

3.2.1 Test Series

The specimens are divided into two main groups – one group where the members are subjected to tension, see figure 3.9, and one group where the members are subjected to compression, see figure 3.10. The figures illustrate the orientation of the force and the joint line. The line through the nail plate represents the main direction of the plate. The specimens shown in the figures are not in scale.

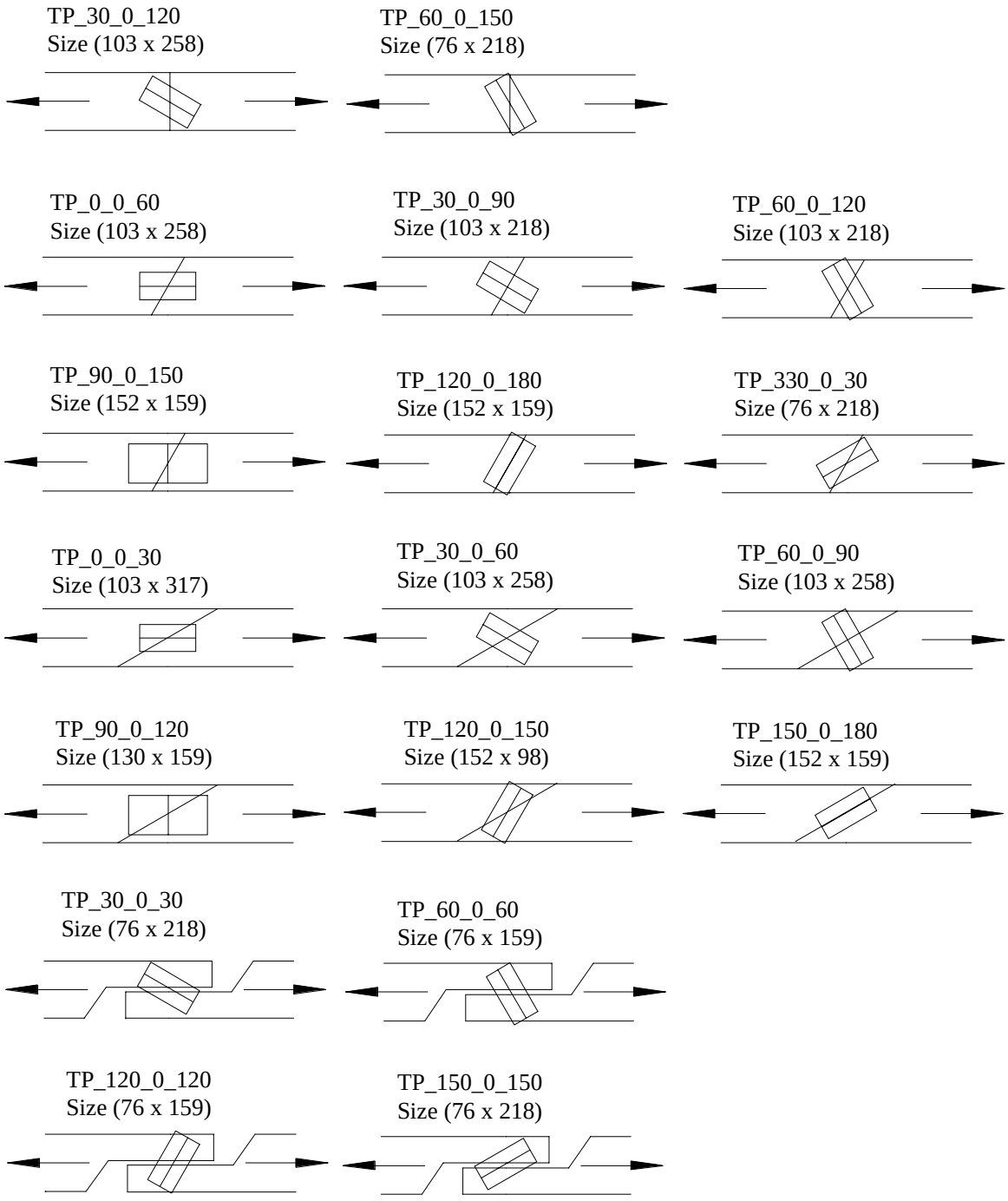

Figure 3.9. Test specimens subjected to tension. Plate sizes in mm (length of the plate perpendicular to the main direction x length of the plate main direction).

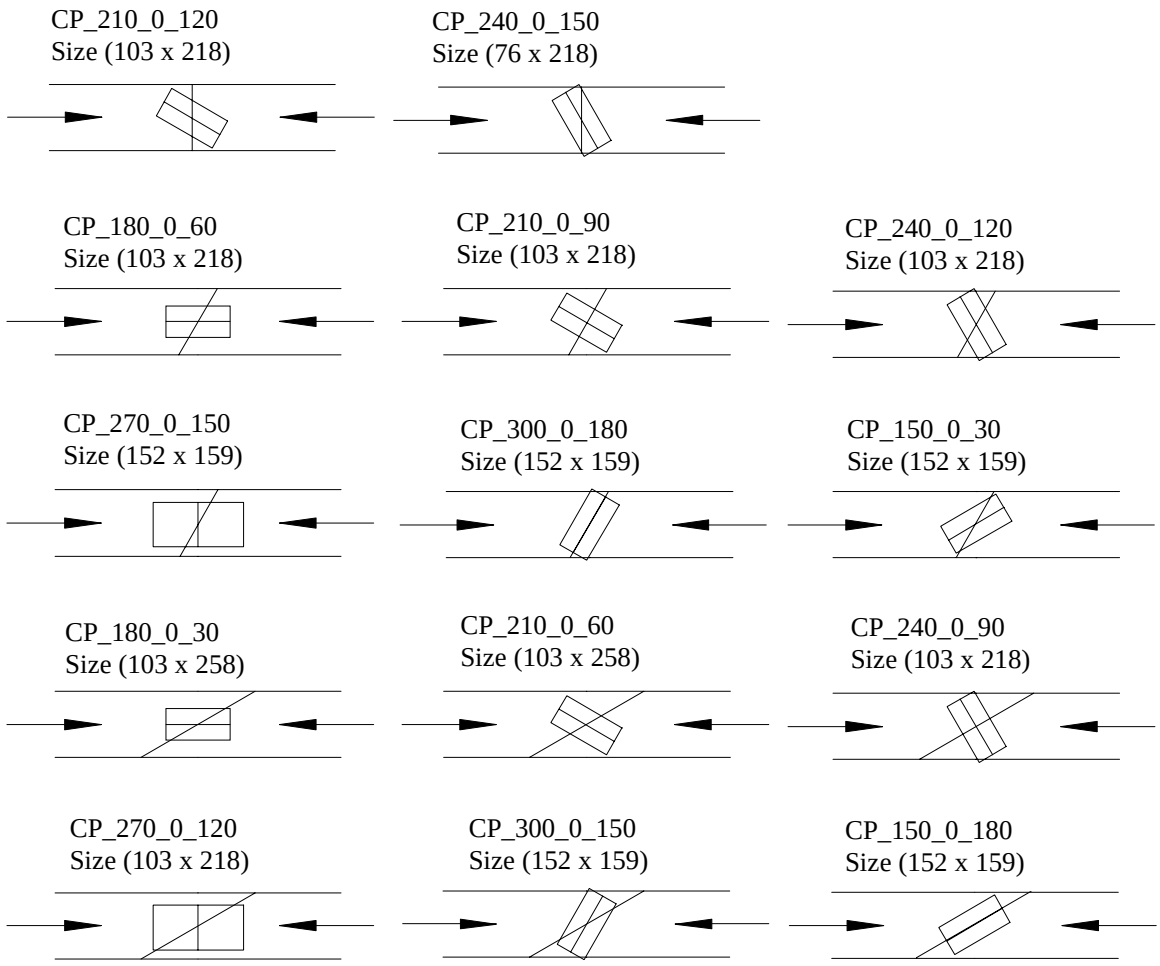

Figure 3.10. Test specimens subjected to compression. Plate sizes in mm (length of the plate perpendicular to the main direction x length of the plate main direction).

All the specimens have a gap of 5 mm between the timber parts to avoid contact. No nails have been removed. The sizes of the nail plates are chosen in order to achieve plate failure and the nail plates are located so that the centre of each nail plate is placed at the centre of the joint line. In the series TP_60_0_150, TP_120_0_150, TP_30_0_30 and TP_150_0_150 the nail plate has been weakened in the joint line by cutting a slit in the plate as illustrated in figure 3.11.

Tests with these four series - with uncut nail plates - have been performed earlier. In these tests anchorage failure was observed for the series TP_60_0_150 and a combination of plate buckling and withdrawal of the nails was seen in the test series TP_120_0_150, TP_30_0_30 and TP_150_0_150. This is also found to be the case for tests performed with other types of nail plates, see e.g. *Lau, P. W. C. (1987).*

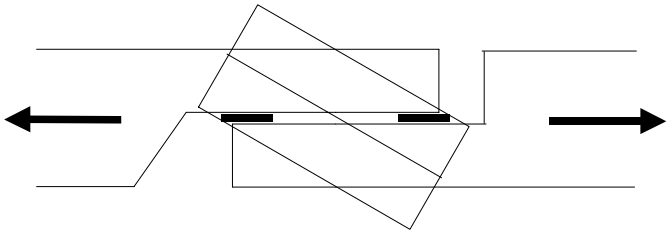

Figure 3.11. Cutting slits in the nail plate to avoid anchorage failure.

The nail plate should not be weakened according to *EN 1075 (1999).*

3.2.2 Comparison of Load-displacement Curves from Tests with TRUSSLAB Calculations

The load-displacement curves for the different tensile tests and results from similar TRUSSLAB calculations are shown in figure 3.12 on page 53. The series are arranged in the same order as in figure 3.9. The force transformed to N per mm of plate along the joint line is shown vertically and the displacement in mm is shown horizontally.

The solid lines represent the test results. Each of the solid lines is an average of the displacement transducer on either side of the test specimen. For some of the series there is only one solid line, which means that only one of the three test specimens in the series has been tested. Again it is noted that some of the tension tests are stopped before the ultimate load is reached.

The dashed lines are the results from calculations in TRUSSLAB and the dots indicate the load level of plate failure predicted by TRUSSLAB.

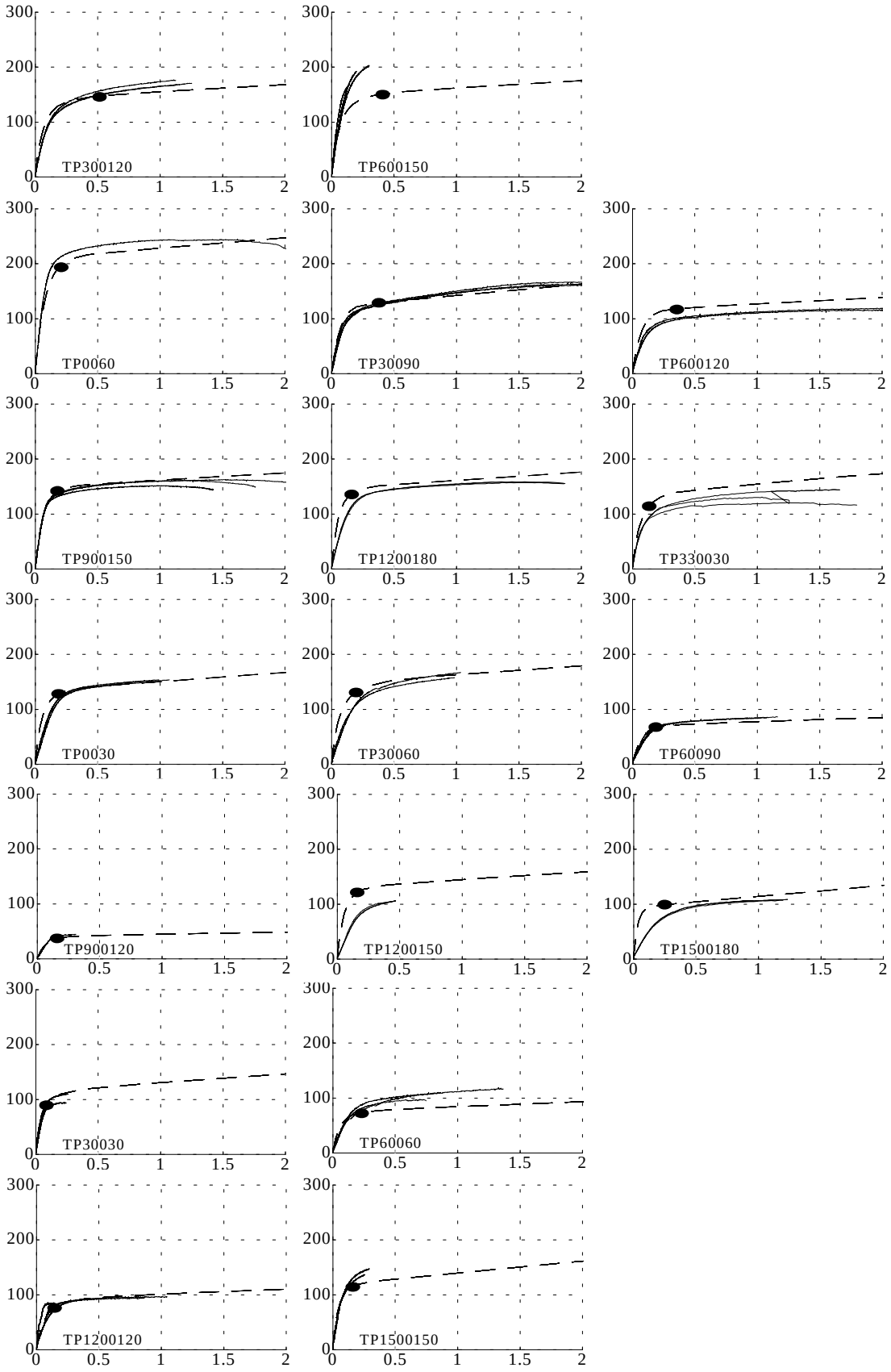

Figure 3.12. Load-displacement curves for the tensile tests.

From the figure it is seen that TRUSSLAB for most of the series is able to predict the load level where the plate starts its plastic behaviour. TRUSSLAB is capable of predicting the initial stiffness as well, but for some of the series the initial stiffness is overestimated by TRUSSLAB (e.g. TP_150_0_180). Furthermore, the load level of plate failure is predicted relatively well by TRUSSLAB.

The test results in figure 3.12 indicate that most of the test specimens have reached a load level where the load is only increasing very slowly with increasing deformation. Therefore, it is estimated that the ultimate load is relatively close to the load level where the tests are stopped.

Figure 3.13 shows two rather complicated failure modes for the test series TP_30_0_120 and TP_60_0_150. The load-displacement curves for these two test series are shown in figure 3.12 at the top.

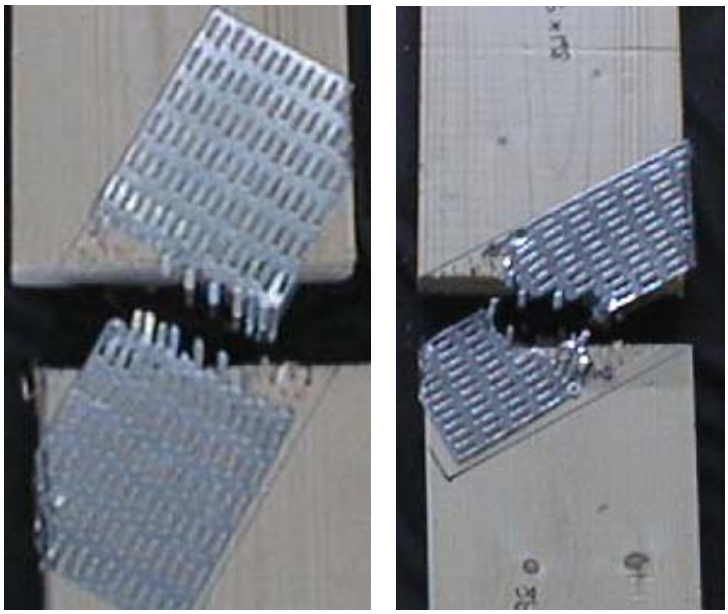

Figure 3.13. Failure modes for the test series TP_30_0_120 and TP_60_0_150.

In the plate element it is assumed that the deformations and failure occur in the joint line, which is not always true as can be seen in figure 3.13. For the series TP_60_0_150 (shown to the left in figure 3.13) TRUSSLAB underestimates the load level where yielding occurs.

It should be noticed that there is only a little variation between the three curves within each of the test series.

Figure 3.14 illustrates the load-displacement curves for the compression tests and the dashed lines show the corresponding results from TRUSSLAB, where a dot indicates plate failure. Again the force per mm of plate over the joint line is shown vertically and the displacement is shown horizontally.

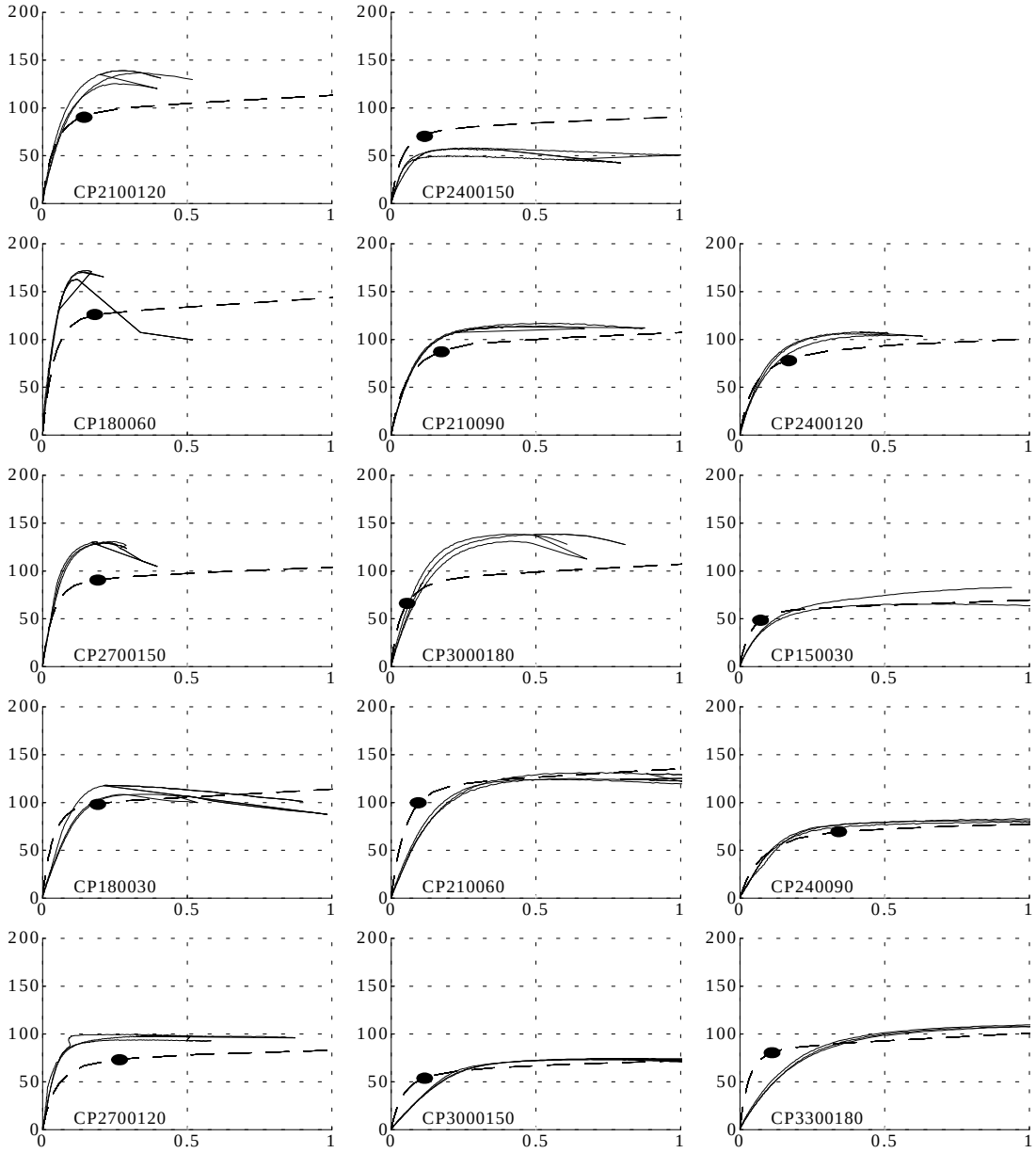

Figure 3.14. Load-displacement curves for the compression tests.

For the compression series the results from the calculations in TRUSSLAB are not as close to the test results as they are for the tensile test series. This may be caused by the fact that the load level where the nail plate starts buckling is dependent on the location of the nails near the joint line. In some of the series the nails are located close to the joint line in such a way that the plate can carry more load - compared with the results from TRUSSLAB - before it starts buckling. In other series the opposite situation may occur. Furthermore, the size of the gap between the timber members may have an influence on the load level where the plate starts buckling.

In some of the compression tests the plate buckling does not follow the joint line, see figure 3.15.

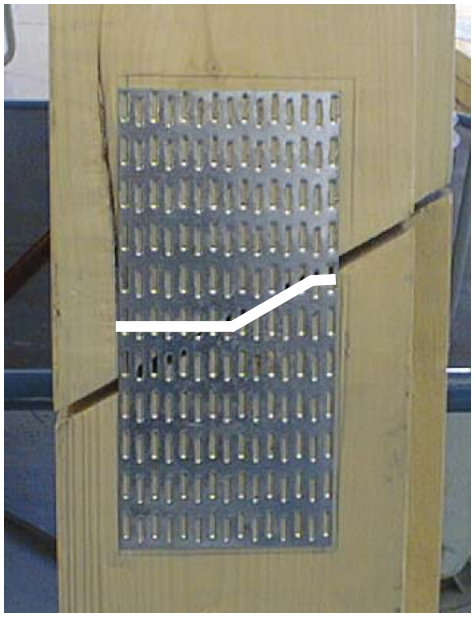

Figure 3.15. Compression test where buckling did not follow the joint line.

TRUSSLAB is not able to predict such kind of buckling because the deformations of the plate element are assumed to follow the joint line.

3.2.3 Comparison of Ultimate Loads from Tests with Eurocode 5 and TRUSSLAB

In 1981 Norén presented a theory for the plate capacity, see *Norén, B. (1981)*. In 1985 Bovim and Aasheim - *Bovim, N. I. & Aasheim, E. (1985)* - compared results from this theory with test results for one specific type of nail plate. They found that the theory given by Norén gave a good prediction of the plate capacity. Aasheim and Solli - *Aasheim, E. & Solli, N. K. (1990)* - made a proposal to implement this design method into Eurocode 5, which was done in the version of the Eurocode in 1993, see *Eurocode 5 (1993).*

Källsner and Kangas - *Källsner, B. & Kangas, J. (1991)* - performed tests with 6 other types of nail plates and compared the results with the theory. It was found that for the tension tests the theoretical capacities were mostly rather good. For the shear tests the theoretical values were close to the measured values when the nail plate had a staggered arrangement of nail holes, see figure 3.16 a). However, when the nail plate had an orthogonal nail hole line situation, as shown in figure 3.16 b), the theory overestimated the shear capacity when the angle α was about 30° and 135° and underestimated the shear capacity when α was in the range from 45° to 90°.

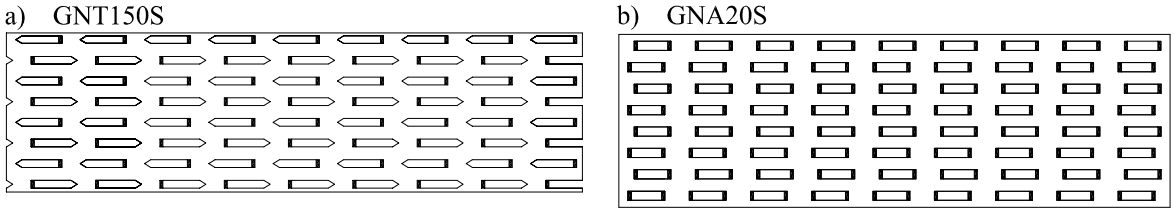

Figure 3.16. a) Staggered arrangement of nail holes. b) Orthogonal arrangement of nail holes. The difference between the two types of nail plates may be even more well-defined than shown in the figure.

Based on that, Kevarinmäki and Kangas suggested a modified design method with two modification factors used to make these estimations more accurate when nail plates with an orthogonal arrangement of the nail holes are considered, see *Kevarinmäki, Ari & Kangas, J. (1995)* or *Kevarinmäki, Ari (2000)*. This modified design method is implemented into a final draft of the Eurocode 5 from 2001, see *Eurocode 5 (2001)*. In this final draft of Eurocode 5 it is suggested to use the method for both nail plates with a staggered arrangement as well as nail plates with an orthogonal arrangement of the nail holes.

The two design methods are described in the following.

Plate Capacity According to Eurocode 5 from 1993

The nail plate is subjected to a force *F* and a moment *M*, see figure 3.17.

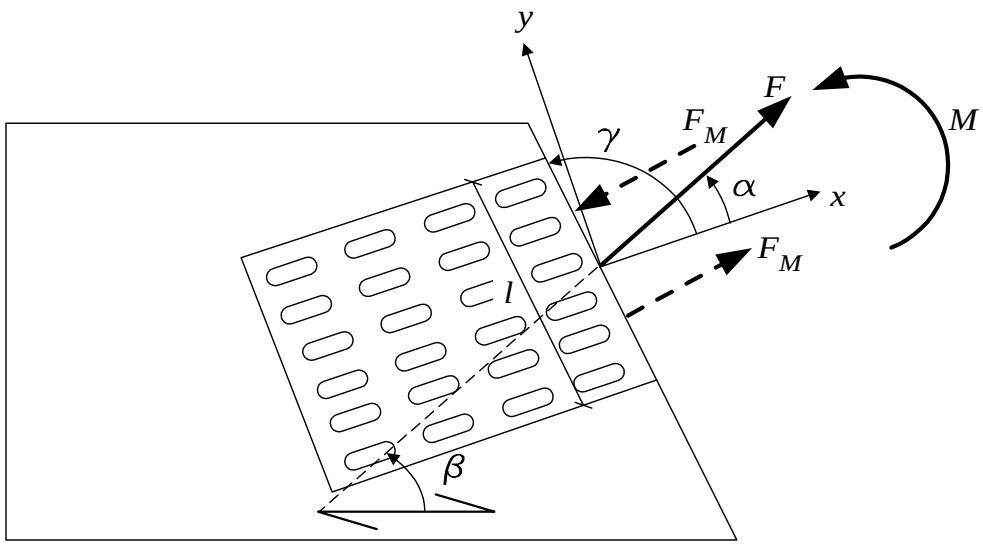

Figure 3.17. Geometry of a nail plate loaded by a force F and a moment M.

The force F_x in the plate main direction (*x*) and the force F_y in the direction perpendicular to the main direction (*y*) are determined by:

$$F_x = F\cos(\alpha) \pm 2F_M \sin(\gamma) \tag{3.5}$$

$$F_y = F\sin(\alpha) \pm 2F_M \cos(\gamma) \tag{3.6}$$

where F_M is given by the plastic assumption:

$$F_M = 2\frac{M}{l} \tag{3.7}$$

The forces F_x and F_y should satisfy the condition:

$$\left(\frac{F_x}{R_x}\right)^2 + \left(\frac{F_y}{R_y}\right)^2 \le 1 \tag{3.8}$$

where R_x and R_y are the strength values of the plate capacity in the *x* and *y* directions, respectively. R_x and R_y are determined by:

$$R_x = \max\begin{cases} f_{n,0} l \sin(\gamma) \\ f_{v,0} l \cos(\gamma) \end{cases} \qquad f_{n,0} = \begin{cases} f_{t,0} \ if \ F_x > 0 \\ f_{c,0} \ if \ F_x \le 0 \end{cases} \tag{3.9}$$

$$R_y = \max\begin{cases} f_{n,90} l \cos(\gamma) \\ f_{v,90} l \sin(\gamma) \end{cases} \qquad f_{n,90} = \begin{cases} f_{t,90} \ if \ F_y > 0 \\ f_{c,90} \ if \ F_y \le 0 \end{cases} \tag{3.10}$$

In the formulas:

$f_{t,0}$ is the tension strength in the plate main direction $(\alpha = 0^\circ)$
$f_{t,90}$ is the tens. strength perpendicular to the plate main direction $(\alpha = 90^\circ)$
$f_{c,0}$ is the compression strength in the plate main direction $(\alpha = 0^\circ)$
$f_{c,90}$ is the comp. strength perpendicular to the plate main direction $(\alpha = 90^\circ)$
$f_{v,0}$ is the shear strength in the plate main direction $(\alpha = 0^\circ)$
$f_{v,90}$ is the shear strength perpendicular to the plate main direction $(\alpha = 90^\circ)$

Plate Capacity According to the Final Draft of Eurocode 5 from 2001

The difference between this method and the one in the Eurocode 5 from 1993 is the way R_x and R_y are determined:

$$R_x = \max\begin{cases} f_{n,0} l \sin(\gamma - \gamma_0 \sin(2\gamma)) \\ f_{v,0} l \cos(\gamma) \end{cases} \qquad f_{n,0} = \begin{cases} f_{t,0} \ if \ F_x > 0 \\ f_{c,0} \ if \ F_x \le 0 \end{cases} \tag{3.11}$$

$$R_y = \max\begin{cases} f_{n,90} l \cos(\gamma) \\ k f_{v,90} l \sin(\gamma) \end{cases} \qquad f_{n,90} = \begin{cases} f_{t,90} \ if \ F_y > 0 \\ f_{c,90} \ if \ F_y \le 0 \end{cases} \qquad k = \begin{cases} 1 + k_v \sin(2\gamma) \ if \ F_y > 0 \\ 1 \qquad\qquad\qquad if \ F_y \le 0 \end{cases} \tag{3.12}$$

The value of γ_0 is determined from shear tests with $\alpha = \gamma = 30^\circ$ and the value of k_v is determined from two shear tests in the range $45^\circ \le (\alpha = \gamma) \le 85^\circ$. The values are determined so the left side of formula (3.8) is equal to 1. From the test results the value of γ_0 is determined to 13°. The value of k_v is determined from only one series of shear tests with $\alpha = \gamma = 60^\circ$ and the value is determined to 0.3.

Plate Capacity in TRUSSLAB

A problem with the above failure conditions arises if the nail plate covers more than one straight joint line. In Eurocode 5 (2001) the following is suggested:

"If the plate covers more than two elements then the forces in each straight part of the connection line should be determined so that the equilibrium is fulfilled and that the condition in 3.8 is satisfied in each straight part."

The condition in 3.8 corresponds to formula (3.8) in this thesis. In TRUSSLAB the plate element is composed of beams with nonlinear material properties. If the nail plate covers e.g. two straight parts the forces at the midpoint of each straight part can be determined from the sectional forces at the ends of the small beams. When more than one joints line is considered it seems, however, that the plate design rules in Eurocode 5 lead to wrong load capacities. To explain this two similar joints, as shown in figure 3.18, are analysed.

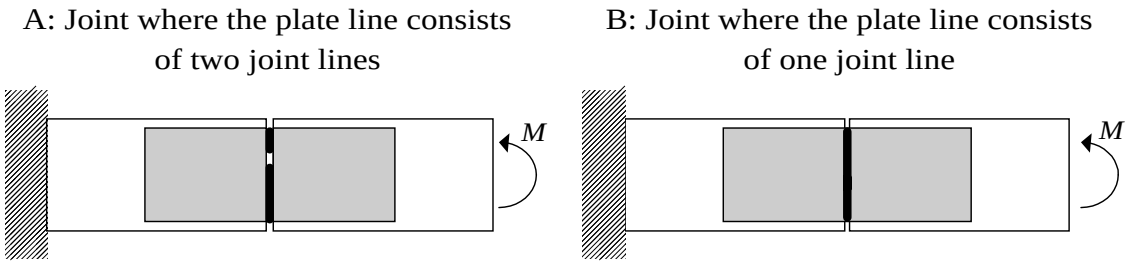

Figure 3.18. Two similar joints where the expressions in Eurocode 5 lead to different load capacities.

In joint type A the nail plate is divided into two straight joint lines, whereas in joint type B the nail plate is treated as one straight line. In practice the joints only cover one line, but could easily be converted to a joint with two straight lines if one of the line parts in joint type A is rotated by a small angle. In TRUSSLAB the nail plates are identical for the two cases A and B.

In order to design the nail plate according to Eurocode 5, sectional forces are to be at the middle of each joint line as shown in figure 3.19. The moment M_1 is smaller than M_2 for two reasons:

1. The lengths of the joint lines are different.
2. The plate becomes plastic in compression at a lower stress level than in tension.

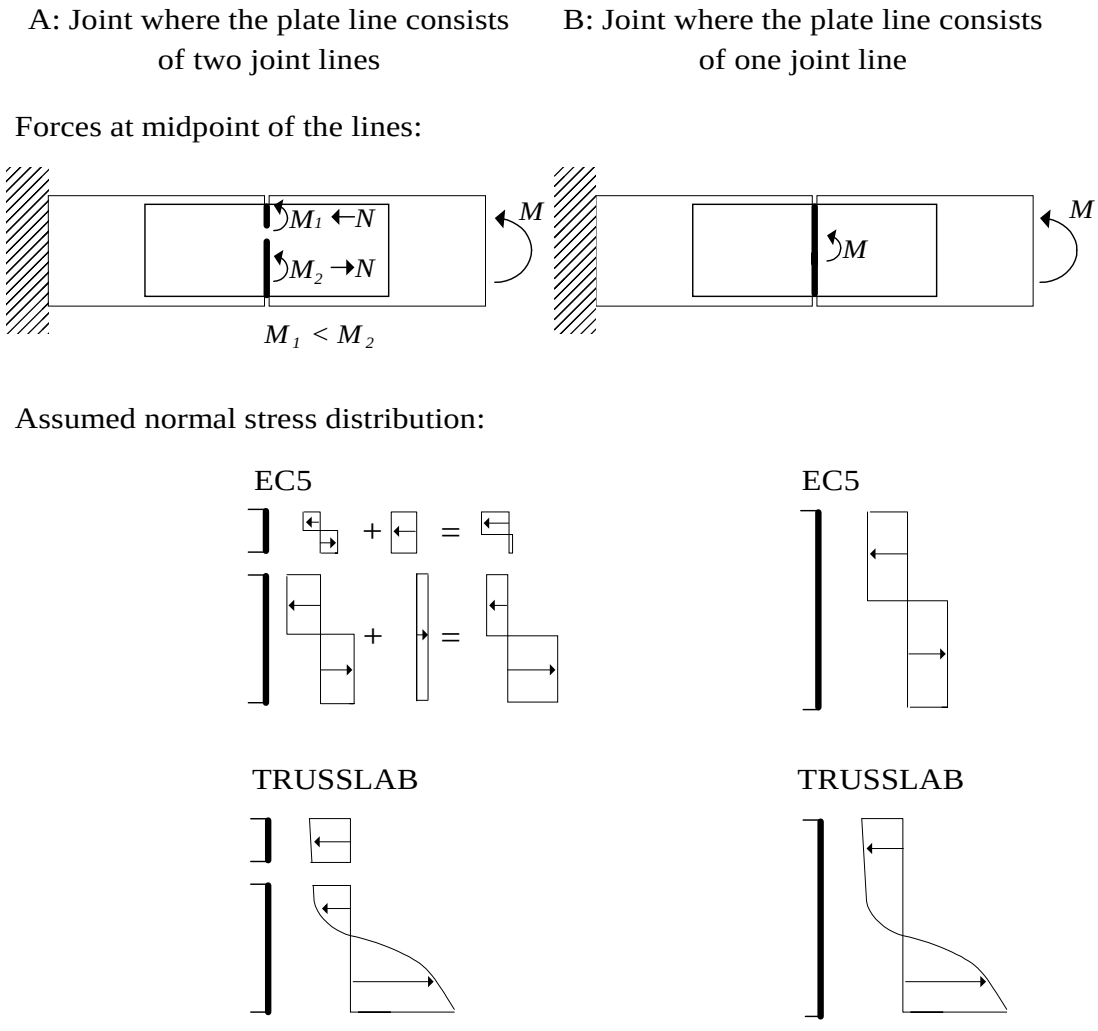

Figure 3.19. Sectional forces and stresses at the middle of each straight part.

From the figures it is seen that the two similar joints are treated differently in Eurocode 5 and a consequence is that the load-carrying capacity of joint type A is approximately 50% less than the load-carrying capacity of joint type B.

In the test series in this chapter the problem described above is non-existing, but for a more complex joint as shown in figure 3.20 the problem will arise. In the figure two possible failure modes in the nail plates are shown with thick lines. It should be noted that the outer leg goes to the top of the rafter.

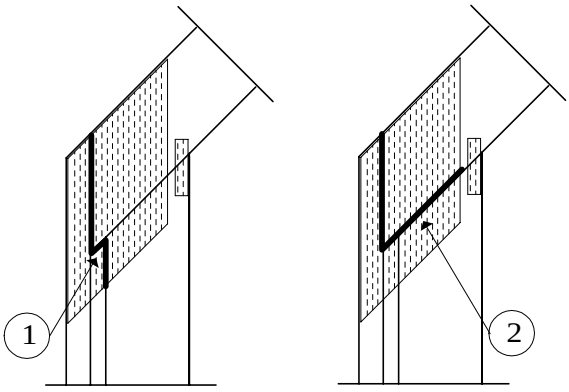

Figure 3.20. Complex joint type where two possible failure modes are shown.

From the calculated sectional forces at each of the midpoints of the straight plate parts 1 and 2, respectively, it is found that plate failure according to Eurocode 5 (2001) arises at an unrealistically low load level for part 1 of the plate. For part 2 of the plate the failure load level according to Eurocode 5 (2001) is significantly higher. However, since part 2 includes part 1 of the plate it seems unrealistic that part 1 fails and part 2 does not fail at the same load level.

Due to the above problems a different method for predicting plate failure has been implemented into TRUSSLAB.

The axial stresses are determined at 5 points at each end of each of the small steel beams – see e.g. section 2.3. The shear stresses are assumed to be equally distributed over the cross-sectional area, see figure 3.21.

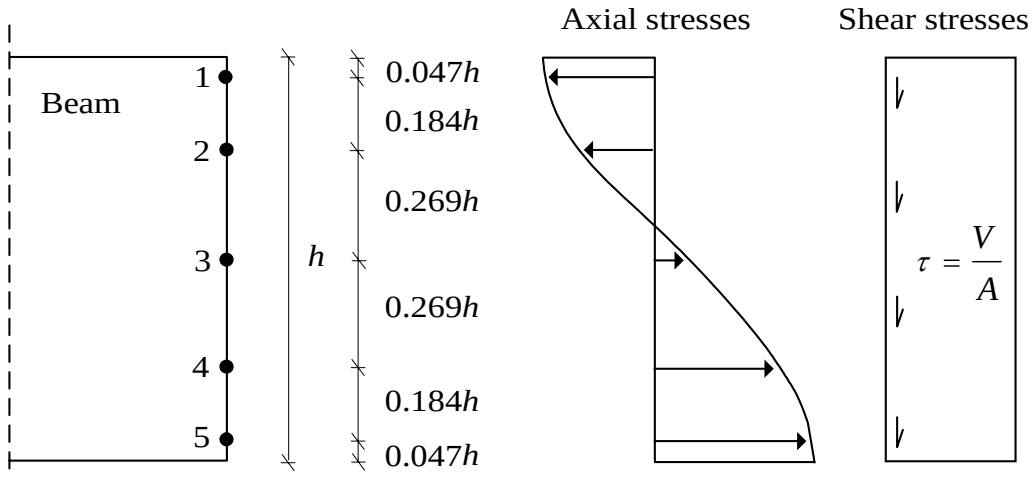

Figure 3.21. Stress distribution at the ends of the small steel beams.

A failure condition could be to check whether the axial stress and the shear stress at each of the 5 points fulfil e.g. v. Mises failure condition. However, in the plate element in TRUSSLAB some assumptions are made:

1) The complicated geometry of a nail plate is converted into a simple model where beam elements are used to connect two nail groups.

2) The beams may have the sizes (length x height) 8x8 mm and 4x12 mm and for the 8x8 mm beams Bernoulli beam theory cannot be used – however, in TRUSSLAB Bernoulli beam theory is used anyway.

3) Prestresses arise due to the production of the nail plates. They influence the stress distribution in the nail plate and this is not taken into account in TRUSSLAB.

4) The deformations at the ends of the beams are calculated from the deformations at the centre of the nail groups (the nail groups are assumed to perform stiff-body movements).

These assumptions may be the explanation why a failure check as that mentioned above will result in ultimate load levels that are not equal to the ultimate load levels achieved by testing.

Different failure conditions have been implemented and tested in TRUSSLAB and the following failure conditions are found to predict the load level of failure relatively precisely:

- At points 2 and 4:

$$\left(\frac{\sigma_x}{\sigma_{u,t}}\right)^2 \le 1 \quad if\ \sigma_x \ge 0$$

$$\left(\frac{\sigma_x}{\sigma_{u,c}}\right)^2 \le 1 \quad if\ \sigma_x < 0$$

- At point 3:

$$\left(\frac{\sigma_x}{\sigma_{u,t}}\right)^2 + \left(\frac{\tau}{\tau_u}\right)^2 \le 1 \quad if\ \sigma_x \ge 0$$

$$\left(\frac{\sigma_x}{\sigma_{u,c}}\right)^2 + \left(\frac{\tau}{\tau_u}\right)^2 \le 1 \quad if\ \sigma_x < 0$$

The fact that the stresses at points 1 and 5 are not used in a failure check means that yielding in the outer fibres of the steel beams are allowed. Furthermore, the shear stresses in the failure check at points 2 and 4 are not included.

$\sigma_{u,t}$, $\sigma_{u,c}$ and τ_u are ultimate stresses in tension, compression and shear, respectively. The values of $\sigma_{u,t}$, $\sigma_{u,c}$ are determined from the basis tests and the value of τ_u is determined from calibration to the basic test where the beams are subjected to both moment and shear forces at the beam ends. The values are determined for both types of steel beams (beams parallel to the main direction of the nail plate and beams perpendicular to the main direction of the nail plate). For the nail plate type GNA20S the values are shown in table 3.2.

	$\sigma_{u,t}$ [N/mm^2]	$\sigma_{u,c}$ [N/mm^2]	τ_u [N/mm^2]
Beams parallel to the main direction	488	250	300
Beams perpendicular to the main direction	483	250	430

Table 3.2. Ultimate stresses for GNA20S used in TRUSSLAB as failure conditions for the plate element.

Comparison

Comparisons between ultimate loads from the test results, the predictions given by TRUSSLAB and the design methods given in Eurocode 5 (1993) and Eurocode 5 (2001) are shown in the figures 3.22, 3.23, 3.24 and 3.25. The values from the test results are the average of the recorded maximum load levels. The predictions given by the equations in Eurocode 5 are based on the test results from the six basic tests.

The results from the tests are indicated by ∗. The results from Eurocode 5 (2001) are shown by a continuous line while the results from Eurocode 5 (1993) are shown by a dashed line. When only a continuous line is shown the results from the two different methods in the Eurocodes are identical.

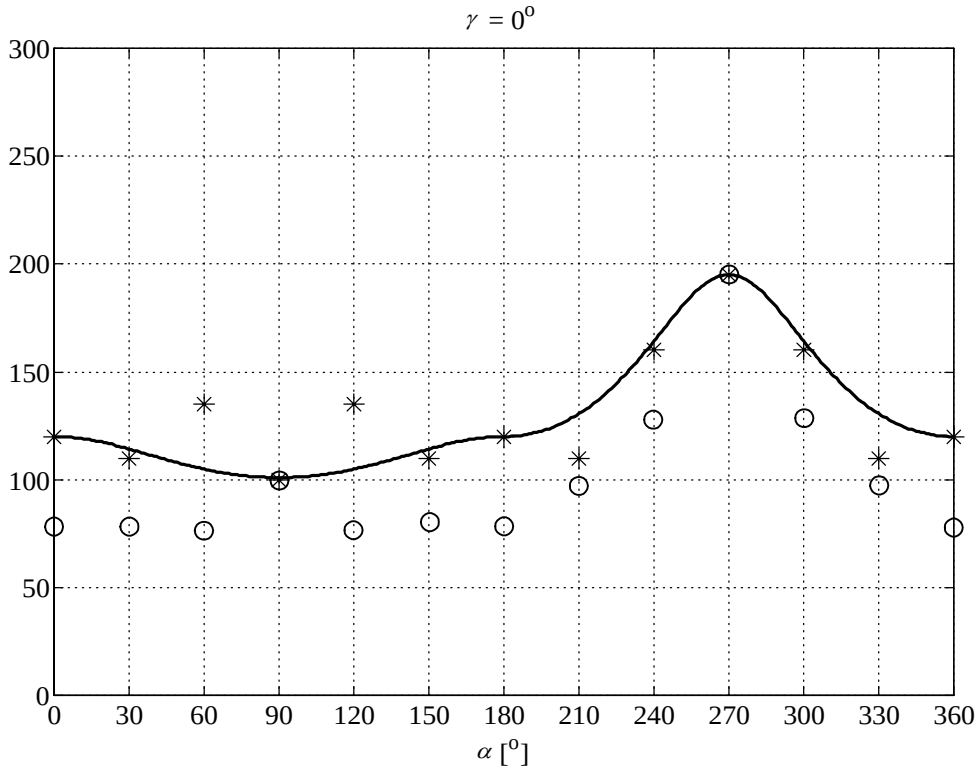

Figure 3.22. Comparison between tests (∗), TRUSSLAB (o) and Eurocode 5. The load is shown on the vertical axis in N/mm along the joint line.

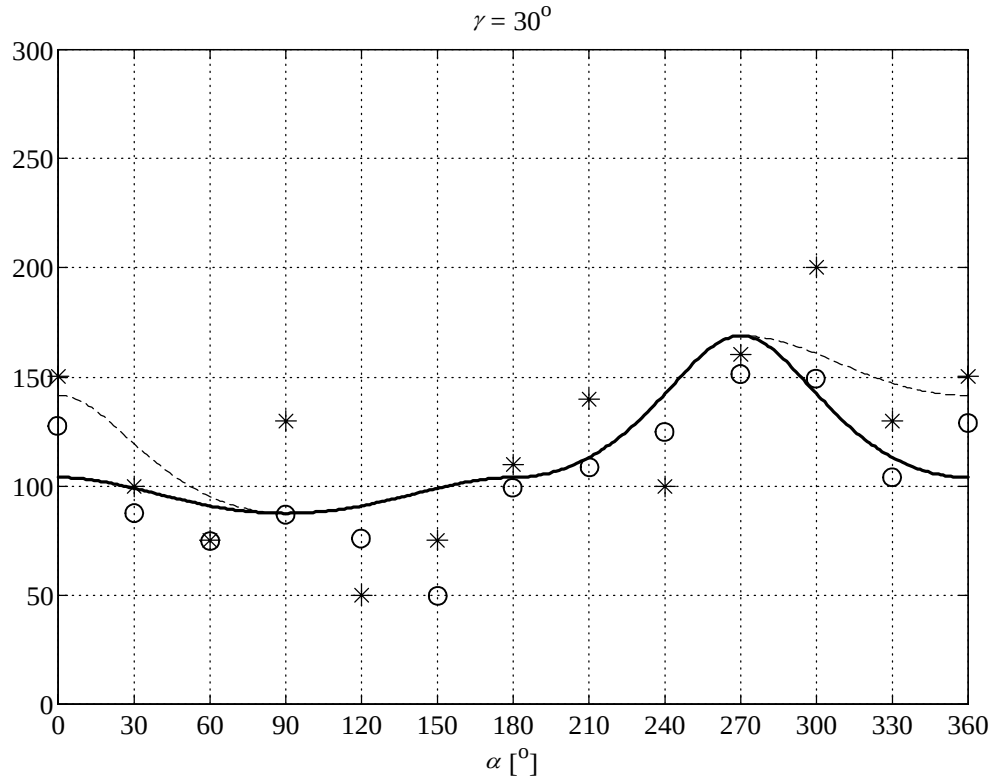

Figure 3.23. Comparison between tests (∗), TRUSSLAB (o) and Eurocode 5. The load is shown on the vertical axis in N/mm along the joint line.

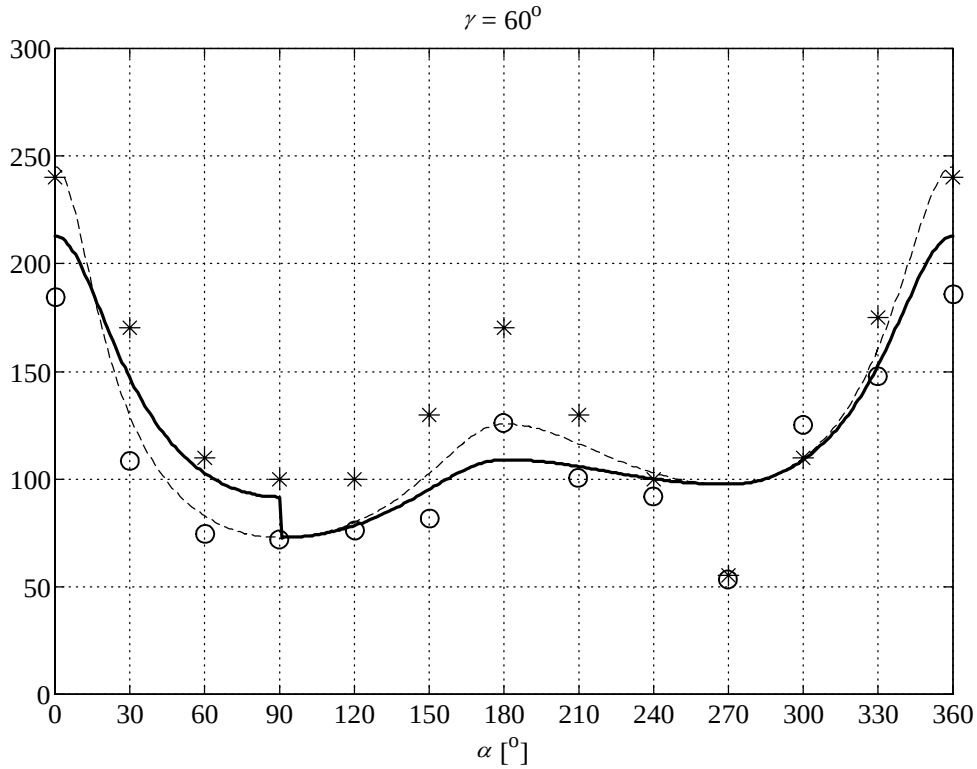

Figure 3.24. Comparison between tests (∗), TRUSSLAB (o) and Eurocode 5. The load is shown on the vertical axis in N/mm along the joint line.

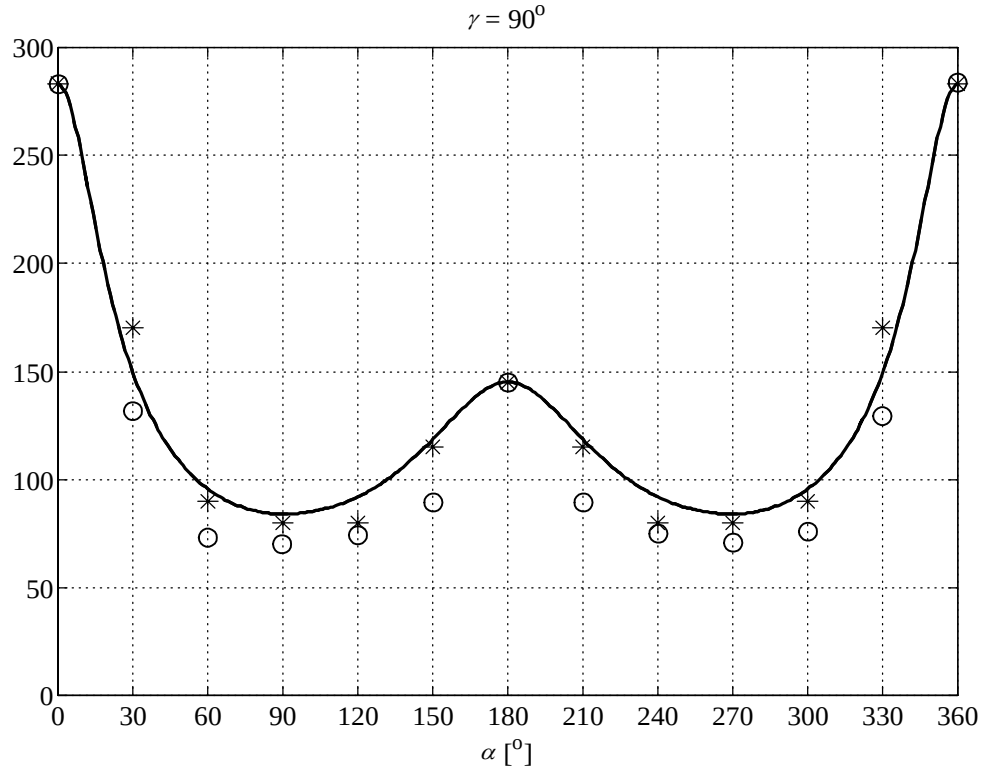

Figure 3.25. Comparison between tests (∗), TRUSSLAB (o) and Eurocode 5. The load is shown on the vertical axis in N/mm along the joint line.

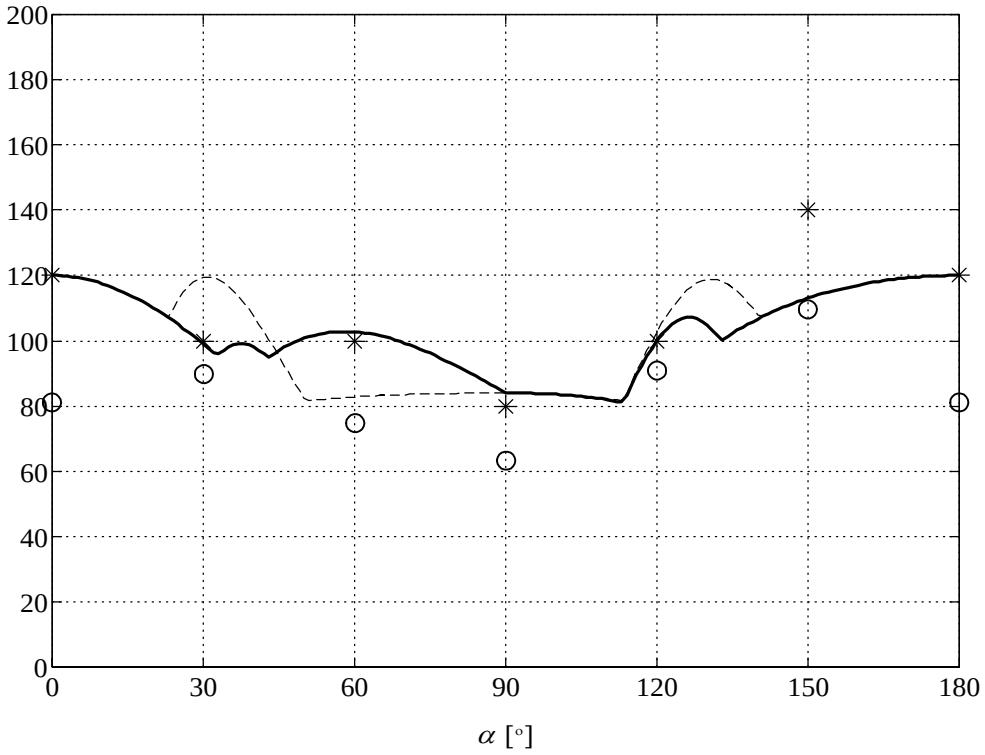

Figure 3.26. Shear tests with $\alpha = \gamma$. Tests (∗), TRUSSLAB (o) and Eurocode 5. The load is shown on the vertical axis in N/mm along the joint line.

For most of the cases the methods given in Eurocode 5 give a good prediction of the plate capacities for different angles of α and γ. In figures 3.23 and 3.24 it seems that the 1993 version of the Eurocode gives a better estimate of the plate capacity compared with the final draft from 2001.

From figure 3.26 with all the shear tests it is seen that the final draft of Eurocode 5 is better in estimating the plate capacity compared with the version from 1993. It is seen how the use of the two additional parameters results in decrease of the plate capacities in the area around $\alpha = \gamma = 30^\circ$ and 135° and increase of the plate capacities, when $45^\circ \le (\alpha = \gamma) \le 90^\circ$.

When comparing the estimated plate capacities from Eurocode 5 with the test results it seems that Eurocode 5 gives a relatively good estimate of the plate capacity. In several cases the predictions given by Eurocode 5 give higher ultimate loads than those found from the tests. The predicted ultimate loads given by TRUSSLAB are always lower than the results from the tests, but in general relatively close to the test results.

3.3 Conclusions on the Plate Capacities

TRUSSLAB is able to predict the stiffness for most of the test series. When comparing the load levels where TRUSSLAB predicts yielding or buckling with the test results, it is seen that TRUSSLAB is able to predict the load level relatively

precisely, even though TRUSSLAB is better at predicting yielding in tension than at predicting buckling when the plate is subjected to compression.

For structural safety reasons it is assumed that it is more important that TRUSSLAB is better at predicting tension than compression. This is because in most practical situations there are timber members to transfer contact forces if the plate starts buckling earlier than predicted, while no structural member can transfer additional forces if the plate fails in tension (consider e.g. a heel joint of a truss). However, to get a precise description of the behaviour of joints with nail plates it is important to have a model that can predict plate buckling.

When planning the tensile tests (in order to get the plate properties) special care can be taken to avoid anchorage and timber failure before the plate has started yielding/failing. This can be ensured if a larger nail plate is used and if this nail plate is weakened in the joint line by cutting in the plate as shown previously in figure 3.11. It may, however, be discussed if this should be done or not. In practical situations the nail plates are not cut and since TRUSSLAB is developed to reflect the behaviour of practical joints it seems illogic that the nail plates were cut. However it seems impossible to design a test specimen for TP_60_0_150 where anchorage failure is avoided without cutting in the plate.

The nail plates are uncut in the six basic test series used to determine the plate properties for the plate element in TRUSSLAB.

Screws have in some cases been used to increase the anchorage capacity in order to avoid anchorage failure. The screws are normally located as far from the joint line as possible to assure that they do not influence the plate capacity. For the series TP_60_0_150 the screws are placed close to the joint line, which may have an impact on the failure mode and on the plate capacity, since the screws are located in the area that is considered to belong to the plate element.

From comparisons between ultimate loads from the test results and from the predictions given by Eurocode 5 it is found that both of the methods given in the 1993 version of the Eurocode 5 and in the final draft from 2001 give a good estimate of the plate capacities for this specific type of nail plate.

In general the predicted ultimate loads given by TRUSSLAB are lower than those found in the tests. However, they are relatively close to each other in many cases (0%-35%).

Table 3.3 shows the average of the maximum recorded loads per mm of joint line for each of the six basic tests together with the 5-percentile strength achieved from the Danish approval for the MiTek GNA20S nail plate, see *Boligministeriet, Bygge- og boligstyrelsen, MK-Godkendelse, (1994)* and from *TRÆ 31 (1995)*.

The values in table 3.3 for compression strengths – indicated by $^{*)}$ - are given by the Swedish approval *Typgodkännandebevis 1690/87 (2001)* due to the fact that these values do not occur in the Danish approval.

	$f_{t,0}$	$f_{c,0}$	$f_{t,90}$	$f_{c,90}$	$f_{v,0}$	$f_{v,90}$
MK-approval (5-percentile)	268	109*)	174	88*)	89	89
Test results (mean values)	283	145	195	101	120	84

*Table 3.3. Test results versus MK-approval. Units in N/mm. The values indicated by *) are from the Swedish approval.*

In all cases but one, the strength values from the tests exceed the values in the approvals. This is probably because the values from the tests are the mean of the recorded maximum values while the values in the MK-approval are the 5-percentile. Anyhow, in *Urfjell, S. B. & Anneling, R. (1991)* it has been shown that tests with nail plates performed at 5 different laboratories can give different results, which might also explain the difference. Normally, there is only a relative small difference between mean values and characteristic values when steel is considered. However, the tests used to determine $f_{t,0}$, $f_{v,0}$ and $f_{v,90}$ are stopped before the ultimate load is reached, but it does not change the fact that the results from the tests give higher strength values compared with the values in the approval.

During the production of the nail plate, the stamping process of the holes introduces a lot of prestresses in the nail plate, which may also affect the test results. TRUSSLAB is not able to deal with these prestresses, which may also explain a difference between the tests results and calculations in TRUSSLAB.

Modification of the test results with regard to the actual thickness of the individual nail plate and the yield strength of the nail plate have not been considered. This is normally done when approvals of nail plates are made.

Due to an assumption that the already performed tests gave some compression load capacities that were too high, additional tests with the two basic test series (CP_180_0_90 and CP_270_0_180) have been performed. Both the MiTek GNA20S and the MiTek GNT150S nail plates were tested. However, in three of the four new test series the load capacities were found to be even higher (up to 50%). A number of different additional tests were performed to find the explanation for this load increasing:

- The gap between the timber members was varied between 2 and 6 mm.
- Different sizes of nail plates were tested to analyse if there could be a size effect.
- Two nail plates located symmetrically on either side and with mutual distance to see if this gave a higher load capacity compared with a centred nail plate on either side, see figure 3.27.
- The nail plates were moved to ensure that the weakest part of the nail plate were located above the joint line, see figure 3.28.

- The side supports were loosened to see if it affected the load capacity.
- Recreation of the previous test specimens with exactly the same sizes and locations of the nail plates was attempted.

However, none of these initiatives could explain the increasing load capacities of the new tests. The only differences from the previous test were:

- The timber members were not conditioned to 85% relative humidity before the test specimens were produced. The tests were carried out right after production. It should, however, not affect the capacity of the nail plate.
- The specimens were not produced at the truss plant, but in the laboratory. The timber members were aligned by a steel beam, and the nail plates were pressed in one at the time.
- The nail plates are produced from different coils in the two test programmes.

The two last-mentioned points are the only explanations found that may cause the higher load capacities. But it seems strange that one of the four series gave results identical with the results from the tests performed earlier.

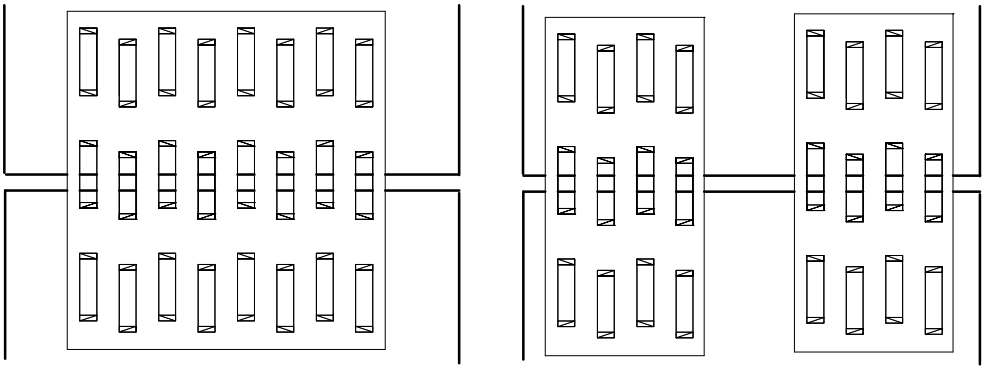

Figure 3.27. Additional test specimen where the nail plate is divided into two nail plates with the same number of steel beams over the joint line. The nail plate is cut to ensure this.

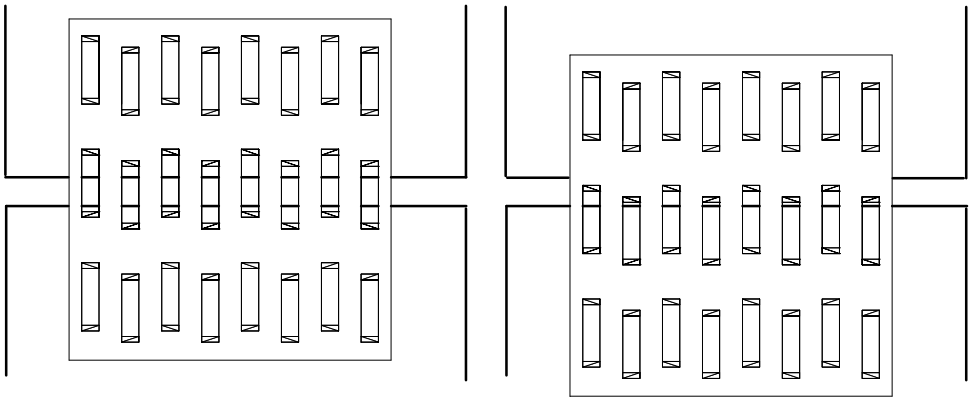

Figure 3.28. Additional test specimen where the nail plate is moved to see the influence on the plate capacity.

3.4 Properties of the Nail Element in TRUSSLAB

The stiffness of a nail group is modelled by a nail element in TRUSSLAB. As input in TRUSSLAB the stiffness parameters of the nails for different combinations of the force, plate and grain direction are needed. In this section the properties needed as input in TRUSSLAB are determined. Furthermore, calculations with TRUSSLAB are compared to test results with the expressions given in the Eurocode 5. For a detailed description of the nail element in TRUSSLAB, see section 2.2.

3.4.1 Basic Tests Used to Determine the Properties of the Nail Element

The four basic test series are shown in figure 3.29. In the basic tests the timber, the force and the nail plate are rotated in steps of 90°. These four tests are suggested by others - see e.g. *Foschi, R. O. (1977)* and *EN1075 (1999)*.

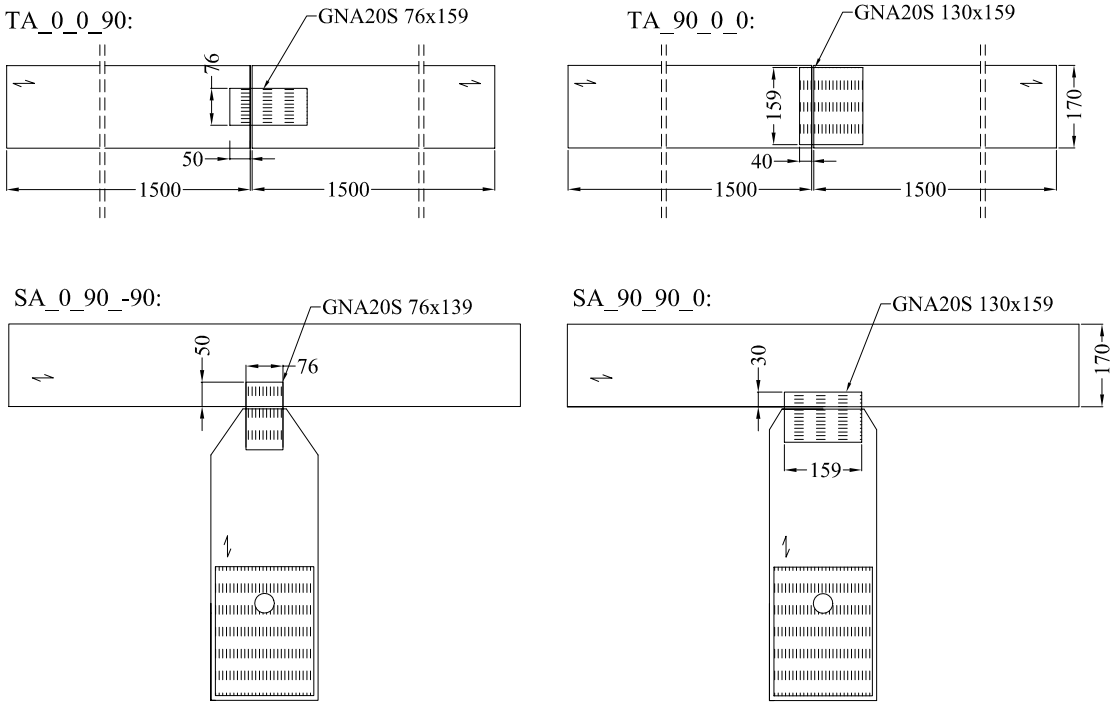

Figure 3.29. Basic test series used to determine the properties of the nail element in TRUSSLAB. The main direction of the nail plate is illustrated by the shading.

The gap between the timber members is 5 mm - *EN1075 (1999)* suggests not less than 2 mm. For each of the four series, 6 specimens have been tested.

The notation of the specimens is SA_α_β_γ (Special test arrangement Anchorage values) and TA_α_β_γ (Tension test arrangement Anchorage values). For a description of the test arrangements, see appendix A and for a definition of the angles α, β and γ, see figure 3.3.

A nail close to the edges of the timber may not carry as much load as a nail located at a distance from the edges. In the test standard *EN 1075 (1999)* it is suggested not

to take the nails into account if they are located at a distance either less than 5 mm from an edge or less than 10 mm in the grain direction from the end of the timber member. This causes an increase in the calculated load capacity of the nails. In this study, however, it is decided that the nails in the edge area can carry a load that should not be neglected because in some of the test series a significant number of nails are located in that area. Furthermore, in *Lau, P. W. C. (1986)* it is shown that a nail with an edge distance of 5 mm has a load capacity of approximately 45% of the full load capacity when the nail is located at a distance of 20 mm to the edge. The tests were performed with the direction of force, the nail plate and the timber similar to the test series named SA_0_90_-90 in figure 3.29. In *Nielsen, J. & Rathkjen, A. (1994)* tests have shown that the full load and stiffness capacity is obtained with nails placed at a distance greater than or equal to 10 mm from the timber edge. These tests were performed with the direction of force, the nail plate and the timber similar to the test series named TA_0_0_90 in figure 3.29.

In the light of the above-mentioned tests it has been chosen to take only half of the total number of nails in the area within 10 mm from the edge into account and these nails are then assumed to be fully active. This is done for all the test series. In general the number of nails is determined for each test specimen by counting before testing.The load-displacement curves for the four basic test series are shown in figure 3.30. The load is converted to N per mm^2 of the anchorage area that is determined from the assumed number of fully active nails. It should be noted that the tests are continued until failure.

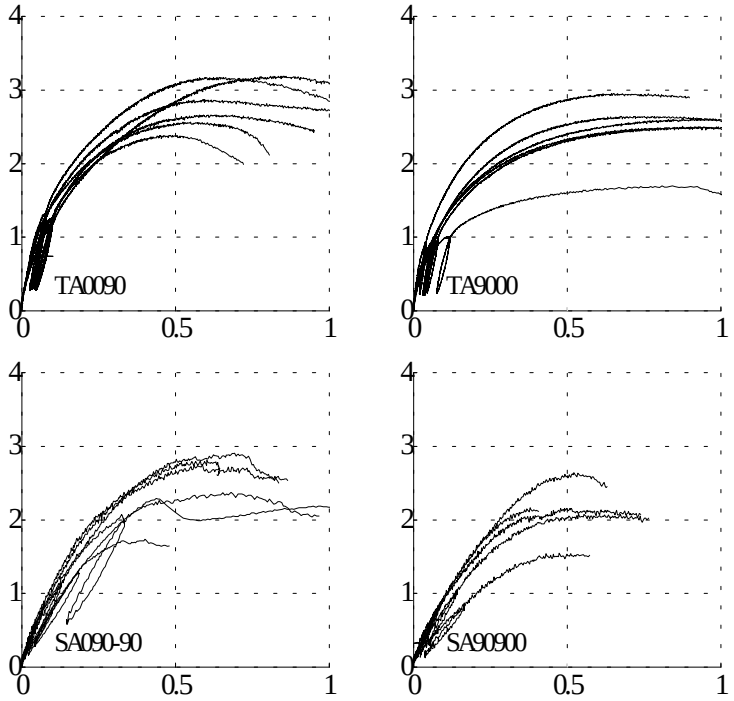

Figure 3.30. Load-displacement curves for the four basic test series used to determine the properties of the nail element in TRUSSLAB. The load is shown vertically in N/mm^2 and the deformation on the horizontal axis in mm.

The three parameters *k*, *kk* and p_0, shown in figure 3.31, have to be determined for each of the four basic test series.

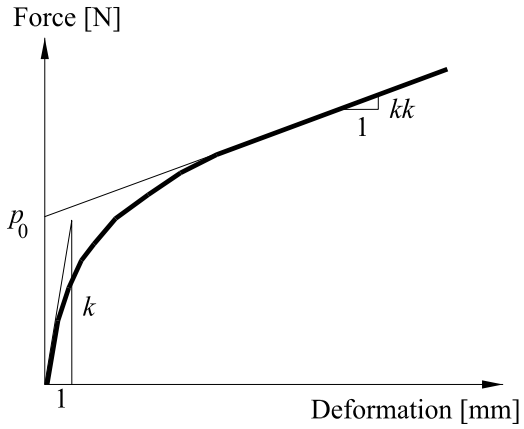

Figure 3.31. Illustration of the three input parameters for each of the four basic test series.

The parameters are determined so the curve drawn using these parameters is some kind of an average of the test results for the current basic test series. Other more refined methods could have been used, but since there is a large variation within the test results for each test series the method used is assumed to be sufficient. In *Wolfe, Ronald W. & McCarthy, Monica (1987)* different methods to determine the parameters have been used and there may be a difference up to 10% of the estimated values depending on the chosen method.

Timber failure, as shown in figure 3.32, occurred in the test series SA_0_90_-90 and SA_90_90_0. The failure in the timber is a kind of splitting. The cracks in the timber do not proceed through the thickness of the beams. The withdrawal of the nails in the upper left-hand corner of the nail plate is a consequence of the splitting in the timber.

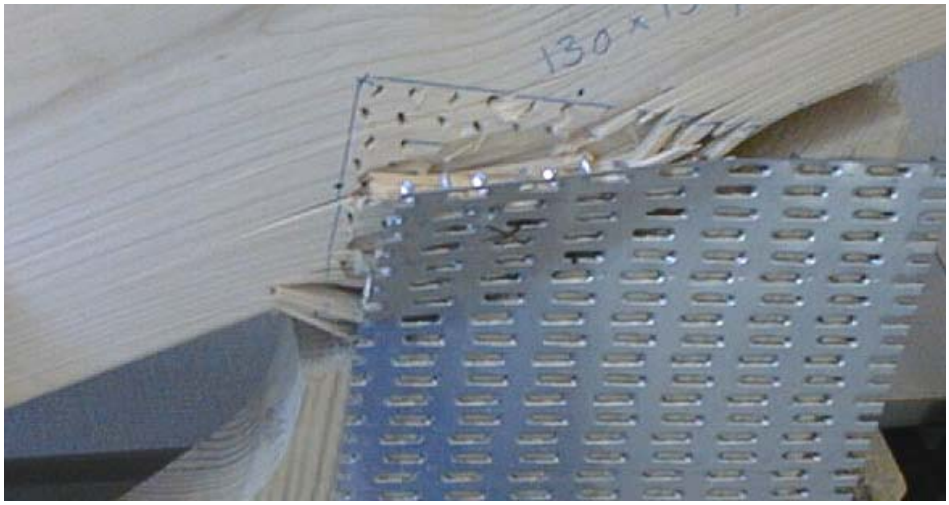

Figure 3.32. Picture of timber failure that occurred in some of the tests used to determine the properties of the nail element.

The failure in the timber occurred in spite of the fact that the edges of the supports were located close to the nail plate. Additional tests have shown that the timber failure can be prevented only by removing some of the nails near the edge and by testing a small number of nails. Figure 3.33 shows test results from the series SA_0_90_-90 and SA_90_90_0 with and without timber failure. The load is converted to one nail.

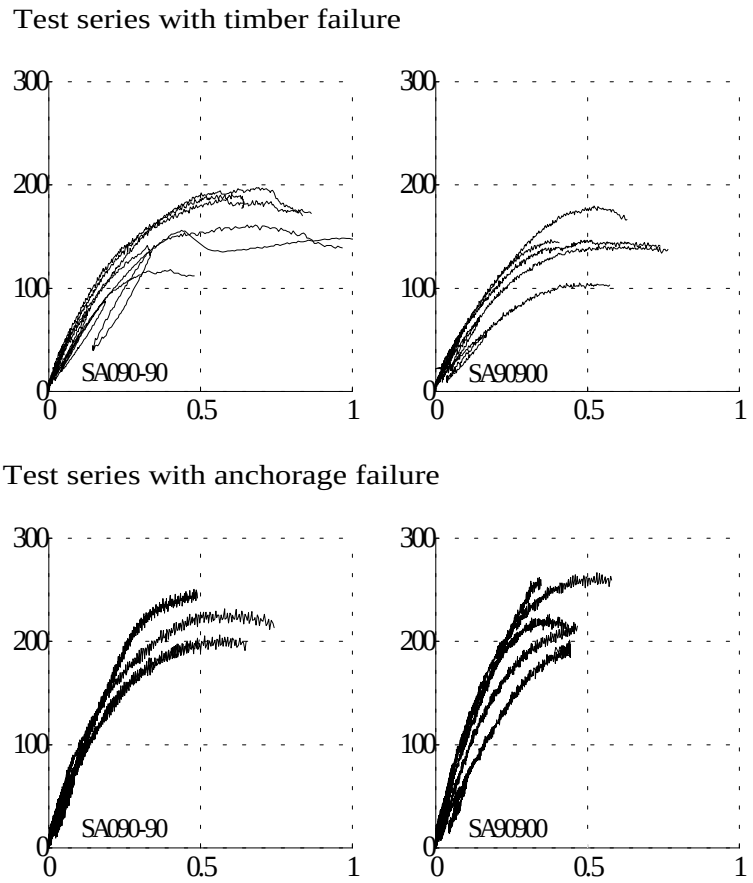

Figure 3.33. Two test series where timber failure occurs, and the same two test series where timber failure are omitted. The load is shown vertically in N/nail and the deformation is shown on the horizontal axis in mm.

As expected the load capacity of the joints is lower when timber failure develops.

In practice and in EN1075 no nails are removed to avoid timber failure in joints with nail plates and, therefore, it seems logic to derive the properties for the nail element from the tests where timber failure occurred.

In *Kevarinmäki, Ari (2000)* it is mentioned that the timber failure described above is often seen when the angle β between the force direction and the fibre direction is different from 0°.

The parameters for the four basic series are listed in table 3.4. The values are given per nail and they are determined from the tests where nothing is done to prevent failure in the timber.

α, β	k [N/mm]	kk [N/mm]	p_0 [N]
0, 0	1200	1	180
90, 0	1000	1	170
0, 90	800	1	180
90,90	700	1	150

Table 3.4. Anchorage parameters for the MiTek GNA20S nail plate. The values are per nail.

The values of *kk* are takes as 1 and not 0 due to the way the calculations are performed in TRUSSLAB. It is chosen to take k as a multiple of 100 and p_0 as a multiple of 10.

A comparison of calculations with TRUSSLAB and the test results from the four basic test series is shown in figure 3.34.

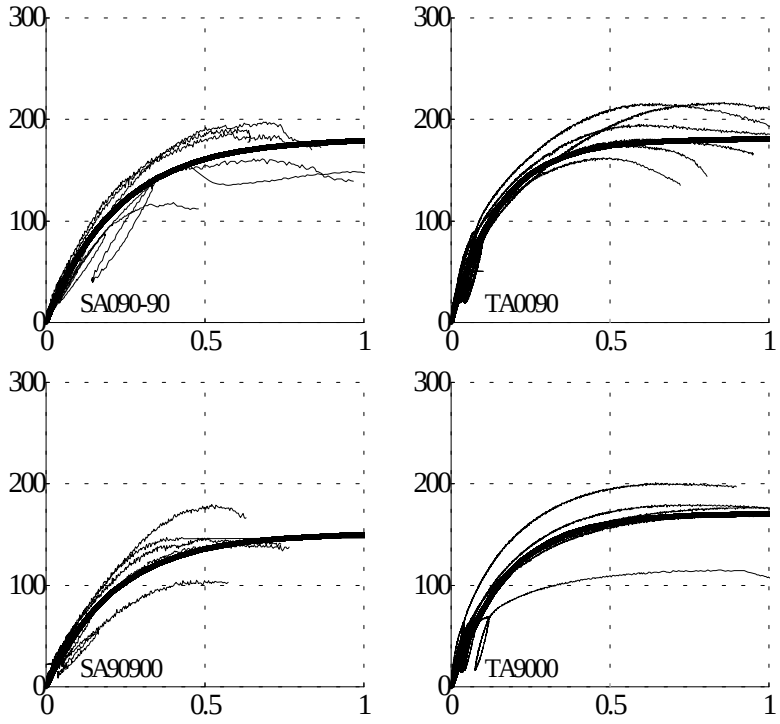

Figure 3.34. Comparison of TRUSSLAB and test results for the four basic test series. The load per nail shown vertically is measured in N, and the displacement shown horizontally is measured in mm.

In figure 3.34 it is seen that TRUSSLAB, with the chosen values for *k*, *kk* and p_0, predicts the average of the load-displacement curves for each of the four basic series.

In *Nielsen, J. & Rathkjen, A. (1994)* a large number of tests have been performed with nail plate type GNA20S in order to analyse the anchorage capacity. Results from three of these are comparable with the test series SA_0_90_-90, TA_0_0_90 and TA_90_0_0 and the average maximum loads per nail for these series are 220 N/nail, 220 N/nail and 140 N/nail, respectively. The corresponding values from the tests in this test programme are 170 N/nail 191 N/nail and 169 N/nail. The difference between the test programmes is up to 30%. In the tests performed by Nielsen and Rathkjen the moisture content in the timber was 11% at the time of production of the test specimens and at the time of testing. At the time the test specimens in this test programme were produced, the moisture content in the timber was 16-18% (according to EN1075).

It should be noted that the results of the tests with anchorage capacities are dependent on the local wood properties.

3.5 Comparison of Anchorage Test Results with TRUSSLAB Calculations and Eurocode 5

In total, 120 tests have been performed including the 24 basic tests. The tests are used to verify the theory behind the nail element in the TRUSSLAB model.

3.5.1 Test Series

The test series are shown in figure 3.35. The moisture content of the timber is in the range 9-12% at the time of testing. The average density of the timber is determined as 470 kg/m^3 when the moisture content in the timber was 14-18%.

The direction of the nail plate, the force direction and the fibre direction are rotated in steps of 30°. The sizes and the location of the nail plates have been chosen so that failure occurs in the desired area (the upper beams in the figure). No nails have been removed.

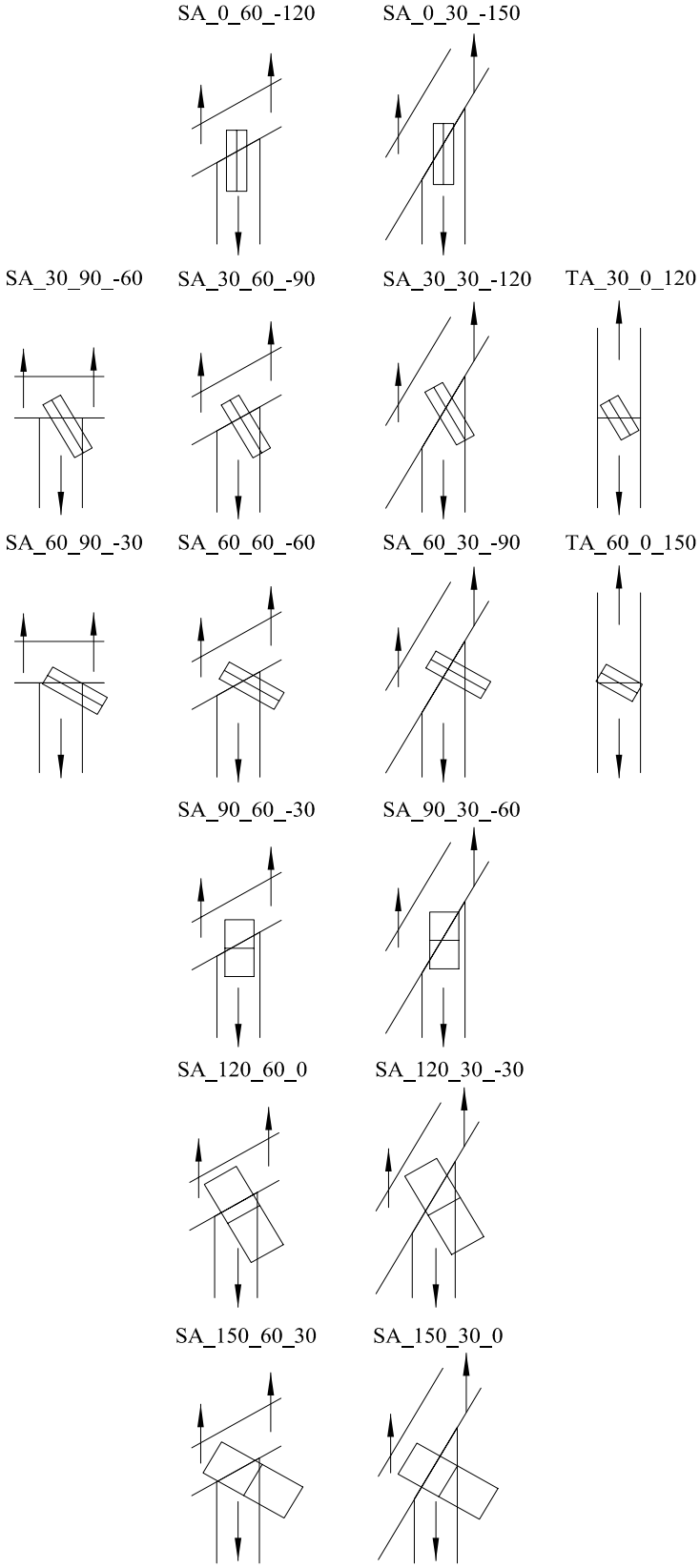

Figure 3.35. Test specimens used to get the load-displacement curves for different combinations of α, β and γ. The figure is not in scale. Nail plate type GNA20S.

3.5.2 Comparison of Load-Displacement Curves from Tests with TRUSSLAB Calculations

The results from the tests are shown in figure 3.36 and the results from calculations with TRUSSLAB are shown as a thick line. The load is shown vertically and is measured in N/nail and the displacement, shown horizontally, is measured in mm. In the figure the specimens are arranged in the same order as in figure 3.35. Again it is noted that the tests are continued until failure.

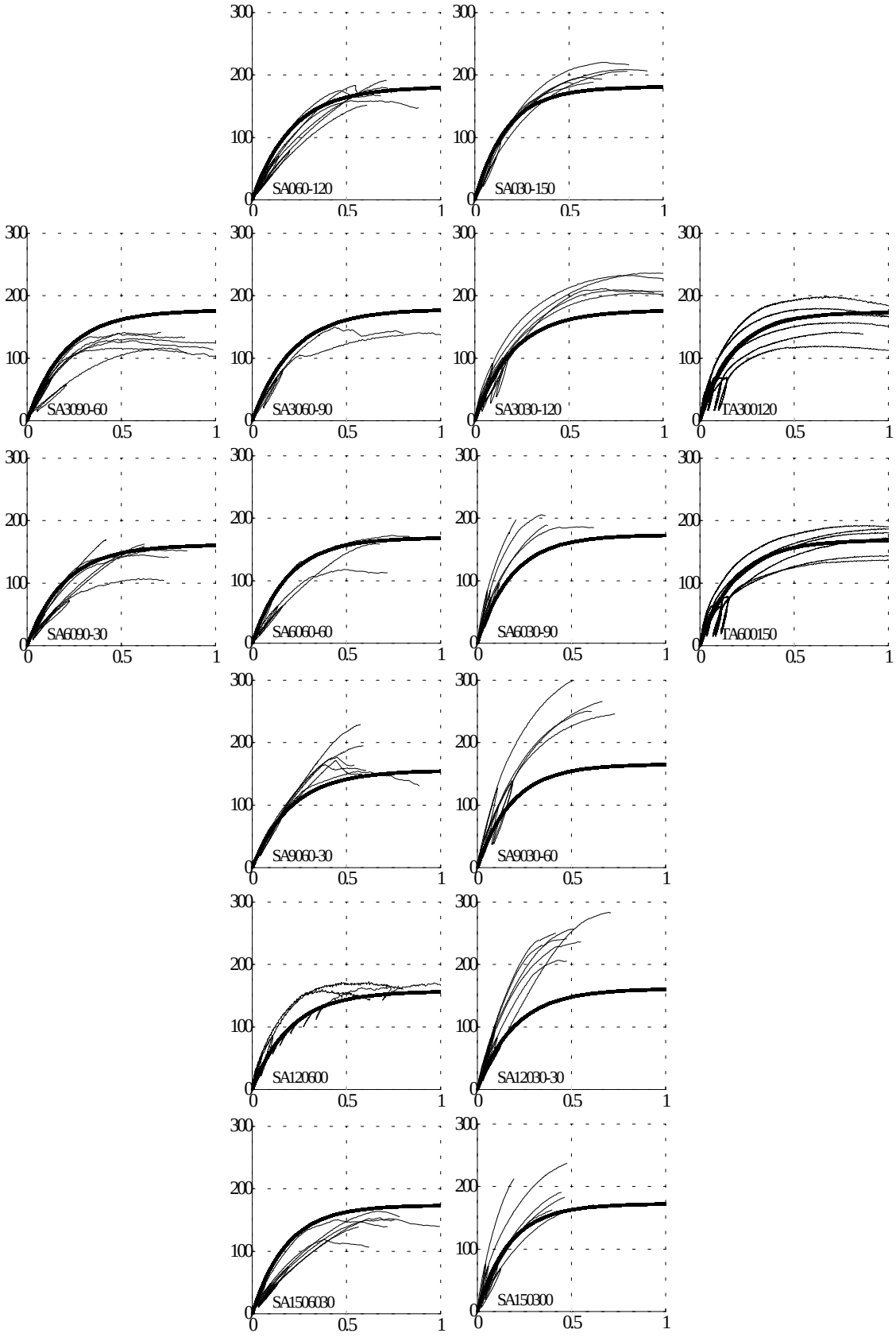

Figure 3.36. Test results versus results from TRUSSLAB calculations.

Timber failures are observed for all of the test series except for the four series where the force direction is parallel to the timber direction (TA_0_0_90, TA_30_0_120, TA_60_0_150 and TA_90_0_0).

For many of the test series there is a big difference between the highest and the lowest ultimate loads, which is caused by the fact that the anchorage capacity is dependent on the properties of the timber. From an analysis of the test results it has been found that a high density of the timber can not always explain a high anchorage capacity but some local properties (e.g. the orientation of the grains or knots in the area where the nail plate is pressed in) of the timber may have an effect. In *Wolfe, Ronald W. & McCarthy, Monica (1987)* it was found that there is no consistent effect of the modulus of elasticity of the timber on the anchorage capacity. A lot of the curves have some jumps in the loads due to suddenly arising cracks in the timber.

When all the factors affecting the anchorage capacity are taken into consideration it is evaluated that TRUSSLAB is able to predict the average load slip behaviour for several of the specimens quite well.

3.5.3 Comparison of Ultimate Load from Tests with Eurocode 5

The test results are compared with results from calculations with the expressions given in Eurocode 5. Simple linear interpolation could have been used between the test results, see *Whale, L. R. J. (1995)*, but Eurocode 5 also contains a presumption, which requires the definition of three constants. The procedure to find these constants is based on the description given in *Whale, L. R. J. (1995).*

Anchorage Capacity According to the Final Draft of Eurocode 5 (2001)

According to the method in Eurocode 5 the anchorage capacity in the grain direction ($\beta = 0^\circ$) is given by:

$$f_{a,\alpha,0} = \begin{cases} f_{a,0,0} + k_1\alpha & for \quad \alpha \le \alpha_0 \\ f_{a,0,0} + k_1\alpha_0 + k_2(\alpha - \alpha_0) & for \quad \alpha_0 < \alpha < 90^\circ \end{cases} \tag{3.13}$$

where

$f_{a,0,0}$ is the anchorage strength for $\alpha = \beta = 0^\circ$

k_1, k_2 and α_0 are fitted constants found as described in the following.

For an arbitrary combination of α and β the anchorage strength is given by:

$$f_{a,\alpha,\beta} = \max\begin{cases} f_{a,\alpha,0} - (f_{a,\alpha,0} - f_{a,90,90}) \cdot \beta / 45^\circ & \text{if } \beta \le 45^\circ \\ f_{a,0,0} - (f_{a,0,0} - f_{a,90,90}) \cdot \sin(\max(\alpha,\beta)) \end{cases}$$

$$f_{a,\alpha,\beta} = f_{a,0,0} - (f_{a,0,0} - f_{a,90,90}) \cdot \sin(\max(\alpha,\beta)) \quad \text{if } 45^\circ < \beta \le 90^\circ \tag{3.14}$$

The constants k_1, k_2 and α_0 are found from a lower-bound bilinear relationship for the four test series with ($\beta = 0^\circ$), see figure 3.37.

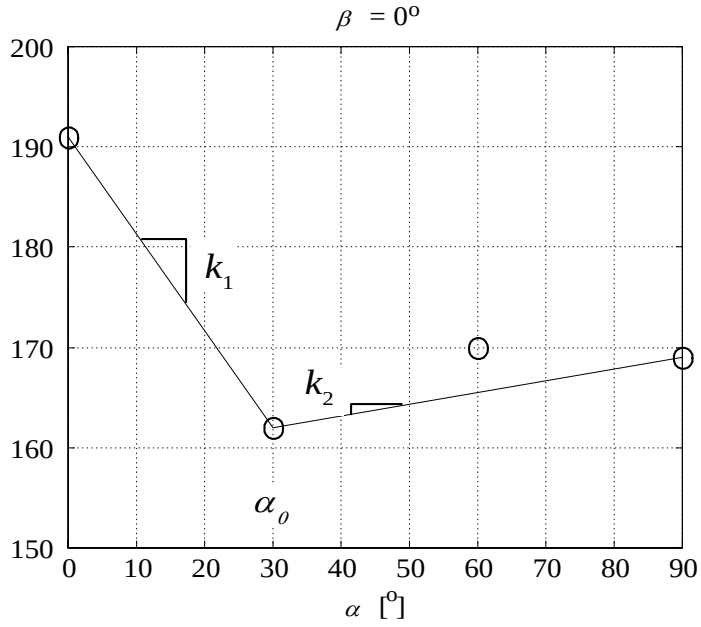

Figure 3.37. Determination the constants k_1, k_2 and α_0. The test results are indicated by a ○. The anchorage capacity per nail is shown in N along the vertical axis.

The anchorage stresses should satisfy the condition:

$$\left(\frac{\tau_F}{f_{a,\alpha,\beta}}\right)^2 + \left(\frac{\tau_M}{f_{a,0,0}}\right)^2 \le 1 \tag{3.15}$$

where τ_F and τ_M are the actual anchorage stresses found by:

$$\tau_F = \frac{F_A}{A_{ef}} \qquad \tau_M = \frac{M_A}{W_p} \tag{3.16}$$

F_A is the force acting on the plate at the centroid of the effective area and M_A is the moment acting at the centroid of the effective area. A_{ef} is the effective area and W_p is the plastic rotational section modulus determined by:

$$W_p = \int_{A_{ef}} r dA \tag{3.17}$$

where r is the distance from the centroid of the effective anchorage area to the area dA. W_p can be determined by numerical integration.

From the test results the constants are determined as $k_1 = -0.99$ N/nail per $^\circ$, $k_2 = 0.12$ N/nail per $^\circ$ and $\alpha_0 = 30^\circ$. It should be noted that the constants are normally determined from tests with α = 0°, 15°, 30°, 45°, 60°, 75° and 90° - here the constants are determined from only four tests with α = 0°, 30°, 60° and 90°.

The values $f_{a,0,0} = 191$ N/nail and $f_{a,90,90} = 144$ N/nail are determined as the average of the maximum anchorage value of each of the six tests in the two test series TA_0_0_90 and SA_90_90_0.

Comparison

The test results versus the calculated anchorage values from Eurocode 5 are illustrated in this section. The results from the tests are indicated by a ✱ and the results from Eurocode 5 are shown as a continuous line.

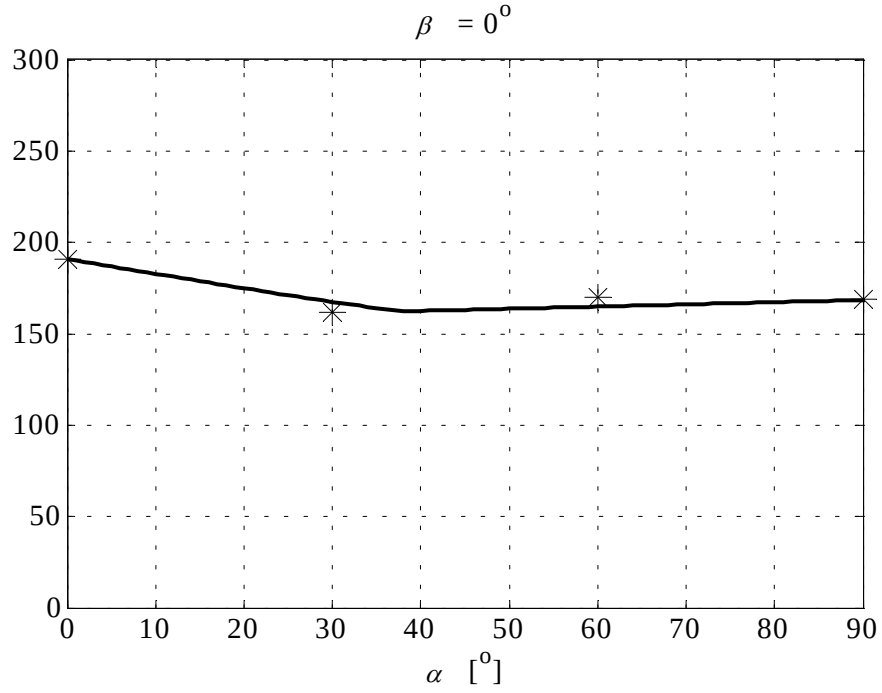

Figure 3.38. Comparison between tests (✱) and Eurocode 5. The anchorage capacity is shown on the vertical axis in N per nail.

When β = 0° the predictions by Eurocode 5 are close to the test results.

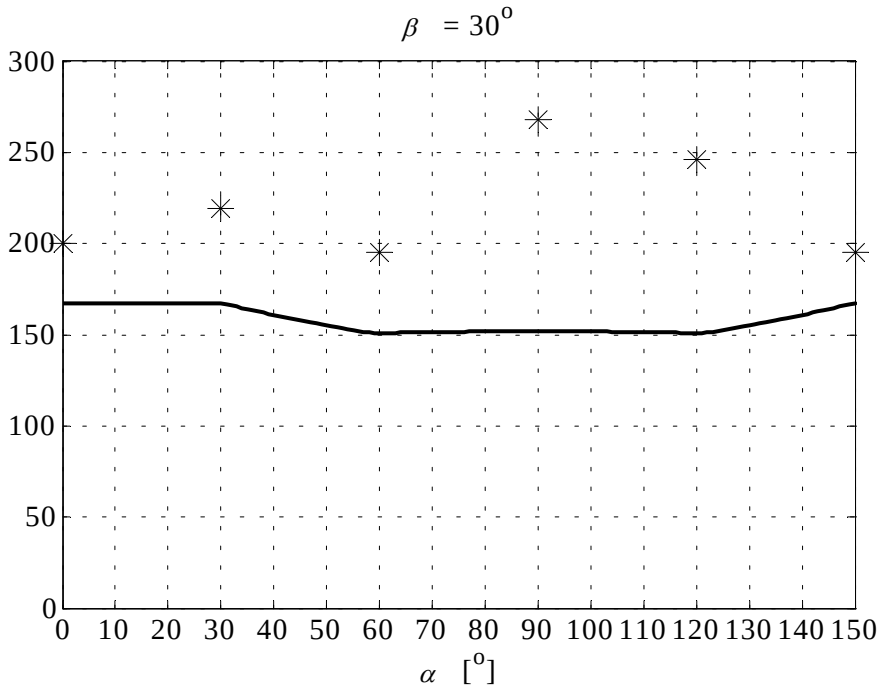

Figure 3.39. Comparison between tests (✳) and Eurocode 5. The anchorage capacity is shown on the vertical axis in N per nail.

When $\beta = 30^{\circ}$ Eurocode 5 predicts a lower anchorage capacity than that found in the tests (on the safe side).

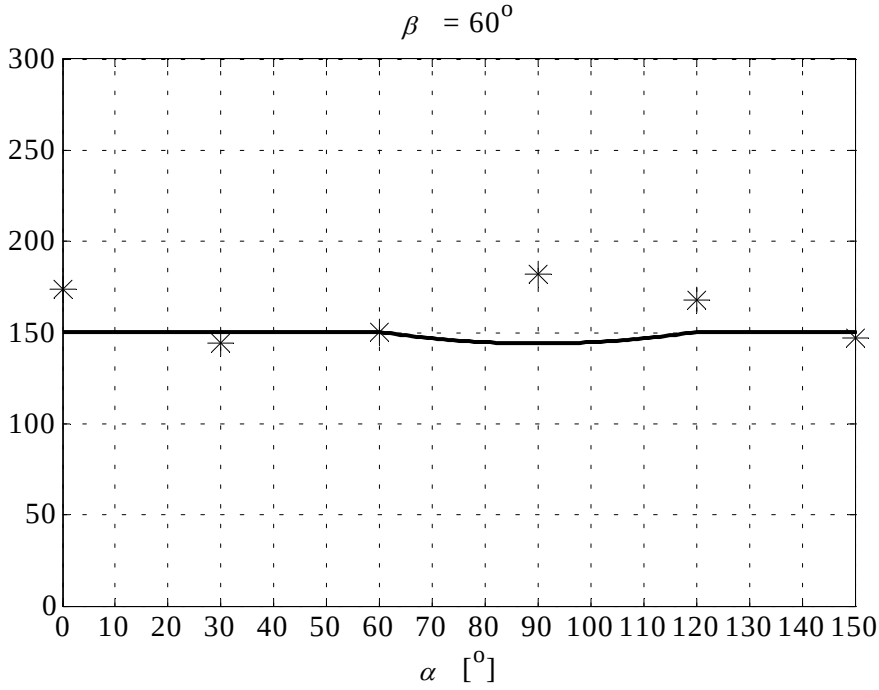

Figure 3.40. Comparison between tests (✳) and Eurocode 5. The anchorage capacity is shown on the vertical axis in N per nail.

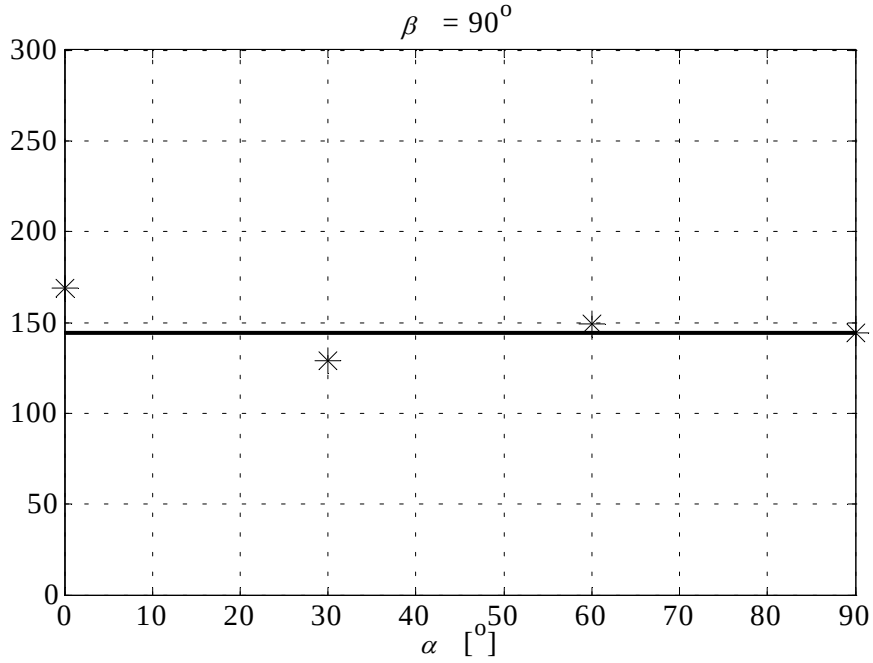

Figure 3.41. Comparison between tests (∗) and Eurocode 5. The anchorage capacity is shown on the vertical axis in N per nail.

For $\beta = 60^\circ$ and $\beta = 90^\circ$ the test results are quite close to the values achieved with the expressions in Eurocode 5.

3.6 Conclusions on the Anchorage Capacities

As shown in figure 3.32, timber failure is the dominating failure mode in the test series performed. Due to the variation of the properties of the timber, large variations in the stiffness and in the anchorage capacities are seen in the test results. This makes it difficult to make a precise modelling of the nails, but it is found that TRUSSLAB gives a reasonable estimation of the load-displacement curves for the tested joints. A method to eliminate timber failure could be to use a test specimen as shown in figure 3.42.

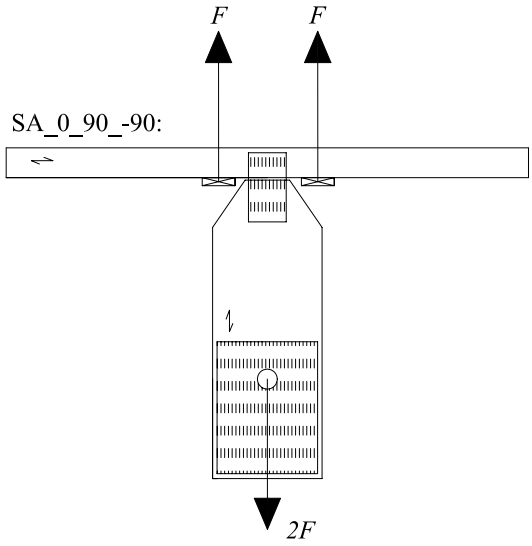

Figure 3.42. Test specimens where the risk for timber failure is eliminated.

The risk of timber failure is eliminated since the nail plate almost covers the height of the horizontal beam.

In *Wolfe, Ronald W. & McCarthy, Monica (1987)* it is shown that a comparison between different studies indicates a huge difference in the achieved properties of the nails.

A comparison between the test results and the expressions given in Eurocode 5 shows that Eurocode 5 in most cases gives a relatively good estimation of the anchorage capacity of the nail plate, and the formulas from Eurocode 5 are therefore implemented in TRUSSLAB.

4 Analysis of Nail Plate Type MiTek GNT150S

In total 42 tests have been performed with the nail plate type MiTek GNT150S. From these tests the parameters needed as input in TRUSSLAB are determined. Besides the basic test series, no additional tests with other combinations of the timber, force and plate directions have been performed to verify the theory for the plate and nail element. For a test description and the test arrangements see appendix A. Some typical pictures of the failure modes are found in appendix B.

The test results are compared with results from calculations with TRUSSLAB.

The geometry for the GNT150S nail plate is shown in figure 4.1.

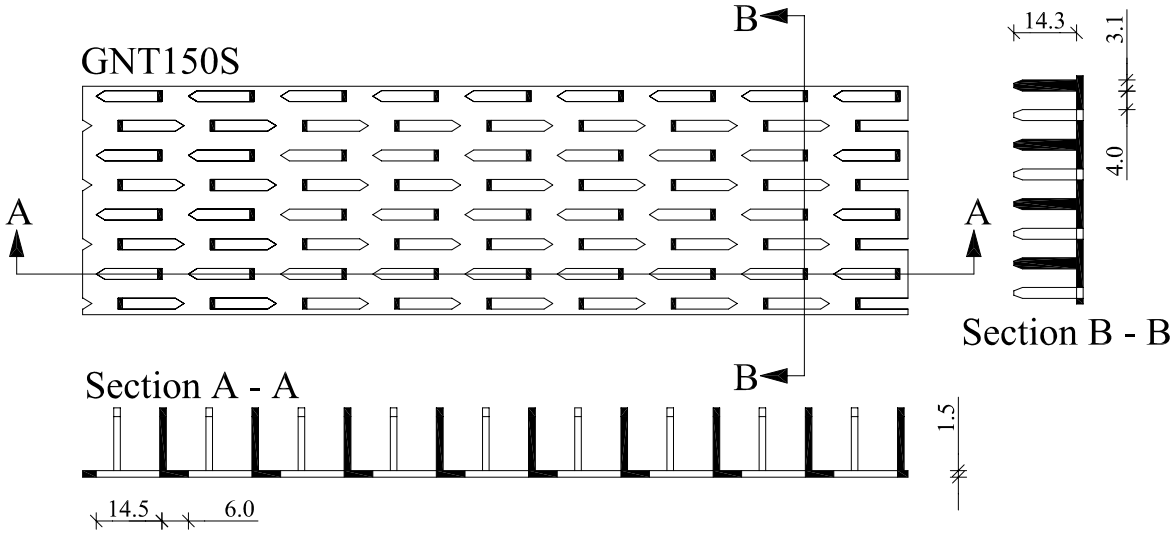

Figure 4.1. Geometry of the MiTek GNT150S nail plate. Dimensions in mm.

The nail density is 0.00672 nails/mm^2. The nail plates are galvanized and are produced by punching the nails from a thin steel plate.

The difference between the GNT150S and the GNA20S nail plates is the thickness of the steel, the geometry of the nails and the number of nails per hole. The GNT150S has only one nail per hole whereas GNA20S has two nails per hole. Furthermore, the GNT150S nail plate has a staggered arrangement of nail holes while the nail holes of GNA20S are located orthogonally, as mentioned earlier.

For a more detailed description of the determination of the plate properties, see section 3.1.1 where the method is described for the nail plate type GNA20S. Similarly for determination of the nail properties, a more detailed description is given in section 3.4.1.

4.1 Properties of the Plate Element in TRUSSLAB

To determine the properties of the plate element that reflects the behaviour of a GNT150S nail plate, the test series in figure 4.2 are used. Three specimens are tested within each test series. The height of the timber beams is 170 mm and the thickness is 45 mm. The gap between the members is 5 mm.

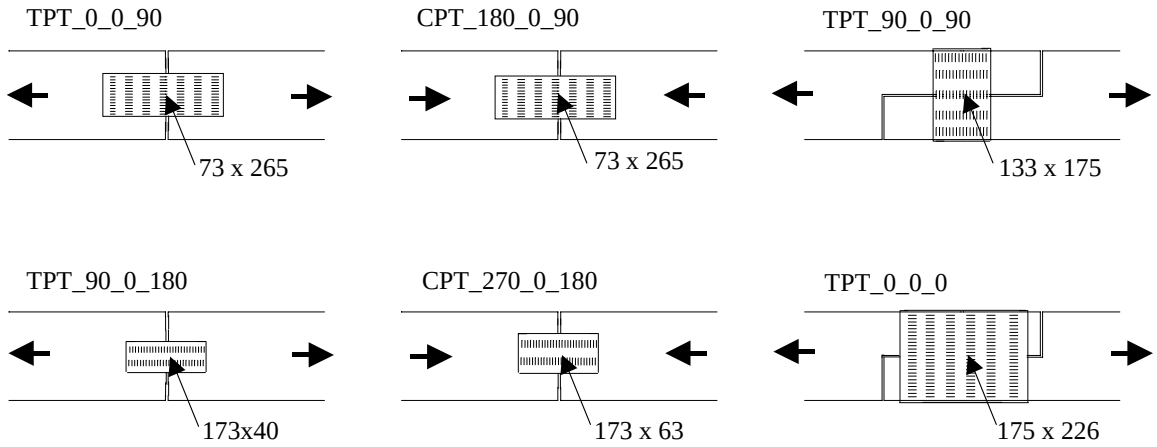

Figure 4.2. Basic test series used to determine the properties for the plate element in TRUSSLAB for the MiTek GNT150S nail plate. Dimensions in mm.

The notation of the specimens is TPT_α_β_γ (Tension test arrangement Plate values GNT150S nail plate) and CPT_α_β_γ (Compression test arrangement Plate values GNT150S nail plate), where α, β and γ are defined as in section 3.1.1.

To avoid timber failure, the two test series TPT_0_0_0 and TPT_90_0_90 are weakened in the joint line and to avoid anchorage failure, the nail plate is weakened for the series TPT_0_0_90. The weakening is done by cutting slits in the nail plate and thereby reducing the length of the joint line.

From an analysis of the test results the parameters shown in table 4.1 are found.

	Beams in plate main direction	Beams perpendicular to plate main direction
$\sigma_{y,t}$ [N/mm^2]	400	180
$\varepsilon_{y,t}$	0.0067	0.0173
$\sigma_{y,c}$ [N/mm^2]	265	250
$\varepsilon_{y,c}$	0.0044	0.0240
L [mm]	8.0	5.0
h [mm]	4.0	7.0
t [mm]	1.5	1.5
E [N/mm^2]	60000	10400
E_p [N/mm^2]	900	300

Table 4.1. Parameters for the plate element for the MiTek GNT150S nail plate.

The distance between the beams in the main direction of the nail plate is 7.1 mm and the distance between the beams perpendicular to the main direction of the nail plate is 20.5 mm.

An illustration of the geometry of the beams for the GNT150S nail plate is shown in figure 4.3.

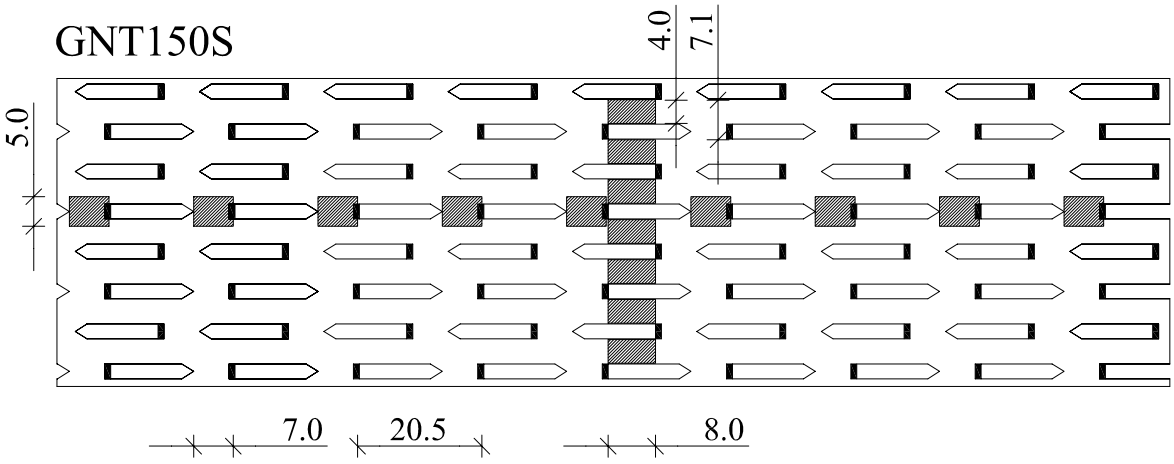

Figure 4.3. Geometry for the beams in the plate element for the GNT150S nail plate. Dimensions in mm.

For the nail plate type GNT150S the failure values needed as input in TRUSSLAB are shown in table 4.2.

	$\sigma_{u,t}$ [N/mm^2]	$\sigma_{u,c}$ [N/mm^2]	τ_u [N/mm^2]
Beams parallel to the main direction	453	283	275
Beams perpendicular to the main direction	211	275	430

Table 4.2. Ultimate stresses for GNT150S used in TRUSSLAB.

The test results together with results from TRUSSLAB for the six basic test series are shown in figure 4.4. The results from the tests are shown as continuous lines and the results from TRUSSLAB as dashed lines. The force is converted to N per beam and the deformation along the horizontal axis is measured in mm.

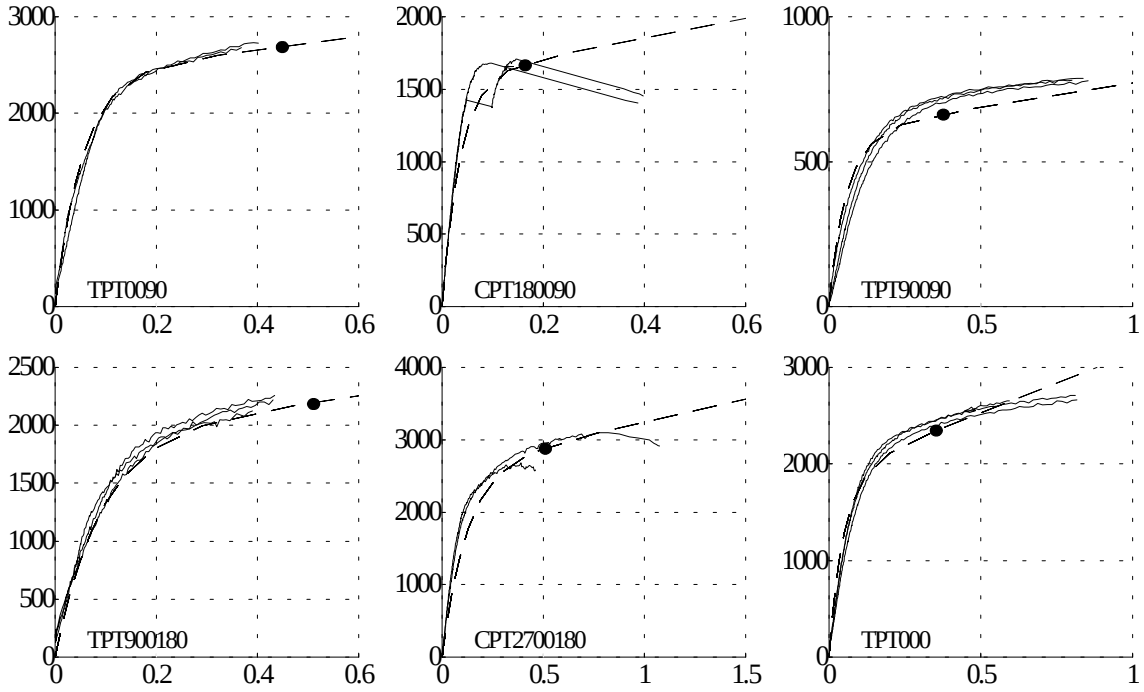

Figure 4.4. Load-displacement curves for the basic tests and corresponding TRUSSLAB calculations for the GNT150S nail plate.

It is seen that the variation between the three identical tests is small. TRUSSLAB is able to predict the behaviour quite well except for the series CPT_180_0_90 and CPT_270_0_180 where TRUSSLAB expects an increase in the load capacity after the buckling has occurred, while the tests show that the load is decreasing.

4.2 Conclusions on the Plate Capacities

According to the test standard *EN 1075 (1999)* the nail plates should not have been weakened in the joint line. It is evaluated, however, that the weakening of the nail

plates for the series TPT_0_0_0, TPT_90_0_90 and TPT_0_0_90 has not affected the plate capacities in any way, since the weakening is performed to avoid anchorage failure due to a too small anchorage area for the series TPT_0_0_90 and to avoid bending/tension failure of the timber in the series TPT_0_0_0 and TPT_90_0_90.

For the four tension tests the displacement transducers were dismounted after yielding occurred, but before the ultimate load was reached. For the two compression tests the displacement transducers were not dismounted before failure.

From a comparison between the test results and results from calculations with TRUSSLAB it is concluded that TRUSSLAB estimates the behaviour of the deformation over the joint line well, except for the compression tests where TRUSSLAB overestimates the load capacity after buckling has occurred.

Table 4.3 shows the average of the maximum recorded load per mm of plate for each of the six basic tests together with the characteristic 5-percentile achieved from the Danish approval for the MiTek GNT150S nail plate, see *Boligministeriet, Bygge- og boligstyrelsen, MK-Godkendelse, (1996)* and from *TRÆ 31 (1995).*

The values in table 4.3 for compression strengths – indicated by *) - are given by the Swedish approval *Typgodkännandebevis 5019/86 (2001)* due to the fact that these values do not occur in the Danish approval.

	$f_{t,0}$	$f_{c,0}$	$f_{t,90}$	$f_{c,90}$	$f_{v,0}$	$f_{v,90}$
MK-approval (characteristic values)	433	184*)	130	160*)	130	148
Test results (mean values)	384	239	108	141	111	131

*Table 4.3. Test results versus MK-approval. Units in N/mm. The values indicated by *) are from the Swedish approval Typgodkännandebevis 5019/86 (2001).*

All values from the MK-approval except one are higher than the values achieved by the tests. This is the opposite of what is achieved for the GNA20S nail plate. An explanation to this is that the tests with the GNT150S nail plate are stopped earlier than the tests with the GNA20S nail plate, which can be seen from size of the deformations at the time when the tests were stopped. The tests with the GNT150S nail plate have been performed by two students as a part of their B.Sc.-thesis - see *Nørgaard, M & Thomsen, K. B. (2001)* - and not by the author. It should, however, be noted again that the tests are stopped before the ultimate load is reached, but after the plate has started yielding.

4.3 Properties of the Nail Element in TRUSSLAB

The properties of the nail element for the GNT150S nail plate are determined from results of the test series shown in figure 4.5. Six specimens are tested within each test series. The height of the timber beams is 170 mm and the thickness is 45 mm. All tests are continued until failure.

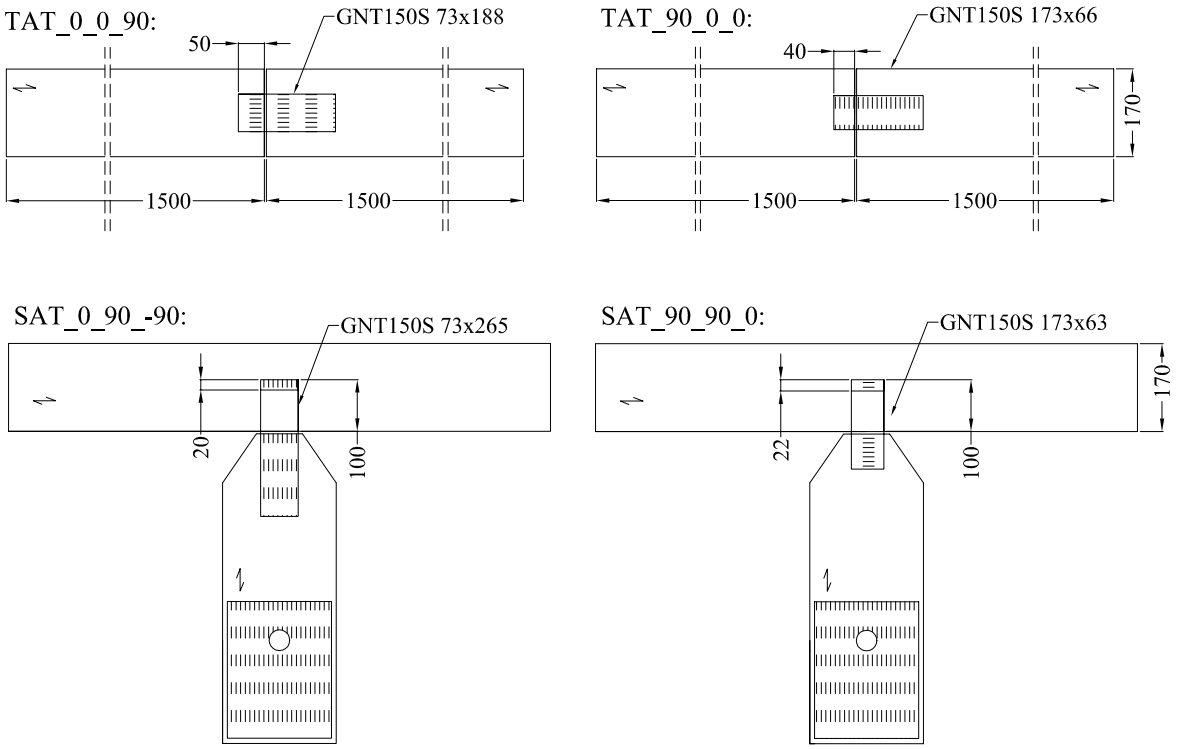

Figure 4.5. Test series used to determine the properties of the nail element for the GNT150S nail plate.

The notation of the specimens is TAT_α_β_γ (Tension test arrangement Anchorage values GNT nail plate) and SAT_α_β_γ (Special test arrangement Anchorage values GNT nail plate) where α, β and γ are defined as in section 3.1.1.

In the series SAT_0_90_-90 and SAT_90_90_0 some of the nails have been removed to avoid timber failure. As mentioned in the chapter where the GNA20S nail plate is analysed, it is estimated that the most realistic properties are found when nothing is done to avoid timber failure. Unfortunately, the properties for the GNT150S nail plate are partly determined from two test series, where timber failure is avoided. This may give stiffness properties and ultimate loads that are too high for these two cases.

The properties for the nail element are given in table 4.4. The values are given per nail.

α, β	k [N/mm]	kk [N/mm]	p_0 [N]
0, 0	1100	1	440
90, 0	1500	1	330
0, 90	1500	1	650
90,90	2000	1	620

Table 4.4. Anchorage parameters for the MiTek GNT150S nail plate. The values are per nail.

The values of *kk* are taken as 1 and not 0 due to the way the calculations are performed in TRUSSLAB.

The results from the four test series together with the calculations with TRUSSLAB are shown in figure 4.6. The results from TRUSSLAB are shown as a thick continuous line and the dots indicate the ultimate load level given by the expressions in Eurocode 5 with $k_1 = -1.22$ N/nail per $^\circ$, $k_2 = 1$ N/nail per $^\circ$, $\alpha_0 = 90^\circ$, $f_{a,0,0} = 440$ N/nail and $f_{a,90,90} = 620$ N/nail. These values are only determined from the four basic test series and should therefore be used with care. The load is given in N per mm^2 of the effective anchorage area (as for the MiTek GNA20 nail plate).

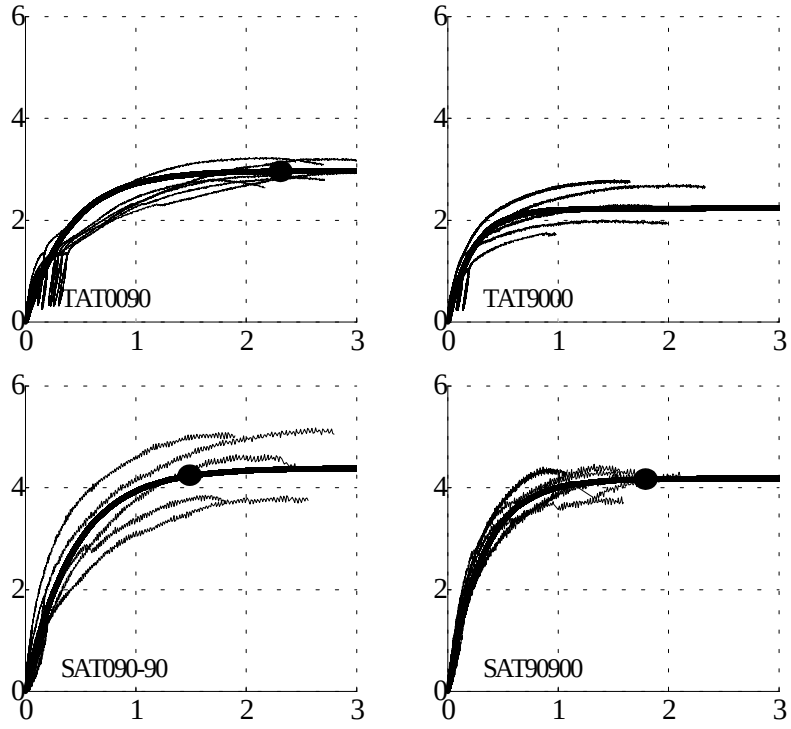

Figure 4.6. Test results and results from TRUSSLAB for GNT150S nail plate. The load on the vertical axis is measured in N/mm^2 and the deformation on the horizontal axis is in mm.

As seen from the figure, TRUSSLAB is able to predict the behaviour quite well with the chosen values for *k*, *kk* and p_0. The results also show that the nails have higher load capacity when the load is applied perpendicularly to the grain direction, which may be caused by the fact that special care has been taken to avoid timber failure. For the series TAT_90_0_0 failure is predicted at a load level on 4.1 N/mm^2, which is caused by the high load capacities when the load is applied perpendicularly to the grain direction.

4.4 Conclusions on the Anchorage Capacities

In total 24 tests have been performed to determine the properties of the nail element for the GNT150S nail plate. Timber failures are not observed in the tests. This gives high load and stiffness properties when the load is applied perpendicularly to the grain direction.

A comparison between the test results and calculations with TRUSSLAB shows that TRUSSLAB predicts the load-displacement curves well. The failure formulas from Eurocode 5 are implemented in TRUSSLAB and for three of the four basic series they predict the load level of failure well. For the series TAT_90_0_0, however, failure is observed at a load level of 2.2 N/mm^2, whereas TRUSSLAB and Eurocode 5 predict the ultimate load level to be 4.1 N/mm^2 (therefore, failure is not indicated in figure 4.6 for test series TAT_90_0_0).

5 Analysis of Knee Joints

The knee joint is part of a frame truss as shown in figure 5.1. The slope of the rafters is 45° for the tested knee joints.

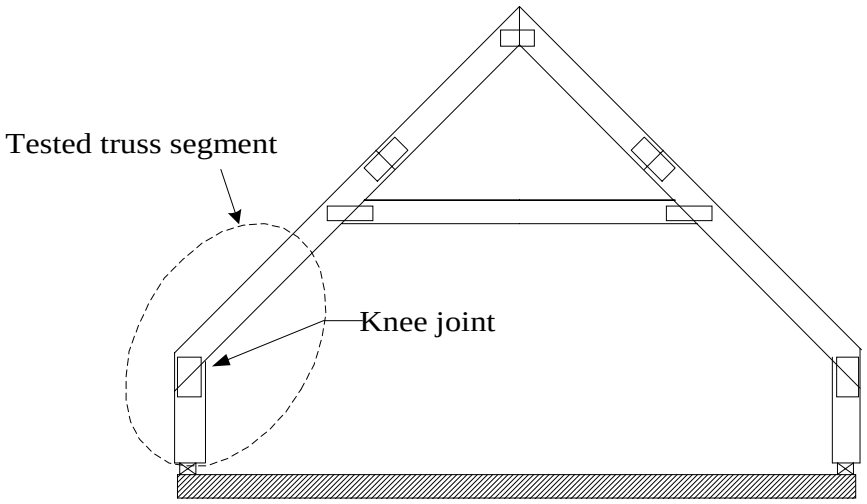

Figure 5.1. Illustration of frame truss and knee joint.

In total 60 tests with 24 different types of knee joints have been performed. The aims of the tests are to verify and improve TRUSSLAB and to find a good design of the knee joint. In order to do so, members of The Association of Manufacturers of Roof Trusses in Denmark have cooperated.

At Aalborg University the knee joint has been investigated earlier and tests have been performed as well. In 1990 and 1991 some full-scale static and dynamic tests were performed on frame trusses with different designs of the knee joints, see *Hansen, F. T., Mortensen, N. L., Kloch, S. & Hansen, L. P. (1990/1991)*. In 1992 *Mortensen, N. L. & Kloch, S. (1992)* performed additional tests and analysis of knee joints. These tests showed that it is important to cover the upper end of the top chord with a nail plate to avoid splitting of the rafter, see figure 5.2.

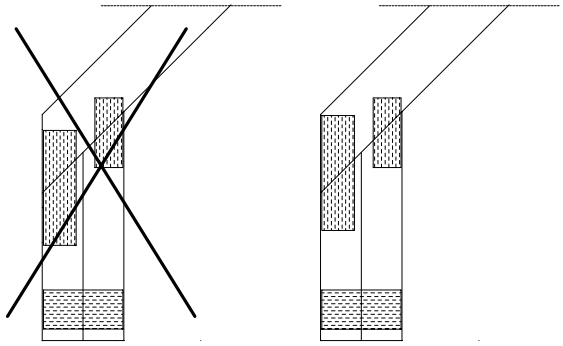

Figure 5.2. Location of nail plate to avoid splitting of the rafter.

The 60 tests in this project with knee joints were performed by two students as part of their B.Sc.-thesis, see *Nørgaard, M. & Thomsen, K. B. (2001)*. The tests were divided into two test programmes in order to perform some pilot tests and afterwards improve the design of the joint and perform additional tests. In the present thesis the tests are treated as one programme.

The results of the tests are compared with results of calculations in TRUSSLAB. It is shown how a finite element model is set up in TRUSSLAB and a parameter analysis is made for some of the relevant parameters and elements. For a test description see appendix C.

5.1 Test Series

The test specimens are made of Swedish spruce of strength class K24 (S10). Two different types of nail plates are used: MiTek GNA20S and MiTek GNT150S with a thickness of 1.0 and 1.5 mm, respectively. For a detailed description of the nail plates, see chapters 3 and 4. The thickness of the timber beams is 45 mm and in order to limit the number of test series it has been chosen to use one fixed total height of the rafter (245 mm) and two different total widths of the legs (290 mm and 360 mm). Further limitations are mentioned in the introduction to the thesis.

The length of the rafter in the test series has been taken as 2 m. This gives a combination of sectional forces in the knee joint that corresponds to a frame truss spanning 7 m and loaded with dead load only (roof and ceiling).

The 24 different test series are shown in the figures 5.3, 5.4, 5.5 and 5.6. To give an overview of the different test series not all dimensions are shown in the figures. For detailed drawings of the test series, see appendix C.3.

The letters A-K give the notation of the specimens. A ‘T’ denotes a ‘Thin’ leg and the numbers ‘20’ and ‘150’ in the series name denote the plate type used in the knee joint. ‘2R’ denotes that the rafter consists of two beams. ‘2P’ denotes that two plates have been impresses on top of each other – double plates (this is done to all the nail plates except the one at the bottom of the leg). In all the series - except series K - the same GNT150S nail plate has been used for the nail plate located at the bottom of the leg.

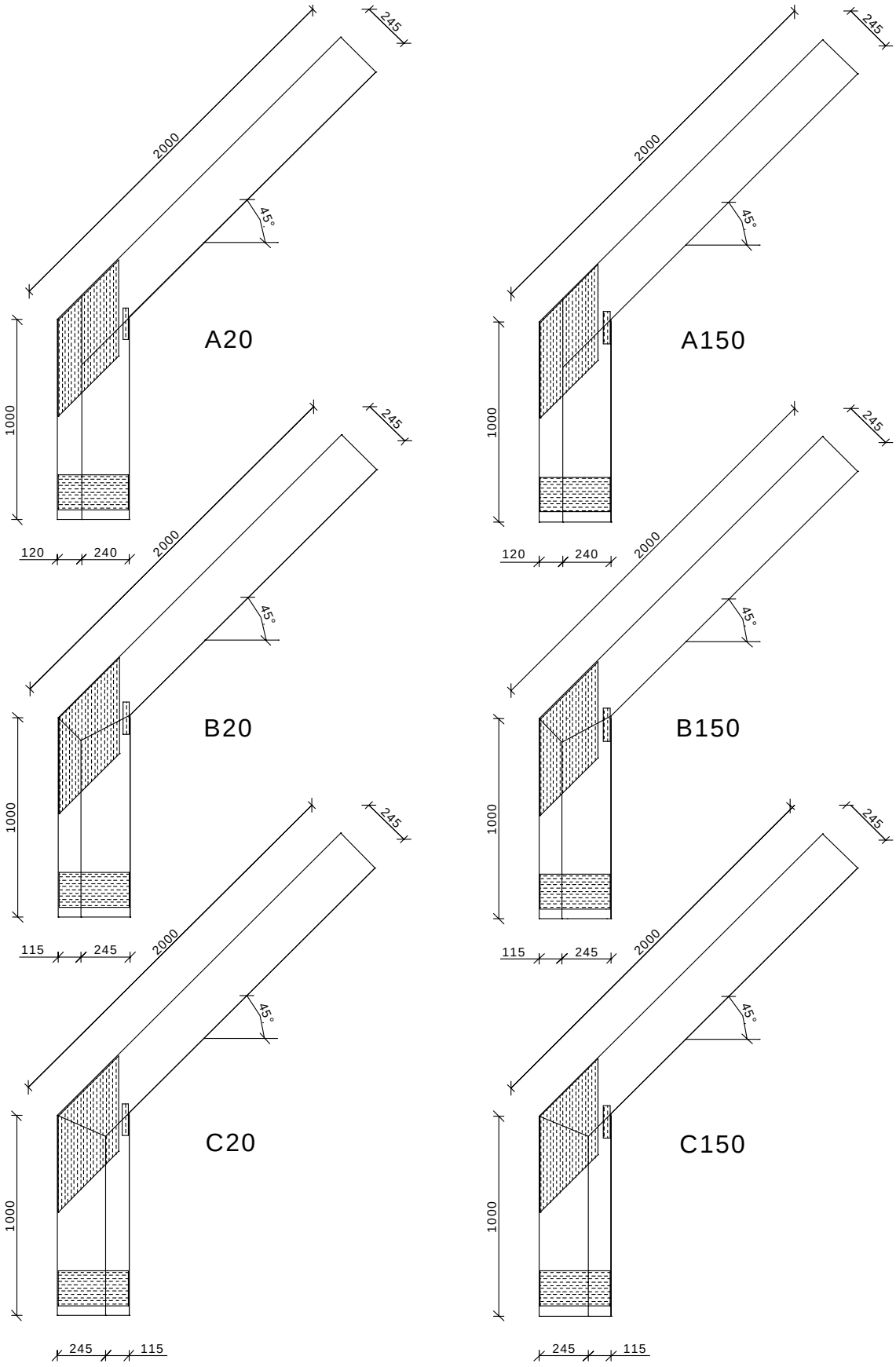

Figure 5.3. A20, A150, B20, B150, C20 and C150. Dimensions in mm.

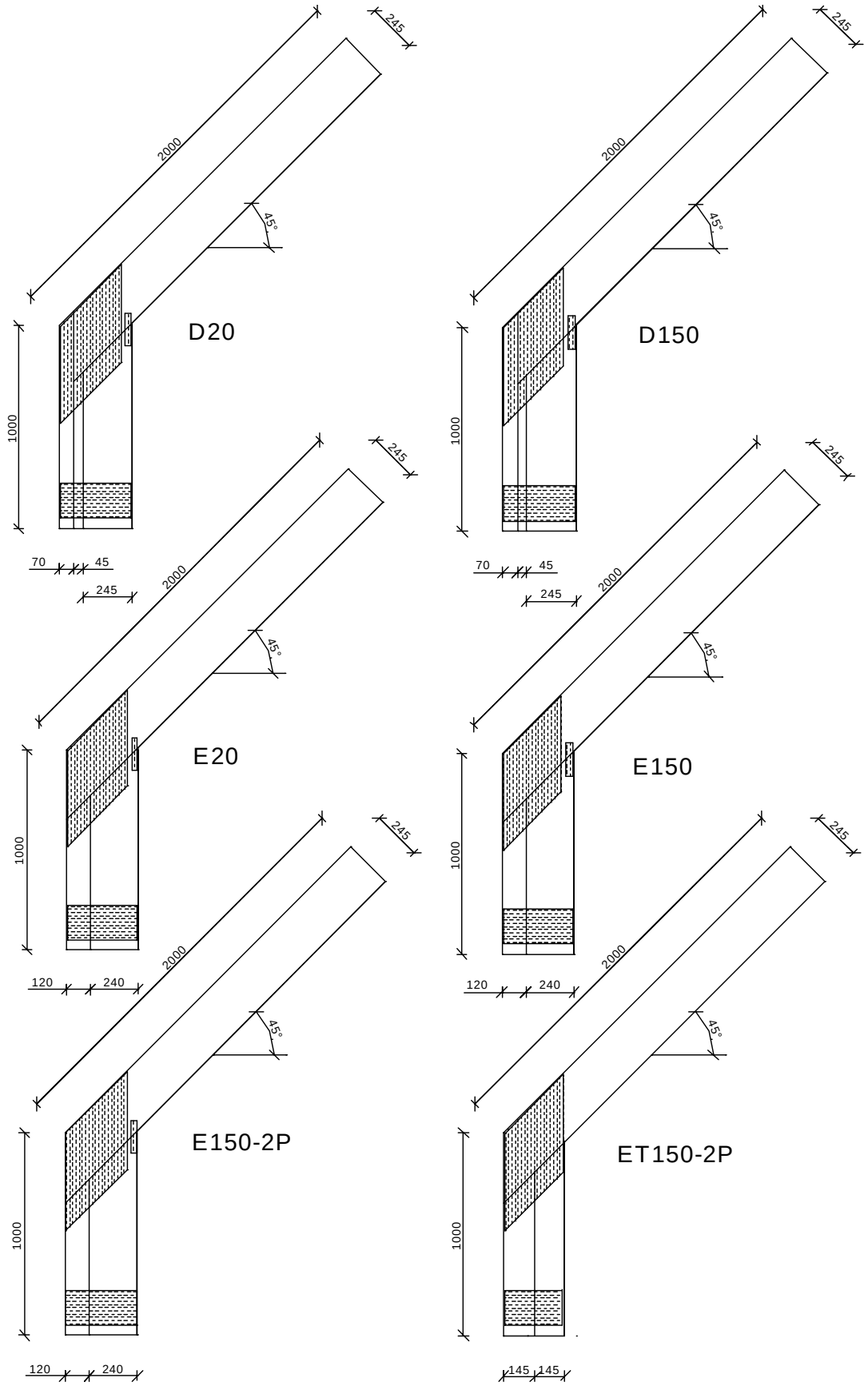

Figure 5.4. D20, D150, E20, E150, E150-2P and ET150-2P. Dimensions in mm.

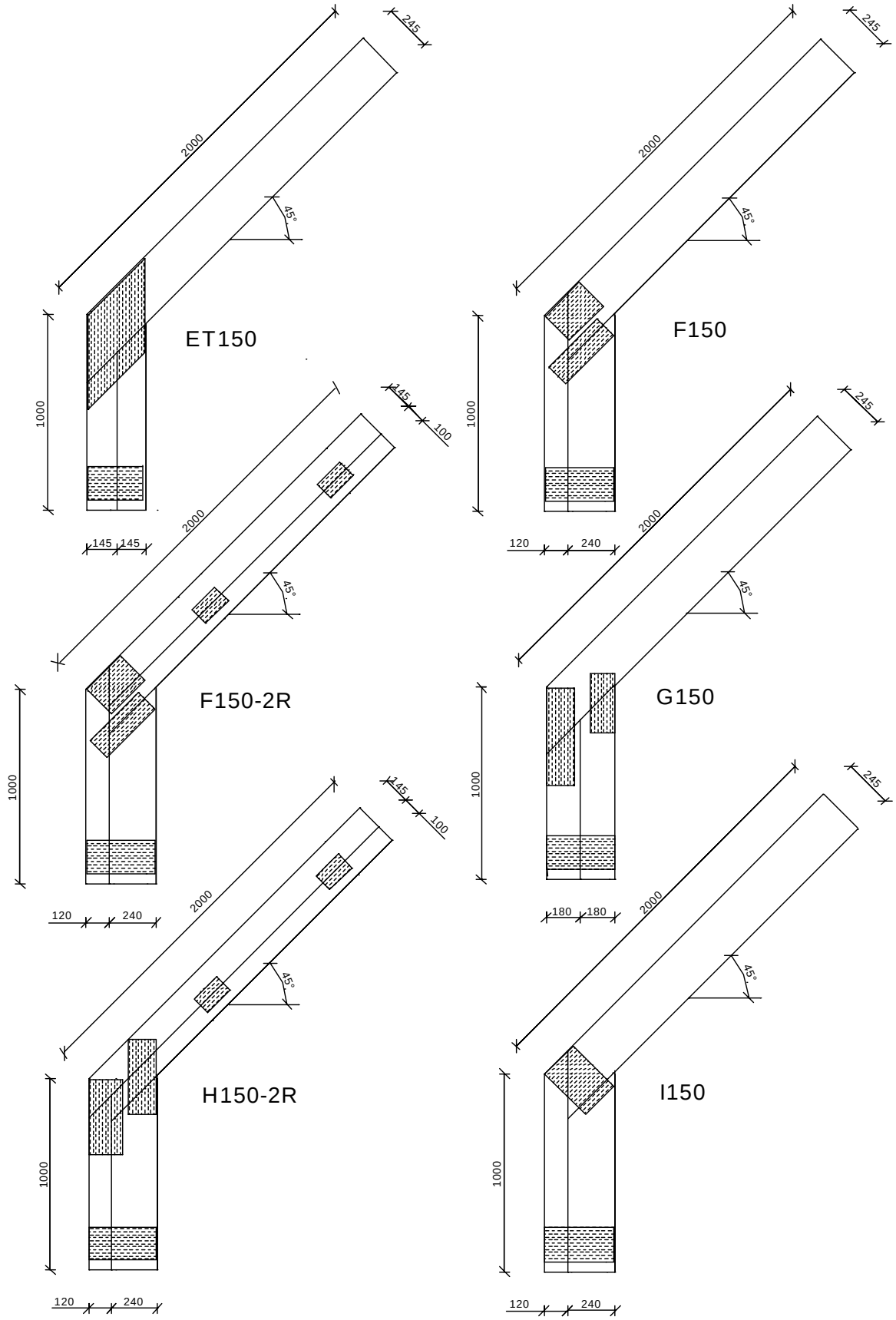

Figure 5.5. ET150, F150, F150-2R, G150, H150-2R and I150. Dimensions in mm.

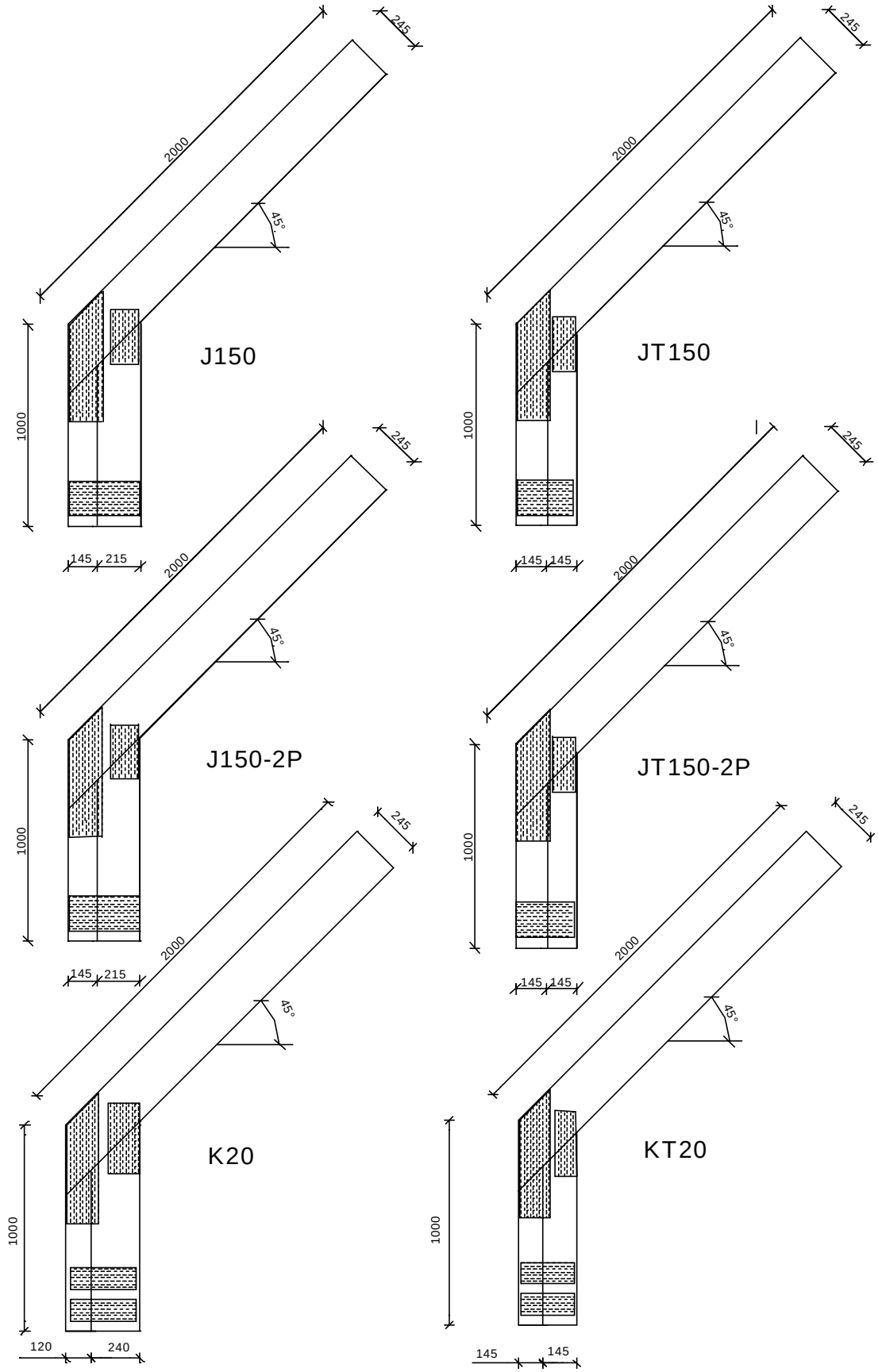

Figure 5.6. J150, JT150, J150-2P, JT150-2P, K20 and KT20. Dimensions in mm.

In the series where the outer leg continues to the top of the rafter (see e.g. the series A and D in figures 5.3 and 5.4) it is the intention that it shall prevent splitting of the rafter.

When planning the series B and C the same argumentation is used. In these series, however, no contact forces can be transferred between the rafter and the outer leg as in the series A and D (under the given load). However, the 'arm' to transfer the moment from the rafter to the legs is bigger compared to the series A and D. The series B and C may be difficult to manufacture due to the fact that height of the timber beams should be precise to produce a joint with minimal gaps between the timber members. However, the height of timber beams is often varying and a rafter with a target height of 245 mm can often be found with a height of only 243 mm.

Series E is used to verify whether it is a good solution to let the rafter continue uncut to the edge or to let the outer leg continue to the top of the rafter as in series A and D.

The series F150 and F150-2R are used to analyse the effect when the rafter consists of one beam versus the situation when the rafter is composed of two beams.

The series G150 is tested because it is a common way to produce a knee joint (normally only with one beam in the leg). The series H150 and I150 are used to test the TRUSSLAB model and are only of theoretical interest.

The series J and K and the different variations of the series E are all made on the basis of the experience from the first test programme. It is interesting to see what influence a thin leg has on the stiffness and strength of the knee joint. Furthermore, it will show if two nail plates impressed on top of each other will improve the behaviour of the knee joint. Series K is assumed to be a good design when only a GNA20S nail plate is used.

Before the test specimens were produced the moduli of elasticity were measured for the uncut beams. This was done when the timber had a moisture content of approximately 16% according to 20° and 85% relative humidity. The moduli of elasticity are later adjusted to the moisture content of the timber at the time when the knee joints were tested. The rest of the storing, manufacturing and testing is performed according to *DS/EN 26 891 (1993).*

5.2 TRUSSLAB Model for a Knee Joint and Parameter Analysis

In this section it is explained how a finite element model of a knee joint is set up in TRUSSLAB. Furthermore, the influence of some of the parameters of the knee joint is analysed. For a detailed description of the special elements in the finite element model, see chapter 2.

5.2.1 TRUSSLAB Model of a Knee Joint

In figure 5.7 an example of a TRUSSLAB model is shown.

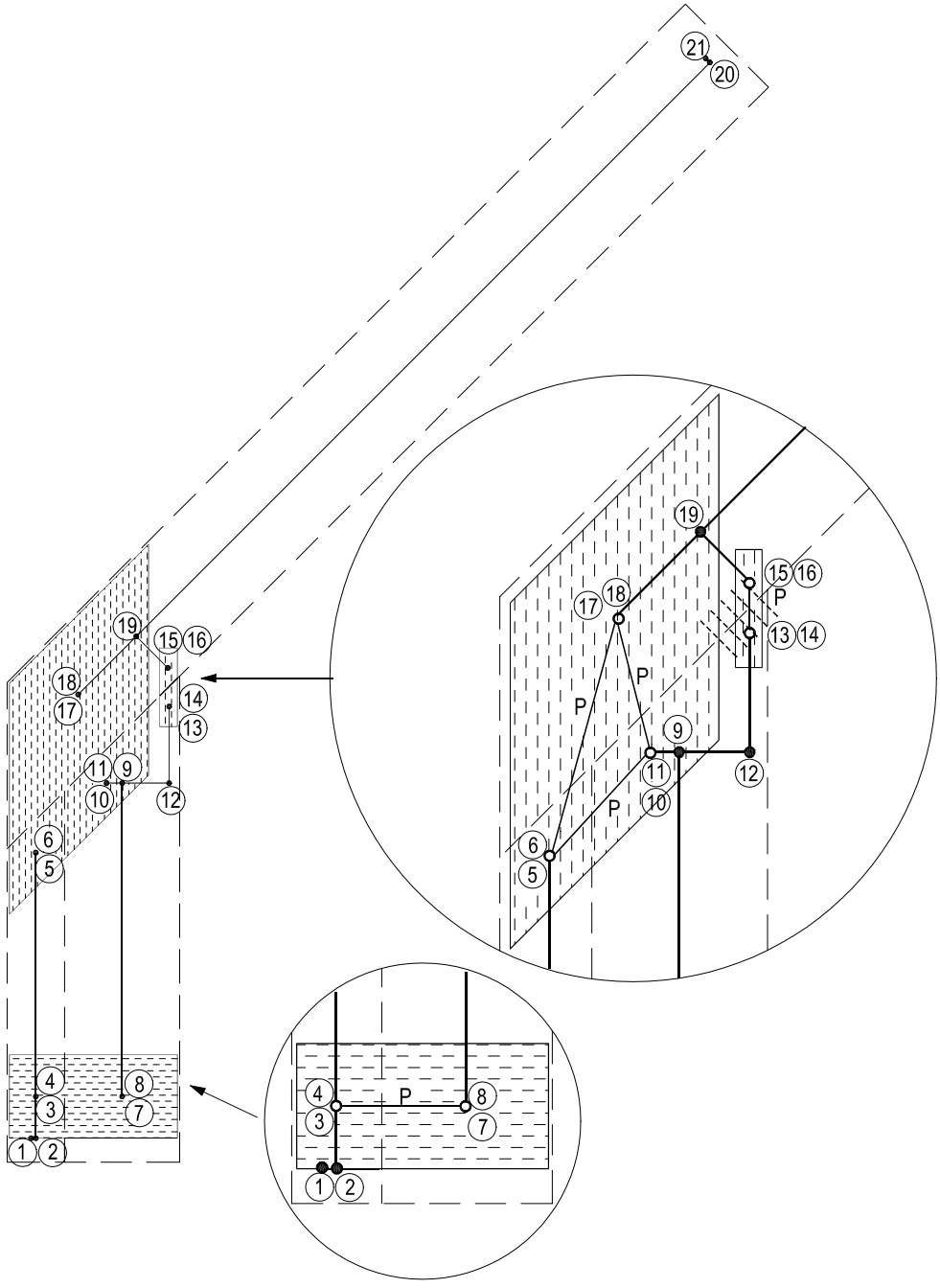

Figure 5.7. TRUSSLAB model for knee joint type E150.

The node numbers are shown in a circle ① and the location of the nodes is shown as a small dot - • or ◦.

The three timber beams are modelled by Timoshenko beam elements. The influence of using Bernoulli beams is analysed later in this chapter. They are located at the symmetry line of each of the beams in the knee joint. Auxiliary beam elements are used to transfer forces from e.g. a nail element to the symmetry line

(see e.g. the element from node 9 to node 12). There are six auxiliary elements in the knee joint type E150 (1-2, 9-10, 9-12, 12-13, 15-19 and 20-21).

The nail elements are indicated by a small circle ◦ and each nail element connects two nodes that are located at the centre of each nail group - one node on the timber and one node on the plate (see e.g. the element from node 7 to node 8). When calculating the strength and stiffness of the nail groups no reduction in the anchorage area is made (no effective area).

A plate element connects two nail elements and is shown with a line denoted P (see e.g. the element from node 4 to 8).

The contact element is indicated by a number of dashed lines – each indicating one of the contact beams in the contact element. In figure 5.7 the contact element connects the nodes 13 and 15.

The location of the nodes 1 and 21 at the supports is chosen so that they correspond to the rotational axes in the test set-up.

Besides the locations of the nail plates, the parameters needed as input in TRUSSLAB for the nail and plate elements are given in sections 3.1.1 and 3.4.1 for the GNA20S nail plate and in sections 4.1 and 4.3 for the GNT150S nail plate.

The input parameters for the timber beams are given by the size of the timber beams (thickness and height) and from the measured moduli of elasticity. It is assumed that the modulus of elasticity is the same for the uncut beams and for the beam sections after the beams are cut into the required dimensions.

The auxiliary elements are assumed to be stiff elements compared to the timber beams and are given a modulus of elasticity of 50000 N/mm^2 and a shear modulus of 5000 N/mm^2 – see also the parameter analysis.

The contact element is given the same properties as the properties for compression perpendicular to the grain direction – i.e. a modulus of elasticity of 350 N/mm^2 according to *DS 413 (1998)*.

5.2.2 Parameter Analysis

The influence of the different uncertain or variable parameters in TRUSSLAB is analysed in this section. For the beams the modulus of elasticity is an uncertain parameter and, furthermore, calculations are performed with Bernoulli beam theory and Timoshenko beam theory. The influence of the stiffness of the auxiliary elements is investigated as well.

Due to the unclear test results from the additional plate compression tests, see section 3.3, it is analysed how a 25% weakening and a 25% reinforcement of the properties for the nail element and the plate elements change the results in TRUSSLAB. Furthermore, the influence of the contact element is analysed.

Since the second order theory is not included in TRUSSLAB (by establishing equilibrium of the deformed structure) it is also estimated how large the error is. The result from this is used when the test results are compared with calculations from TRUSSLAB.

The influence of the different parameters is illustrated via changes in the load-displacement curves for the knee joints. The direction of the load is shown in figure 5.8.

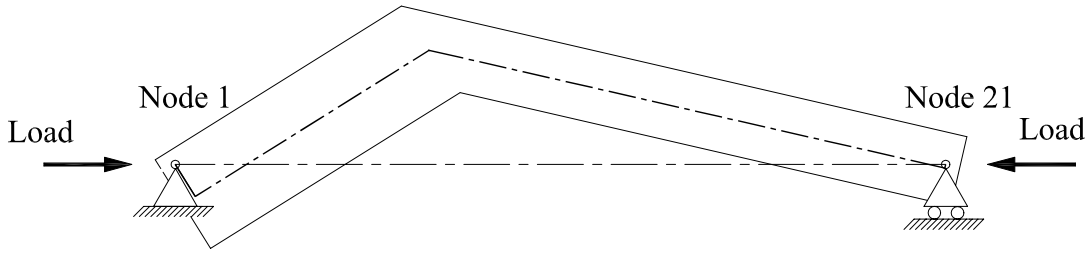

Figure 5.8. Illustration of load direction.

The deformation is measured in the same direction.

Influence of Moduli of Elasticity of the Timber Beams

The modulus of elasticity for each of the beams in the TRUSSLAB model is taken as an average value of the measured moduli of elasticity for the corresponding uncut beams. However, at least two assumptions will make the modulus of elasticity an uncertain parameter:

1. It is assumed that the modulus of elasticity for the cut timber section is the same as for the uncut beam (the timber beams for the knee joints are cut from beams with a length up to 5.1 m).

2. For each of the uncut beams two different moduli of elasticity are measured – one where the beam is bending up and one where the beam is bending down (both are bending around the strong axis). In the TRUSSLAB model the average value is used, but in some cases there is a rather big difference between the two values – up to 20%. However, further tests and analyses have shown that these differences are caused by the test setup used. It is estimated that the average value of the measured moduli is close to the real one and no further corrections are made.

Therefore, the influence of a change of ±10% in the moduli of elasticity is tested. It is assumed that the influence is more or less independent of the type of test series and it has been chosen to make the changes on the timber beams of the knee joint type E150.

The load-displacement curves for the cases are shown in figure 5.9.

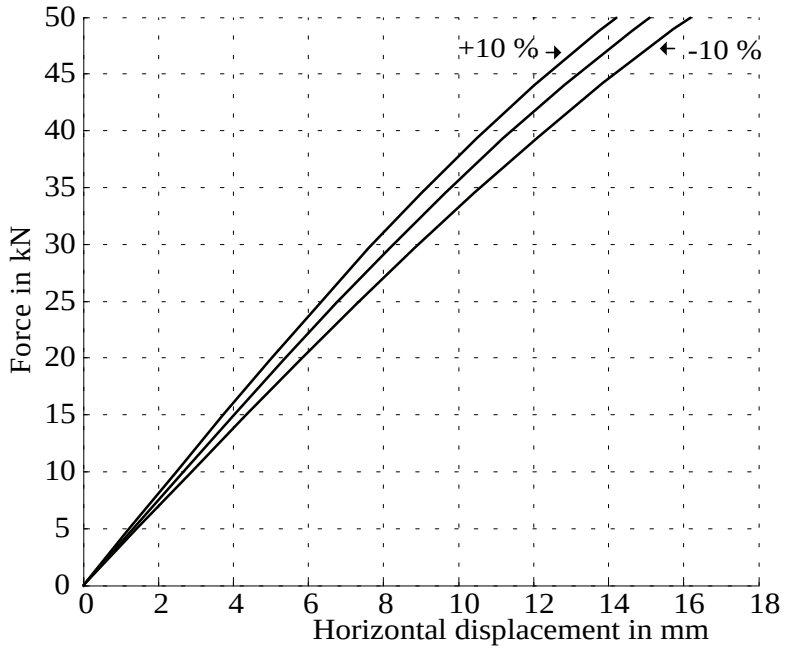

Figure 5.9. Load-displacement curves for the test series E150 when the moduli of elasticity are increased and decreased by 10%.

When the moduli of elasticity are increased by 10% the horizontal deformation is decreased by 7%. The opposite is seen when the moduli of elasticity are decreased by 10%.

As expected the modulus of elasticity has an influence on the behaviour of the frame. In the TRUSSLAB models an average of the two measured moduli of elasticity is used.

Influence of Beam Theory

The timber beams can be modelled as either Timoshenko or Bernoulli beams – see e.g. the description of the beam element on page 12. Again it is assumed that the effect is independent of the type of knee joint and the series E150 is chosen.

Figure 5.10 illustrates the difference between the load-displacement curves when the timber beams are modelled by Timoshenko and Bernoulli beams.

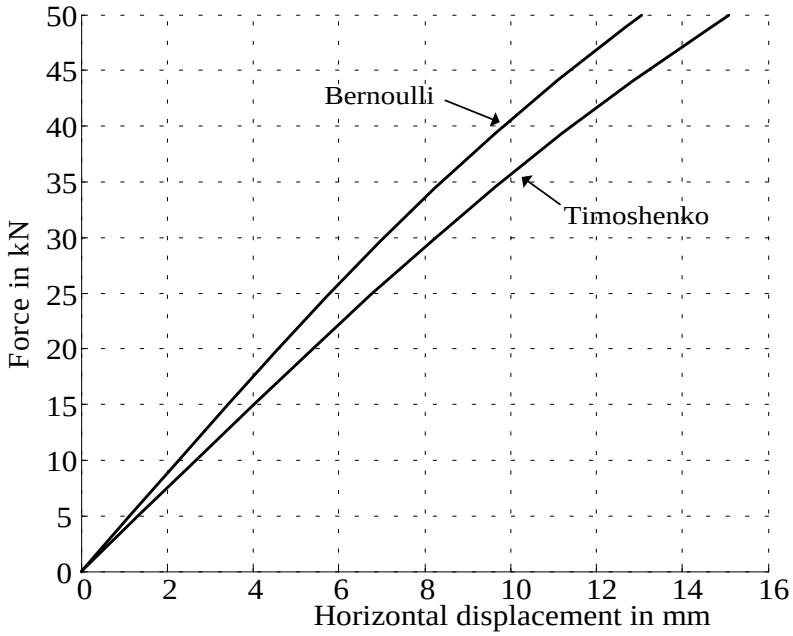

Figure 5.10. Load-displacement curves when the beams are modelled by Timoshenko and Bernoulli theory.

When using Timoshenko beams the horizontal deformation at maximum load level increases by 15%. It is chosen to model the timber beams as Timoshenko beams, since the contribution from the shear forces is included in the deformations.

Influence of the Stiffness of the Auxiliary Elements

The stiffness of the auxiliary elements has an impact on the load-displacement curves. The effect is dependent on the type of knee joint, since the lengths of some of the auxiliary elements are different from model to model. Two different sets of parameters have been used to analyse the effect – see table 5.1. G is the shear modulus and h is the height of the beam.

	E [N/mm^2]	G [N/mm^2]	h [mm]
Stiff auxiliary elements	50000	5000	150
Weak auxiliary elements	350	700	300

Table 5.1. Parameters for stiff and weak auxiliary elements.

The parameters for the weak auxiliary elements have been chosen so that the modulus of elasticity corresponds to the direction perpendicular to the grain direction, since all the auxiliary elements coincide with this direction. The height of the beams is estimated to be 300 mm.

In figure 5.11 the load-displacement curves are shown for the knee joint types C150 and E150. The force is shown vertically in kN and the deformation is shown on the horizontal axis in mm.

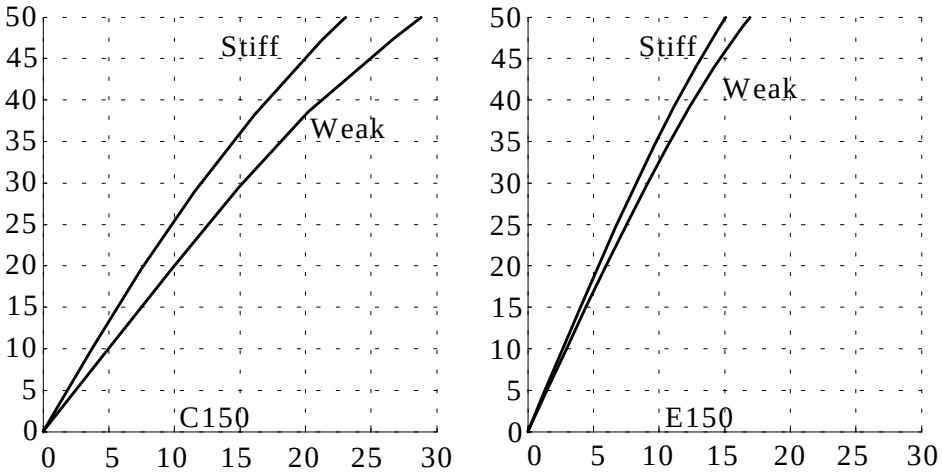

Figure 5.11. Influence of stiffness of auxiliary elements.

For the knee joint type C150 the deformation increases by 22% at a load level of 50 kN when the parameters for the auxiliary elements are changed from stiff to weak. Similar changes increase the deformation by only 7% for the knee joint type E150. Additional analyses have shown that in particular one auxiliary element causes these relatively large changes for the knee joint type C150. The element connects nodes 19 and 20 and is shown in figure 5.12.

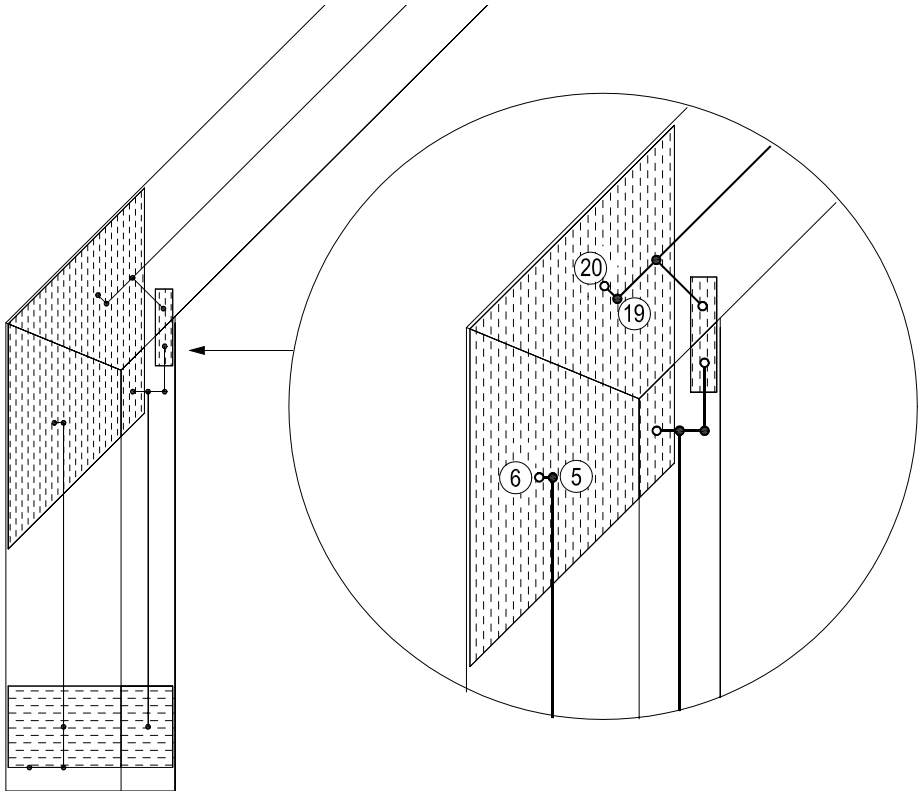

Figure 5.12. Auxiliary element whose properties are important for the stiffness of the knee joint type C150.

In figure 5.13 some small changes have been made to the size of the nail plate in the knee joint type C150. These changes cause the auxiliary element from node 19 to 20 to disappear and therefore the stiffness of this auxiliary element is no longer important.

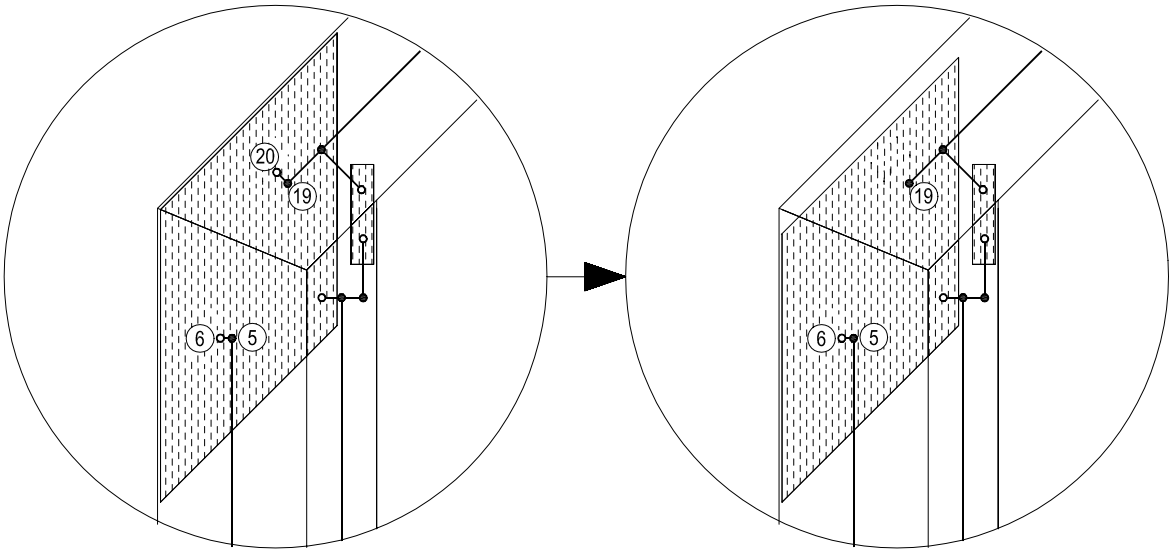

Figure 5.13. Changes of nail plate area so that the stiffness of the auxiliary element is no longer important.

Normally a reduction in the size of the nail plate - as shown in figure 5.13 - will result in a knee joint with decreasing stiffness. However, if the auxiliary elements are given the weak properties the opposite occurs. Due to this reason the auxiliary elements are given the stiff properties.

Influence of the Properties of the Plate Element

The influence of the properties of the plate element is analysed by increasing and decreasing the stress level, respectively, where the plate beams start yielding in tension and buckling in compression with 25%. The stiffness parameters for the plate element are not changed. The changes to the properties are illustrated in figure 5.14.

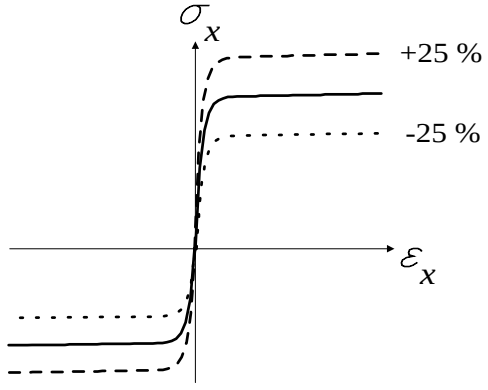

Figure 5.14. Changes in plate properties.

The load-displacement curves with the changed plate properties are shown in figure 5.15.

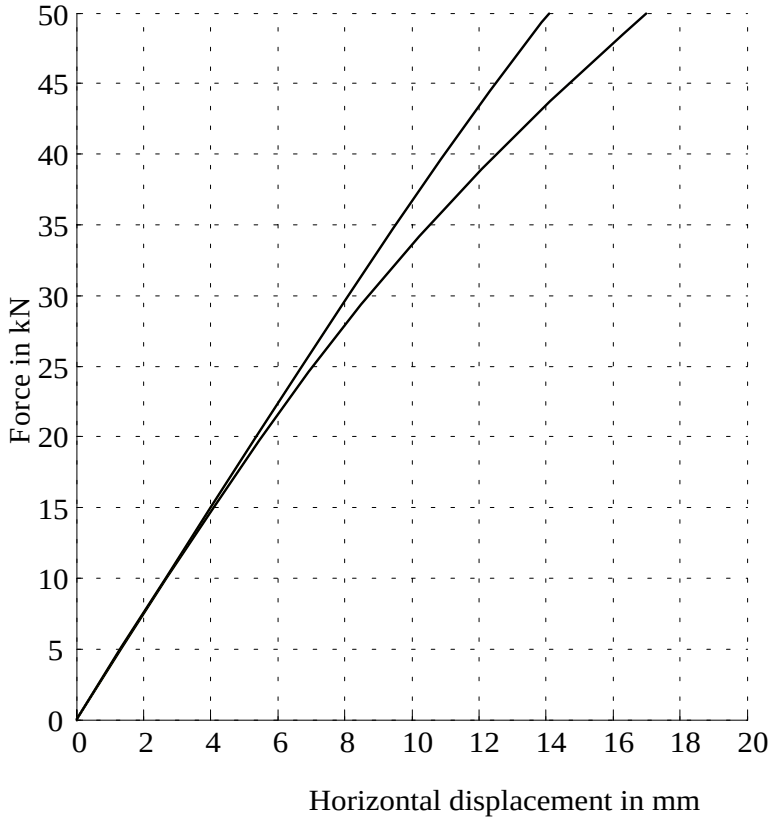

Figure 5.15. Influence on load-displacement curve when the plate properties are weakened by 25% and reinforced by 25%.

The changes do not affect the initial stiffness of the knee joint, but at a load level of 50 kN the difference between the two calculated horizontal displacements is 21%.

It is concluded that even a relatively large change in the plate properties (as illustrated in figure 5.14) does not affect the initial stiffness, but gives changes in the behaviour of the joint at higher load levels.

It should be noted that E150 only consists of the nail plate type GNT150S but it is assumed that the influence of the plate properties is similar for knee joints with the plate type GNA20S.

Influence of the Properties of the Nail Elements

The properties of the nail elements are changed in a similar way as the properties for the plate element were changed (the stress level where the nails start behaving plastic is decreased/increased by 25%, see e.g. figure 5.14). The influence on the load-displacement curve for the knee joint type E150 is shown in figure 5.16.

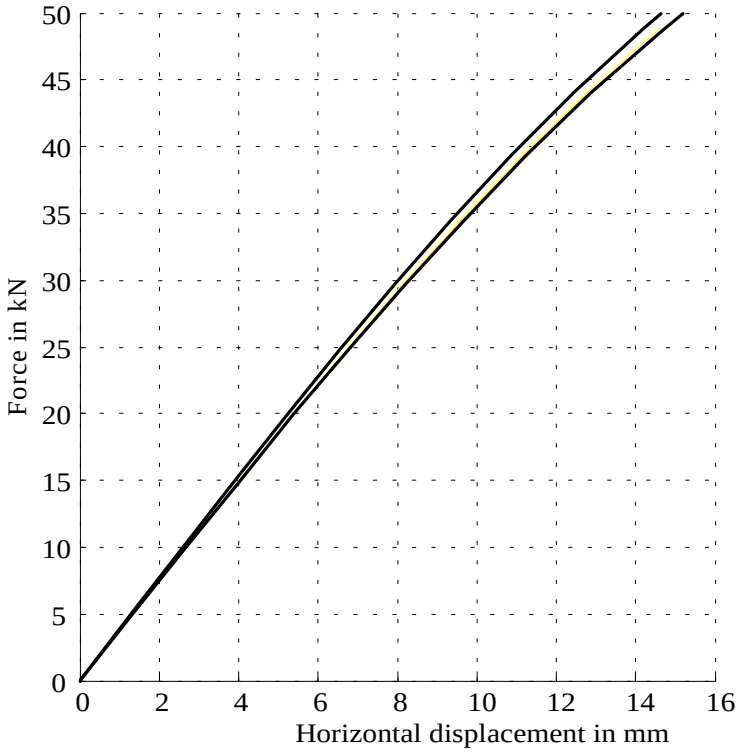

Figure 5.16. Influence on load-displacement curve when the nail properties are weakened by 25% and reinforced by 25%.

The changes only slightly affect (3.5%) the behaviour of the knee joint. Again it should be noted that E150 only consists of the nail plate type GNT150S, but it is assumed that the influence of the nail properties is similar for knee joints with the plate type GNA20S. However, for other types of the knee joint the changes may result in larger differences in the load-displacement curves. This could be the case for those knee joint types, where the anchorage stresses are close to the anchorage capacity.

Influence of the Properties of the Contact Elements

The influence of the different parameters of the contact elements is analysed. The analysis only considers the contact element that connects the rafter with the inner leg – see e.g. figure 5.7. Four conditions are considered:

- Mutual differences between the force levels, where contact occurs for the different types of knee joint.
- Influence of the location of the nodes that the contact element refers to.
- Influence of contact or not and the influence of the gap size.
- Influence of the length of the contact beam elements.

The load level where contact between the rafter and the inner leg of the knee joint occurs is shown in table 5.2 for some of the knee joints. In these calculations the initial gap of the contact elements is taken as 1 mm.

A150	B150	C150	D150	E150	F150	J150
43 kN	38 kN	38 kN	38 kN	41 kN	11 kN	50 kN
A20	B20	C20		ET150		JT150
40 kN	25 kN	30 kN		42 kN		38 kN

Table 5.2. Load level where the gap is closed and contact develops. The initial gap size is taken as 1 mm.

As seen from the table the load levels are different when contact develops. However, a tendency is that the gap closes earlier for the knee joints with the GNA20S nail plate compared to the knee joints with the GNT150S nail plate (see the knee joint types A, B and C). This is also expected since the GNT150S nail plate has higher stiffness and load capacity in compression than the GNA20S nail plate.

It is also seen that contact develops at a low load level for the series F150. This may be due to the fact that there is no nail plate in the region between the inner leg and the rafter in this series.

When considering the series E150, ET150, J150 and JT150 it is difficult to obtain a clear indication whether a thin leg causes the gap to close at a lower load level or not. It should be noted that the moduli of elasticity for the timber beams used in these four series are of the same order so that this cannot explain the unexpected results.

If the gap size is taken as 0.1 mm the contact is established at a significantly lower load level. For series A150 the gap is closed at a load level of 8 kN if the initial gap size is taken as 0.1 mm.

A model of series A150 without the small nail plate at the inner corner of the knee joints has been tested. Contact is then present at a load level of 31 kN and the influence on the horizontal displacements is 8% (initial gap size taken as 1 mm). As expected the analysis shows that the horizontal displacements increase when the nail plate is removed from the model.

To analyse if the location of the nodes to which the contact element refers has an influence on the load level where the gap closes, two different TRUSSLAB models with knee joint type C150 have been set up. In one model the contact element connects nodes 14 and 16, whereas in the other model the contact element connects nodes 14 and 26, see figure 5.17.

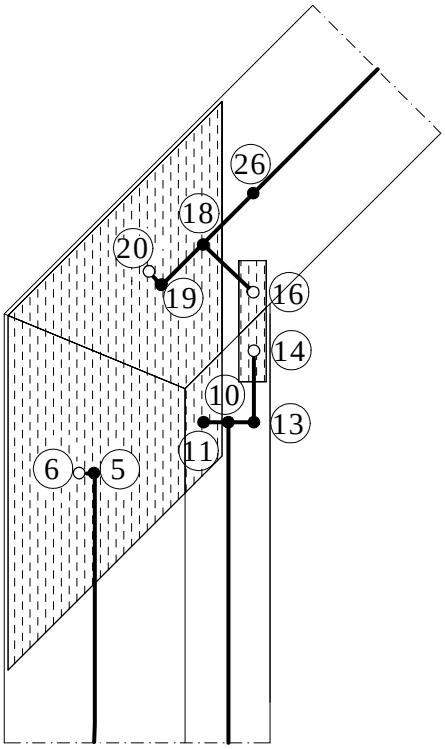

Figure 5.17. Location of nodes for the knee joint type C150.

From the load-displacement curves it is found that the horizontal deformation at maximum load level only differs by less than 1.5% for the two TRUSSLAB models. Furthermore, the load levels where the gaps are closed are almost identical. It is concluded that the choice of nodes for the contact element only slightly changes the behaviour of joints.

The influence of the size of the gap is shown in figure 5.18, where the knee joint type C150 is used again. Four models with different gaps have been set up to see the effect of the size of the gap and to see which effect is has whether the contact element is active or not. The load-displacement curves for these models are shown in figure 5.18.

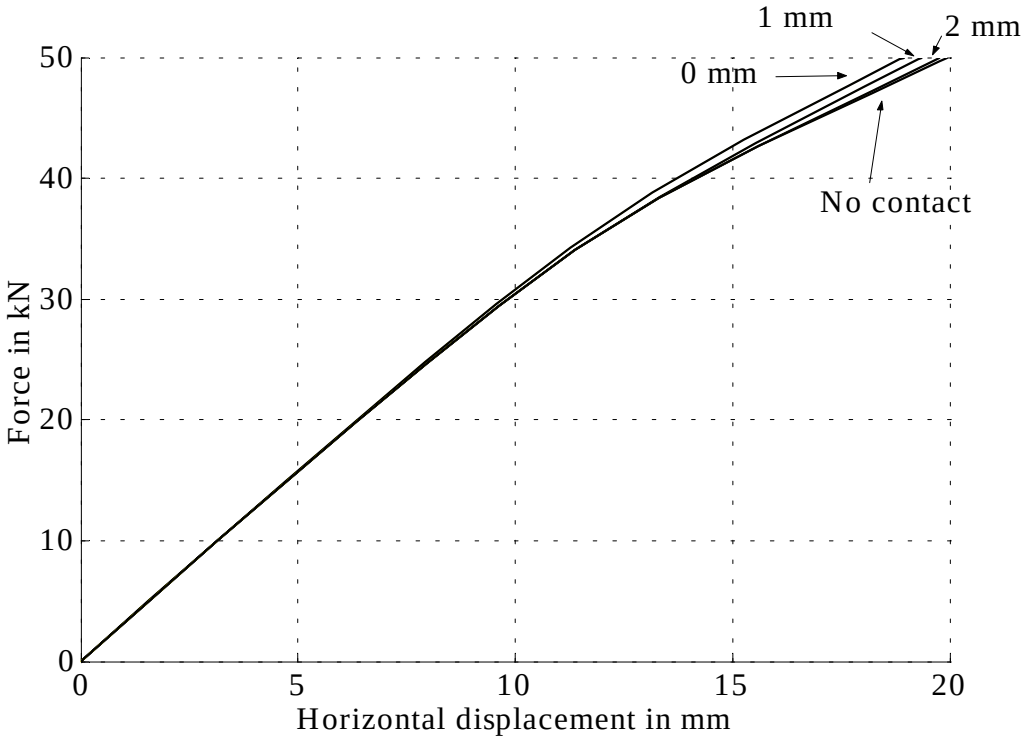

Figure 5.18. Knee joint type C150 with and without the contact element between the rafter and the inner leg.

The difference between the model with full contact and the model with no contact is 5% when the displacements at maximum load level are considered. For the model with an initial gap size of 1 mm, the contact element is activated at a load level of 38 kN while the load level is 45 kN for the model with an initial gap of 2 mm.

It is chosen to use a gap size of 0.1 mm for all the contact elements. Due to the relatively precise production of the knee joints this seems to be a reasonable choice.

Two models with the length of the contact beams taken as 20 mm and 100 mm, respectively, show that the difference in the behaviour of the knee joint is minimal. In the further TRUSSLAB calculations it is chosen to take the length of the beams in the contact element as 100 mm.

Influence of Second Order Theory

To analyse the influence of second order theory a model has been set up in a finite element program CALFEM, where it is possible both to use first order theory and second order theory (CALFEM is a finite element toolbox to MATLAB and is developed at Lund University, Sweden). The model only uses five beam elements, see figure 5.19.

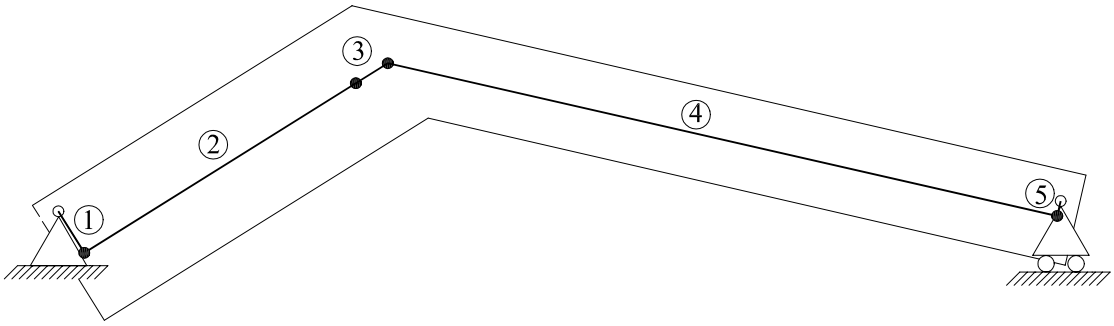

Figure 5.19. Finite element model used to analyse the effect of second order theory.

The elements no. 2 and no. 4 are given the properties of the leg and the rafter, respectively. Element no. 3 is used to model the behaviour of the joint. The properties of this element are determined so the deformation of the knee joint is of the same order as in TRUSSLAB (a horizontal displacement on 20 mm at a load level on 50 kN).

The load-displacement curves for the models are shown in figure 5.20.

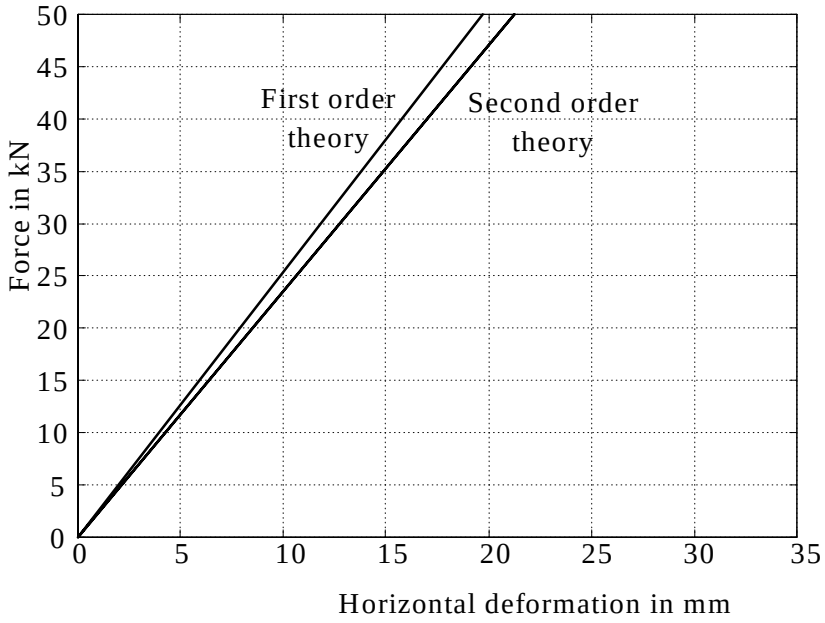

Figure 5.20. Difference between first and second order theory.

Use of the second order theory causes the deformations to increase by 8%.

5.3 Comparisons Between Test Results and Results from TRUSSLAB

The results from the knee tests are compared with results from calculations using TRUSSLAB. Comparisons are made of load-displacement curves and of the ultimate loads and failure modes.

5.3.1 Load-Displacement Curves

During testing the displacements are measured at four or five different locations – see appendix C.2.3. A comparison between the measured horizontal displacements (number 1 in figure 5.21) and the calculated corresponding displacements is made for all the test specimens. Furthermore, for some of the test specimens a comparison between the measured displacement between the inner leg and the rafter (number 2 in figure 5.21) and the shear displacement between the two legs (number 3 in figure 5.21) is performed. The rest of the displacement transducers are not used for comparison.

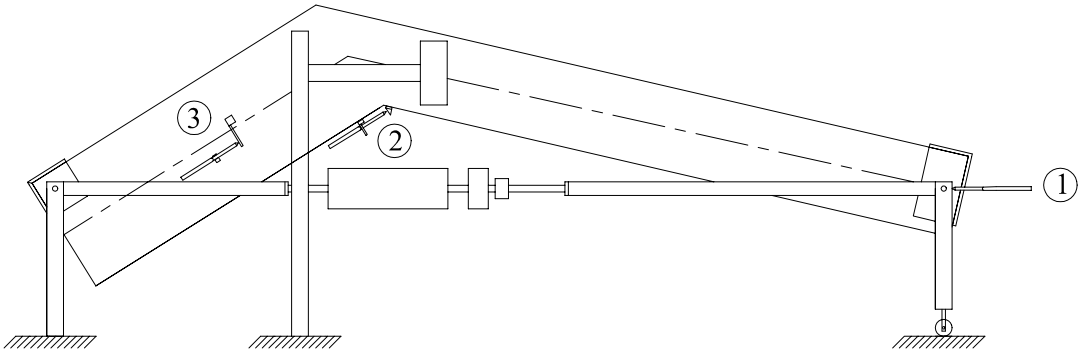

Figure 5.21. Location of displacement transducers used for comparison.

In order to "add" the effect of second order theory the calculated displacements in TRUSSLAB are multiplied by 1.08. This is the factor for the overall displacement.

The measurements collected during the initial loading and unloading procedure are omitted in the shown load-displacement curves because in many cases they only disturb the plots. The calculated load-displacement curves from TRUSSLAB are given a horizontal offset to make the curves comparable with the curves from the tests (the initial slip is omitted).

The measured load-displacement curves are shown as thin lines while the corresponding curves given by TRUSSLAB are shown as thick lines.

In the figures 5.22 to 5.45 comparisons between the tests and TRUSSLAB are shown. Only the horizontal deformation is considered in these figures. In the four cases where two nail plates are on top of each other it should be noted that no calculations have been made in TRUSSLAB. The results from the testing of these four series are shown for comparison with the rest of the series. The calculations in TRUSSLAB are proceeded up to a load level on 50 kN and are not stopped due to failure in the timber or in the nail plate.

The testing is stopped close to failure and the displacement transducers are dismounted. Then the testing is proceeded until failure is reached and the ultimate load level is noted. The load levels increase 0-2 kN after the displacement transducers are dismounted and before the ultimate load level is reached.

In TRUSSLAB only one model is made for each of the test series. Each of the timber beams in the models is given an average modulus of elasticity that is calculated from the timber beams in the corresponding test specimens, i.e. the modulus of elasticity for the rafter in the series A20 is determined as an average value of the two moduli of elasticity for the two rafters in the test series A20.

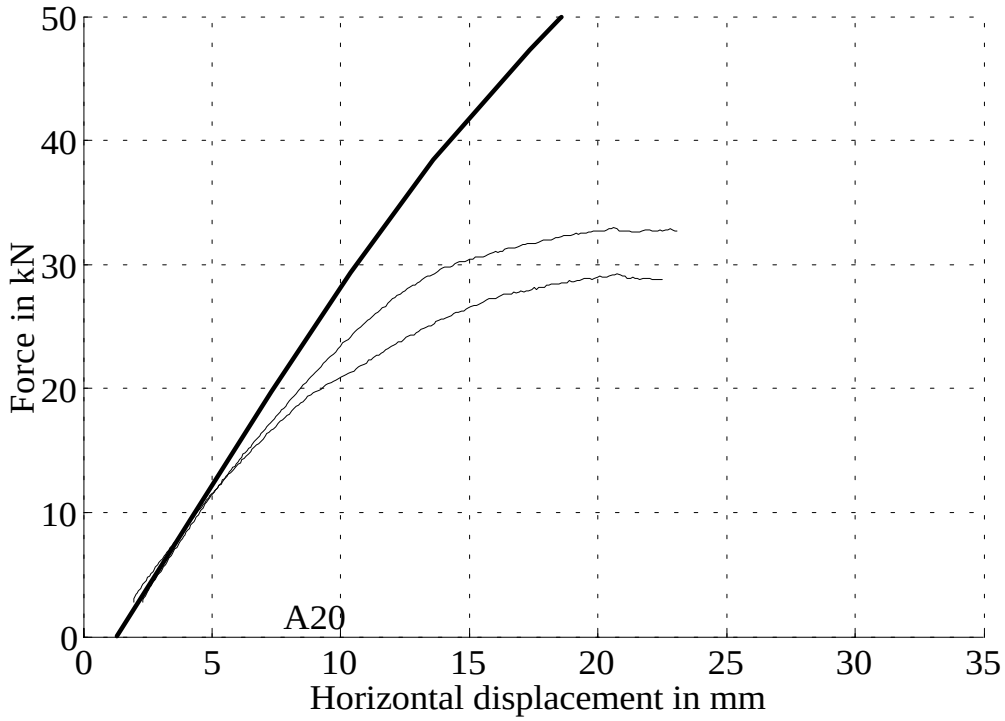

Figure 5.22. Load-displacement curves for series A20.

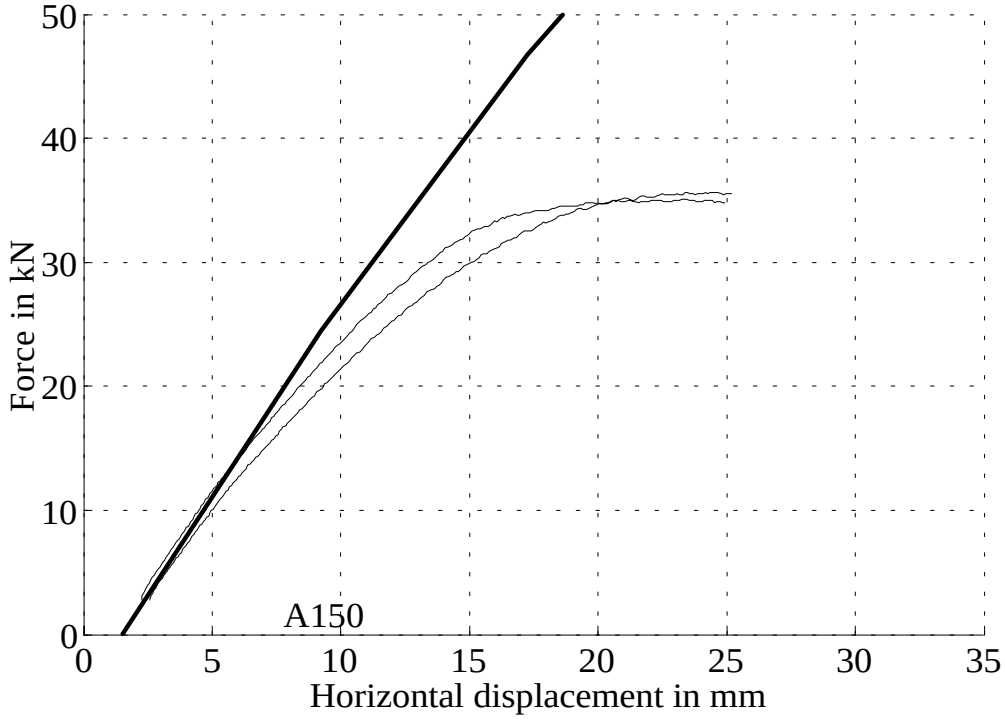

Figure 5.23. Load-displacement curves for series A150.

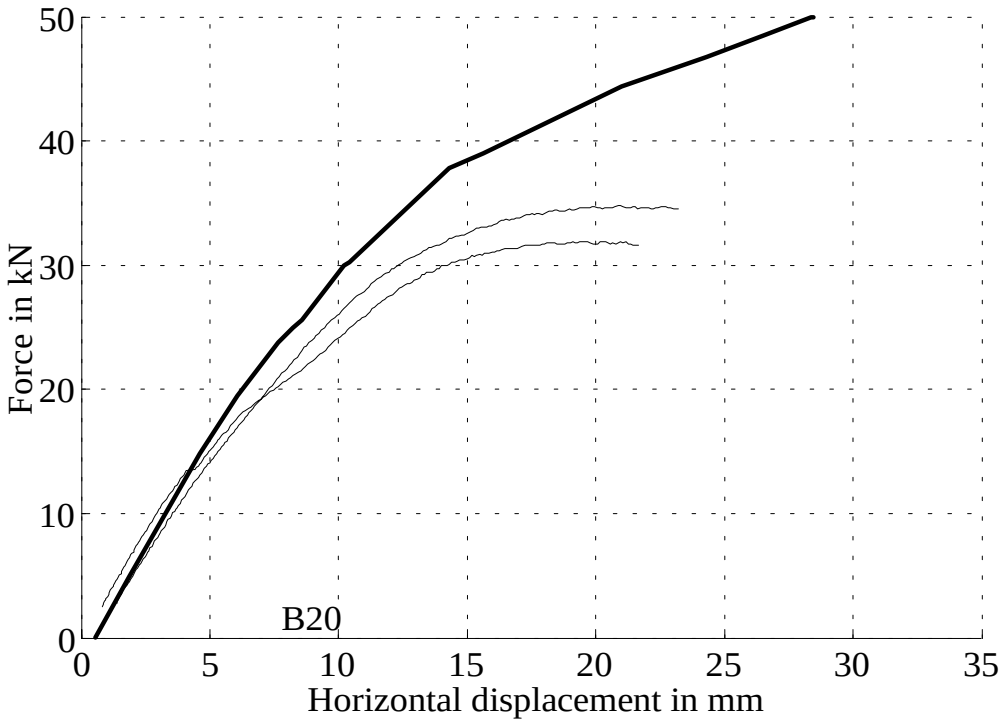

Figure 5.24. Load-displacement curves for series B20.

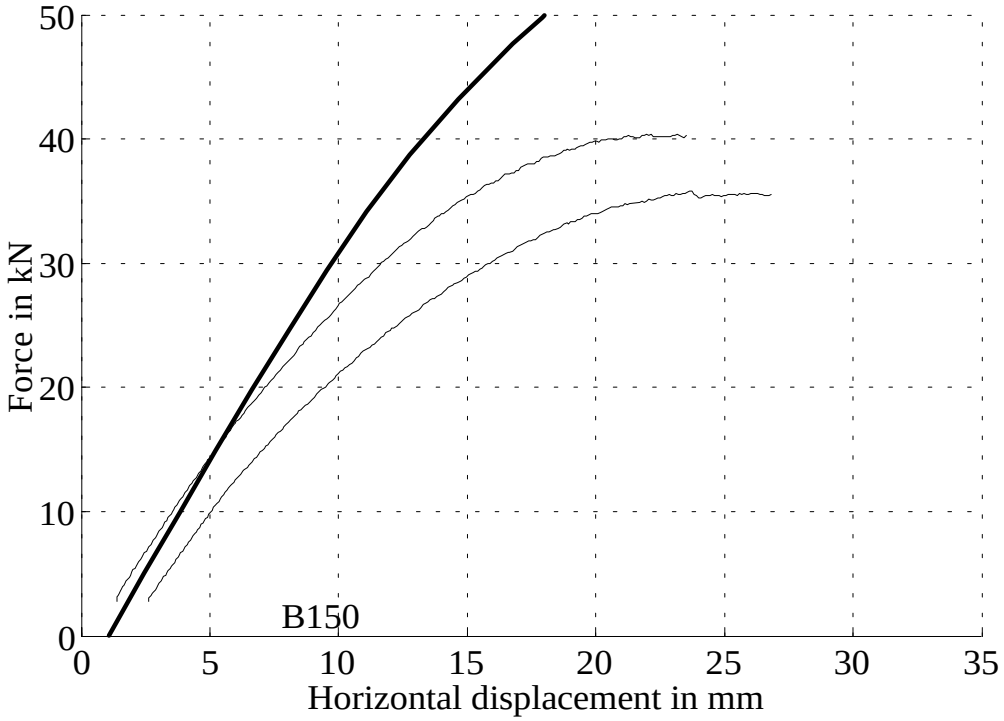

Figure 5.25. Load-displacement curves for series B150.

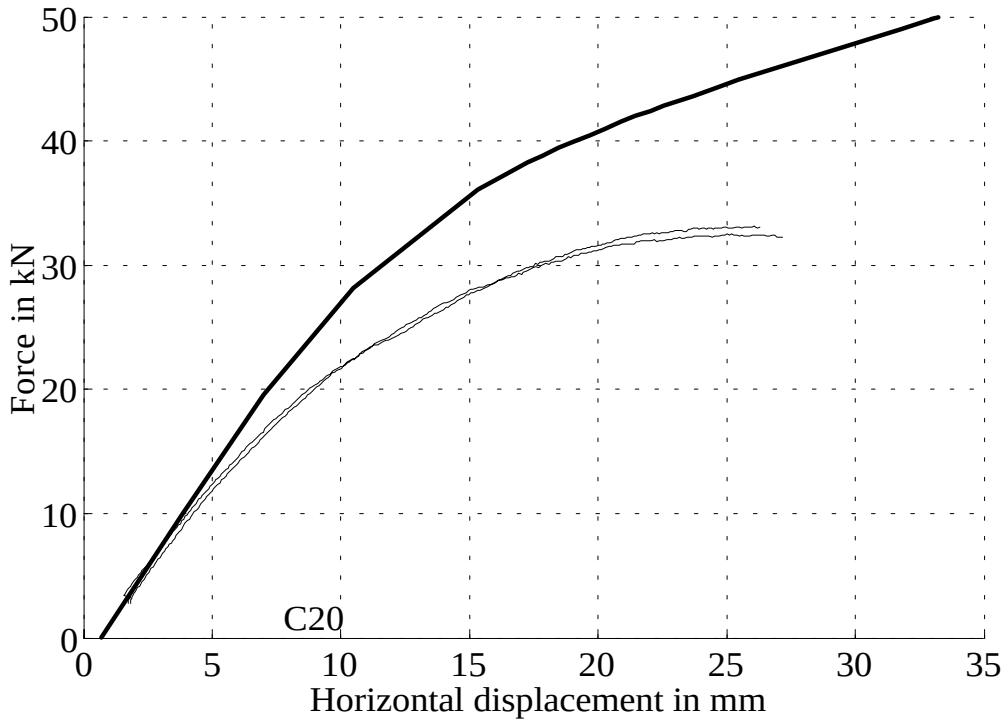

Figure 5.26. Load-displacement curves for series C20.

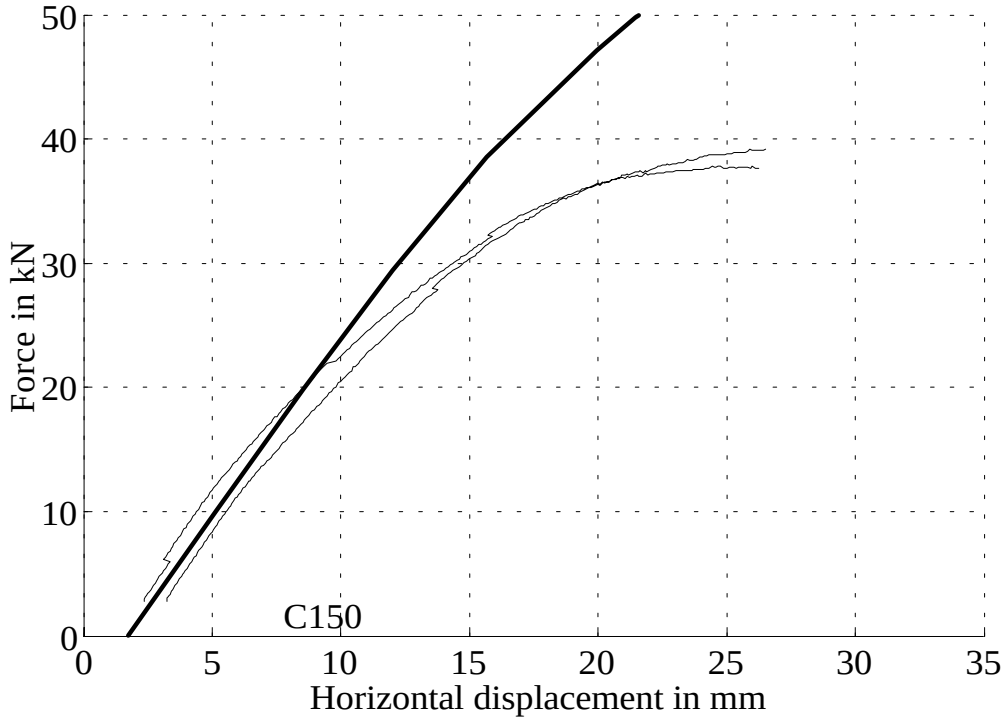

Figure 5.27. Load-displacement curves for series C150.

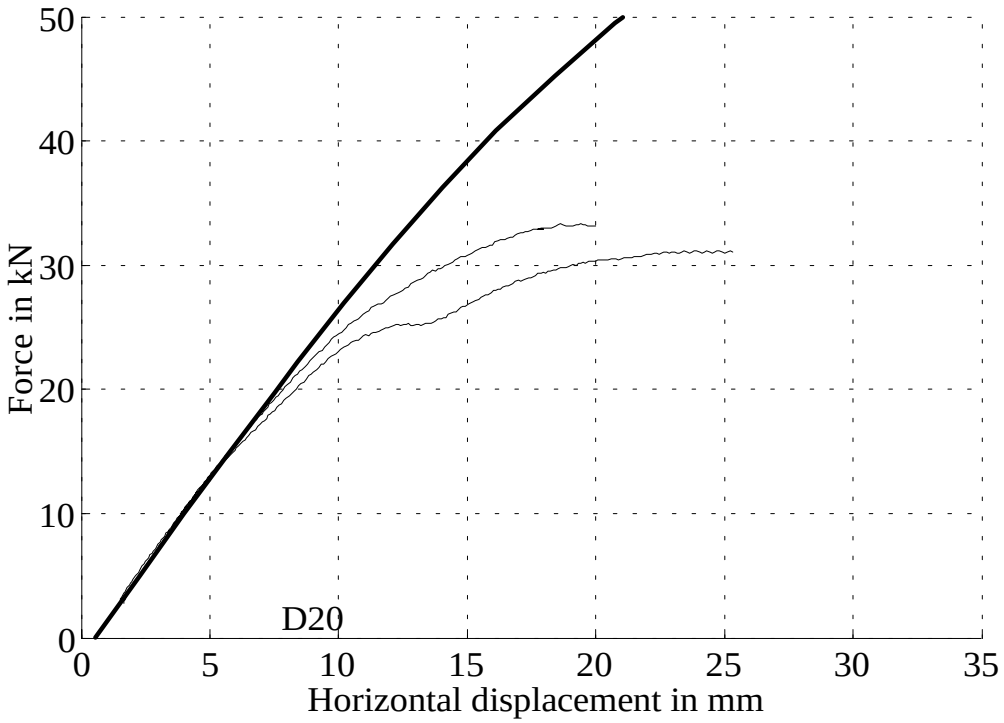

Figure 5.28. Load-displacement curves for series D20.

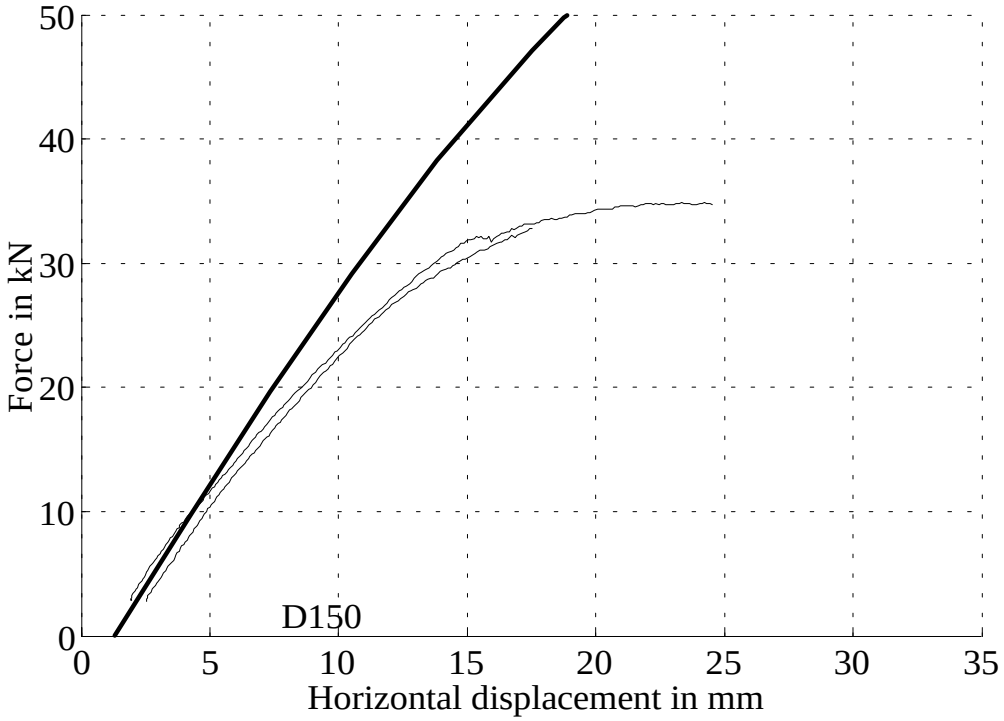

Figure 5.29. Load-displacement curves for series D150.

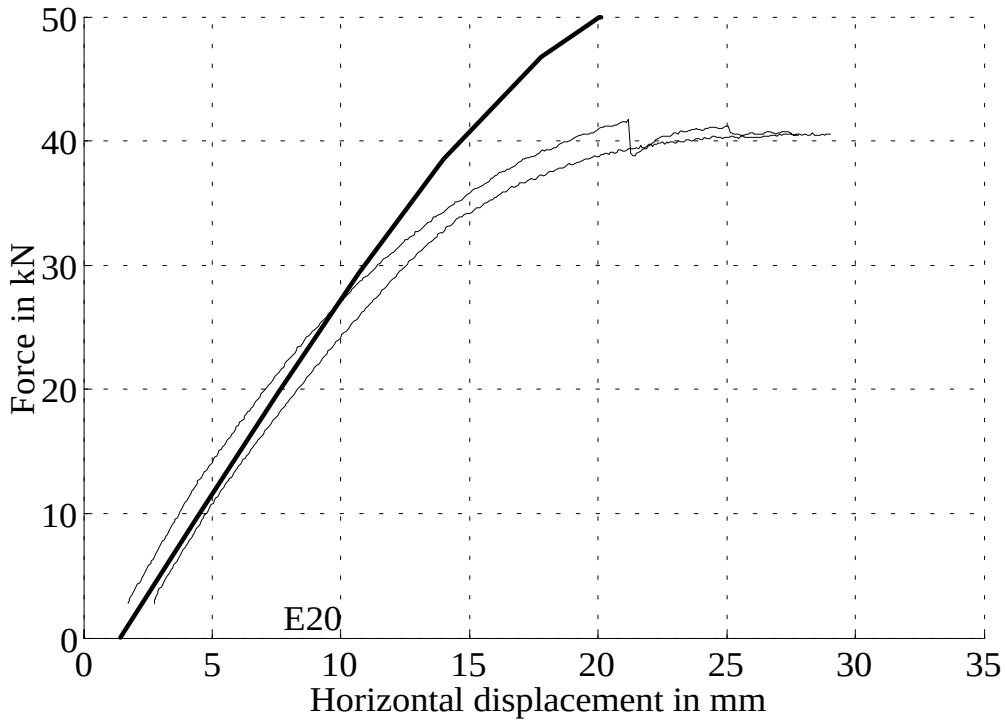

Figure 5.30. Load-displacement curves for series E20.

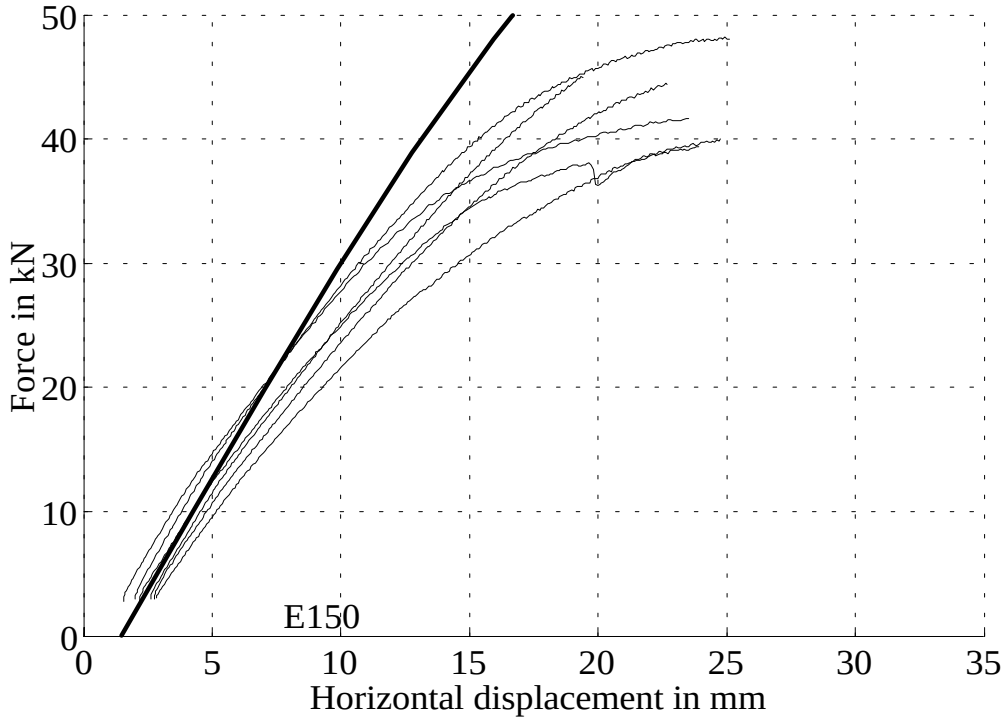

Figure 5.31. Load-displacement curves for series E150.

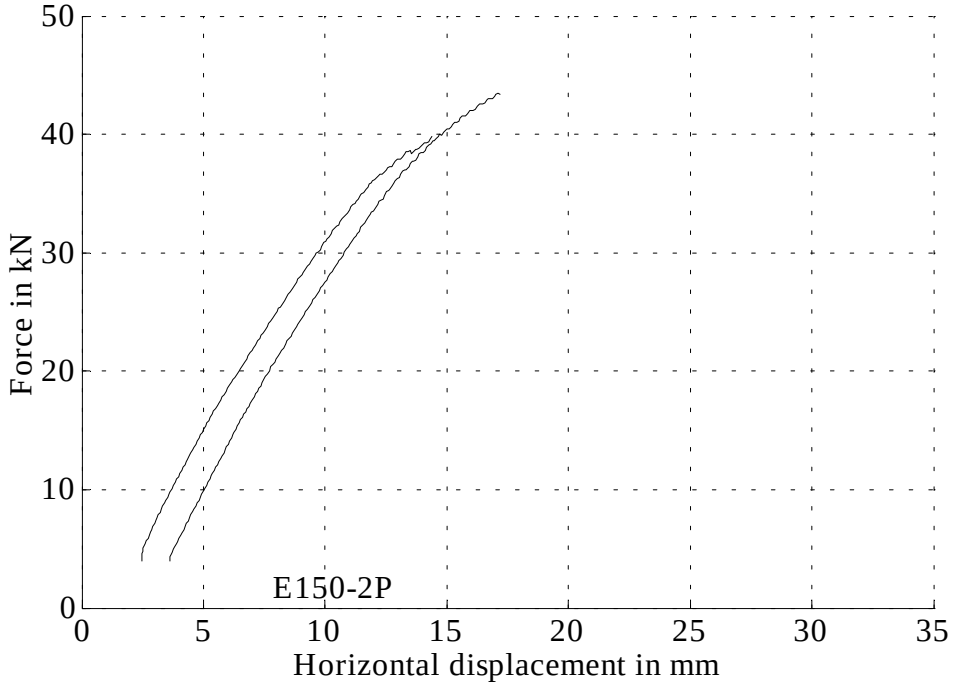

Figure 5.32. Load-displacement curves for series E150-2P. No predictions are given by TRUSSLAB since the properties of two nail plates on top of each other have not been determined.

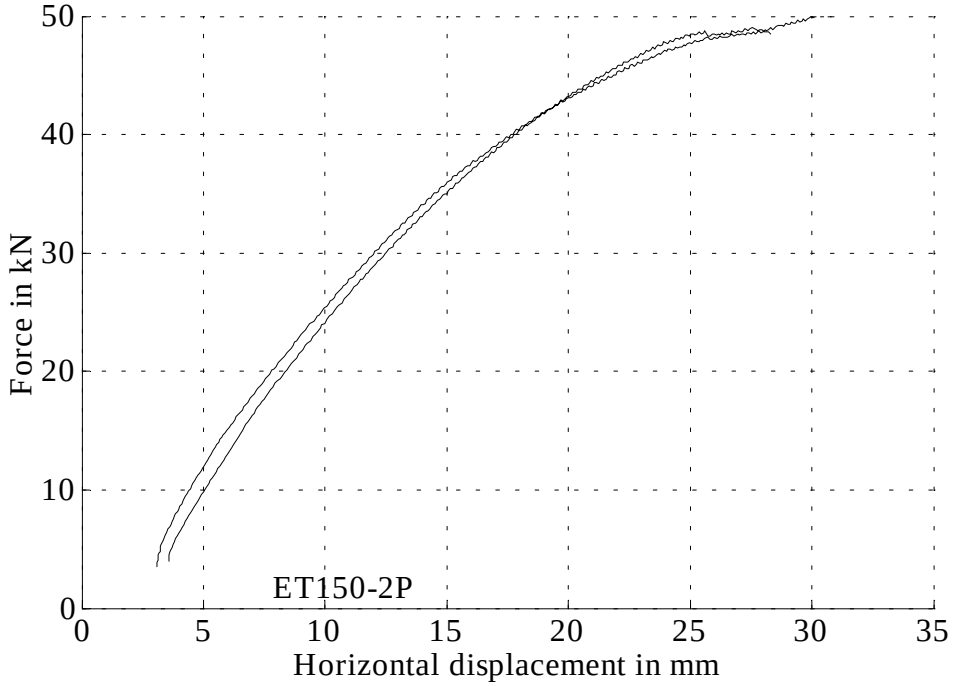

Figure 5.33. Load-displacement curves for series ET150-2P. No predictions are given by TRUSSLAB since the properties of two nail plates on top of each other have not been determined.

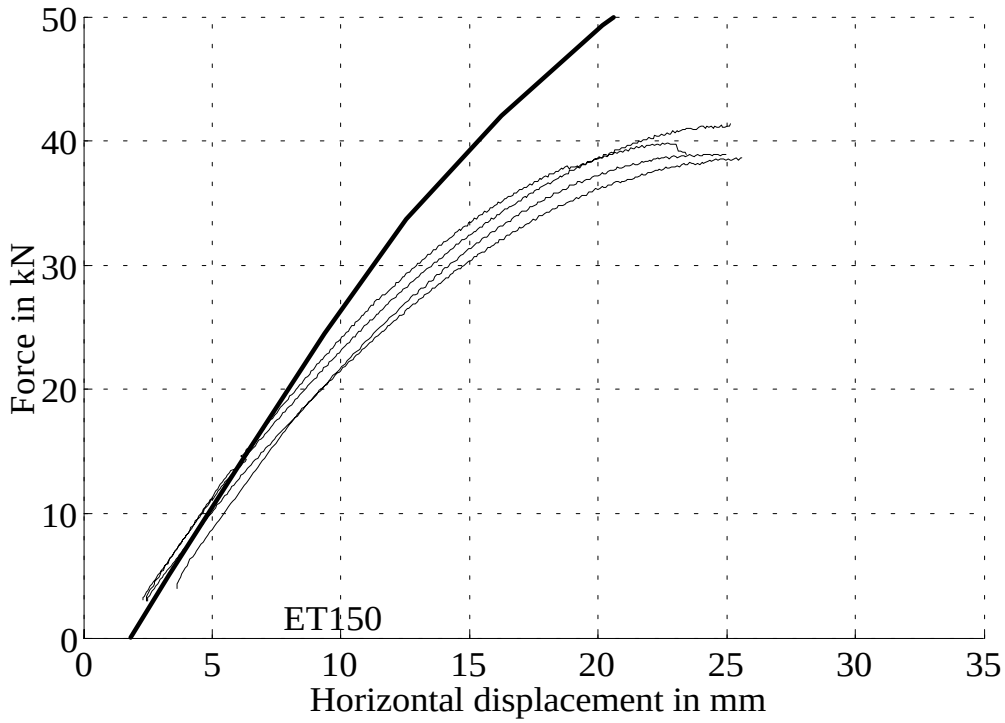

Figure 5.34. Load-displacement curves for series ET150.

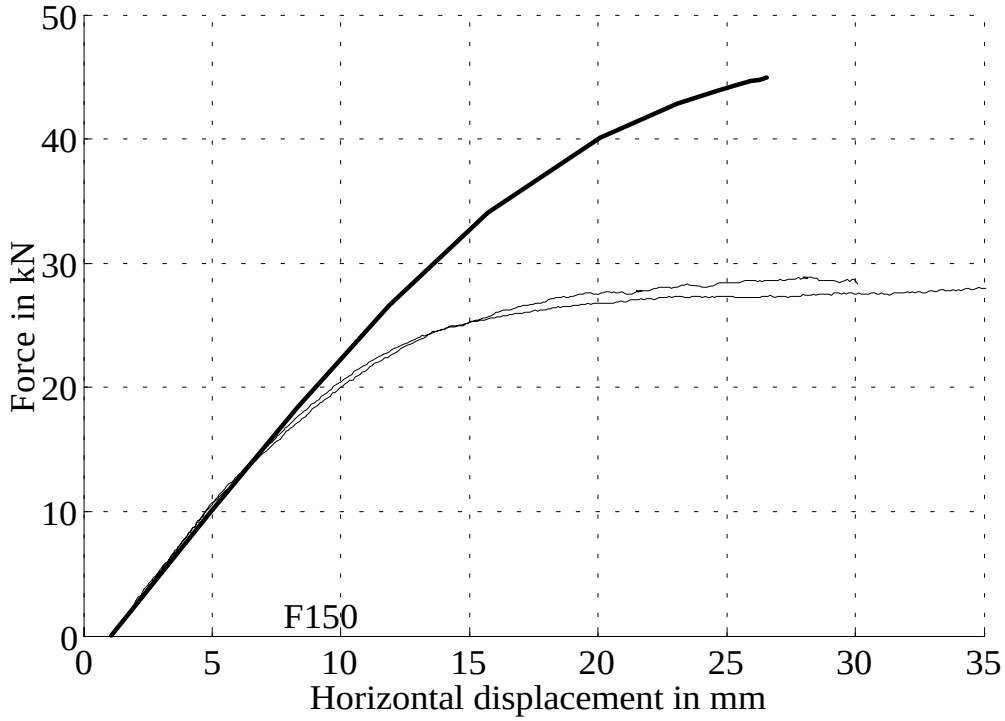

Figure 5.35. Load-displacement curves for series F150.

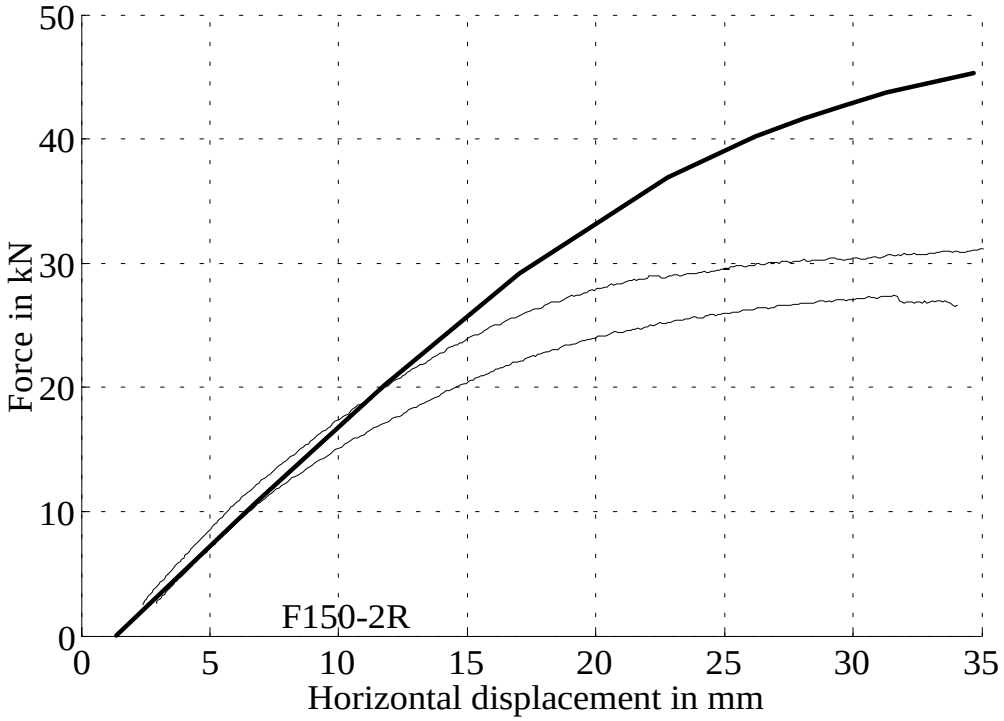

Figure 5.36. Load-displacement curves for series F150-2R.

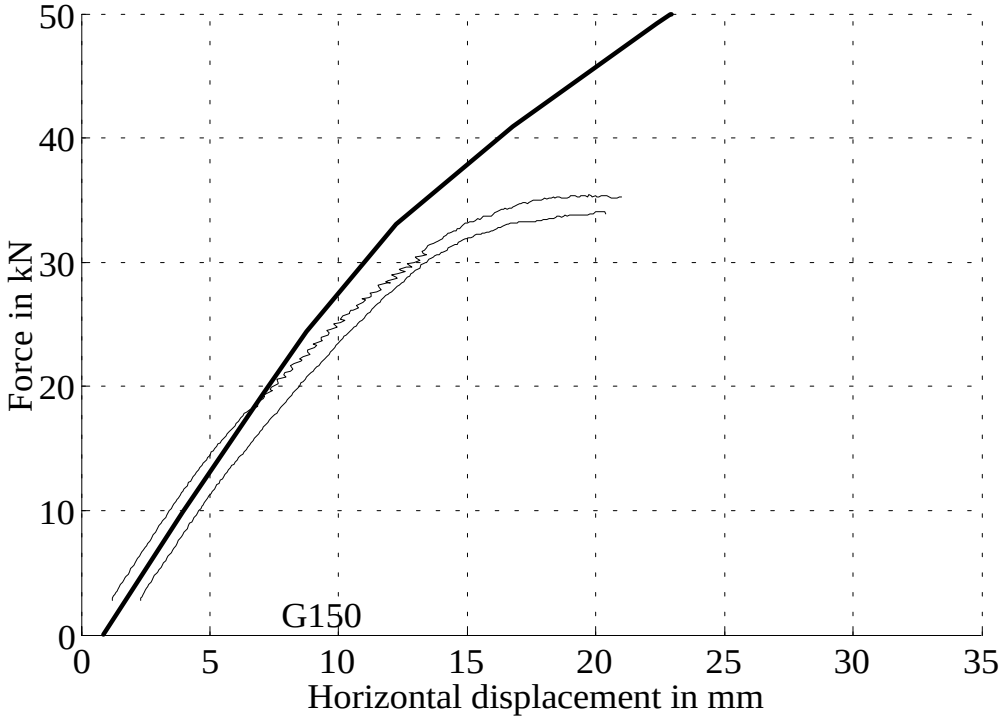

Figure 5.37. Load-displacement curves for series G150.

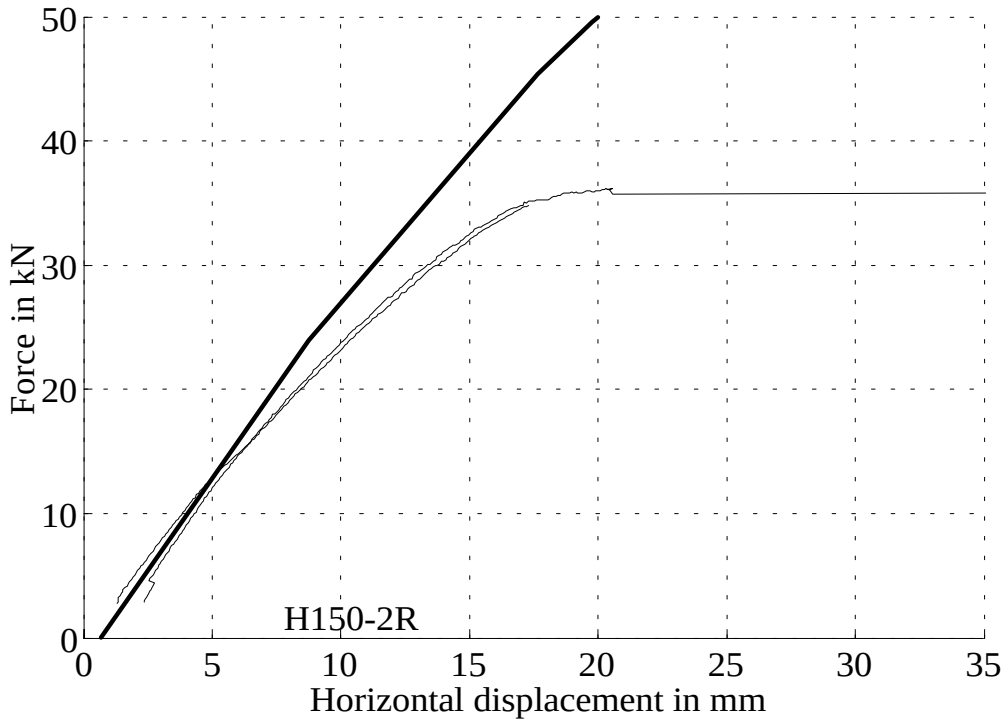

Figure 5.38. Load-displacement curves for series H150-2R.

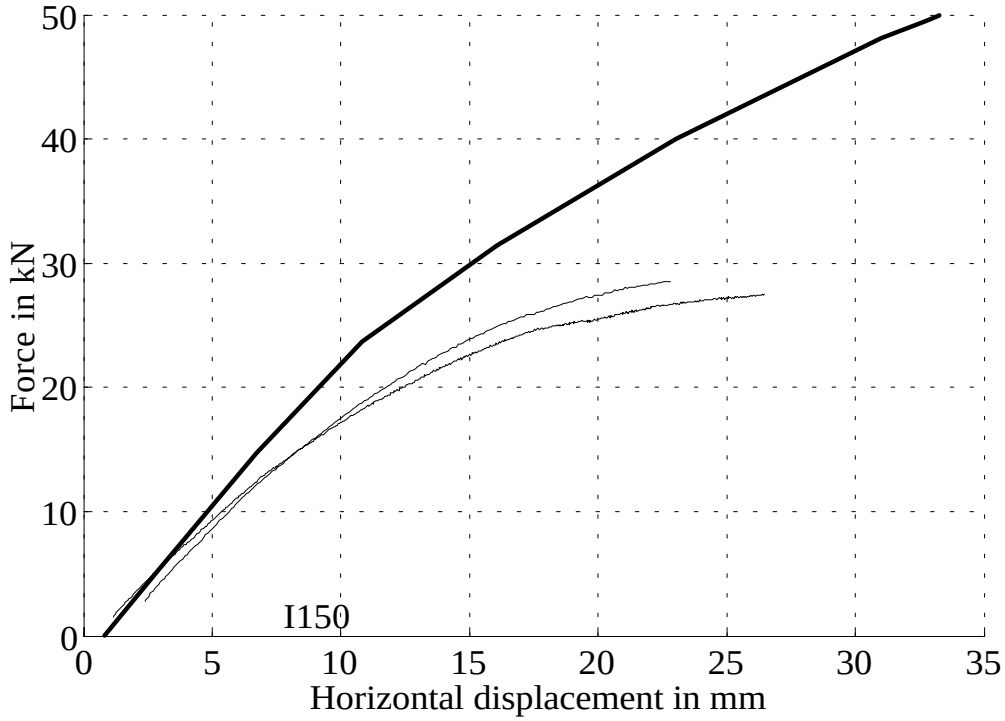

Figure 5.39. Load-displacement curves for series I150.

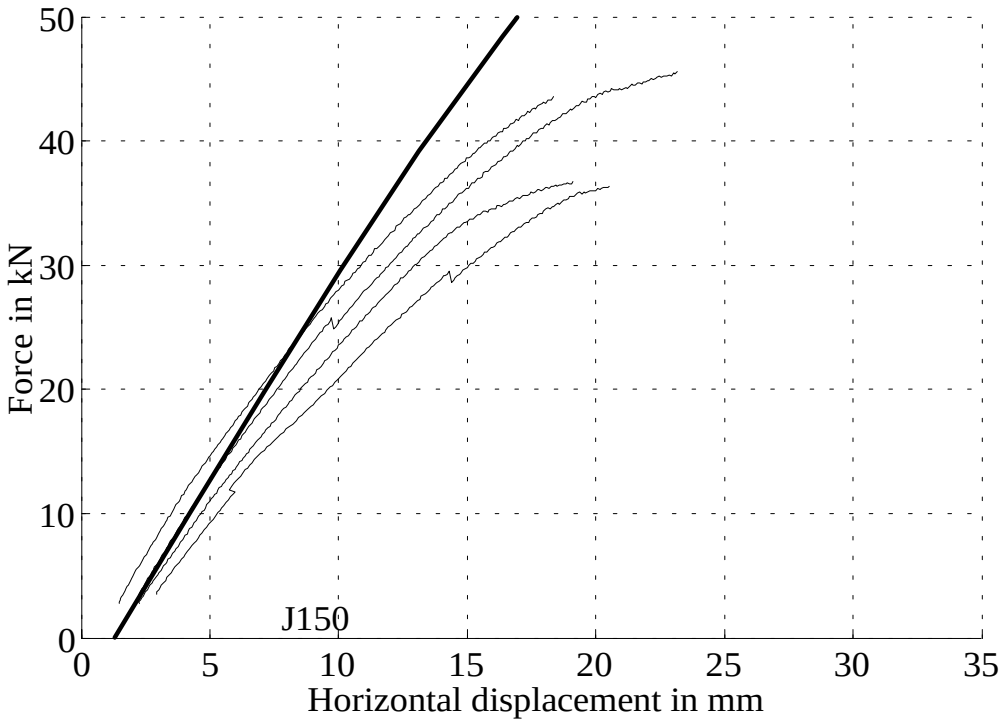

Figure 5.40. Load-displacement curves for series J150.

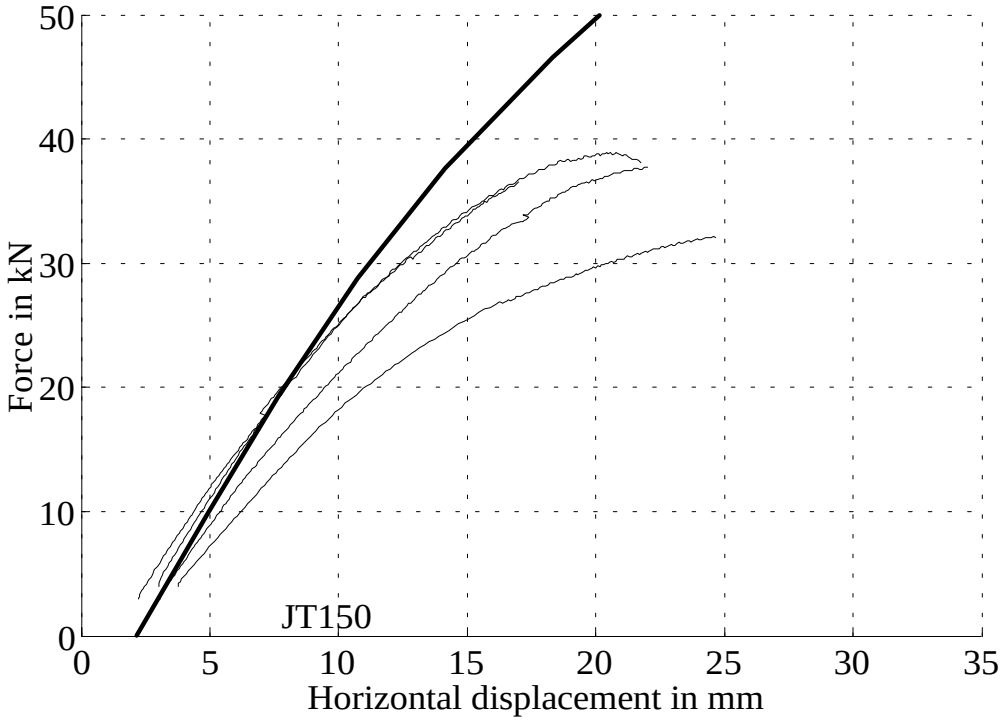

Figure 5.41. Load-displacement curves for series JT150.

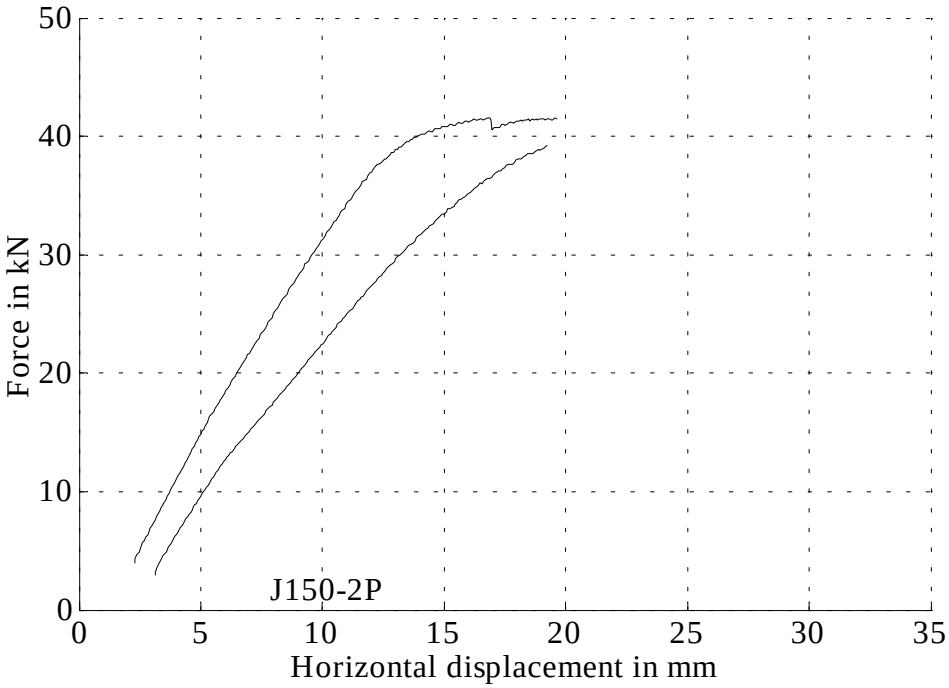

Figure 5.42. Load-displacement curves for series J150-2P. No predictions are given by TRUSSLAB since the properties of two nail plates on top of each other have not been determined.

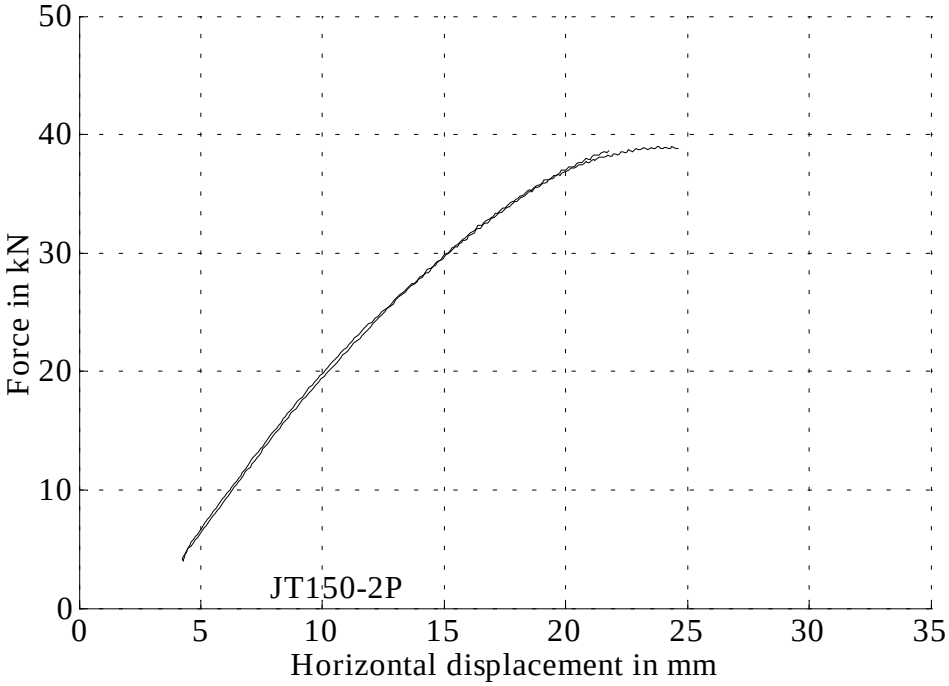

Figure 5.43. Load-displacement curves for series JT150-2P. No predictions are given by TRUSSLAB since the properties of two nail plates on top of each other have not been determined.

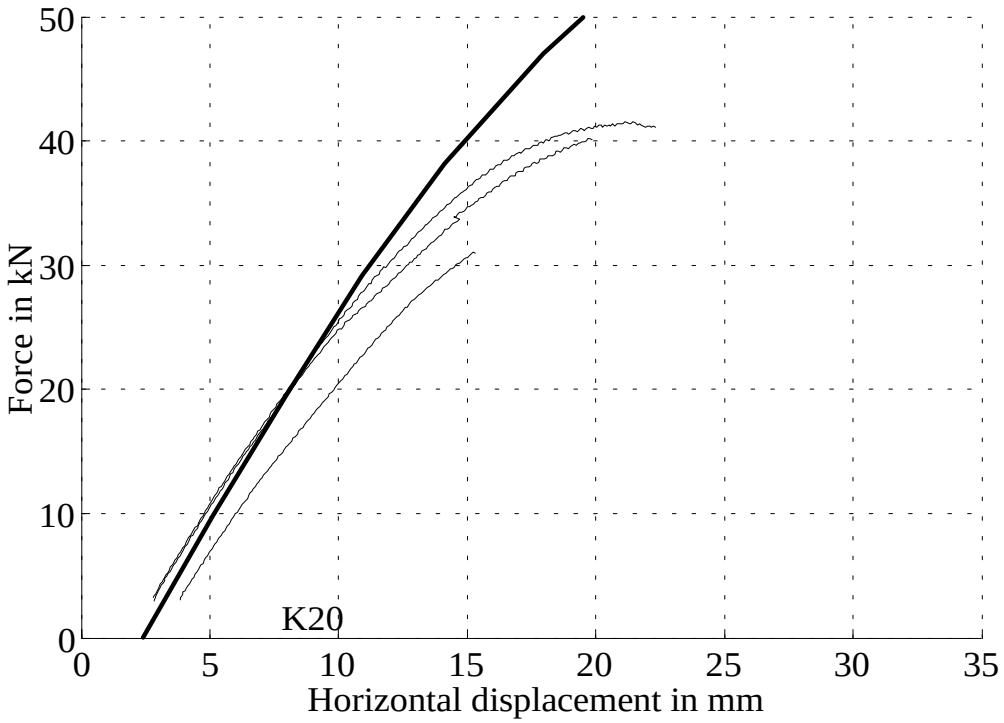

Figure 5.44. Load-displacement curves for series K20.

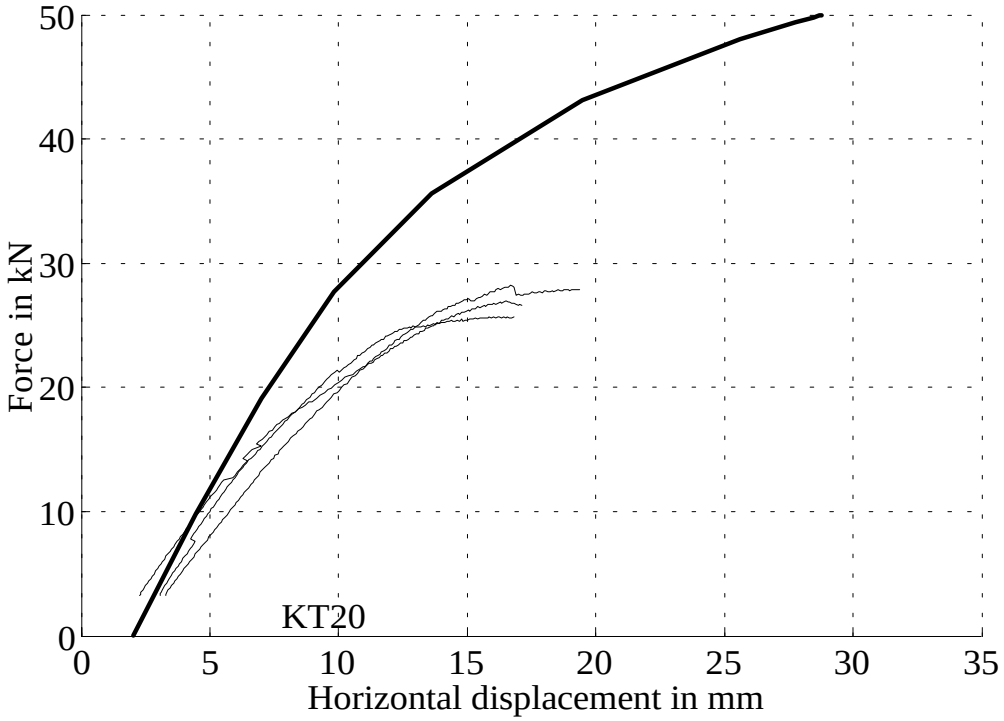

Figure 5.45. Load-displacement curves for series KT20.

For the TRUSSLAB models of the series F150-2R and H150-2R it has been necessary to add an extra auxiliary element to make the models behave as the test specimens. This is caused by the support conditions in the test set-up, where the support of the rafter covers both the upper and the lower beam (these two series are produced from a rafter that is composed of two beams). The extra auxiliary element ensures that the rafter beams are unable to perform a mutual shear deformation near the support.

In table 5.3 it can be seen for which series the initial stiffness is predicted well by TRUSSLAB and if the initial stiffness is over- or underestimated (the initial stiffness is determined in the load range 0-10 kN). Furthermore, it is indicated at which load level (40%, 50% or 60% of maximum load level in the tests) TRUSSLAB starts deviating from the test results.

	Initial stiffness			Load level at deviation		
	Under-estimating 10-20%	OK ±10%	Over-estimating 10-20%	40%	50%	60%
A20		X		X		
A150		X			X	
B20		X			X	
B150		X		X		
C20		X		X		
C150		X			X	
D20		X				X
D150		X		X		
E20		X			X	
E150		X		X		
ET150		X		X		
F150		X				X
F150-2R		X				X
G150		X				X
H150-2R		X		X		
I150			X	X		
J150		X		X		
JT150		X			X	
K20		X			X	
KT20			X	X		

Table 5.3. Comparison between results from TRUSSLAB and test results.

From the table it is seen that most of the models in TRUSSLAB are able to predict the initial stiffness well. Again, it is noted that to include the second order theory the deformations in TRUSSLAB have been multiplied by 1.08.

TRUSSLAB is able to predict the behaviour of the knee joints up to a load level of 40-60% of the maximum load level. At higher load levels TRUSSLAB overestimates the stiffness of the joints. The reason for the overestimation may be found in one or more of the following explanations:

- The timber is assumed to show linear-elastic behaviour. In most of the test series compression parallel to the fibres resulted in failure (kinking band) followed by large plastic deformations. This is observed in the rafter near the contact zone with the inner leg. Furthermore, there is a biaxial stress situation in the same area due to the contact forces between the inner leg and the rafter and the bending moment in the rafter. This biaxial stress situation is not taken into account in TRUSSLAB.

- TRUSSLAB is not able to treat the development of cracks/splitting in the timber. In many test series cracks developed at the end of the rafter or in the inner leg.

For the two test series E150 and J150 the measurements from the displacement transducers that measure the deformation between the rafter and the inner leg and the shear between the legs have been compared with corresponding deformations from TRUSSLAB, see e.g. figure 5.21 for the location of the displacement transducers. The figures 5.46 and 5.47 show the deformation between the rafter and the inner leg, and the figures 5.48 and 5.49 show the shear deformation between the legs. Additional auxiliary elements are used in TRUSSLAB to determine the deformations at the relevant locations.

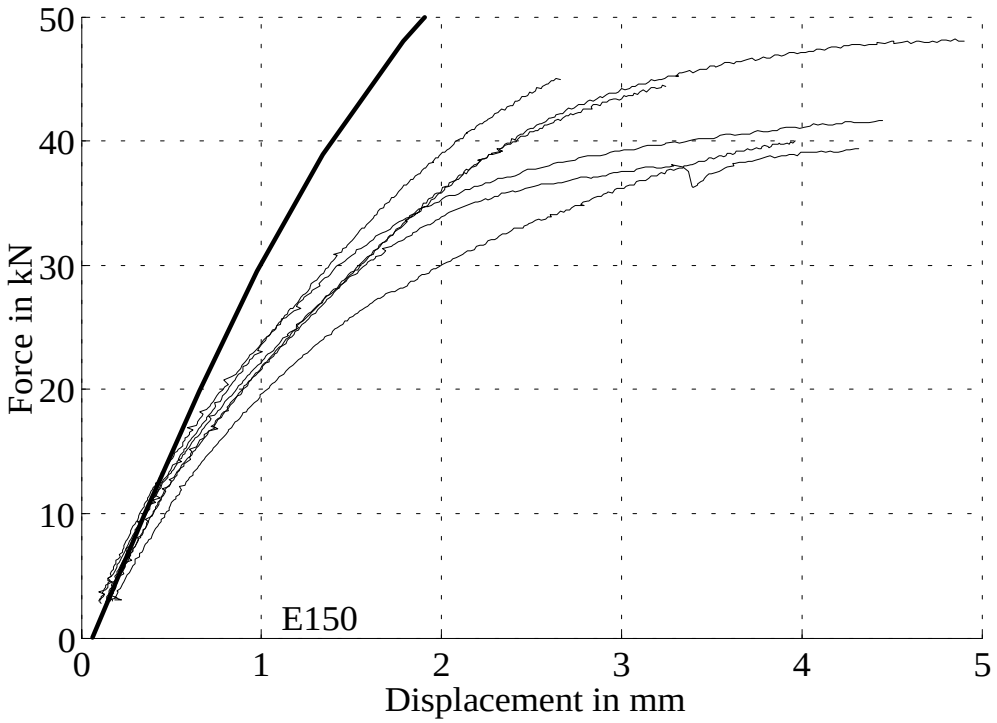

Figure 5.46. Deformation between the rafter and the inner leg for series E150.

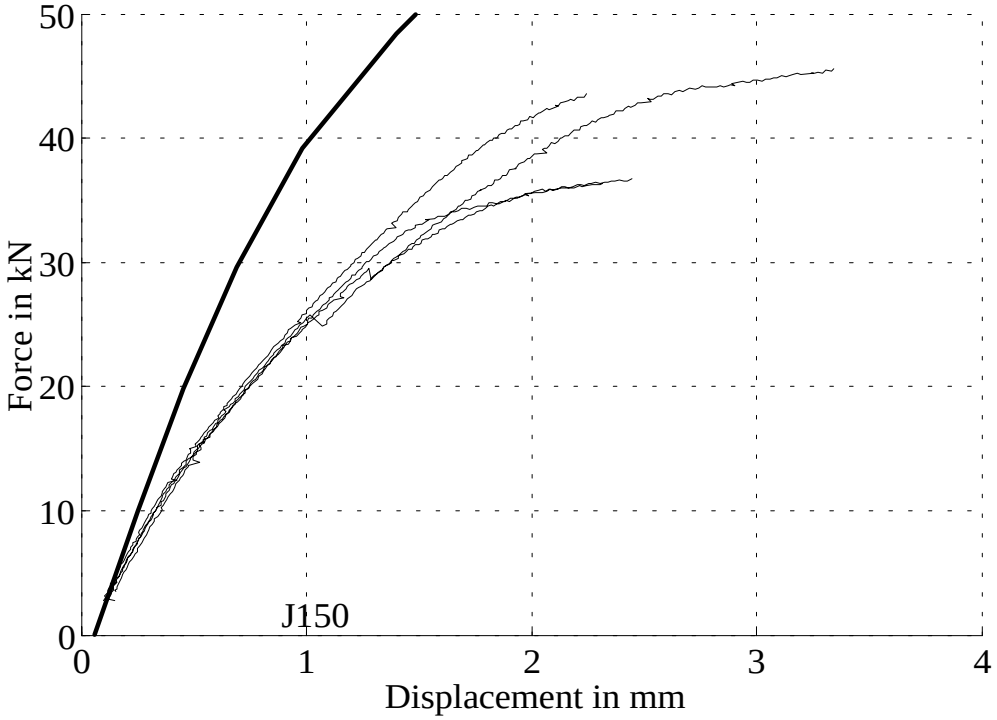

Figure 5.47. Deformation between the rafter and the inner leg for series J150.

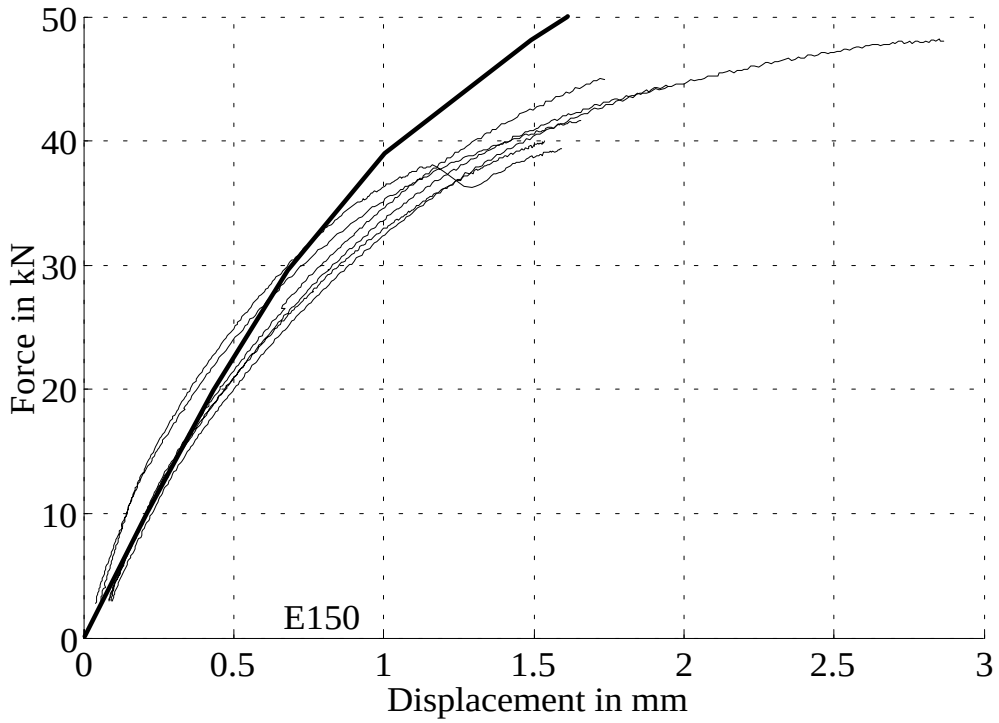

Figure 5.48. Shear deformation between the legs for series E150.

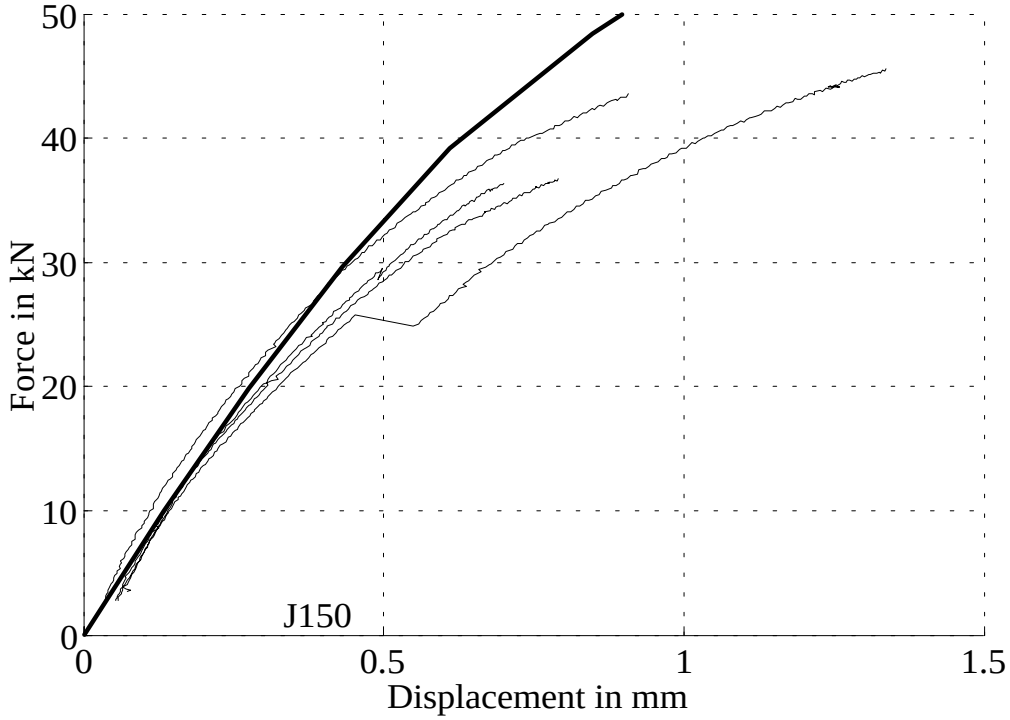

Figure 5.49. Shear deformation between the legs for series J150.

For the series E150 it is seen that TRUSSLAB is able to predict the initial stiffness, while TRUSSLAB overestimates the stiffness at higher load levels. For series J150

the same tendency is seen when the shear deformation is considered, but an overestimation of the initial stiffness is observed for the deformation between the rafter and the inner leg.

5.3.2 Failure Modes and Ultimate loads

During testing the following failure modes are observed – see also figure 5.50:

Timber:
- Compression failure in the rafter parallel to the grain - kinking band.
- Large compression deformations perpendicular to the grain in the rafter at the contact zone between the rafter and the inner leg.
- Shear failure in the rafter or in the leg.
- Splitting of the rafter or the leg.
- Moment failure (tension) in the rafter.

Nail plate:
- Anchorage failure/withdrawal of nails.
- Compression failure/buckling of the nail plate.
- Tension failure in the nail plate
- Shear failure in the nail plate.

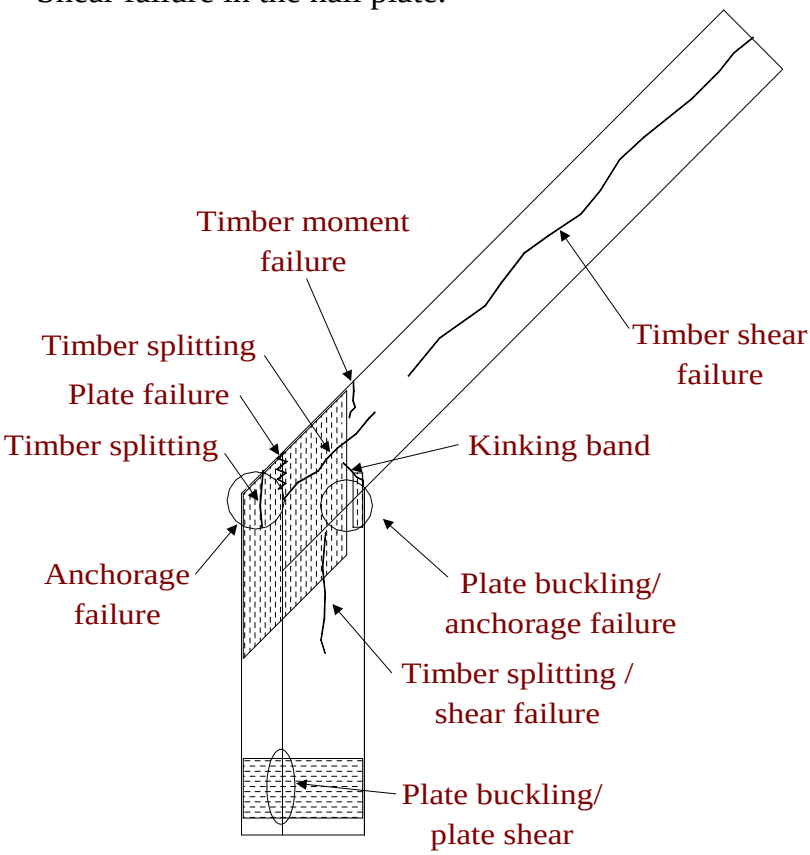

Figure 5.50. Illustration of failure modes.

The two first-mentioned failure modes in the timber (kinking band and large compression deformations perpendicular to the grain direction) are often seen in combination with each other. In some of the test series, however, it is difficult to

determine whether kinking band is present or not due to the nail plate that is covering the timber in this area (e.g. test series A). It has therefore been chosen always to assume that the two failure modes are present if large compression deformations perpendicular to the grain direction are observed in the area.

Photographs of some of the failure modes are shown in the figures 5.51 to 5.56.

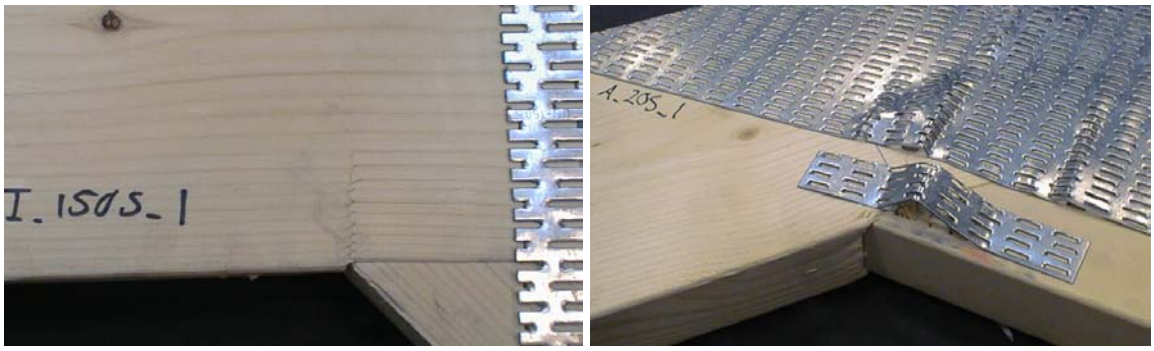

Figure 5.51. Compression between rafter and inner leg, kinking band and plate buckling.

Figure 5.52. Shear failure in the rafter and in the leg.

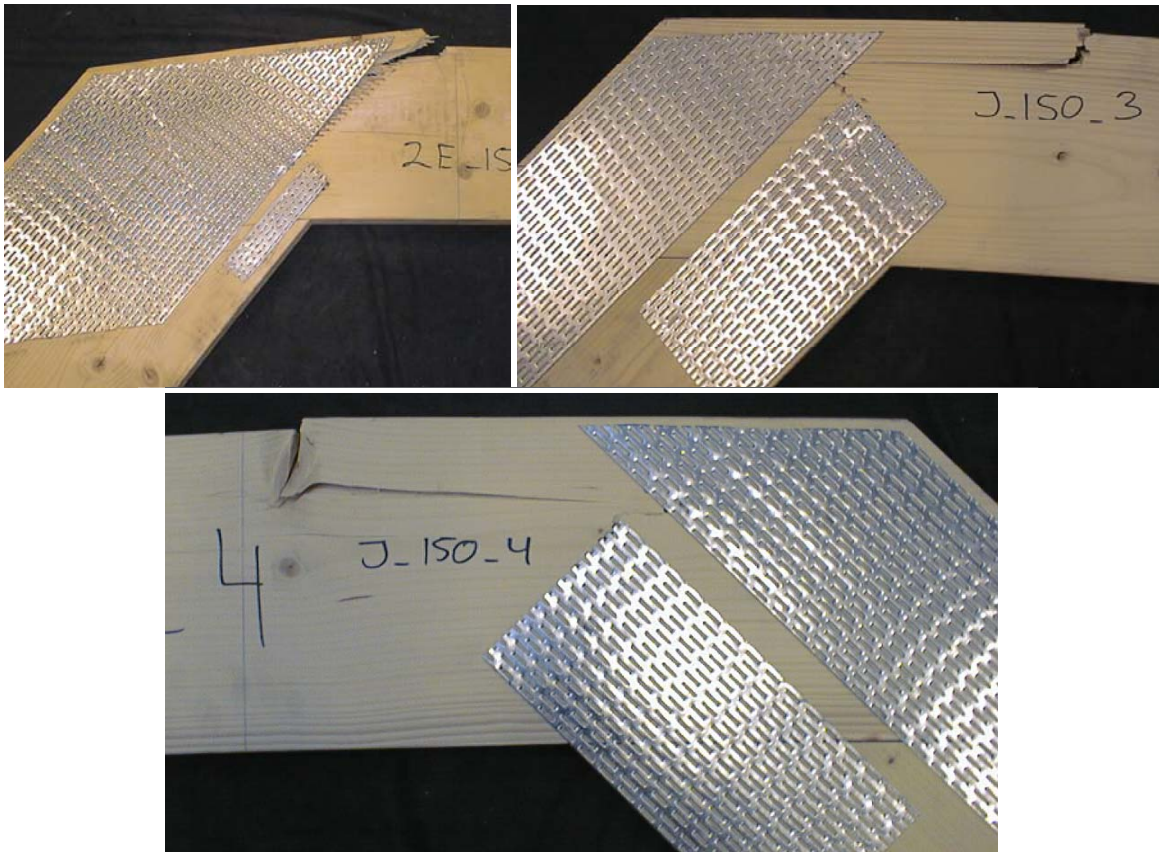

Figure 5.53. Moment tension failure in the rafter.

Figure 5.54. Anchorage failure at the outside corner.

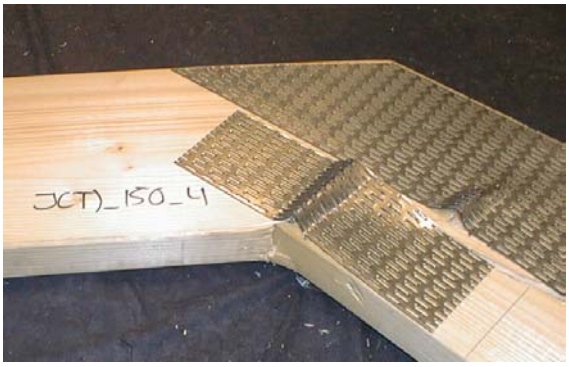

Figure 5.55. Plate buckling.

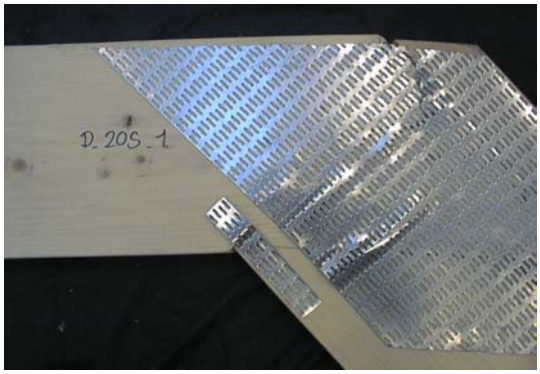

Figure 5.56. Tension failure in the nail plate between the outer leg and the rafter and buckling at the inner corner.

Some of the failure modes are a consequence of other failure types. E.g. in some cases anchorage or plate failure may develop due to splitting of the rafter.

TRUSSLAB is able to predict plate failure (shear, tension and compression failure) and anchorage failure (no reduction in the anchorage area is made). Furthermore, failure criteria for combinations of tension, compression and moment failure and pure shear failure in the timber are implemented in TRUSSLAB. However, TRUSSLAB is not able to predict the splitting/shear failures parallel to the grain direction that are observed in some of the test series in the rafter and in the leg.

In the figures 5.57 to 5.66 the observed failure modes from the tests are compared with the failure modes predicted by TRUSSLAB.

The failure modes from the tests are listed in the order they are observed and the average maximum load level is noted. In the figures timber failures are divided into three groups: “Timber splitting”, which includes shear failures, “Timber”, which covers combined bending and tension failures and “Compression perpendicular and kinking band”. “Plate” covers both plate tension and shear failure and plate buckling. “Nail” denotes anchorage failure.

For each of the predicted failure modes in TRUSSLAB it is also noted when the failure is registered. The calculations in TRUSSLAB are performed with load steps of approximately 2-3 kN and the failure check is made after equilibrium has been established for each load step. The calculations in TRUSSLAB are proceeded without any changes when failure is predicted.

All failure parameters used in TRUSSLAB are mean values. For the timber, mean values for strength class K24 are used. The values are calculated from the 5-percentile listed in the Danish timber code *DS 413 (1998)* and a logarithmic normal distribution with a coefficient of variance of 20%. The values are listed in table 5.4.

	f_m	f_t	f_c	$f_{c,90}$	f_v
Characteristic values [MPa]	24.0	16.0	20.0	3.5	3.0
Mean values [MPa]	34.0	23.0	28.0	5.0	4.3

Table 5.4. Strength values for K24 timber.

Where:

f_m is the bending strength
f_t is the tension strength
f_c is the compression strength
$f_{c,90}$ is the compression strength perpendicular to the grain direction
f_v is the shear strength

The strength values have not been modified by any load duration factor. In the Danish timber code *DS 413 (1998)* and in *Eurocode 5 (2001)* there is a modification factor of 0.9 of the strength values if the load is a short-term load (less than one week) and a modification factor of 1.1 if the load is an instantaneous load (e.g. wind load and accidental load).

A few special comments are given after each figure, but general comments on the results are given after figure 5.66.

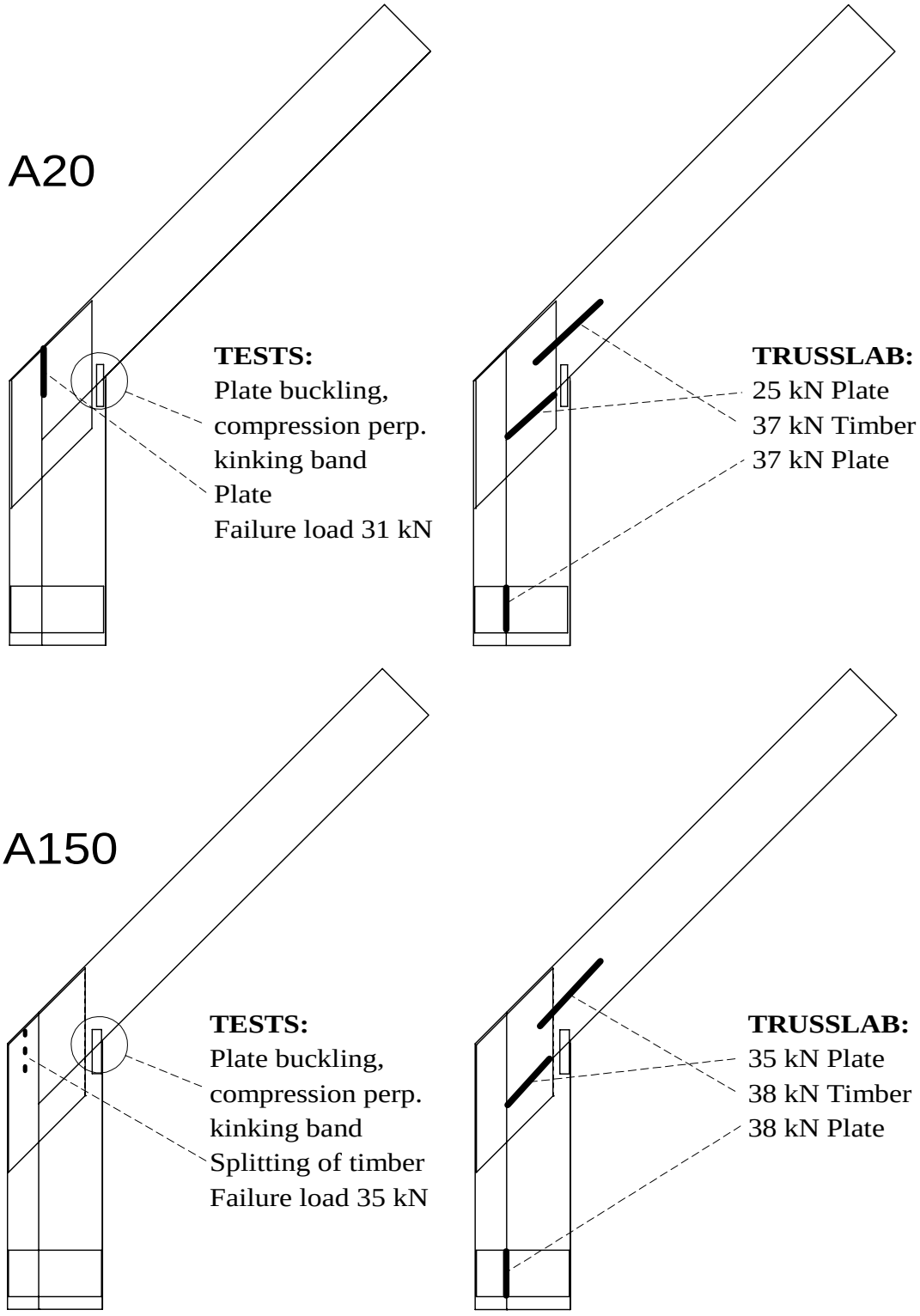

Figure 5.57. Failure modes for series A20 and A150.

The first plate failures predicted by TRUSSLAB for the series A20 and A150 are caused mainly by compression in the plate beams located near the contact zone, which is also observed in the tests. In series A150 splitting is the main reason for failure.

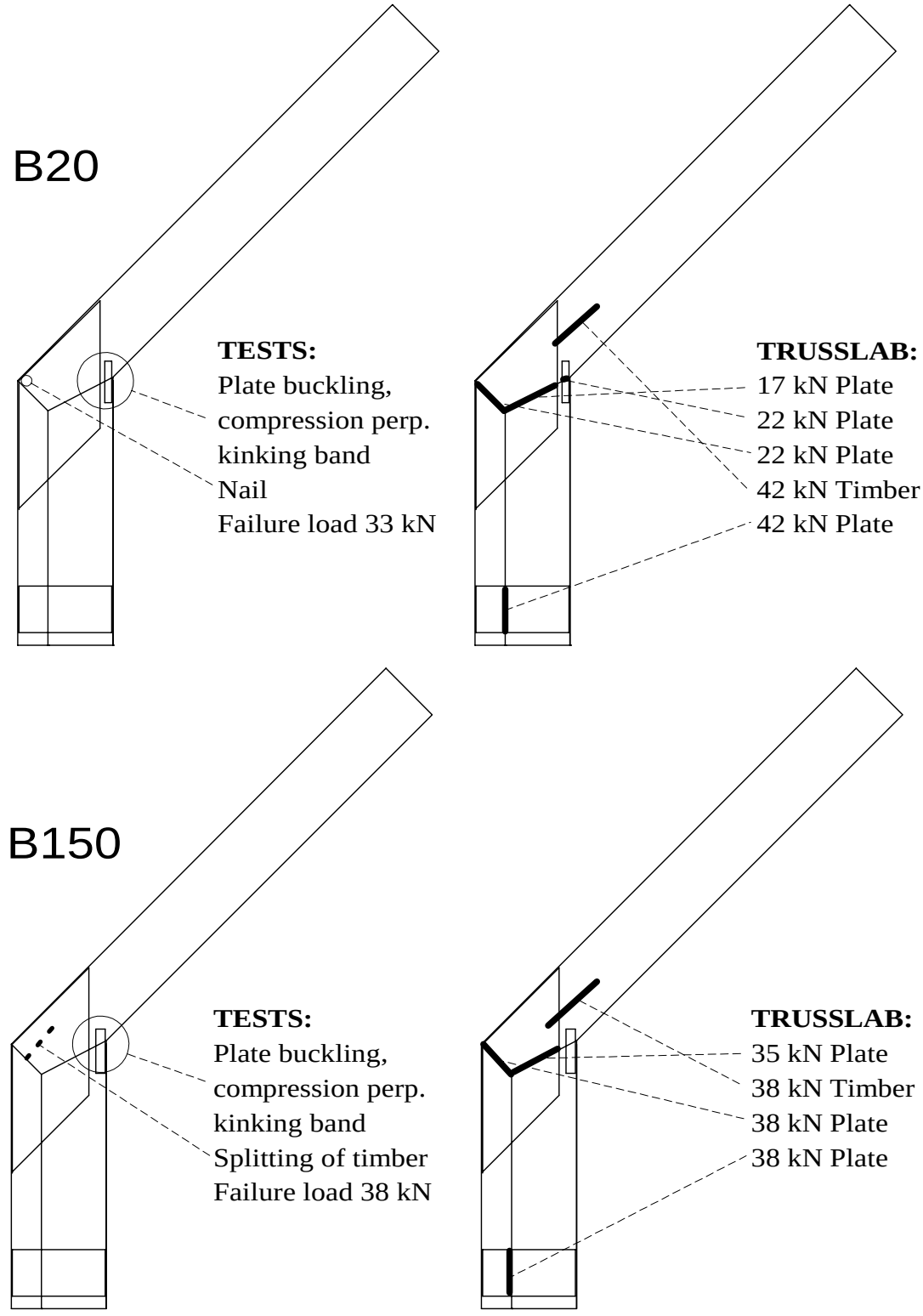

Figure 5.58. Failure modes for series B20 and B150.

For series B20 plate failure at the outer corner of the knee joint is predicted at an unexpectedly low load level (22 kN) and TRUSSLAB is not able to predict the nail failure in this area, which is the main reason for failure in this test series. In series B150 splitting is the main reason for failure.

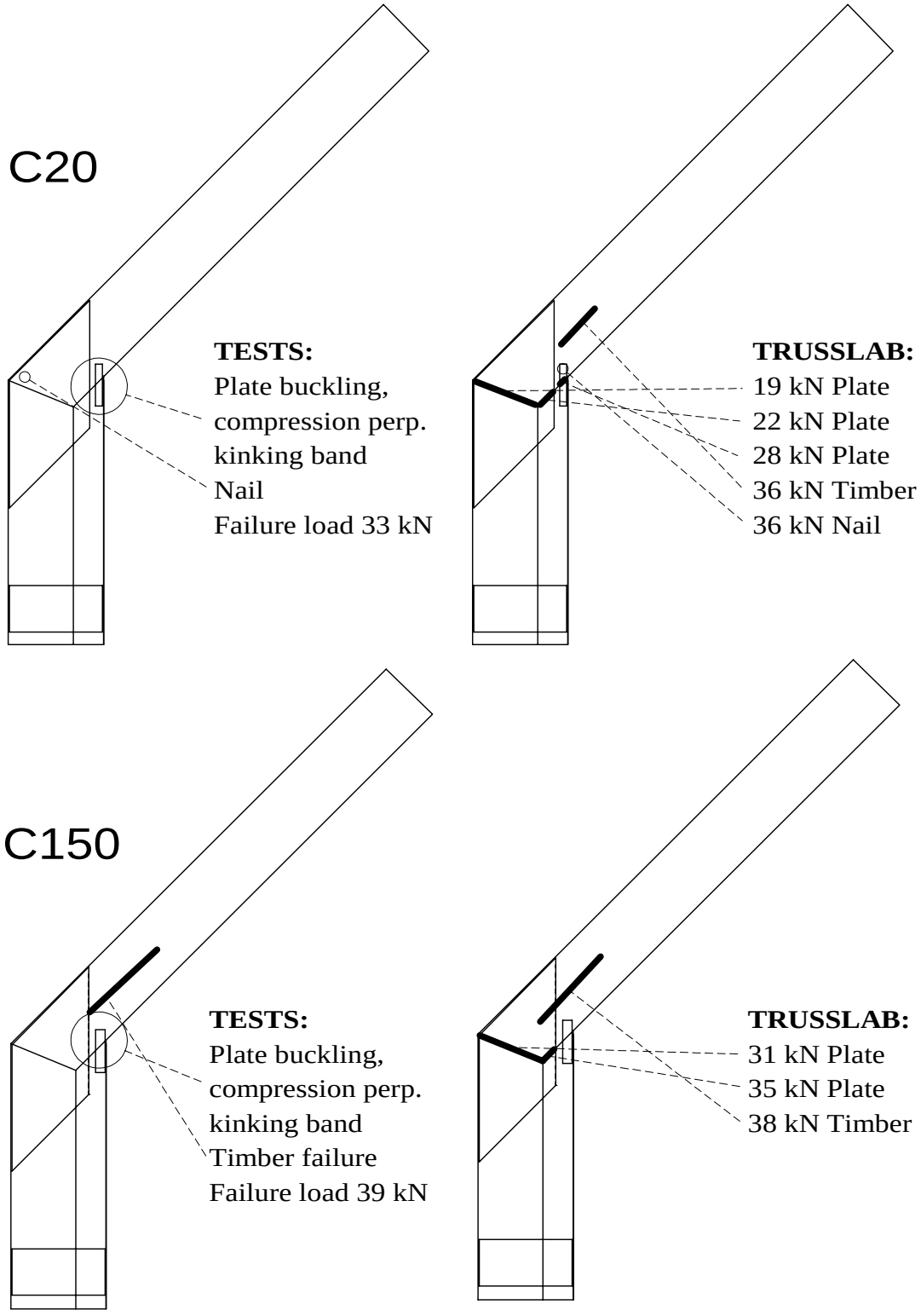

Figure 5.59. Failure modes for series C20 and C150.

As for series B20 the plate failure at the outer corner of the knee joint for series C20 is predicted at an unexpectedly low load level (22 kN) and TRUSSLAB is not able to predict the nail failure in this area, which is the main reason for failure in the tests.

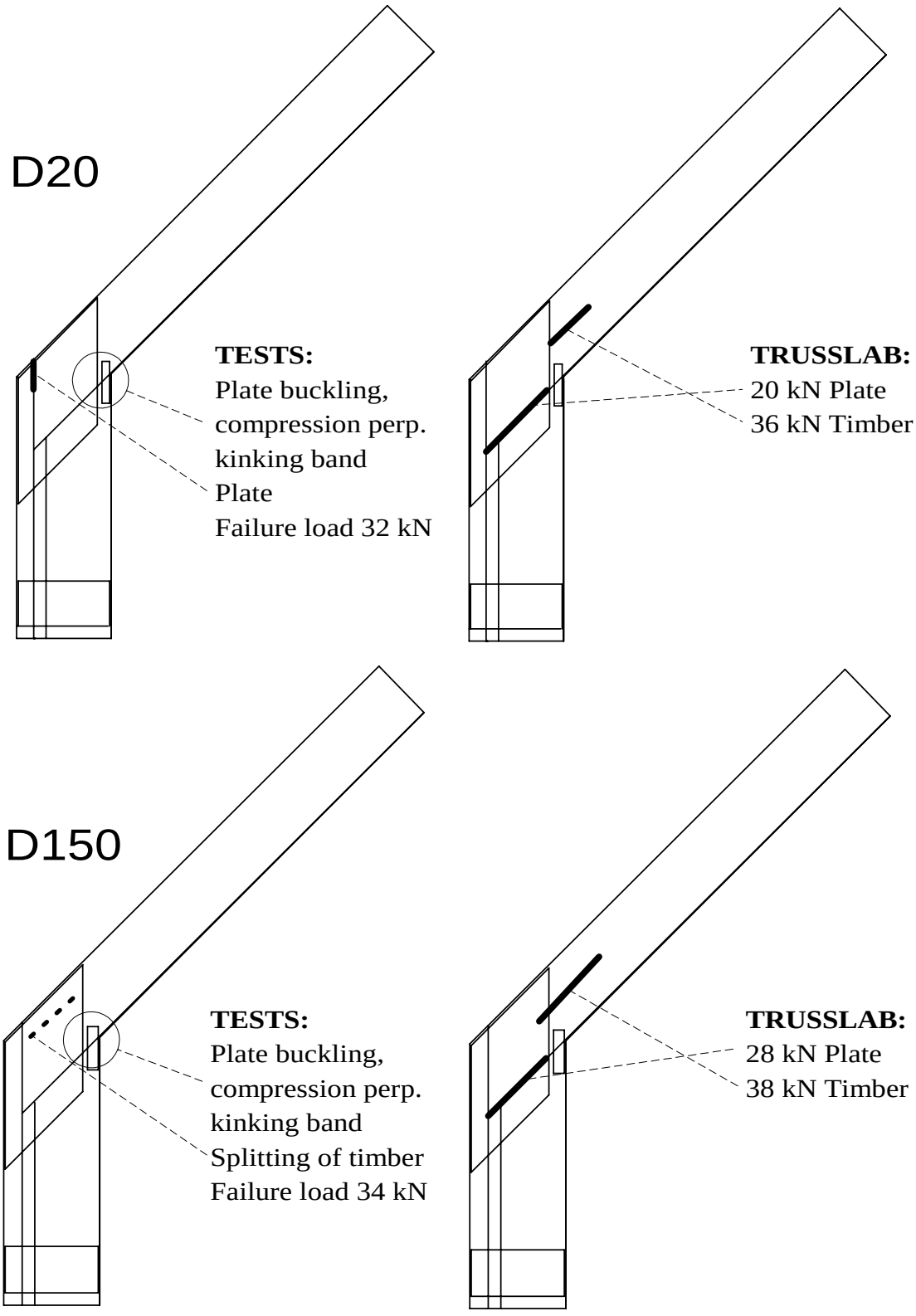

Figure 5.60. Failure modes for series D20 and D150.

For series D20 TRUSSLAB does not predict plate failure at the outer corner of the nail plates in the knee joint. In series D150 splitting is the main reason for failure.

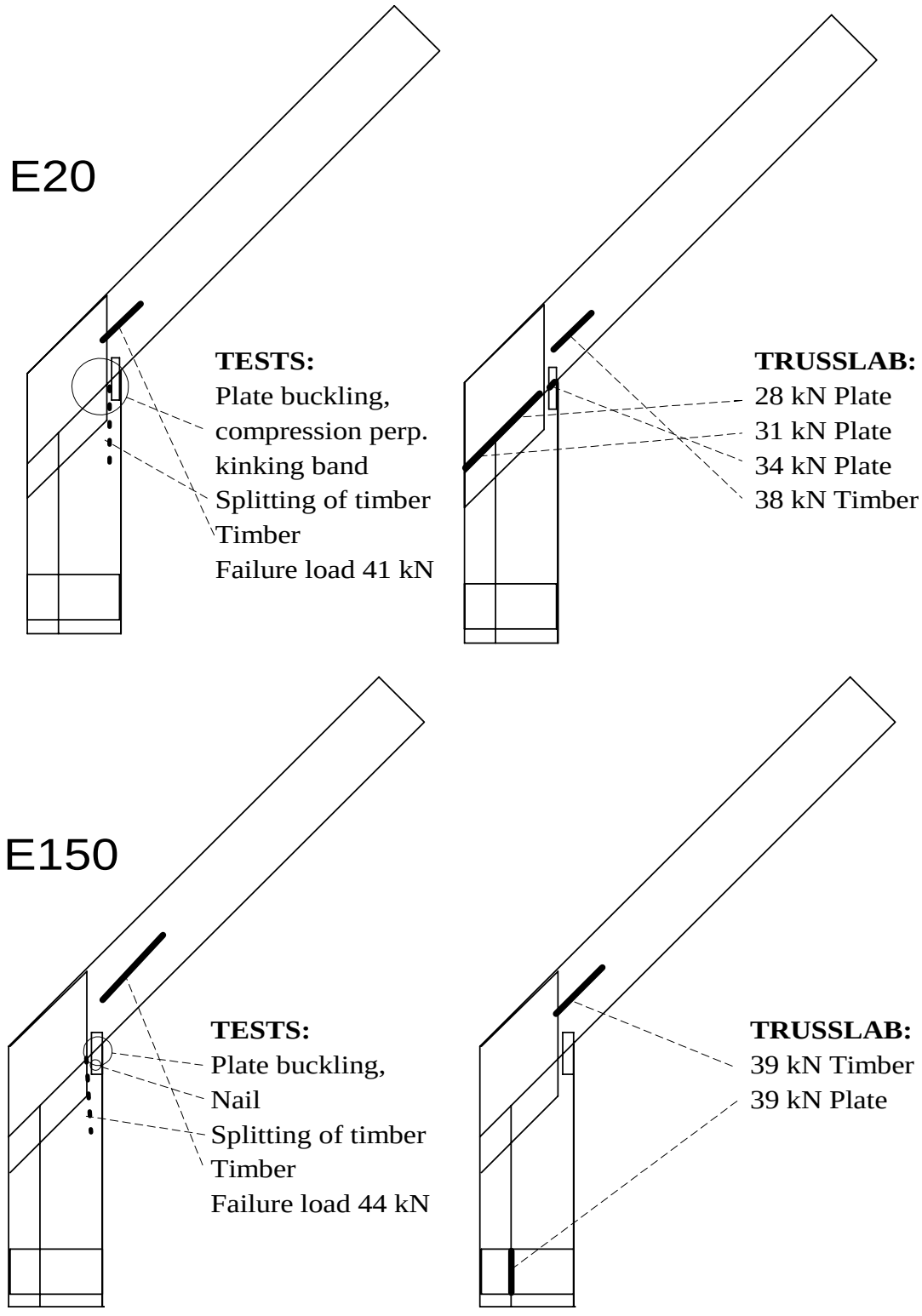

Figure 5.61. Failure modes for series E20 and E150.

In both test series splitting occurred in the timber, which is a failure mode that is not implemented in TRUSSLAB.

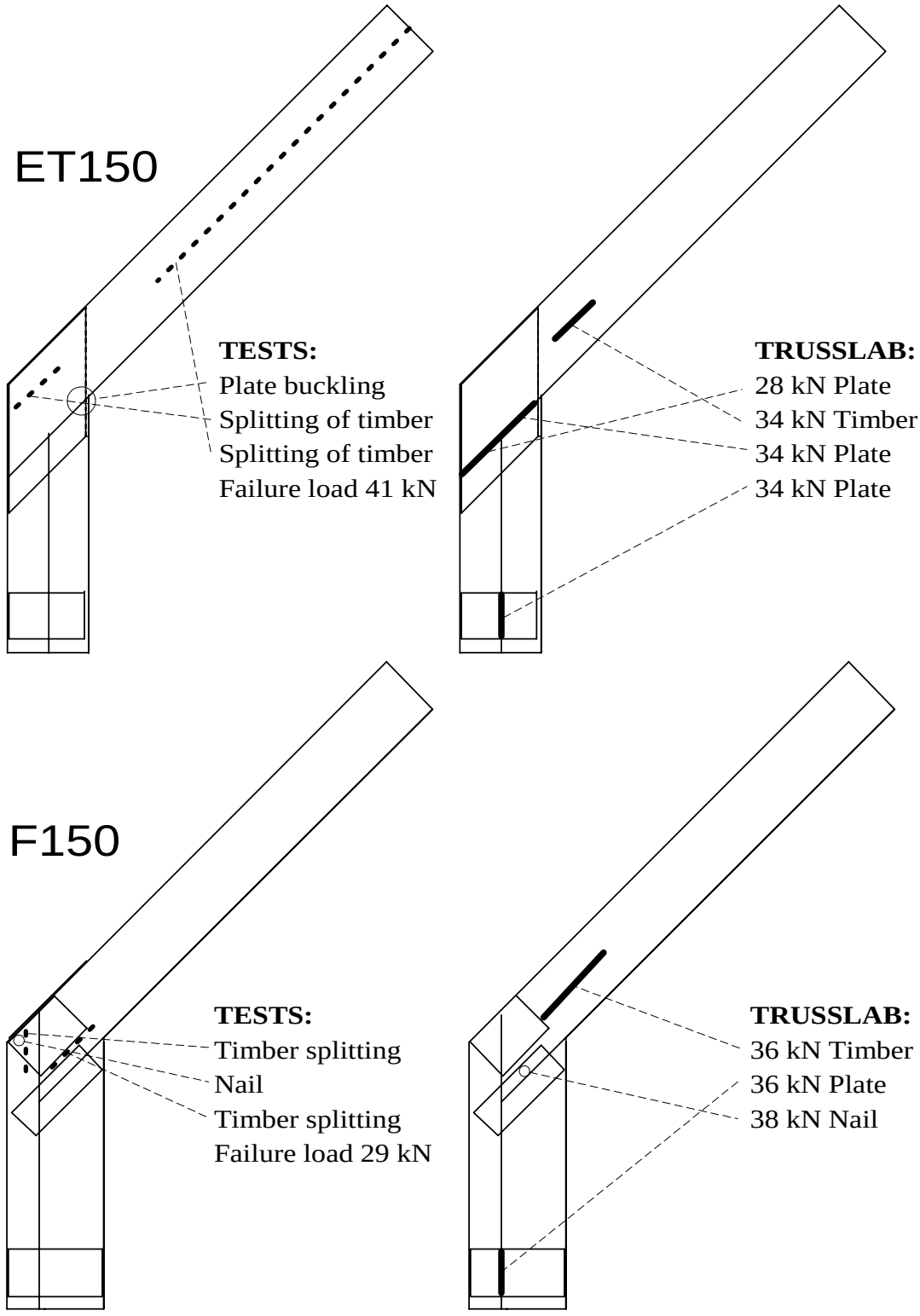

Figure 5.62. Failure modes for series ET150 and F150.

For test series F150 it is surprising that the first failure predicted by TRUSSLAB is at a load level of 36 kN. This can be caused by the fact that many forces have been transferred by contact between timber members. In series ET150 and F150 splitting is the main reason for failure.

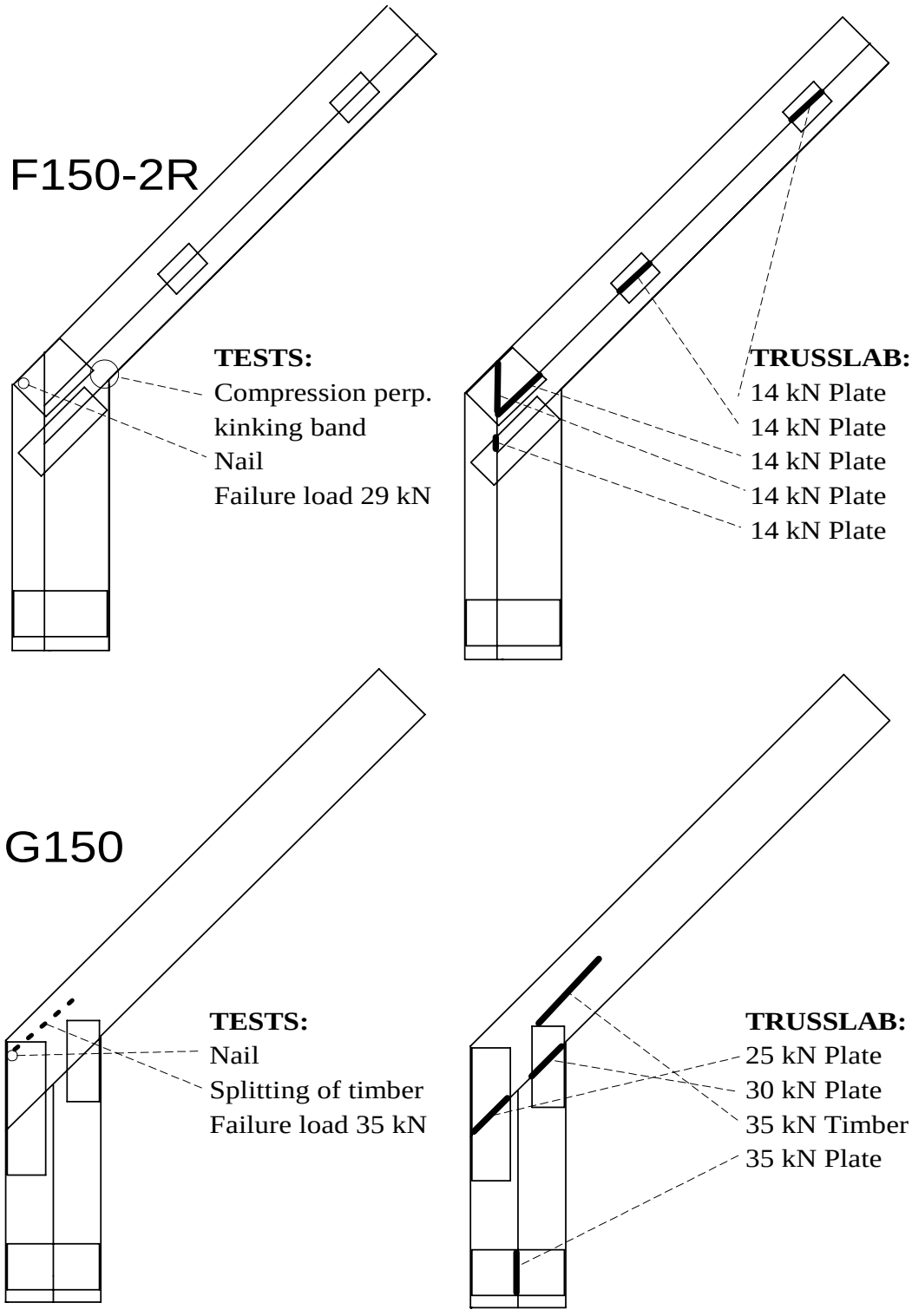

Figure 5.63. Failure modes for series F150-2R and G150.

In neither of the series TRUSSLAB predict nail failure, but for the series G150 the nail failure may be caused by timber splitting. No buckling of the nail plate is observed for series G150 in the contact zone in the tests.

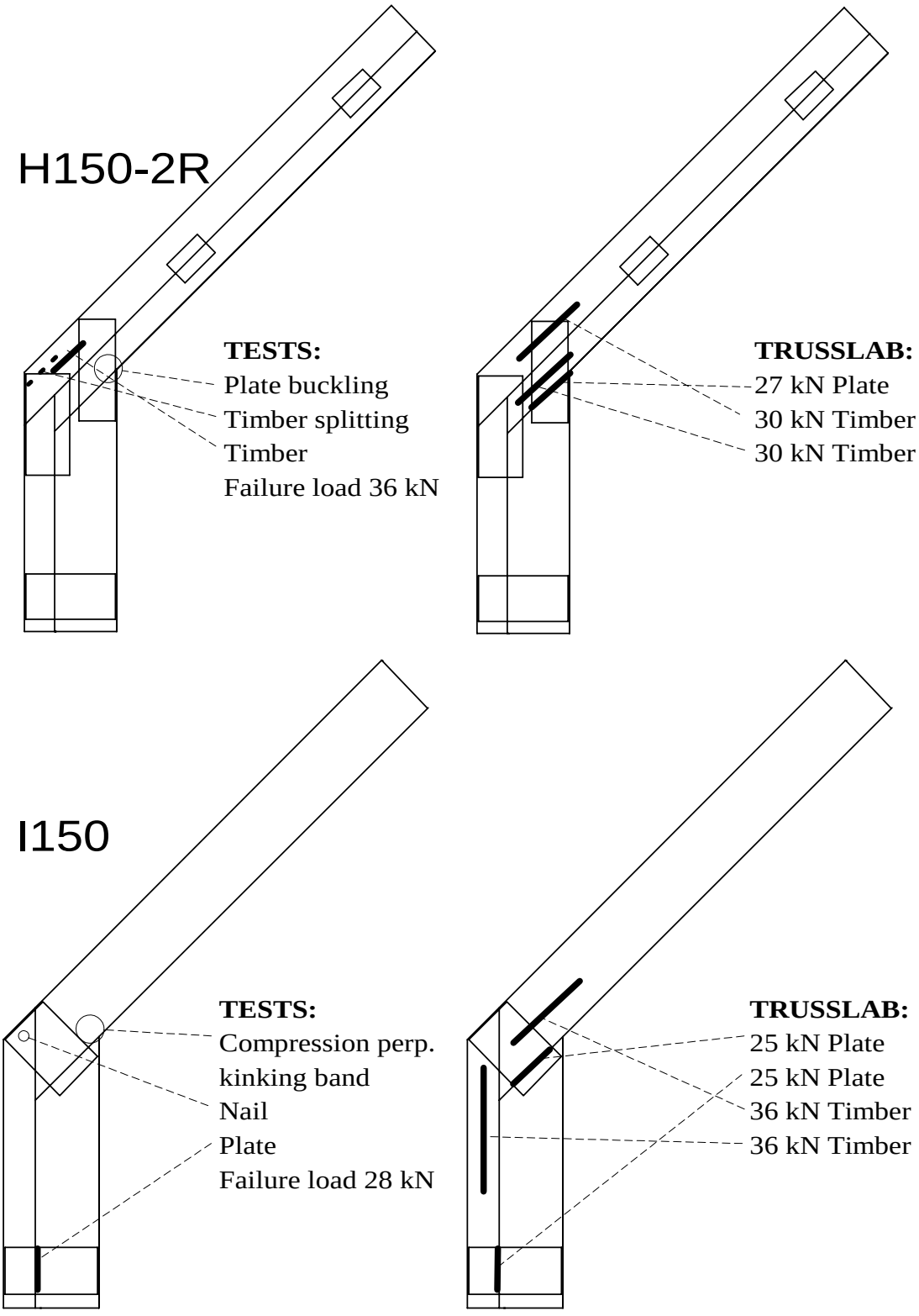

Figure 5.64. Failure modes for series H150-2R and I150.

Series I150 is the only series where shear deformations are observed in the nail plates at the bottom of the legs.

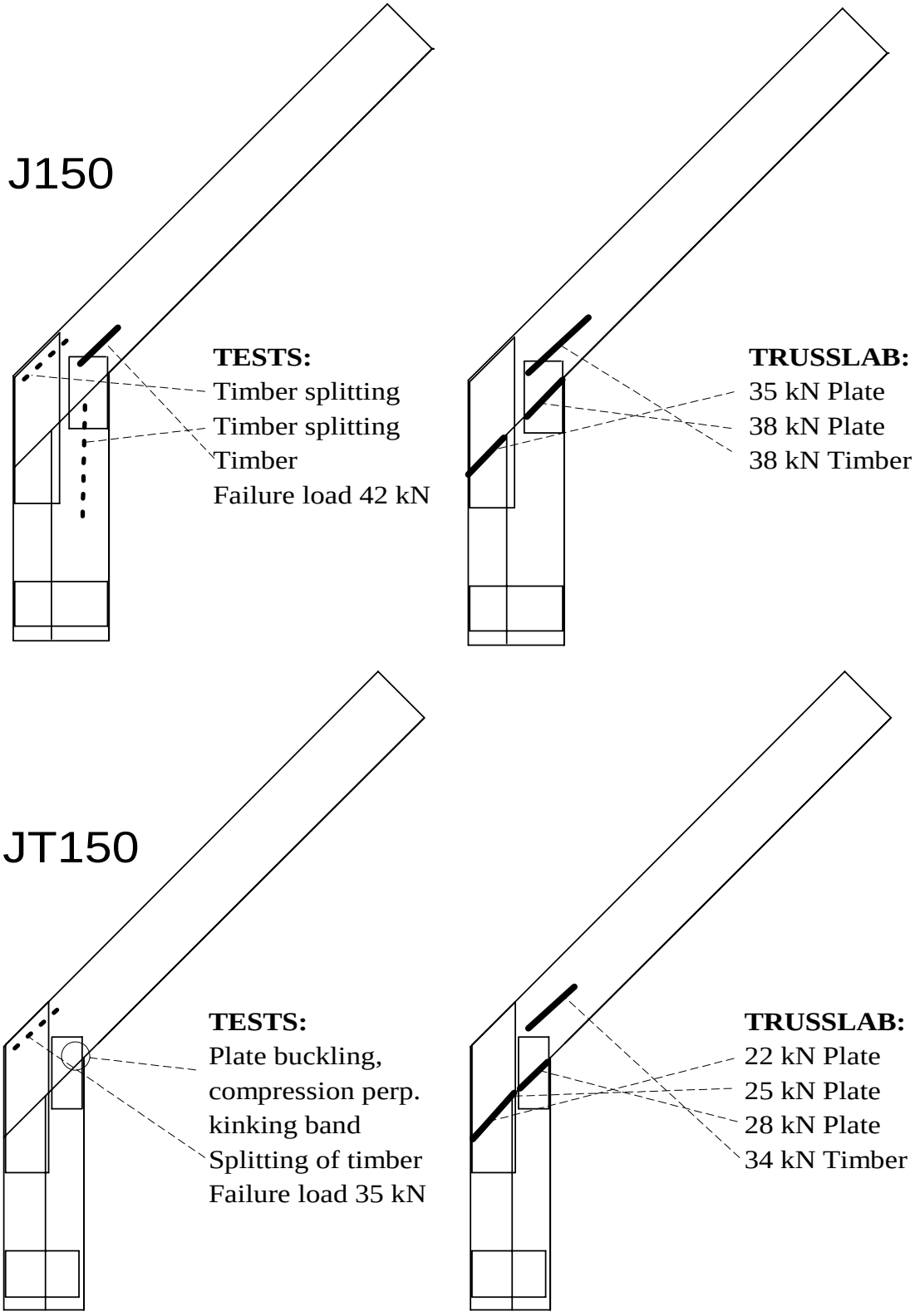

Figure 5.65. Failure modes for series J150 and J150.

For series J150 no buckling of the nail plate in the contact zone is observed in the tests. In series JT150 splitting is the main reason for failure.

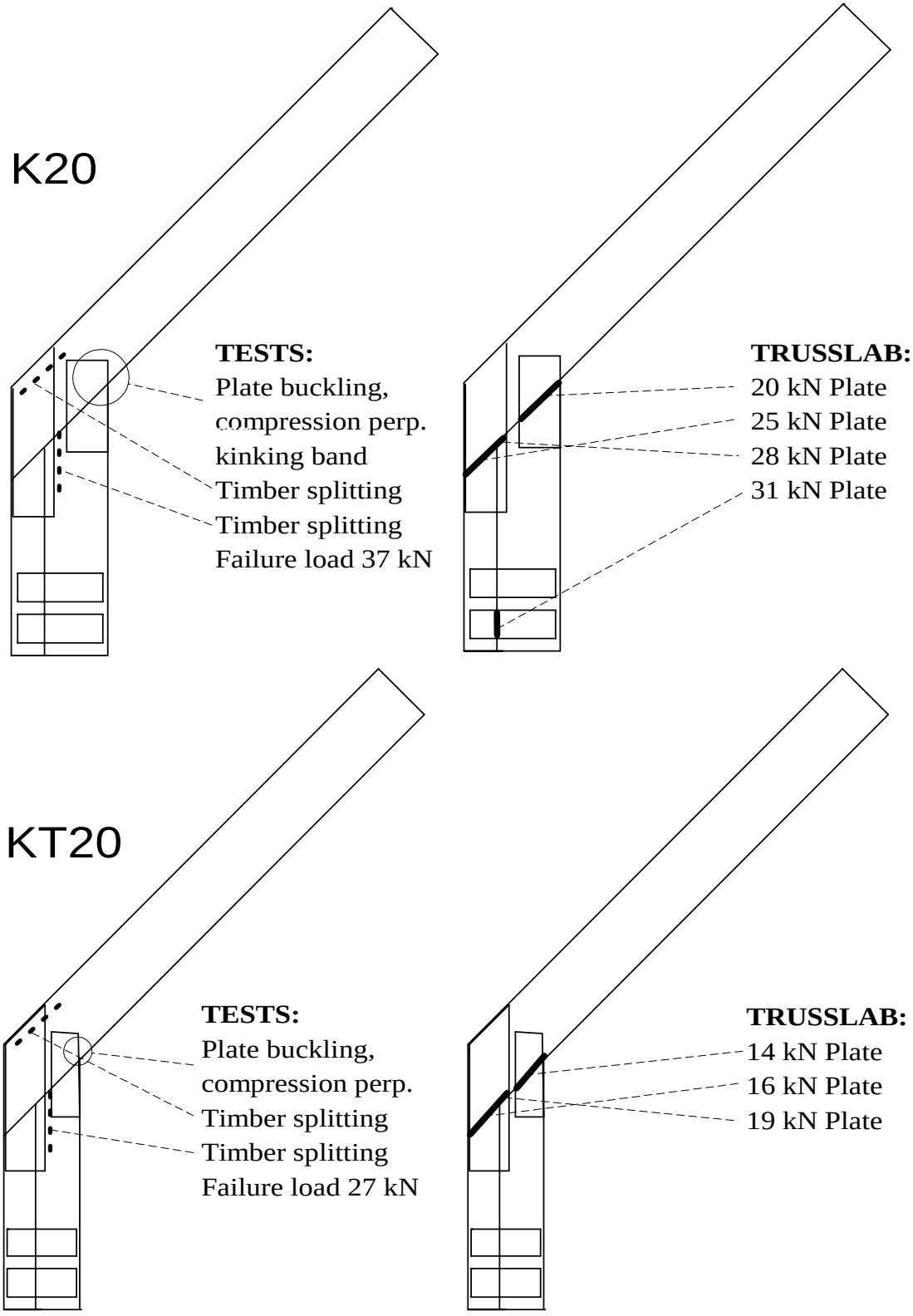

Figure 5.66. Failure modes for series K20 and KT20.

Both of the series failed due to timber splitting. For the series KT20 TRUSSLAB predicts plate failure at a relatively low load level in the outer nail plate in the knee joint.

In general there seems to be relative major differences between the failure modes and ultimate loads found in the tests and those predicted by TRUSSLAB. In TRUSSLAB the "first" failures are predicted at a load level of 50-100% of the maximum ultimate loads found in the tests. However, some comments should be made on this fact:

- In TRUSSLAB compression failure in the plate is the main reason for plate failure at a low load level for many of the series – e.g. series A20 where plate failure occurs at 25 kN in the compression zone. In the tests buckling of the nail plate in this zone is also observed, but the load capacity of the joint has not been reached due to compression between the timber members.

- When calculating the anchorage capacity in TRUSSLAB it is based on the strength values attained from the basic tests where the nails in the anchorage area are centrally loaded. The sizes of the nail plates in these tests are relatively small compared to the sizes of the nail plates used in the knee joints. These things may make a difference but it is difficult to say whether these differences will result in predictions that are on the safe or unsafe side. In the TRUSSLAB models of the knee joints all nails are assumed to be able to carry full load – also the nails close the joint lines. In practice these nails may only have a load-carrying capacity of 50% of a nail with full capacity – see also the discussion in section 3.4.

- TRUSSLAB predicts timber failure at the bottom of the outer leg at a load level of 20-35 kN. Due to the support conditions and due to the reinforcing nail plate located in this area this failure mode is restricted during testing. To clarify the figures 5.57 to 5.66 it is chosen not to illustrate this failure mode in the figures.

A clear method to improve the failure conditions in TRUSSLAB and to make TRUSSLAB predict failure modes and loads that are closer to the test results does not seem to exist, since the failure conditions implemented in TRUSSLAB were relatively close to the test results in all the "simple" tests performed with the GNA20S nail plate. However, in all the "simple" anchorage tests with the GNA20S the nail groups are only centrally loaded, whereas in the knee joints the nail groups are also loaded with a moment. In other literature eccentrically loaded nail groups have been investigated and tested. In *Blaβ, H. J., Ehlbeck, J. & Kurzweil, L. (1997)* test results are compared with the expressions in Eurocode 5 (1993). In *Kevarinmäki, Ari (2000)* comparisons between tests and the expressions in Eurocode 5 (2001) are made and quite reasonable results are found when using the expressions for the anchorage capacity similar to those in the final draft of Eurocode 5 (2001). In TRUSSLAB the expressions from Eurocode (2001) are implemented.

It should also be noted that splitting of the timber is not implemented in TRUSSLAB and that the timber is modelled by linear elastic beam elements. If the

timber was modelled by nonlinear beam elements the forces may be transferred in a different way, since the stiffness would then be dependent on the stresses in the timber beams.

In the test series A to E plate buckling is observed in the small nail plate in the contact zone between the rafter and the inner leg. TRUSSLAB, however, does not predict failure in this nail plate in all these five test series. The reason for this can be found when having a closer look at the deformations in the individual beams in the main direction of the plate. In figure 5.67 a deformed plot for a section of the test series A20 is shown.

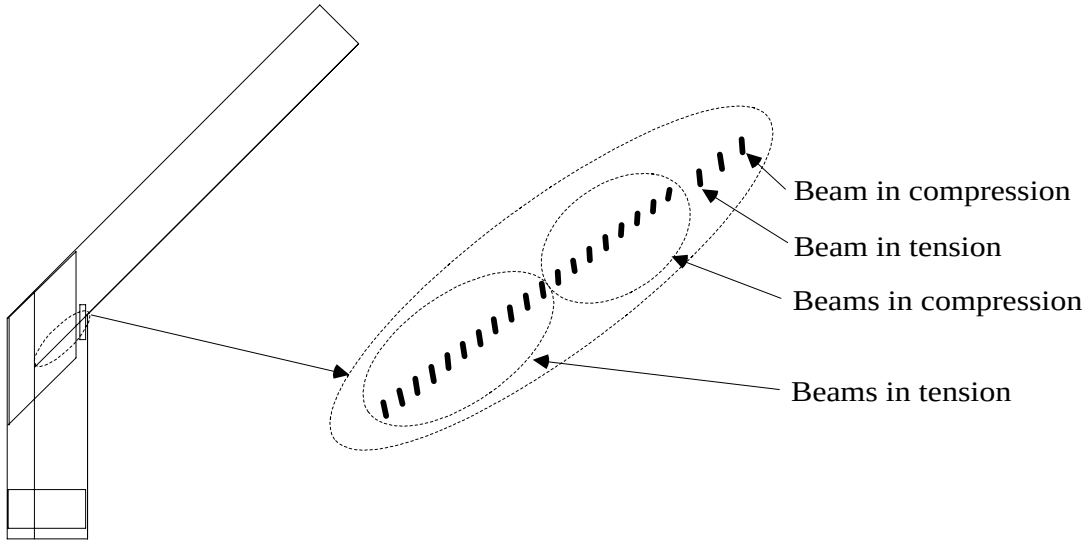

Figure 5.67. Deformed plot for a section of the test series A20. The three beams to the right are parts of the small nail plate, whereas the rest of the beams is part of the large nail plate.

In TRUSSLAB the deformation of the beams is not continuous between the two plate elements and this results in the fact that plate failure is not predicted in the small plate that connects the inner leg and the rafter.

However, the photographs shown in figure 5.68 indicate that the small plate may not buckle as much as the large plate, but this was not the case for all of the test series.

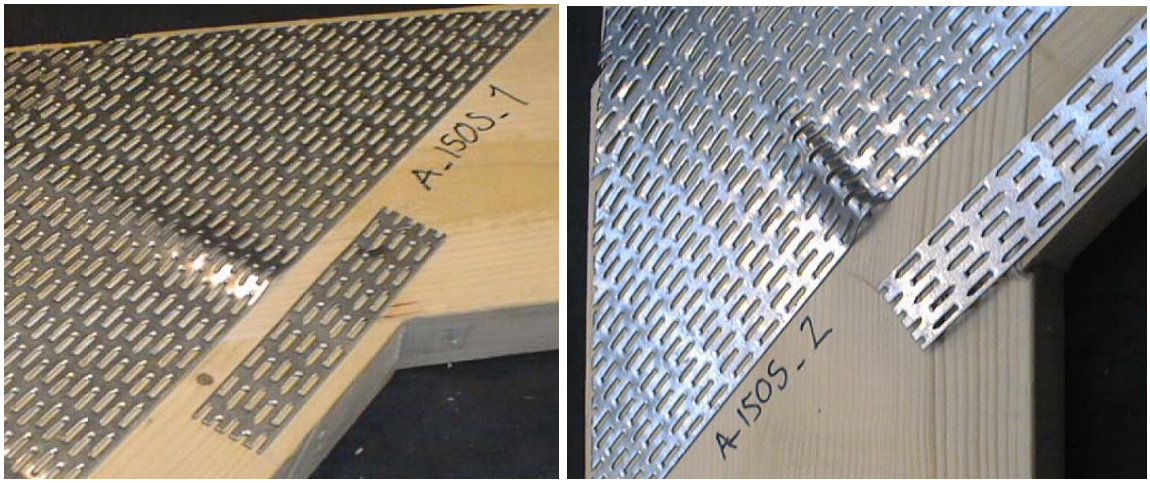

Figure 5.68. Buckling of nail plate for test series A150.

From figure 5.68 it is also observed that the buckling line is not following the joint line between the leg and the rafter, which is assumed in the theory of the plate element.

5.4 Choice of Promising Designs for Knee Joint

The different test series will be compared with each other and some promising designs for the knee joint are determined.

The failure moment in the knee joint is calculated on the basis of an eccentricity of 397 mm for the knee joints with a leg width of 360 mm and an eccentricity of 407 mm for the knee joints with a leg width of 290 mm. A definition of the eccentricity *e* is shown in figure 5.69.

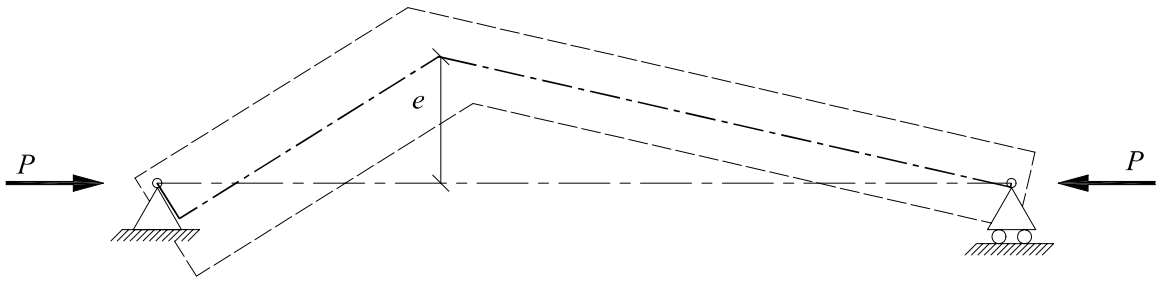

Figure 5.69. Definition of the eccentricity used for calculation of the failure moment.

The failure moment is calculated from the initial eccentricity although the eccentricity increases by up to 5% during testing. This is on the safe side.

As a comparison between the individual test series table 5.5 shows some important results from the tests. F_{05} is the force at a horizontal deformation of 5 mm, F_{10} is the force at a horizontal deformation of 10 mm, F_{max} is the maximum load and M_{max} is the corresponding maximum moment. All values are mean values of the test specimens in the actual test series and the initial slip is not included when F_{05} and

F_{10} are determined. F_{05} and F_{10} are used as a kind of stiffness measurement, whereas M_{max} is a measurement of the strength of the knee joint.

Series	F_{05} [kN]	F_{10} [kN]	F_{max} [kN]	M_{max} [kNm]
A20	14	24	31	12.3
A150	14	26	35	13.9
B20	16	26	33	13.1
B150	15	26	38	15.1
C20	13	23	33	13.1
C150	14	25	39	15.5
D20	15	25	32	12.7
D150	16	26	34	13.5
E20	17	30	41	16.3
E150	17	30	44	17.5
E150-2P	20	36	44	17.5
ET150-2P	19	31	51	20.8
ET150	17	27	41	16.7
F150	13	22	29	11.5
F150-2R	11	18	29	11.5
G150	15	27	35	13.9
H150-2R	15	26	36	14.3
I150	12	19	28	11.1
J150	16	30	42	16.7
JT150	15	26	35	14.2
J150-2P	18	32	40	15.8
JT150-2P	17	25	40	16.3
K20	16	29	37	14.7
KT20	16	25	27	11.0

Table 5.5. Important results from the individual test series.

From the table it is found that the four series (E150-2P, ET150-2P, J150-2P and JT150-2P) with two nail plates on top of each other have relatively high stiffness values (F_{05} and F_{10}) and high failure moments. However, when these series were manufactured some problems arose: cracks developed in the timber due to the significant number of embedded nails and the pressing had to be repeated several times to ensure that there was no gap between the timber and the nail plate. Furthermore, some of the nails of the upper nail plate were bent during pressing.

As a consequence of this a solution could be to increase the thickness of the nail plate or to use specially fabricated nail plates with a smaller number of nails, which would be more suitable for this propose. In Denmark, however, 1.5 mm is the maximum thickness of nail plates used for manufacturing trusses.

When comparing the series A and D with the series E it is found that the best solution is to let the rafter proceed to the outer corner of the knee joint.

As expected when the rafter consists of two rafters the stiffness decreases by up to 20% but this does not seem to affect the strength of the knee joint, see the series F150 and F150-2R.

When the width of the leg is reduced from 360 mm to 290 mm there are some confusing results. For the test series with two nail plates on top of each other the stiffness is decreasing but the strength is increasing (E150-2P with ET150-2P and J150-2P with JT150-2P). When the modulus of elasticity for the beams in those tests series is investigated no explanation can be found. For the series E150/ET150 and J150/JT150 a decreasing width of the leg results in less stiffness and less strength, which is also expected.

The series E150, ET150, J150 and JT150 seem to be reasonable designs with high stiffness and high strength properties and they were produced without any problems although the pressing should be repeated due to the large sizes of the nail plates. However, the nail plates used for those designs are special nail plates that are cut at an angle of 45º.

5.5 Conclusions

Comparisons between test results and results from calculations with TRUSSLAB show that TRUSSLAB predicts the load-displacement curves quite well up to a load level of 40-60% of the ultimate load level. The main reasons for the overestimation of the stiffness by TRUSSLAB (at higher load levels) are that the timber is modelled by linear elastic beam elements and that cracks and splitting are observed during testing. The ultimate loads and failure modes predicted by TRUSSLAB are in several cases not similar to those found in the tests. This is again in several cases caused by the fact that timber splitting is not implemented in TRUSSLAB.

During manufacture of the test series with two nail plates on top of each other, different problems rose. These problems have to be solved before these types of knee joints should be used. The results from the tests showed, however, high stiffness and strength properties.

The effect of the leg width is a bit unclear. But for the series with one nail plate on either side the stiffness and the strength decrease when the width of the leg is changed from 360 mm to 290 mm.

When the rafter is made up of two beams the stiffness decreased, but it seems that the strength is unaffected.

When designing knee joints it should be considered whether it is a wish to make the knee joint so strong that failure occurs in the timber areas outside the knee joint. This makes the failure mode more brittle and the variance of the ultimate load level increases. However, when designing a frame truss the horizontal deformation at the knee joint is often the critical factor. To avoid large horizontal deformations the rafter is often larger than required from the strength calculations. This is also making the discussion with the failure mode irrelevant.

6 Analysis of Frame Truss

In this chapter a frame truss with knee joint type ET150 is analysed using TRUSSLAB. The dimensions of the timber beams and the sizes and locations of the nail plates are determined by a truss manufacturer according to the Danish codes *DS 413 (1982)*, *DS 410 (1982)* and *DS 409 (1982)*. At present these codes are still used by the Danish truss manufactures.

The dimensions of the frame truss are shown in figure 6.1.

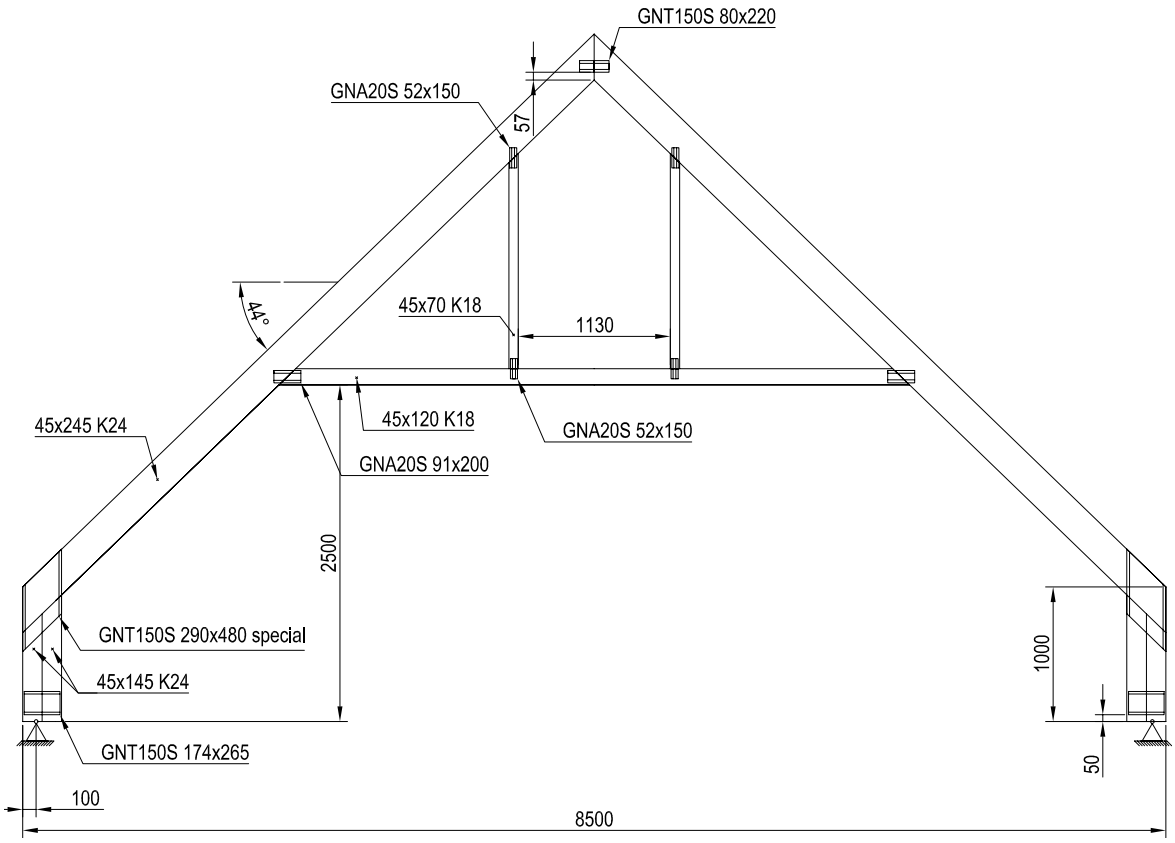

Figure 6.1. Geometry of frame truss. Dimensions in mm.

The truss is symmetrical and the nail plates are located symmetrically around the joint lines at the centre of the joint lines. The main directions of the nail plates are parallel with the two lines drawn through each nail plate.

It should be noted that the width of the leg is changed from 245 mm to 290 mm (compared with the geometry given by the truss manufacturer). This is done to make the results from this analysis comparable with the results from the tests on the knee joints. Furthermore, the leg is made by two beams and not as one solid beam. In practice, the truss is produced in two parts that are jointed together at the building site before erection. The joints are located at the centre of the ceiling tie and at the peak of the truss. In this analysis the peak joint is considered to be a nail plate joint and the joint at the centre of the ceiling tie is ignored due to lack of input information for these building site joints.

The specific truss manufacturer only produces frame trusses where the leg and the rafter are connected with one plywood sheet on both sides. The sheets are glued and nailed to the timber beams. However, if the design value of the bending moment in the knee joint is less than 2.5 kNm, the knee joint is made with nail plates (according to this truss manufacturer).

Two finite element models are set up. One model where the joints are acting either as fully stiff or as a hinge exactly as the model used by the truss manufacturer and one model where all the joints are assumed to be semi-rigid with the special nail, plate and contact elements in TRUSSLAB. The differences in the sectional forces and in the displacements between these two finite element models are compared.

The design values of the sectional forces in the knee joint are compared with the test results of the knee joint type ET150 and it is estimated whether it is reasonable to produce a frame truss with the design given in figure 6.1, where the knee joint is made with nail plates.

Normally the controlling parameter for design of frame trusses is the horizontal displacement at the knee joint. To ensure that the horizontal displacement at the knee joint is not increasing 1/100 times the height of the leg ($1/100 \cdot 1000\,\text{mm} = 10\,\text{mm}$ - guiding request used by truss manufacturers) the timber beams are in this specific case only utilised up to maximum 58% of their capacity according to the calculations performed by the truss manufacturer. The deformations are calculated using the characteristic load values and only one variable load at a time is considered.

6.1 Finite Element Models of Frame Truss

The finite element model of the frame truss where the joints are considered to be either fully stiff or pinned is shown in figure 6.2. The model is similar to the one used by the truss manufacturer (a finite element programme called TrussCon).

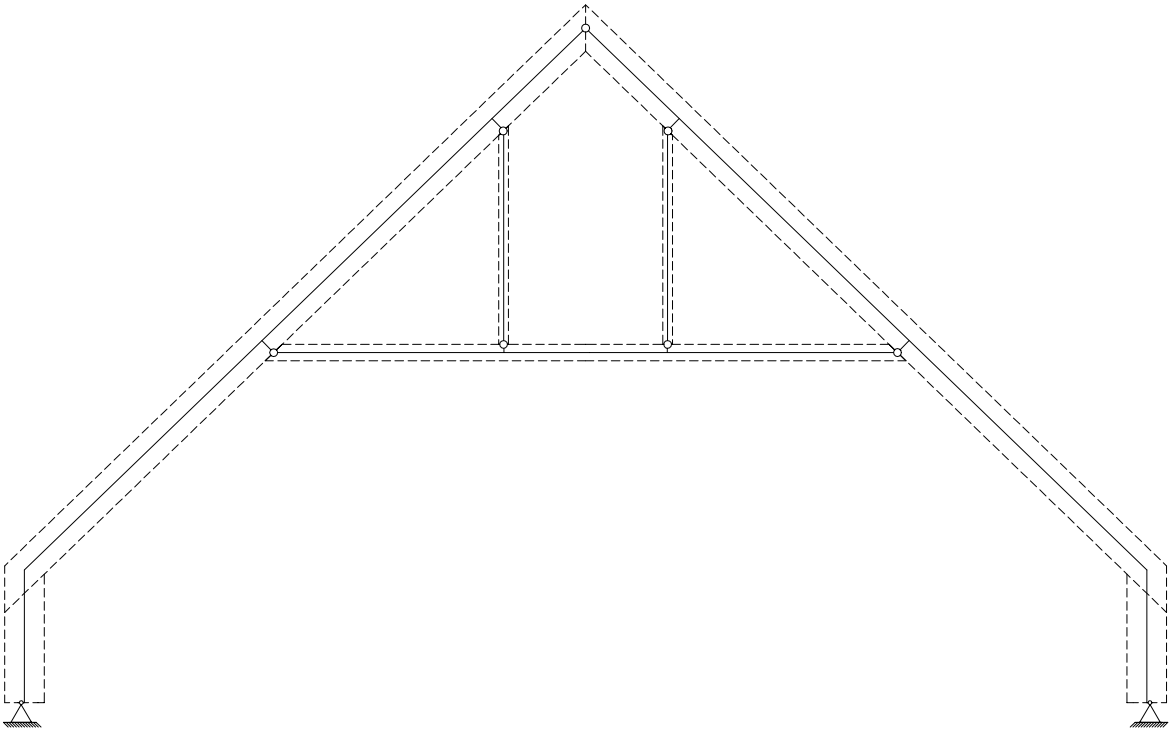

Figure 6.2. Finite element model used in the commercial programme TrussCon for design of timber trusses.

The system lines of the beam elements coincide with the timber centre lines, and small beam elements are used to model the eccentricities in the joints.

For both models the timber beams are modelled by Timoshenko beam elements. The input parameters for the timber beams are given by the size of the beams (thickness and height). The moduli of elasticity and the shear modulus of the beams are determined according to the Danish timber code DS 413 (1982).

In figure 6.3 the corresponding finite element model used in TRUSSLAB is shown.

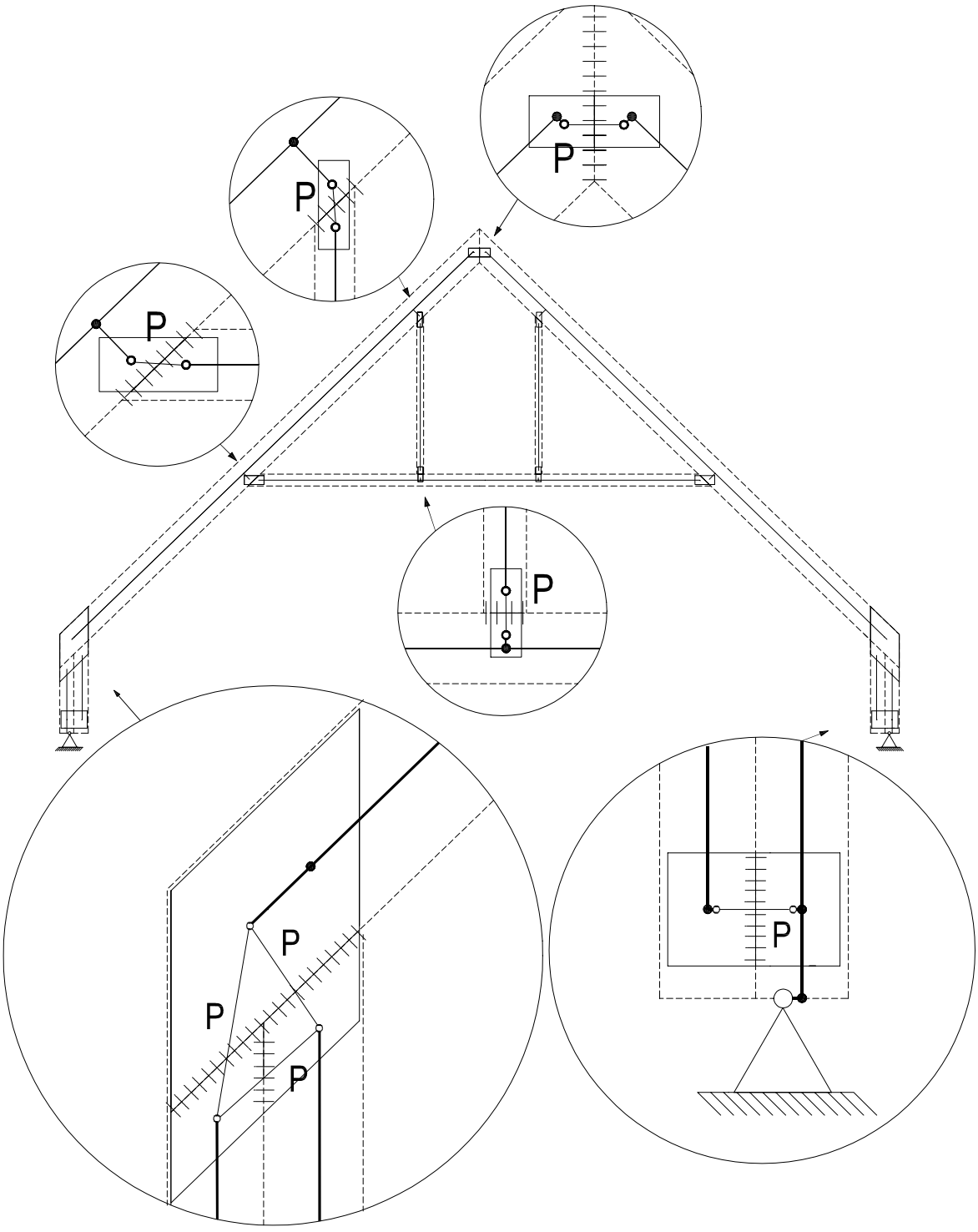

Figure 6.3. Finite element model in TRUSSLAB.

The location of the nodes is shown with a small dot - • or ◦. If the node is indicated by ◦ then a nail element is located at this node.

For both models the auxiliary elements are assumed to be stiff elements compared with the timber beams and they are given a modulus of elasticity of 50000 N/mm^2 and a shear modulus of 5000 N/mm^2 – see also the parameter analysis in chapter

5.2.2. Auxiliary beam elements are used to transfer forces from e.g. a nail element to the symmetry line of a timber beam element.

The nail elements are indicated by a small circle ◦. When calculating the strength and stiffness of the nail groups no reduction in the anchorage area is made (no effective area).

A plate element connects two nail elements and is shown as a line that is indicated by a P.

The contact elements are shown as a number of small solid lines – each indicating one of the contact beams in the contact element. The contact elements are given properties as the properties for compression perpendicular to the grain direction – i.e. a modulus of elasticity of 350 N/mm^2 according to *DS 413 (1998)*. The 1998 version of DS 413 is used in this situation since the strength values for compression perpendicular to the grain direction are almost reduced by half compared to the 1982 version. The strength values are used as the point where the bilinear stress-strain curve changes from elastic stage to “plastic” stage. Two different values (0 mm and 1 mm) of the initial gaps between the timber ends are used to analyse the effect of the gap size (all gaps are taken as either 0 mm or 1 mm)

Besides the locations of the nail plates the parameters needed as input in TRUSSLAB for the nail and plate elements are given in sections 3.1.1 and 3.4.1 for the GNA20S nail plate and in sections 4.1 and 4.3 for the GNT150S nail plate.

6.2 Load Cases

Two load cases from the Danish code *DS 410 (1982)* are considered. The first load combination corresponds to (ultimate limit state):

$$1.0 \cdot \text{dead load} + 0.5 \cdot \text{snow load} + 1.3 \cdot \text{wind on left hand side} + 1.0 \cdot \text{live load}$$

and is shown in figure 6.4.

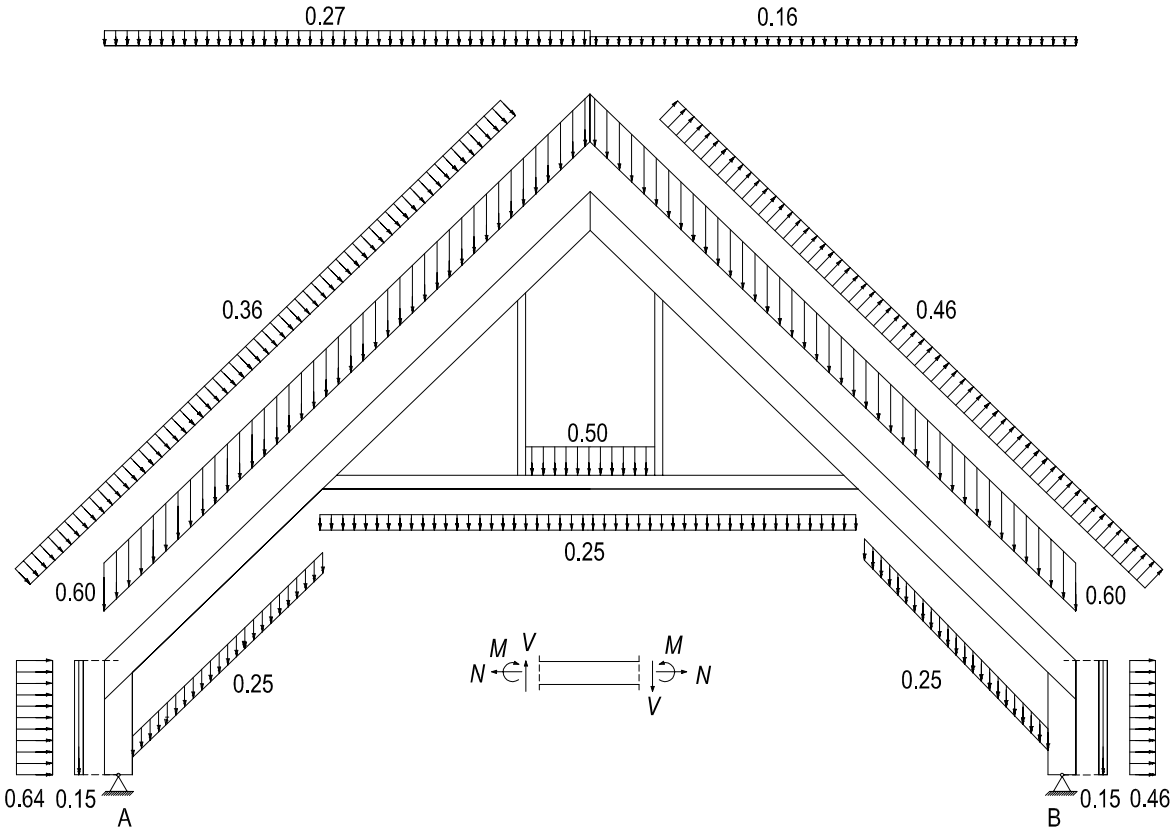

Figure 6.4. Load combination 1 [kN/m].

The load case is chosen because it results in the largest bending moment in the knee joint and the largest utilisations of most of the timber beams and nail plates in the ultimate limit state.

The other load situation corresponds to (serviceability limit state):

$$1.0 \cdot \text{wind load}$$

and is shown in figure 6.5.

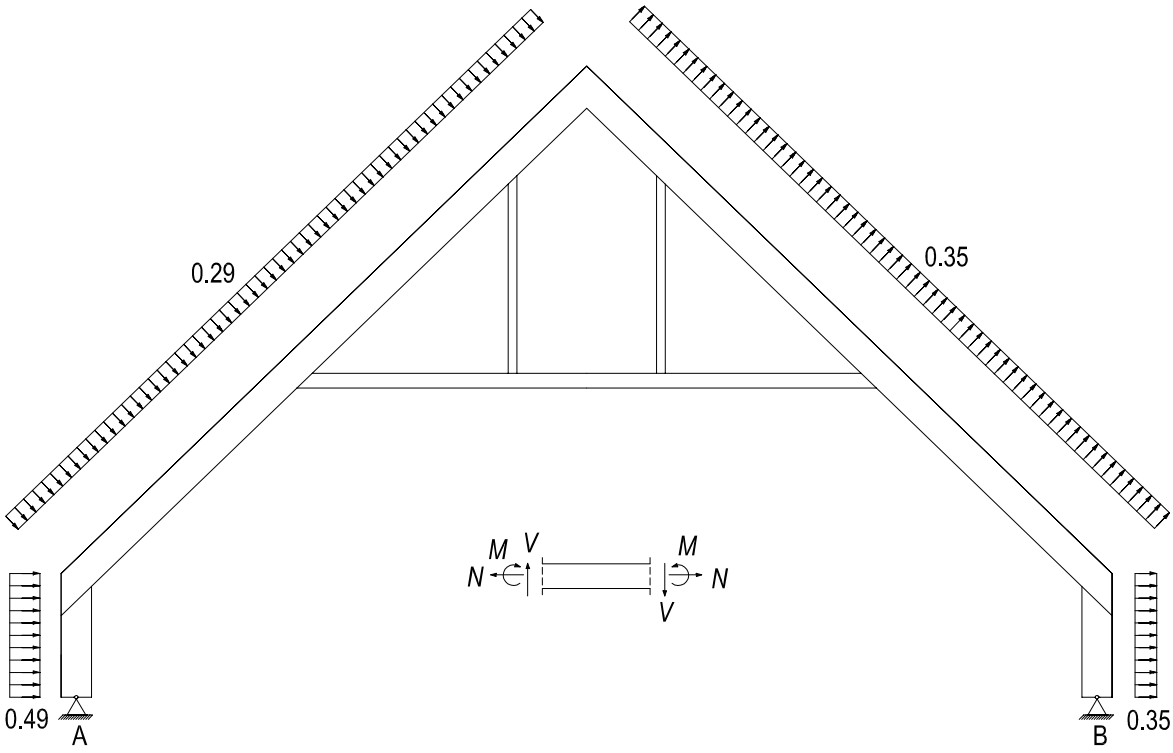

Figure 6.5. Load case 2 [kN/m].

This load situation results in the largest horizontal displacement at the knee joint and is used to evaluate the displacement of the frame truss.

The reactions (considered positive upwards and to the right) for the two finite element models and for the two different load cases are listed in table 6.1.

Finite element model/ Load case	R_{Ah}	R_{Bh}	$\sum R_h$	R_{Av}	R_{Bv}	$\sum R_v$
TRUSSLAB model (Gap = 0 mm)/ Load case 1	0.81	-4.39	-3.58	5.83	6.30	11.60
Model with stiff knee joint/ Load case 1	0.91	-4.48	-3.58	5.83	6.30	11.60
TRUSSLAB model (Gap = 0 mm)/ Load case 2	-1.79	-1.57	-3.36	-0.42	0.18	-0.24
Model with stiff knee joint/ Load case 2	-1.78	-1.57	-3.35	-0.42	0.18	-0.24

Table 6.1. Reaction forces "R" in kN for the different finite element models and load cases. The vertical reaction forces are indicated by a "v" and the horizontal by a "h". The support to the left is indicated by a "A" and the support to the right is indicated by a "B".

From the table it is seen that the sum of the horizontal and vertical reaction forces, respectively, for the different finite element models is similar. It is therefore assumed that the TRUSSLAB model and the model with a stiff knee joint are given with similar loads in each of the two load cases. The differences in the vertical reactions are due to the different stiffness of the two finite element models.

6.3 Comparison of Sectional Forces

The comparison between the sectional forces is based on calculation using load combination 1 (ultimate limit state).

The axial forces for the finite element models are shown in figure 6.6. The distribution of the axial forces in the figure is from the finite element model, where the joints are modelled as fully stiff or pinned joints.

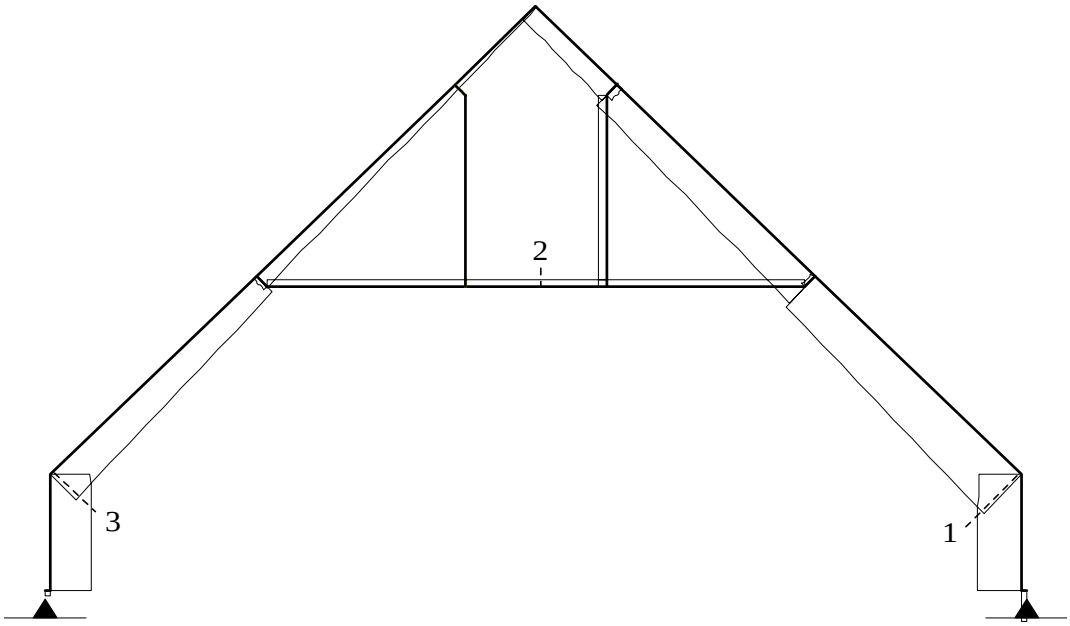

Location:	Truss with stiff knee:	Truss with semi-rigid joints (gap = 0 mm):	Truss with semi-rigid joints (gap = 1 mm)
1	-7.82 kN	-7.75 kN (-1%)	-7.76 kN (-1%)
2	-1.02 kN	-0.48 kN (-53%)	-0.64 kN (-37%)
3	-5.83 kN	-5.00 kN (-14%)	-4.99 kN (-14%)

Figure 6.6. Axial forces in the frame truss.

At the location with maximum axial force (1) the change is less than 1% when the model with stiff knee joint is compared with the TRUSSLAB models. For the two other locations the relative changes in percent are larger and up to 53%. However, this large decrease in the axial force is found at a location where the axial force is relatively small.

In general the axial forces are larger in the model with the stiff knee joint than in the TRUSSLAB models.

The distribution of the shear forces is shown in figure 6.7. The distribution of the shear forces in the figure is from the finite element model where the joints are modelled as fully stiff or pinned joints.

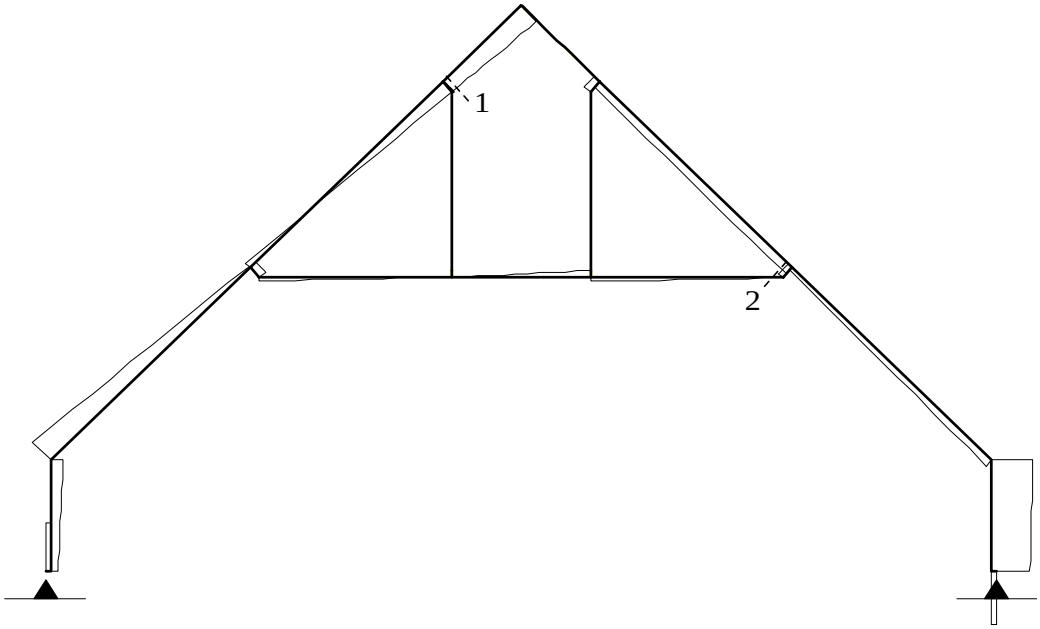

Location:	Truss with stiff knee:	Truss with semi-rigid joints (gap = 0 mm):	Truss with semi-rigid joints (gap = 1 mm)
1	-1.66 kN	-2.06 kN (+24%)	-1.95 kN (+17%)
2	-1.12 kN	-0.71 kN (-37%)	-0.81 kN (-28%)

Figure 6.7. Shear forces in the frame truss.

At location 1 the shear forces are up to 24% larger for the TRUSSLAB models compared with the model with the stiff knee joint. At location 2 the shear forces are reduced by up to 37%.

The distribution of the bending moments for the three models is shown in figure 6.8.

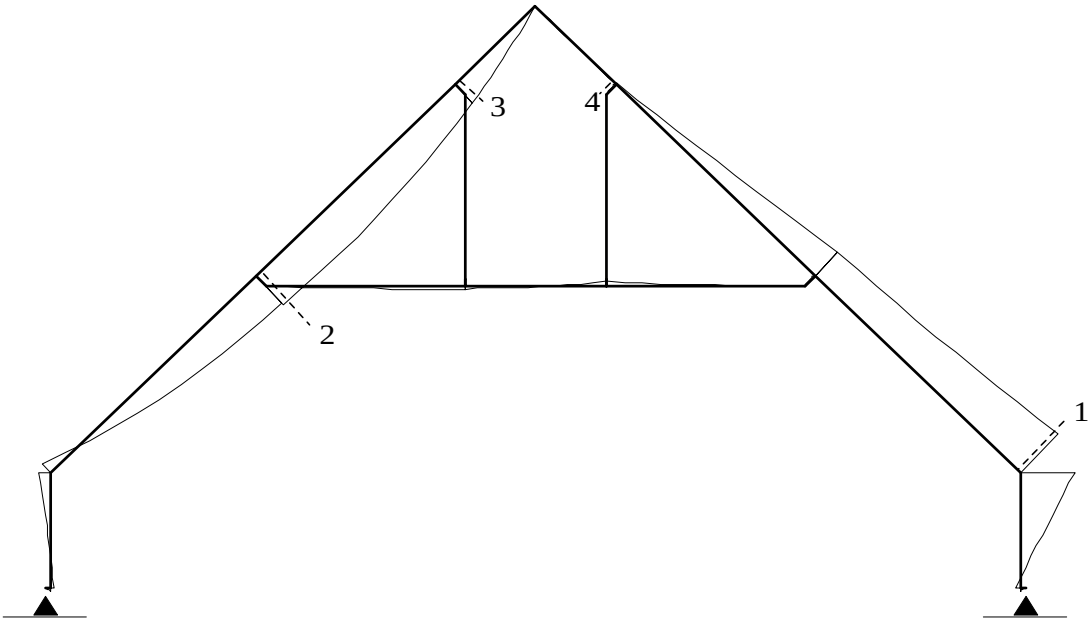

Location:	Truss with stiff knee:	Truss with semi-rigid joints (gap = 0 mm):	Truss with semi-rigid joints (gap = 1 mm)
1	-4.28 kNm	-4.18 kNm (-2%)	-4.22 kNm (-2%)
2	3.12 kNm	2.86 kNm (-8%)	2.83 kNm (-9%)
3	2.03 kNm	1.54 kNm (-24%)	1.71 kNm (-16%)
4	0.05 kNm	-0.53 kNm (+1160%)	-0.35 kNm (-800%)

Figure 6.8. Distribution of bending moments in the frame truss.

At location 1 where maximum moment is present the difference between the models is less than 3%. In general the TRUSSLAB models results in smaller bending moments in the timber beams (except for location 4).

6.4 Comparison of Deformations

The deformations are calculated for the situation where the frame truss is loaded according to load situation 2 (serviceability limit state).

A plot of the un-deformed and the deformed frame truss is shown in figure 6.9.

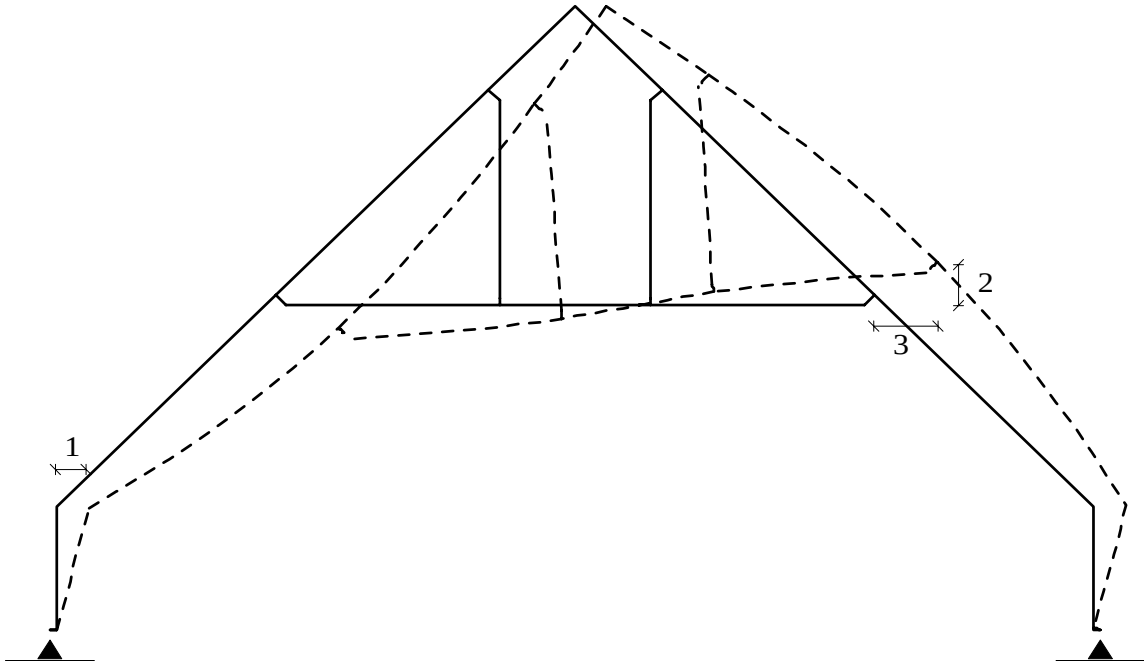

Location:	Truss with stiff joint:	Truss with semi-rigid joints (gap = 0 mm):	Truss with semi-rigid joints (gap = 1 mm)
1	11.44 mm	11.01 mm (-4%)	11.27 mm (-1%)
2	11.50 mm	10.76 mm (-6%)	10.90 mm (-5%)
3	21.93 mm	20.89 mm (-5%)	21.12 mm (-4%)

Figure 6.9. Displacements of the frame truss.

The horizontal displacement at the knee joint is reduced by up to 4% when the model with the stiff knee joint is compared with the TRUSSLAB models. At locations 2 and 3 the resultant displacement is reduced by 5%.

In general the displacements are larger for the model with the stiff knee joint compared with the TRUSSLAB models. This must be due to the fact that the rest of the joints in the TRUSSLAB model are modelled as semi-rigid, whereas they are assumed to be pinned in the model with the stiff knee joint.

6.5 Knee Joint Type ET150 as Part of a Frame Truss

In order to evaluate whether knee joint type ET150 can be used in a frame truss, the deformation and the strength of the joint are considered. From a production point of view the joint should not cause any problems – however, the impressing of the nail plate should be repeated several times if the pressing force is not high enough. The special nail plate can either be delivered from the nail plate producer or cut into the required dimension by a compass saw at the truss plant.

6.5.1 Deformations

The displacements are shown in figure 6.9. The horizontal displacement at the knee joint should not exceed 1/100 of the height of the leg. This demand is made to ensure that the neighbouring building parts (often a brick wall on the outside of the frame truss) are not subjected to large deflections.

With the chosen timber and plate dimensions the horizontal deformation at the knee joint is determined as 11.01-11.44 mm, which exceeds the guidelines by 10-15%. However, in this case the truss manufacturer has accepted the displacement. The displacement could be decreased by e.g. using a 45x290 mm beam as the rafter, which reduces the horizontal deformation to 7.28 mm (35%) for the TRUSSLAB model with the size of the initial gap taken as 1 mm.

6.5.2 Strength of knee joint

Four similar knee joints of type ET150 have been tested, see chapter 5. From the achieved ultimate loads a characteristic value of the moment capacity is calculated according to the method described in *DS 409 (1998) - Annex A*.

The ultimate loads are denoted m_i and they are assumed to be logarithmic normally distributed with an unknown coefficient of variation. In table 6.2 the values are listed.

	1	2	3	4
m_i	42.7 kN	39.9 kN	40.6 kN	39.9 kN
$\ln(m_i)$	3.754 kN	3.686 kN	3.704 kN	3.686 kN

Table 6.2. Ultimate loads for the four tests with knee joint type ET150.

The mean value $\bar{y}$ of $\ln(m_i)$ is determined by:

$$\bar{y} = \frac{1}{n}\sum_{i=1}^{n}\ln(m_i) = 3.707 \text{ kN} \tag{6.1}$$

where *n* is the number of tests (4).

The standard deviation s_y of $\ln(m_i)$ is determined by:

$$s_y = \sqrt{\frac{1}{n-1}\sum_{i=1}^{n}(\ln(m_i)-\bar{y})^2} = 0.032 \text{ kN} \tag{6.2}$$

The characteristic ultimate load m_k is given by:

$$m_k = \exp(\bar{y} - k_s s_y) = 36.7 \text{ kN} \tag{6.3}$$

where k_s is determined by:

$$k_s = k'/\sqrt{n} = 3.26 \tag{6.4}$$

k' is a 5-percentile value in a non-central *t*-distribution with *n*-1 degrees of freedom and the non-central parameter $\lambda = u_p\sqrt{n}$ where u_p is the 95-percentile in the standardised normal distribution function.

With an eccentricity of 407 mm the characteristic bending moment M_k is:

$$M_k = 36.7\ \text{kN} \cdot 0.407\ \text{mm} = 14.9\ \text{kNm} \tag{6.5}$$

In the tests with knee joint type ET150, failure in the timber was the dominating reason for failure. To calculate a design value of the moment capacity for knee joint type ET150 it has therefore been chosen to use the partial factor for timber. In the Danish timber code from 1982 the partial factor for structures produced on fabric under impartial control in normal safety class is 1.35. A design value for the bending moment capacity M_d is therefore determined by:

$$M_d = \frac{14.9\ \text{kNm}}{1.35} = 11.0\ \text{kNm} \tag{6.6}$$

It should be noted that buckling of the nail plate is allowed when the maximum ultimate loads are determined from the test results. The values of the axial force and the shear force in the knee joint in the test set-up are compared with the actual axial and shear forces in the knee joint in the model of the full frame truss in table 6.3. The comparison is made at load levels where the bending moment in the knee joint in the test setup is similar to the bending moment in the knee joint of the full frame truss.

	Test set-up	Full frame truss	Ratio
M [kNm]	-3.44	-3.44	1.00
N [kN]	-9.6	-6.1	1.57
V [kN]	-6.0	-4.8	1.25

Table 6.3. Comparison of sectional forces.

The values of the axial force and the shear force are larger in the test set-up than in the model of the full frame truss (the ratios are larger than 1.00). However, this fact only seems to increase the bending moment capacity of the knee joint if full-scale testing is performed. It is also noted that the number of test specimens is relatively small.

When comparing the design value of the moment capacity achieved from testing (11.0 kNm) with the design value of the bending moment in the finite element

model (4.3 kNm) there is enough moment capacity in the knee joint type ET150 to produce a frame truss with the given dimensions.

In load case 2 no failure is observed when calculations are performed using TRUSSLAB and when using design values of the nail and plate capacities (and with the failure conditions implemented in TRUSSLAB).

The moment capacity calculated from the test results is based on the initial eccentricity in the test set-up and in the finite element model in TRUSSLAB no second order effects have been included either.

Only one load case is considered when determining a design value of the bending moment.

6.6 Conclusions

From comparisons between a finite element model, where the joints are either fully stiff or pinned joints, and a finite element model with semi-rigid behaviour of the joints it is found that:

- The sectional forces at critical sections with peak values are only slightly changed and in most cases the sectional forces are larger in the model with stiff knee joints compared with the model with semi-rigid joints.
- The displacements are in general decreased by up to 6% when a model as TRUSSLAB with semi-rigid joints is used.

For a frame truss under the given load conditions, with the given dimensions and with knee joint type ET150 it is estimated that the strength of the knee joint is sufficient to transfer the given sectional forces. Furthermore, the horizontal displacement at the knee joint is considered to be allowable. Even though the design moment (4.3 kNm) of the knee joint is far from the design moment capacity (11.0 kNm) it is not recommended to increase the span of the frame truss due to the horizontal displacements.

Full-scale tests with the frame truss could verify if the models are able to predict the behaviour of the frame truss.

7 Analysis of Chord Splices

Trusses are often produced with splices in the top chord and in the bottom chord. In Denmark these chord splices are often assumed as rotationally stiff joints in the finite element model and they are designed from the actual sectional forces, according to *Træ 31 (1995)* (the values are not increased as in the final draft of Eurocode 5 as described below). However, in the final draft of Eurocode 5, *Eurocode 5 (2001)* and in the Danish timber code *DS 413 (1998)* the splice joints may only be modelled as rotationally stiff if the actual rotation (under load) would have no significant effect upon member forces. According to Eurocode 5 this requirement is fulfilled if one of the following conditions is satisfied:

- "Splice joints with a load carrying capacity which corresponds at least to 1.5 times the combination of applied force and moment."

- "Splice joints with a load carrying capacity which corresponds at least to the combination of applied force and moment, provided that the wooden members are not subject to bending stresses which are greater than 0.3 times the member bending strength, and the assembly would be stable if all such connections acted as pins."

In this section the influence of chord splices on the member forces and on the deformations will be analysed by means of calculations using TRUSSLAB. The effect of chord splices in a typical fink truss and a typical attic truss is analysed. This investigation is performed to show some of the applications that can be achieved using a finite element model as TRUSSLAB. Furthermore, there is no need for the conditions above if a finite element model with semi-rigid joints as TRUSSLAB is used.

The analysis is not performed to see whether the "new" conditions in the codes are appropriate or not. To do so, additional calculations should be made with a range of different nail plate sizes and locations, but the analysis may give an indication of the influence of chord splices on member forces and deformations for two specific types of trusses with a given nail plates size.

First some experimental bending tests of splice joints performed by *Nielsen, J. (1996)* will be analysed in order to compare the TRUSSLAB model with test results for such types of joints. This analysis is performed because some modifications to the nail, plate and contact elements have been made since the

work done by Nielsen in 1996 and to find the value of *E* for the contact element in the chord splices.

7.1 Bending Tests on Splice Joints

J. Nielsen tested 8 types of splice joints with different sizes and locations of the nail plates, see *Nielsen J. (1996)*. Three of these bending tests are analysed with TRUSSLAB in this chapter. The test set-up is shown in figure 7.1.

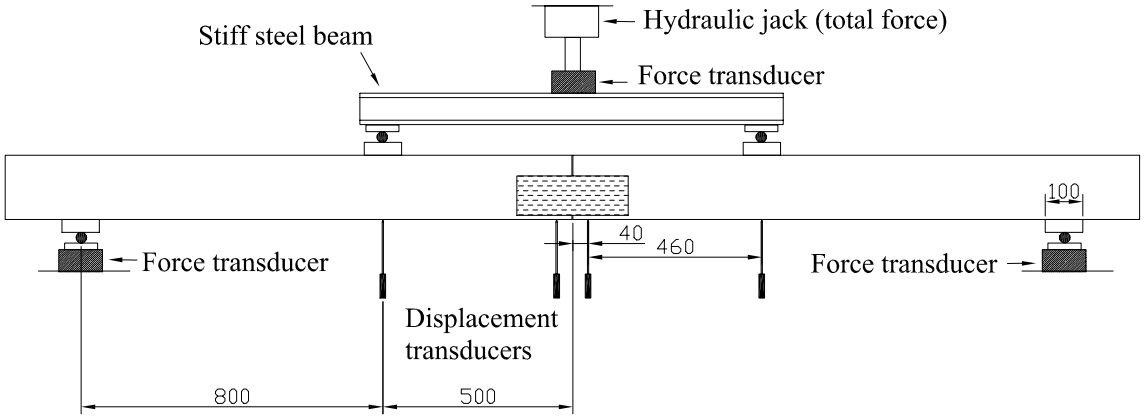

Figure 7.1. Test set-up for bending tests with splice joints. Dimensions in mm.

The three different test series are shown in figure 7.2. Five test specimens are tested in each test series.

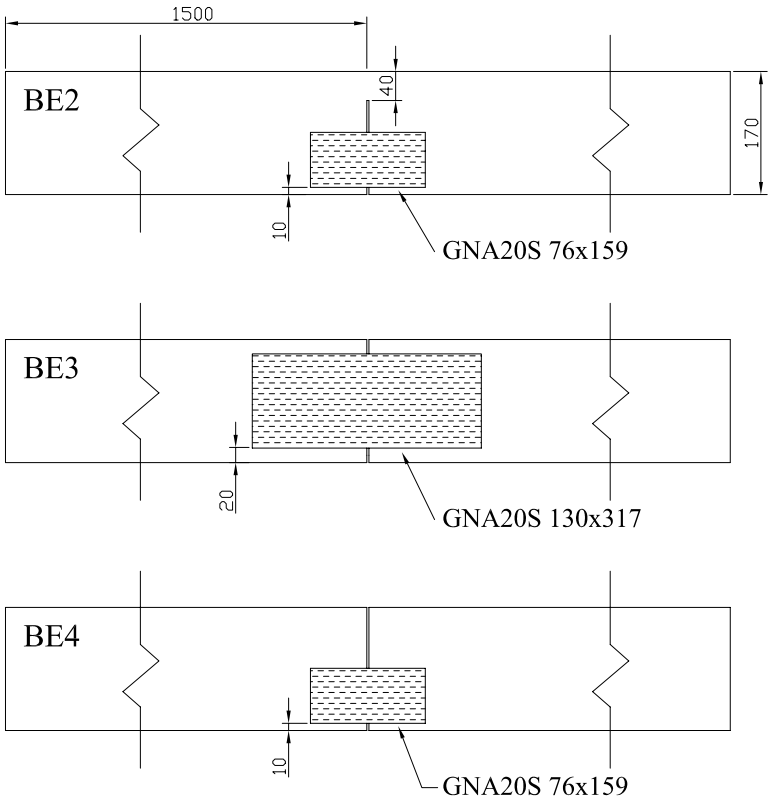

Figure 7.2. Bending test series BE2, BE4 and BE3. Dimensions in mm.

The test series BE2 and BE4 are used to analyse the “butt effect” in the contact zone between the timber ends. In other words, the influence of the phenomena where the grain in the timber ends is pressed into each other is investigated. Test series BE3 is used to compare results from TRUSSLAB with test results.

In the test series BE4 there is no gap between the timber members and the nail plate is only subjected to tension in the given load situation because the nail plate is located eccentrically. The finite element model for test series BE4 is shown in figure 7.3.

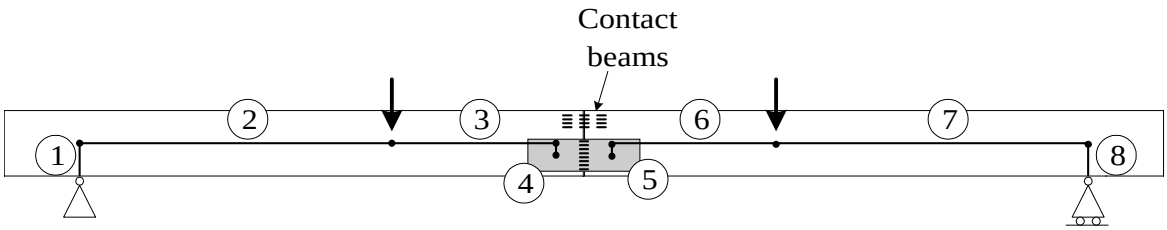

Figure 7.3. TRUSSLAB model for test series BE4. Element numbers for the timber beam elements are shown in a circle.

The properties for the timber beam elements are listed in table 7.1. The timber is Swedish spruce of strength class K24.

Element number	Width mm	Height mm	*E* MPa	*G* MPa
2,3,6,7	45	170	12800	700
1,8	45	150	350	700
4,5	45	200	50000	5000

Table 7.1. Properties for beam elements.

The height of the beams 1 and 8 is estimated considering the width of the support and stress distribution over the height of the beam.

The properties for the nail and plate elements are determined in chapter 3. The initial modulus of elasticity for the contact beams is taken as 1500 MPa and their “plastic” modulus of elasticity is taken as 150 MPa. The word plastic may not be the right word since a possible relief follows the loading curve.

The initial modulus of elasticity for the contact beams is determined so that calculations in TRUSSLAB fit the test results for test series BE4. The plastic modulus of elasticity is taken as 10% of the initial modulus of elasticity. Further investigations of the value of the plastic modulus of elasticity show that for the test series BE3 and BE4 there is only a relatively small change in the behaviour of the joint, no matter if the plastic modulus is taken as 1500 MPa or 150 MPa. However, tests with timber subjected to compression parallel to the grain direction show a

nonlinear stress-strain curve and in TRUSSLAB the curve is simplified to a bi-linear stress-strain curve.

The stress level where the contact beams starts its plastic behaviour is taken as 0.6 times the mean compression strength parallel to the grain direction ($0.6 \cdot 28\text{MPa}$) according to *DS 413 (1998)*.

The load-displacement curves for series BE4 from the tests and from TRUSSLAB are shown in figure 7.4. The predictions by TRUSSLAB are shown as a continuous line while the test results are shown as a dashed line. The curve for the test results is a mean curve for the five different tests and the initial slip is ignored.

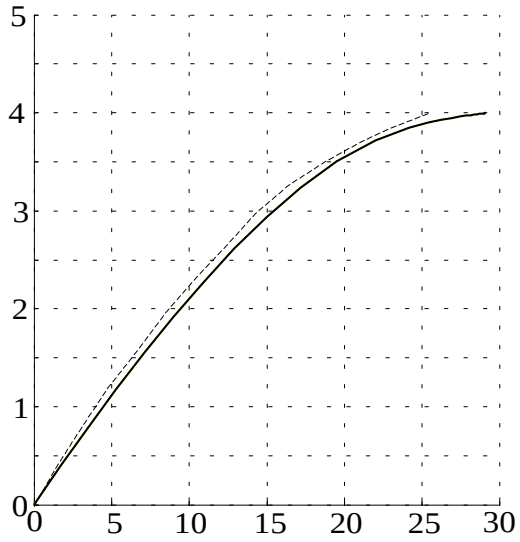

Figure 7.4. Test results from test series BE4 and results from TRUSSLAB calculations. The total load divided by two is shown vertically in kN and the vertical deformation at mid span of the beam is shown horizontally in mm.

As seen from the figure TRUSSLAB predicts the behaviour well with the chosen values of the modulus of elasticity for the contact beams.

To see the influence of the butt effect, test series BE2 should be considered. The results from the test series BE2 together with results from TRUSSLAB are shown in figure 7.5. The predictions by TRUSSLAB are shown as a continuous line and the test results are shown as a dashed line. The curve for the test results is a mean curve for the five different tests and the initial slip is ignored.

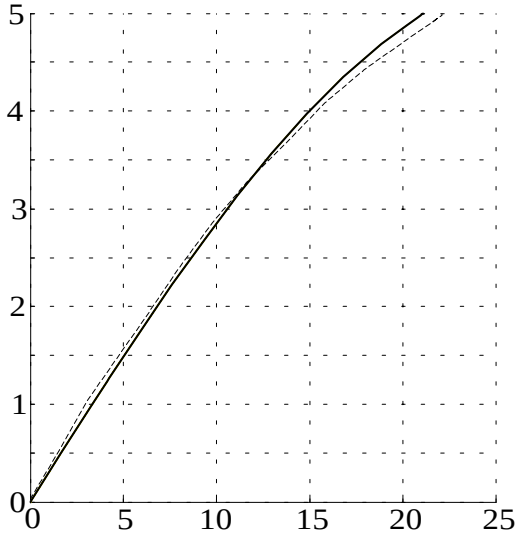

Figure 7.5. Test results from test series BE2 and results from TRUSSLAB calculations. The total load divided by two is shown vertically in kN and the vertical deformation at mid span of the beam is shown horizontally in mm.

No contact element has been used in the TRUSSLAB model since the beams are "connected" with a 45x40 mm (thickness x height) timber beam. The modulus of elasticity for this beam is taken as 12800 MPa and the length is taken as 50 mm. If a contact element with a modulus of elasticity of 12800 MPa is used instead of the 45x40 mm beam a decrease of 10% in the stiffness is observed. This difference is caused by the bending stiffness of the 45x40 mm beam.

When comparing the results from the two test series BE2 and BE4 it is seen that the butt effect results in a decreasing stiffness. However, as mentioned above some of this is caused by the bending stiffness of the 45x40 mm beam.

The results from the test series BE3 are compared with results from TRUSSLAB using the reduced modulus of elasticity (1500MPa/150MPa) for the contact beam (due to the butt effect). In this series there are different sizes of the gap between the timber members. A comparison between test results and TRUSSLAB is shown in figure 7.6.

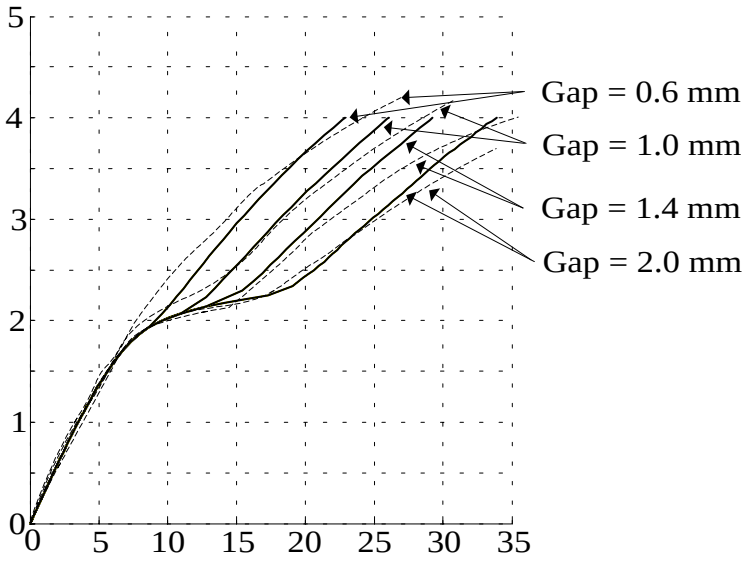

Figure 7.6. Test results from test series BE3 and results from TRUSSLAB calculations. The total load divided by two is shown vertically in kN and the vertical deformation at mid span of the beam is shown horizontally in mm.

TRUSSLAB is able to predict these bending splices well. After contact has been established the stiffness increases. At this part of the load-displacement curves there is a slight overestimation of the stiffness calculated by TRUSSLAB. This can be caused by the fact that for the small plate beams in the TRUSSLAB model the load after buckling in compression is not decreased. From some of the basic tests performed on the GNA20S nail plate it is shown that the load decreases after buckling.

7.2 Influence of Splice Joints in Trusses

The influence of splice joints on deformation and moment distribution is analysed for two specific types of trusses based on the knowledge attained above regarding the modulus of elasticity for the contact beams in the contact element (1500 MPa for the elastic modulus of elasticity and 150 MPa for the ”plastic” modulus of elasticity).

Two different types of trusses are analysed: a fink truss and an attic truss. The timber dimensions and the sizes of the nail plates are determined by a truss manufacturer according to *DS 413 (1982)* and the codes *DS 409 (1982)* and *DS 410 (1982)* (codes of practice for loads and safety of structures). In figure 7.7 and figure 7.8 the two trusses are shown. The trusses are symmetrical and if nothing else is shown on the figures then the nail plates are located symmetrically around the joint lines and at the centre of the joint lines. The main directions of the nail plates are parallel with the two lines drawn through each nail plate.

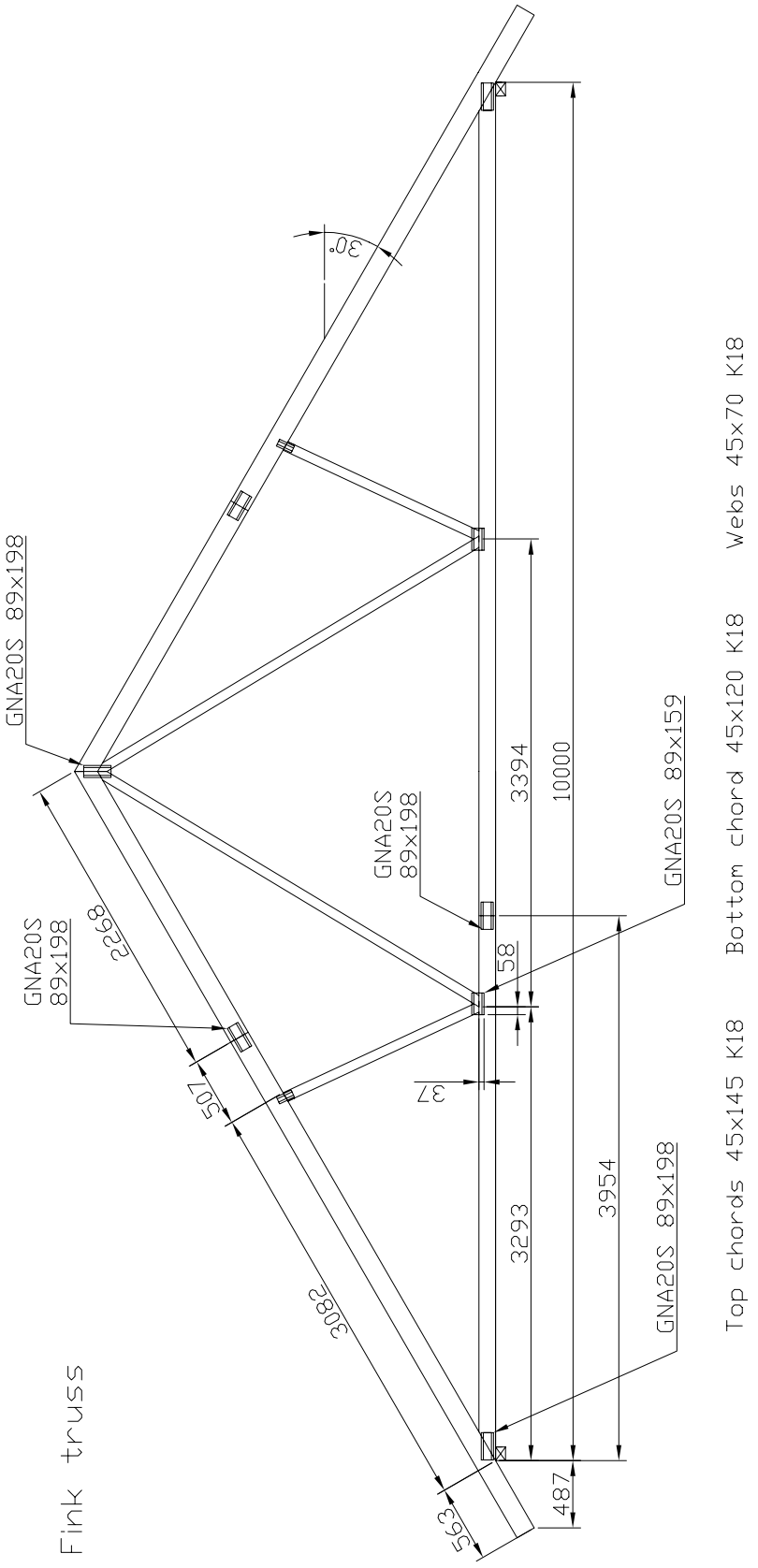

Figure 7.7. Fink truss used for analysis of the influence of splice joints. Dimensions in mm.

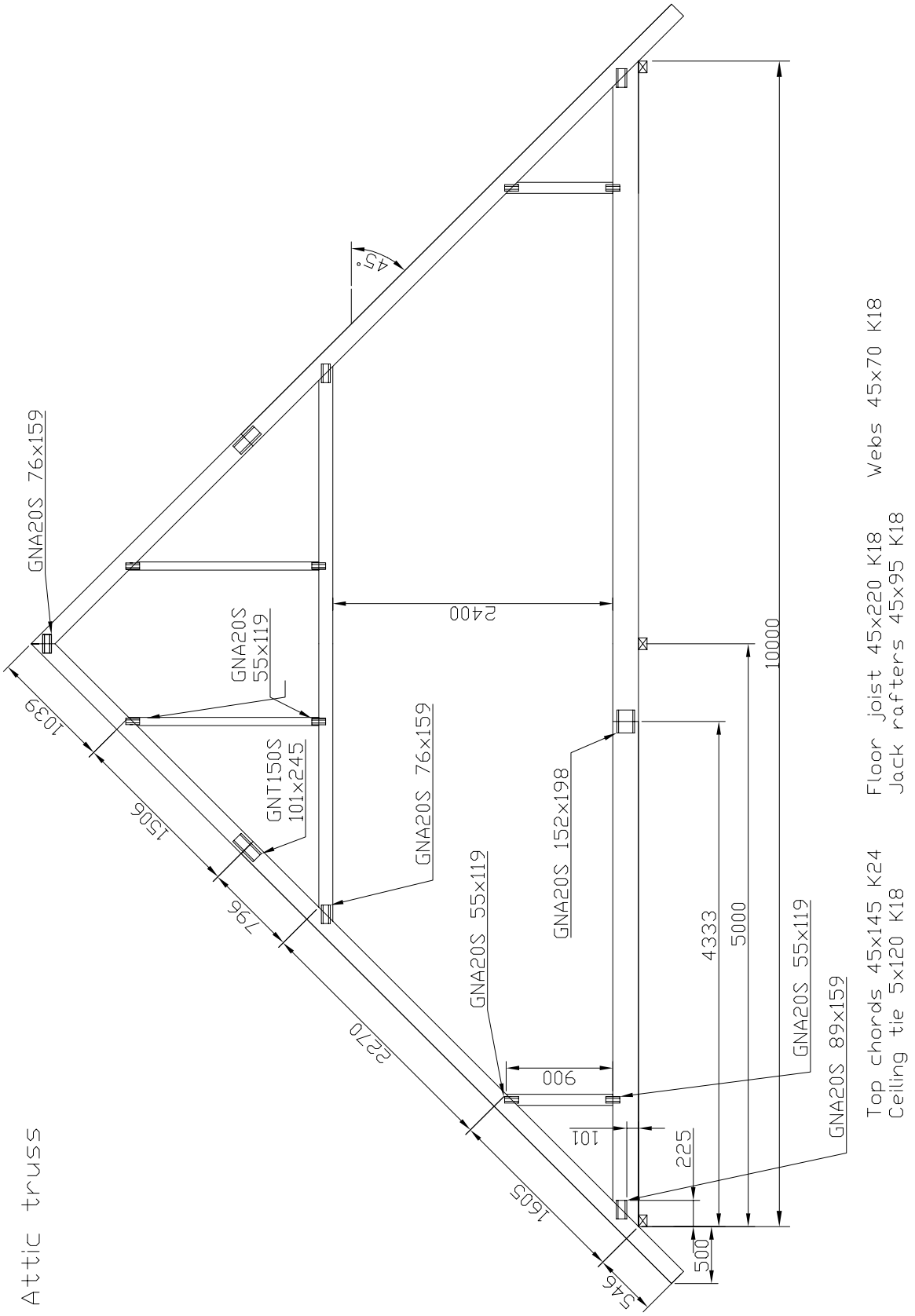

Figure 7.8. Attic truss used for analysis of the influence of splice joints. Dimensions in mm.

The spacing between the trusses is 1000 mm. In addition to the attic truss there is an intermediate floor beam spanning over the three support points. The spacing between these intermediate floor beams is 1000 mm. This decreases the load on the floor joist of the attic truss by 50%.

It should be noted that the attic truss must have additional joints for transportation reasons – in this study they are not considered.

7.2.1 Finite Element Models

To see the influence of the splice joints, two finite element models for each type of truss are set up in TRUSSLAB, namely one model where the splice joints are modelled as fully stiff joints and one model where the splice joints are modelled with nail, plate and contact elements. The rest of the joints in the finite element models are modelled as in the finite element programme used by the truss manufacturer, see figure 7.9 (the splice joints are shown without the special nail, plate and contact elements). The system lines of the beam elements coincide with the timber centre lines, and small beam elements are used to model the eccentricities in the joints.

Since the splice joints are located where the bending moment is close to zero, an extra model with the fink truss is set up. In this model the two splice joints in the top chords are located where the maximum positive bending moment in the upper part of the top chords is present. The nail plates in these splice joints are changed to nail plate type GNT150S with a size of 130x198 mm. The initial gap between the timber members in the chord splices is taken as 1 mm.

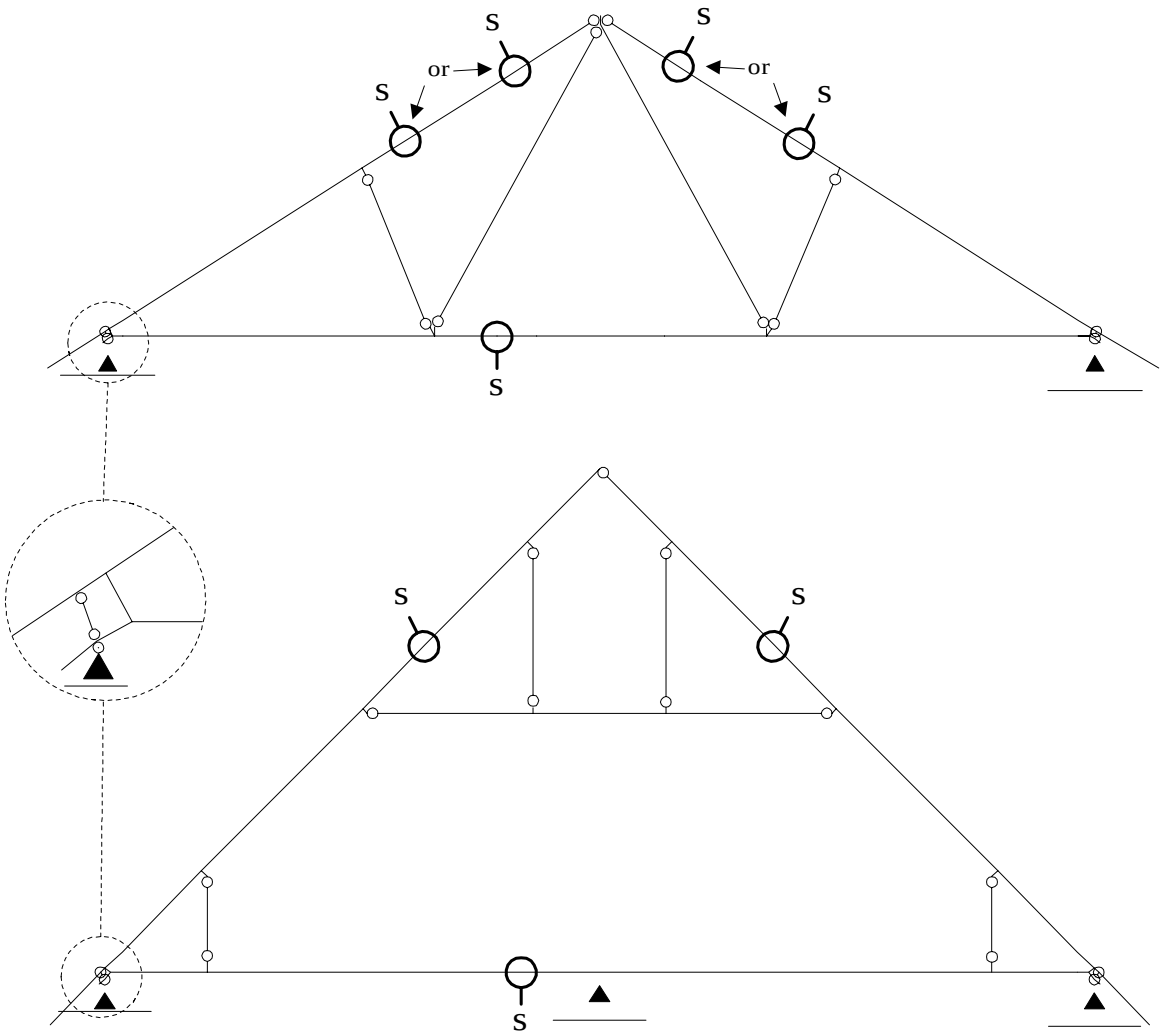

Figure 7.9. Finite element model for the fink truss and the attic truss used for analysis of the influence of splice joints. The location of the splice joints is indicated by a S.

7.2.2 Load Cases

In this analysis only one load case is simulated for each type of truss, see figure 7.10. The specific load cases are chosen, since they are controlling the dimensions of the timber beams and most of the nail plates.

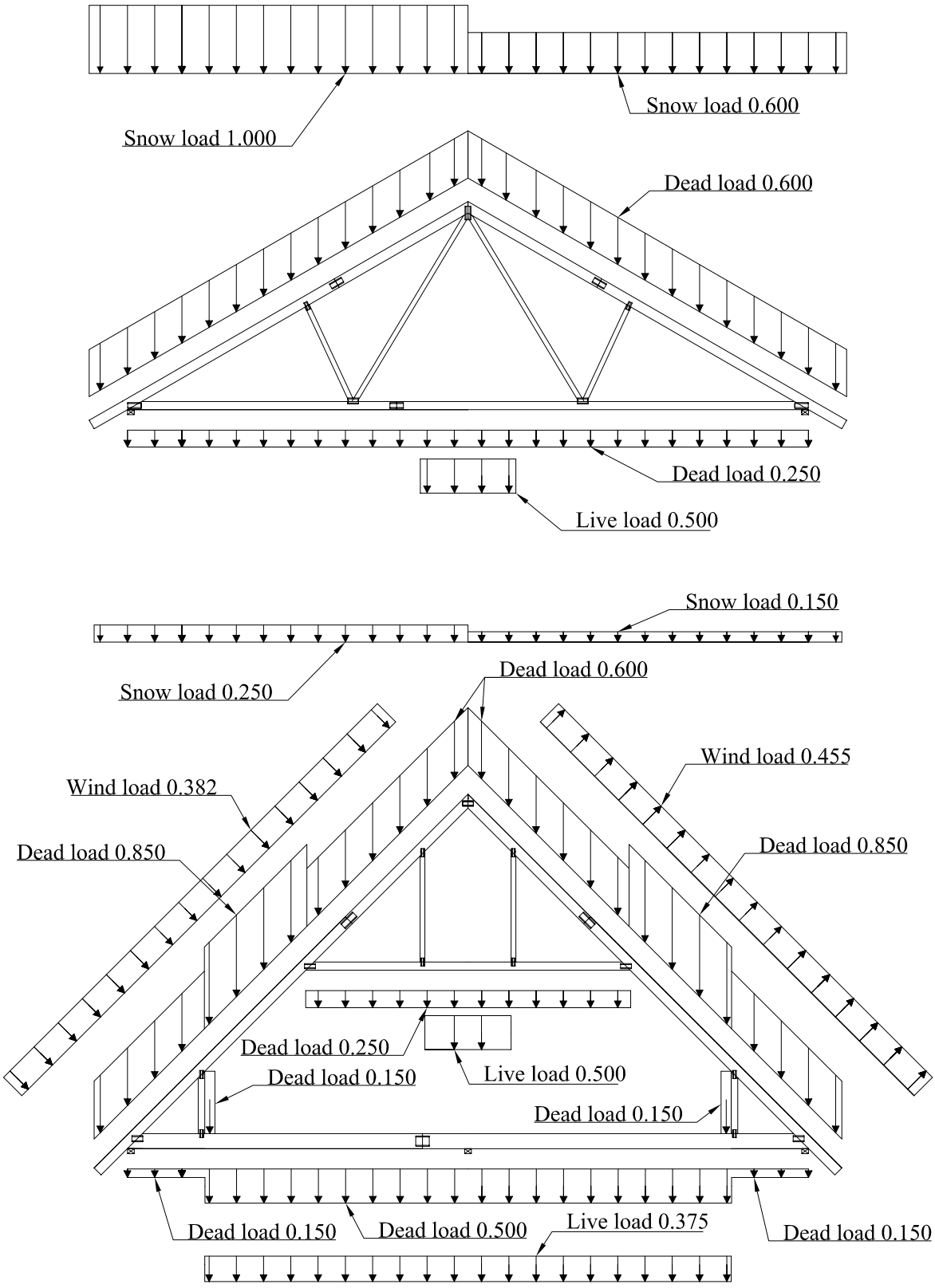

Figure 7.10. Load on trusses. Loads in N/mm. The loads are design values.

The load combination for the fink truss corresponds to:

$$1.0 \cdot \text{dead load} + 1.3 \cdot \text{snow load} + 1.0 \cdot \text{live load}$$

and the load combination for the attic truss is:

$$1.0 \cdot \text{dead load} + 0.5 \cdot \text{snow load} + 1.3 \cdot \text{wind on left - hand side} + 1.0 \cdot \text{live load}$$

7.2.3 Comparison of the Bending Moment Distribution

Calculations show that the changes in the axial and shear forces between the two different finite element models are approximately ± 1%. Therefore, the influence of chord splices is based on comparisons of the distributions of the bending moment and the deformations only.

The distributions of the bending moment for the three finite element models of the fink truss are shown in figure 7.11. The moment curves are almost identical and the moments at four different locations are written below the figure.

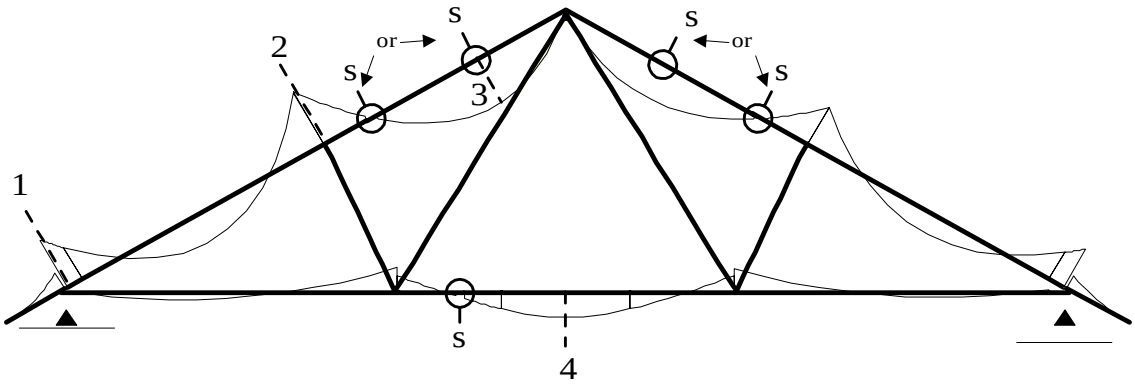

Location:	Truss with stiff splice joints:	Truss with semi-rigid splice joints:	Truss with semi -rigid splice joints located at M_{max}
1	-0.997 kNm	-1.013 kNm (+2%)	-0.986 kNm (-1%)
2	-1.203 kNm	-1.132 kNm (-6%)	-1.293 kNm (+7%)
3	1.087 kNm	0.918 kNm (-16%)	1.050 kNm (-3%)
4	0.459 kNm	0.452 kNm (-2%)	0.459 kNm (0%)

Figure 7.11. Bending moment distribution for the fink truss. The location of the splice joints is indicated by a S.

The two models with semi-rigid behaviour of the splice joints result in a redistribution of the bending moment. The redistribution is caused by the fact that the splice joints are not as stiff as the connected timber members and in a statically undetermined structure the member forces are distributed according the stiffness of the structure.

For the model with the splice joints located close to the points with zero bending moments the overall maximum moment decreases from 1.203 kNm to 1.132 kNm (6%). For the model with the splice joints in the top chords at location 3 (at the point with maximum bending moment for the upper part of the top chords) the maximum moment increases from 1.203 kNm to 1.293 kNm (7%).

When comparing the model with the stiff splice joints to the two models with the semi-rigid splice joints it is found that the largest decrease in the moment distribution is 16% and the largest increase in the moment distribution is 7%.

The distribution of the bending moment for the attic truss is shown in figure 7.12.

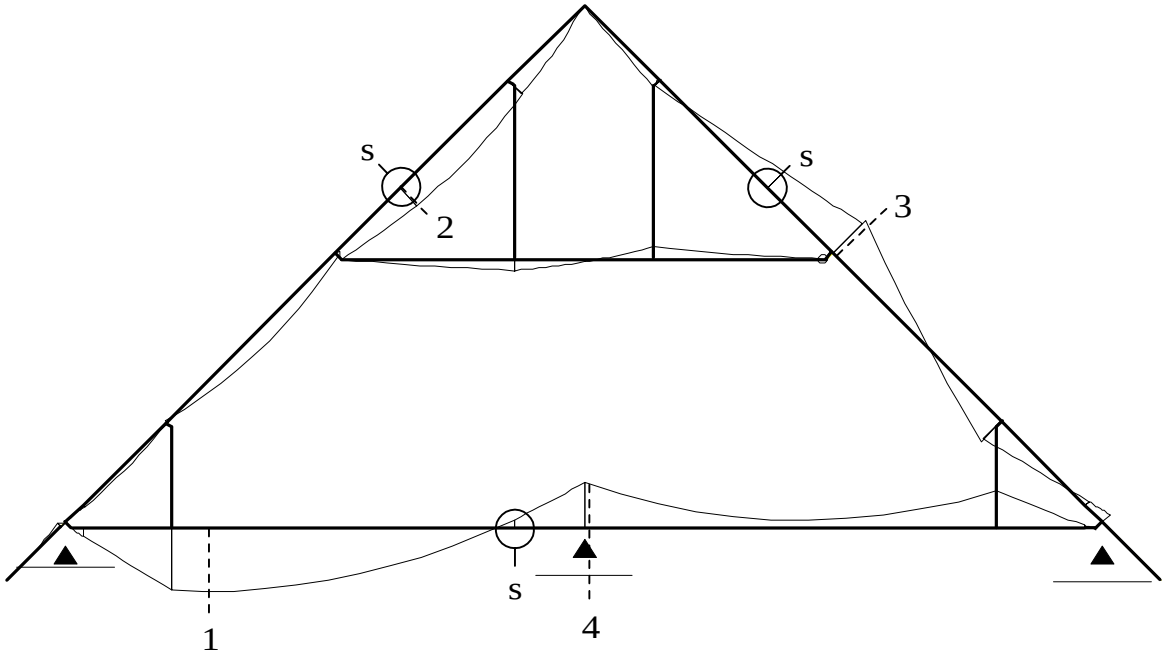

Location:	Truss with stiff splice joints:	Truss with semi-rigid splice joints:
1	-3.257 kNm	-3.362 kNm (+3%)
2	1.205 kNm	1.094 kNm (-9%)
3	-2.329 kNm	-2.268 kNm (-3%)
4	2.292 kNm	2.220 kNm (-3%)

Figure 7.12. Bending moment distribution for the attic truss. The location of the splice joints is indicated by a S.

From the values of the bending moments it is found that the largest increase in the bending moment is 3% at location 1 and the largest decrease in the bending moment is 9% at location 2 where the chord splices in the top chords are located.

The size of the increase in the bending moment is of the same order as found for the fink truss with the size and location of the nail plates given by the truss producer.

7.2.4 Comparison of Deformations

In figure 7.13 the deformations of the fink truss are shown (scaled by a factor of 50). The deformations for the three different models are almost identical and for comparison the deformations at three locations are written below the plot of the deformed structure. The deformations are calculated from the design values of the

loads, and the moduli of elasticity for the timber beams are not multiplied by any modification factor to take the load duration into account.

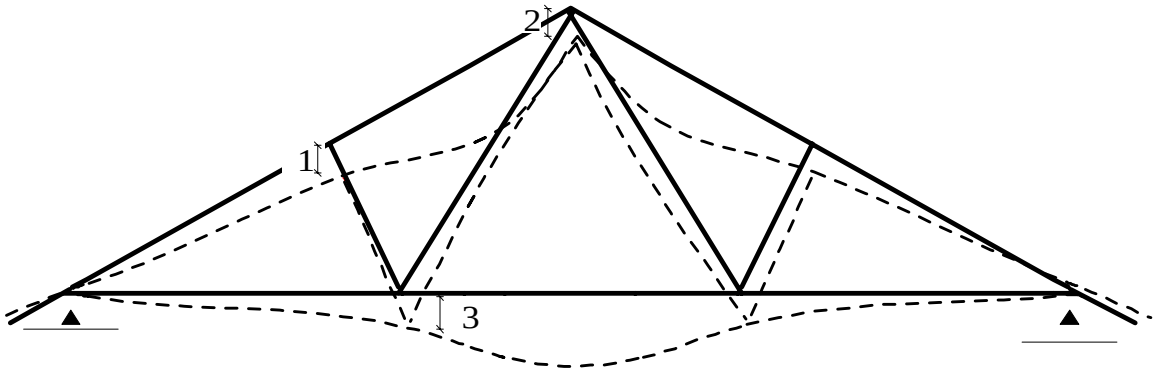

Location:	Truss with stiff splice joints:	Truss with semi-rigid splice joints:	Truss with semi -rigid splice joints located at M_{max}
1	5.79 mm	5.80 mm (0%)	6.14 mm (+6%)
2	5.16 mm	5.22 mm (+1%)	5.62 mm (+9%)
3	6.25 mm	6.29 mm (+1%)	6.71 mm (+7%)

Figure 7.13. Vertical deformations for the fink truss.

The deformations increase when the joints are modelled to be semi-rigid. The increases in the deformations between the model with stiff splice joints and the model with the nail plates located near the points with bending moments close to zero are less than 2%. When the nail plates are located at the maximum bending moment in the upper part of the top chords the deformations increase up to 9%.

Figure 7.14 shows the deformation of the attic truss due to the given loads.

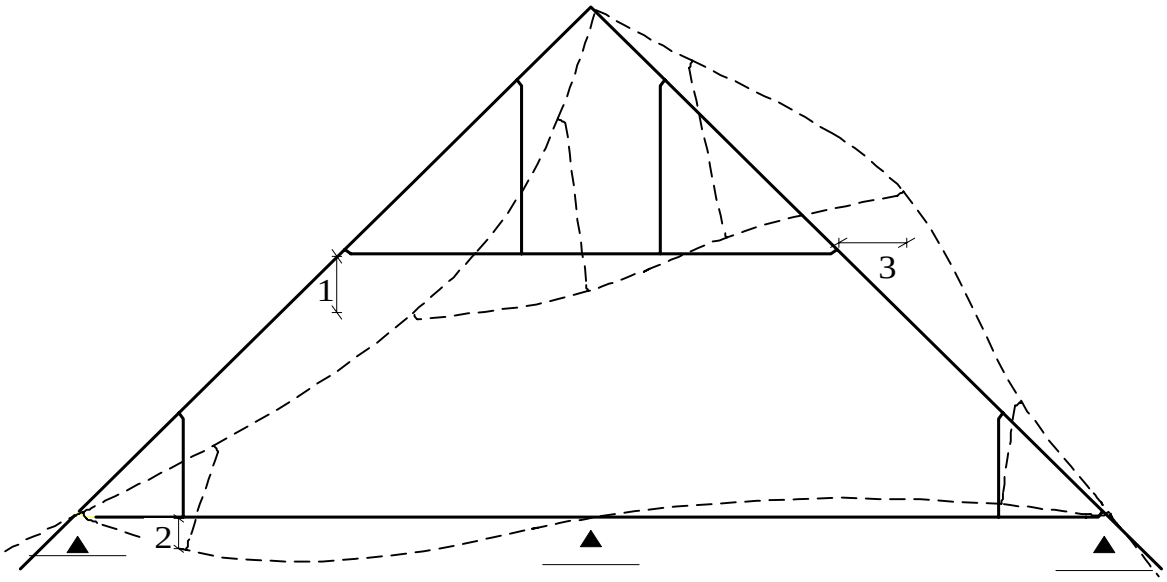

Location:	Truss with stiff splice joints:	Truss with semi-rigid splice joints:
1	27.37 mm	30.26 mm (+11%)
2	14.23 mm	14.65 mm (+3%)
3	27.92 mm	30.86 mm (+11%)

Figure 7.14. Deformations for the attic truss.

The maximum increase in the vertical deformation is 11% found at location 1. An identical percentage increase in the horizontal deformation is found at location 3.

The changes in the deformations of the attic truss are relatively high when they are compared with the changes in the deformations of the fink truss with nail plate size and location determined by the truss manufacturer. An explanation to this may be that there are no points in the rafters of the attic truss with zero moment and, therefore, the influence of the splice joints becomes more significant.

7.3 Conclusions

In the analysis of splice joints subjected to bending it is found that the butt effect should be considered in order to make TRUSSLAB predict the stiffness from the bending tests. However, TRUSSLAB still slightly overestimates the stiffness after contact between the timber members has been established. This can be caused by the fact that it is assumed in the theory behind TRUSSLAB that the nail plate is able to maintain the load level after buckling in compression.

For the model of the fink truss with a size and location of the splice joints as suggested by the truss manufacturer the distribution of the bending moment in TRUSSLAB becomes more favourable compared with the distribution of the bending moment in the model with stiff splice joints since the maximum moment values decreases.

According to the calculations for the fink truss performed by the truss manufacturer the nail plates in the splice joints in the top chords are only utilised by up to 23% of their load-carrying capacity and the nail plates in the splice joint in the bottom chord are utilised 45%. This means that the splice joints fulfil the conditions in Eurocode 5 and can therefore be considered rotationally stiff in the finite element model. It is also calculated that the increase in the vertical deformation is less than 2% when the model with semi-rigid splice joints (located where the bending moments are close to zero) is compared to the model with stiff chord splices. As expected, the influence of the splice joints on the distribution of the bending moment and on the deformation becomes larger if the splice joints in the top chords are located at the point with maximum moment.

For the attic truss the nail plates are utilised 96% and 80% of the load-carrying capacity for the chord splices in the top chords and in the bottom chord, respectively. The bending moments only increase by 3%, but the deformations increase by up to 11% when the model with the semi-rigid joints in the chord splices is compared to the model with stiff joints. These chord splices do not fulfil the conditions in Eurocode 5 and can therefore not be treated as rotationally stiff.

It should be noted that even though the nail plates in the chord splices are utilised close to their load-carrying capacity the influence on the distribution of the bending moments may be relatively small which is seen for the attic truss. The deformations, however, increase by 11%.

The only chord splices where contact between the timber ends is established is in the model of the fink truss where the chord splices are located at the point with maximum bending moment in the upper part of the top chords. If the initial size of the gap is taken as 0.4 mm instead of 1.0 mm, contact is established in most of the top chord splices for both types of trusses. Furthermore, this results in smaller deformations. Further analysis of the gap size shows that if the initial gap size is taken as 0 mm the distribution of the bending moments in the TRUSSLAB model with semi-rigid joints tends to get closer to the bending moment distribution of the model with stiff joints. The maximum percentage increase in the deformations is reduced from 11% to 6% for the attic truss and from 0% to –2% for the fink truss.

The influence of the chord splices would perhaps be different if all joints were modelled in TRUSSLAB. Furthermore, second order theory could change the results.

8 Conclusion

The conclusions of the thesis are divided into two sections. One summarises the contents and some results of each chapter of the thesis. The purpose is to give an overview before the general conclusions are given. Additional suggestions for future work are listed. Finally, a list of items I would change if I should start over again is given.

8.1 Summary of the Thesis

In chapter 1 an introduction to the frame truss is given and four different finite element models are briefly described. The Foschi model is chosen as a basis for further development since it is the model with the best properties for predicting the stiffness of joints and trusses with nail plates.

In chapter 2 the theory behind TRUSSLAB is given. TRUSSLAB is the name for a modified version of the Foschi model, and the joints are modelled by special nail, plate and contact elements. The nail elements are used to model the deformation and strength of nail groups, and the plate elements model the deformation and strength of the nail plate over the joint line. The contact element takes possible contact forces between timber members into account. The material properties of the nail and plate elements are nonlinearly elastic, and the properties of the contact elements are bilinearly elastic.

In chapter 3 the GNA20S nail plate is analysed. The properties of the plate element are determined from six basic tests and the properties of the nail elements are determined from four basic tests. Additional tests are used to verify the theory of the plate and nail elements in TRUSSLAB. Regarding the tests targeted at the plate element, TRUSSLAB predicts the load-displacement curves relatively well, but is better for predicting the load-displacement curve for the nail plates subjected to tension than the nail plates subjected to compression. Considering the tests targeted at the nail element there is greater differences between the test results and the predictions given by TRUSSLAB - both when comparing the stiffness and the ultimate load levels.

In chapter 4 the properties of the plate and nail elements are determined for the GNT150S nail plate.

In chapter 5 knee joints are analysed. 24 different types of knee joints have been tested and the load-displacement curves and the ultimate loads have been registered. When comparing the load-displacement curves with predictions by TRUSSLAB it is found that TRUSSLAB predicts the initial stiffness well. At higher load levels (>40-60% of the ultimate load) TRUSSLAB overestimates the stiffness. This is caused by development of cracks and splitting of the timber and that the timber is modelled by linear elastic material properties. In the compression zone between the leg and the rafter a biaxial stress situation occurred in the rafter, and in many of the tests large deformations were observed in this area. In TRUSSLAB the bilinear contact element takes some of these plastic deformations into account, but the rafter is "only" modelled by a linear elastic beam element.

In several cases the ultimate loads and failure modes predicted by TRUSSLAB are not similar to those found in the tests with the knee joints. This is often caused by the fact that timber splitting is not implemented in TRUSSLAB.

In chapter 6 an analysis of a frame truss is performed using one of the most promising type of knee joints (high stiffness and strength). The frame truss is analysed by a traditional finite element program using either rigid or pinned joints and by TRUSSLAB. In general only small differences (<5%) between the two models are observed, but the displacements and the distribution of the bending moments are more favourable in the TRUSSLAB model.

In chapter 7 the influence of chord splices in a fink truss and in an attic truss is analysed. Results from finite element models similar to those used by a truss manufacturer are compared with models with the special elements in TRUSSLAB. Regarding the fink truss, TRUSSLAB predicts a more favourable bending moment distribution, whereas the displacements are almost unchanged. For the attic truss, however, the displacements increase by up to 3% and the bending moments by up to 11%.

8.2 General Conclusions

The TRUSSLAB model is based on the geometry of the trusses – including the geometry of the joints. The size and the location of the nail plates, the deformations of the nail groups and of the plate regions over the joint lines are included in the model. Furthermore possible contact between timber members is considered. The plate, nail and contact elements are modelled with nonlinear elastic material properties. It may be considered to change the material properties to nonlinear plastic properites to take possible unloading into account.

In general the modified Foschi model is assumed to take important aspects into account - e.g. nonlinearity of the deformation of the joint, the size and the location of the nail plates and contact forces. Furthermore, the sectional forces needed for design of the joints are given directly by the model. Finding the sectional forces is a

problem in e.g. the model with fictitious elements, where assumptions have to be made before the sectional forces in the nail plates can be determined.

It is assumed that the nail plate will maintain the load level after buckling (in the plate element). However, in some of the tests it is observed that the load level decreased rapidly after buckling.

The TRUSSLAB model predicts the behaviour of splices subjected to tension better than the splices subjected to compression. In general TRUSSLAB predicts failure at a lower load level for all the "simple" tests with the GNA20S nail plate compared to the test results.

The failure conditions in *Eurocode 5 (2001)* for the plate capacity are not implemented in TRUSSLAB, since they lead to strange and misleading results when complex knee joints are considered. Therefore, the plate capacity is based on conditions where the stress levels in the plate beams are taken into consideration.

When determining the properties of the nail element timber failure was often observed in the corresponding tests. The failure conditions in *Eurocode 5 (2001)* are implemented in TRUSSLAB since, they predict ultimate load levels relatively close to the ultimate load levels determined in the tests.

From the tests series with the 24 different types of knee joints it is found that the rafter shall proceed to the corner of the knee joint to get a stiff and strong joint. The nail plates shall be located as closely as possible to the top of the rafter and the largest stiffness and strength is attained if the nail plates are cut so they are flush with the top of the rafter (45º).

TRUSSLAB predicts the initial stiffness of the knee joints well, but larger differences are observed when comparing the predicted ultimate load levels and the failure modes with the results from the tests.

Considering the strength and stiffness of knee joint type ET150 it is safe to produce frame trusses with a span of 8.5 m and a geometry as given in chapter 6. For the frame truss TRUSSLAB predicts a more favourable distribution of the bending moments, and the displacements are up to 5% smaller compared with a finite element model similar to the one used by a truss manufacturer.

From the truss manufacturer's point of view it may be a great advantage that frame trusses with a span of 8.5 m (and the given geometry) can be produced with nail plates in all joints. Today the knee joints in such a frame truss would typically be produced using expensive and specially fabricated steel plates with separate nails or with plywood sheets glued and nailed at each side of the joint.

In the analysis of the effect of chord splices on the deformations and sectional forces two types of trusses were modelled. The modelling was performed with a finite element model with the special elements in TRUSSLAB and with a finite element model similar to the one used by a truss manufacturer. For the fink truss

TRUSSLAB predicts a more favourable bending moment distribution, but for the attic truss the maximum bending moment increases by up to 3% and the deformations increases by up to 11%.

In general it is concluded that TRUSSLAB predicts the behaviour of timber joints with nail plates relatively well and that future finite element models for design of timber trusses can use the theory on which TRUSSLAB is based. However, in many areas further research and work is still needed.

8.3 Suggestions for Future Work

As suggestions for future works the following subjects can be considered:

- Tests with several types of nail plates should be performed and the results should be compared with predictions given by TRUSSLAB. This would indicate if the theory of TRUSSLAB can be used for other types of nail plates than the GNA20S and GNT150S.
- Full-scale tests with frame trusses should be performed and corresponding finite element models should be made in TRUSSLAB to see if TRUSSLAB predicts the behaviour well.
- Have a closer look at the nonlinear behaviour and the biaxial stress situation that occur in the contact zone between the rafter and the leg. If possible this could be implemented in TRUSSLAB. This could make TRUSSLAB predict the upper part of the load-displacement curves for the knee joints more accurately.
- Find a method to take the splitting of the timber into account and be able to predict when splitting occurs. This could make TRUSSLAB predict the upper part of the load-displacement curves for the knee joints more accurately.
- Implement second order theory in TRUSSLAB.
- Perform additional tests with knee joints to get a better statistic material.
- Perform tests with knee joints with e.g. different support conditions and different slope of the rafter.

8.4 If I Should Start Over Again With the Knowledge I Have Attained

This section is given to prevent others from repeating some of the mistakes that I have done and to point out some of the areas where things could have been made in another and maybe better way.

Some of the nail plate tests were stopped prior to failure in order not to destroy the displacement transducers. Not all of the tests were continued with the displacement transducers dismounted, which they should have been in order to register the ultimate load levels.

In the tests used to determine the properties of the plate element (section 3.1) and in the additional tests used to verify the theory in TRUSSLAB it should be clear whether the nail plates should be cut or not to avoid withdrawal of nails in parts of the nail plate area, see figure 8.1. In real situations the nail plates are not cut and therefore, the deformations due to the withdrawal of nails will be included in the overall deformation of the truss.

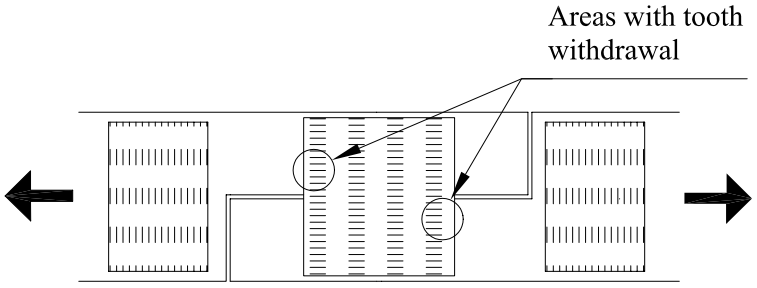

Figure 8.1.Withdrawal of nails in parts of a nail plate if the plate is not weakened in the joint line.

Similar considerations should be made when determining the anchorage capacity. Should some of the nails be removed and should the remaining nails be located far from the timber ends to ensure that timber failure will not appear?

In the theory behind the plate element a relatively sophisticated model is used to include the nonlinearity of the beams (determination of the stresses at several points in each the beams). The method seems to be too sophisticated when considering all the uncertain parameters that are not taken into account (e.g. the complex geometry of the nail plates and prestresses). However, no other method to solve this problem could be found even though a great number of methods were tested. The method given in *Foschi, R. O. (1977)* only considers axial and shear forces at the ends of the beams. Therefore, if a fixed beam is loaded by a shear force at one end then the moment at the other end is not considered. Furthermore, the expressions given in *Nielsen, J. N. (1996)* are not true when a beam is in the plastic stage.

The method used to take the interaction between the two types of beams into account may also seem to be too sophisticated – again considering the uncertain parameters.

9 Summary in Danish

I kapitel 1 introduceres trempelspæret, og fire forskellige elementmetodemodeller bliver kort beskrevet. Som basis for yderligere udvikling vælges Foschis model, da det er den model, der har de bedste egenskaber til bestemmelse af stivheden af samlinger og spær med tandplader.

I kapitel 2 beskrives teorien bag TRUSSLAB. TRUSSLAB er navnet på en modificeret version af Foschis model, og samlingerne er opbygget med specielle tand-, plade- og kontaktelementer. Tandelementerne bliver brugt til at modellere deformationen og styrken af tandgrupper, og pladeelementerne modellerer deformationen og styrken af den del af tandpladen, der er beliggende over fugelinien. Kontaktelementet tager hensyn til eventuelle kontaktkræfter mellem trædele. Materialeegenskaberne for tand- og pladeelementerne er ikke-lineærelastiske og egenskaberne for kontaktelementerne er bi-lineærelastiske.

I kapitel 3 analyseres GNA20S tandpladen. Egenskaberne for pladeelementet bestemmes ved hjælp af 6 basisforsøg, og egenskaberne for tandelementet bestemmes ved hjælp af 4 basisforsøg. En række yderligere forsøg bruges til at verificere teorien bag plade- og tandelementerne i TRUSSLAB. Ud fra forsøgene, der er rettet mod verifikation af pladeelementet, ses det, at TRUSSLAB bestemmer last-flytningskurverne relativt præcist. TRUSSLAB er dog bedre til at bestemme last-flytningskurverne for de situationer, hvor tandpladerne er udsat for træk sammenlignet med de situationer, hvor tandpladerne er udsat for tryk. Mht. forsøgene, der er rettet mod verifikation af tandelementet, er der større forskelle mellem forsøgsresultaterne og resultaterne fra beregningerne vha. TRUSSLAB – både hvad angår stivhed og brudlast.

I kapitel 4 bestemmes egenskaberne for plade- og tandelementerne for tandpladen GNT150S.

I kapitel 5 analyseres knæsamlinger. Der er udført forsøg med 24 forskellige typer af knæsamlinger og last-flytningskurverne og brudlasterne er registreret. Ud fra en sammenligning af last-flytningskurverne fra forsøgene med beregninger vha. TRUSSLAB ses det, at TRUSSLAB forudsiger den initiale stivhed godt. Når lasten er større end 40-60% af brudlasten, så overestimerer TRUSSLAB stivheden. Dette skyldes, at revner i træet udvikles, og der sker flækning, samt at træet er modelleret med lineærelastiske materialeegenskaber. I trykzonen mellem benet og

spærhovedet opstår der en toakset spændingstilstand, og i mange af forsøgene blev der observeret store deformationer i dette område. I TRUSSLAB tages nogle af disse plastiske deformationer i beregning vha. kontaktelementet, men spærhovedet er ”kun” modelleret som et lineærelastisk bjælkelelement.

I en række af forsøgene er de brudlaster og brudformer, som forudsiges i TRUSSLAB, ikke identiske med dem, der blev konstateret ved forsøgene. Dette skyldes ofte, at der ikke tages hensyn til flækning i TRUSSLAB.

I kapitel 6 analyseres et trempelspær, hvor knæsamlingen er udført som en af de mest lovende typer (mht. stivhed og styrke). Trempelspæret analyseres vha. en traditionel elementmodel, hvor samlingerne modelleres enten som charniere eller som stive, samt vha. TRUSSLAB. Generelt er forskellene mellem de to modeller små (<5%), og TRUSSLAB giver den mest gunstige momentfordeling samt mindre flytninger.

I kapitel 7 undersøges indflydelsen af stødsamlinger i et trekantspær samt i et hanebåndsspær. Resultater fra elementmodeller magen til dem, der benyttes af spærfabrikanter, sammenlignes med resultater fra TRUSSLAB, hvor de specielle elementer er benyttet. Mht. trekantspæret, så er momentfordelingen mere gunstig, når TRUSSLAB-modellen benyttes, hvorimod flytningerne er stort set uforandrede. Derimod ses det for hanebåndsspæret, at flytningerne forøges med op til 3% og momenterne med op til 11%, når TRUSSLAB-modellen benyttes.

10 References

Aasheim, E. & Solli, K. H. (1990), 'Proposal for a Design Code for Nail Plates', CIB-W18/23-7-1, Lisbon, Portugal, 1990.

Beineke, L. A. & Suddarth, S. K. (1979), 'Modeling Joints made with Light-Gage Metal Connector Plates', Forest Products Journal, 19(8), 1979.

Berglund, P. & Holmberg, J. (2000), 'CALROOF – Program för modellering av takstolar med hänsyn till eftergivlighed I knutpunkter' (in Swedish) (CALROOF – Program for modelling of trussed considering the deformations of the joints), Lund University, Department of Mechanics and Materials, ISSN 0281-6679, 2000.

Blaβ, H. J., Ehlbeck, J. & Kurzweil, L. (1997), 'Berücksichtigung der Momentenübertragung von Nagelplattenverbindungen bei der Bemessung', Versuchsanstalt für Stahl, Holz und Steine, Abteilung Ingenieurholzbau, Universität Friderciana Karlsruhe, 1997.

Boligministeriet, Bygge- og boligstyrelsen, MK-Godkendelse, (1994), MK 5.60/1034 (in Danish), (Approval for Nail Plate Type GNA20S). August 1994.

Boligministeriet, Bygge- og boligstyrelsen, MK-Godkendelse, (1996), MK 5.60/0925 (in Danish), (Approval for Nail Plate Type GNT150S and GNT150). 1996.

Bovim, N. I. & Aasheim, E. (1985), 'The Strength of Nail Plates', CIB-W18/18-7-6. Beit Oren, Israel, 1985.

Byskov, E. (1982), 'Plastic Symmetry of Roorda's Frame' J. Struct. Mech., 10(3), pp 311-328, 1982-1983.

Chrisfield, M. A. (1997), 'Non-linear Finite Element Analysis of Solids and Structures', Volume 1, 1997.

DS 409 (1982), 'Norm for sikkerhedsbestemmelser for konstruktioner' (in Danish) (Code of Practise for the Safety of Structures), Dansk Standard, 1. udgave/8.oplag, 1982.

DS 409 (1998), 'Norm for sikkerhedsbestemmelser for konstruktioner' (in Danish) (Code of Practise for the Safety of Structures), Dansk Standard, 2. udgave/1.oplag, 1998.

DS 410 (1982), 'Norm for last på konstruktioner' (in Danish) (Code of Practice for Loads for the Design of Structures), Dansk Standard, 3. udgave/7.oplag, 1982.

DS 413 (1982), 'Norm for trækonstruktioner' (in Danish) (Code of Practice for the structural use of timber), Dansk Standard, 4. udgave/6.oplag, 1982.

DS 413 (1998), 'Norm for trækonstruktioner' (in Danish) (Code of Practice for the structural use of timber), Dansk Standard, 5. udgave/1.oplag, 1998.

DS/EN 384 (1995), 'Structural timber – Determination of characteristic values of mechanical properties and density', 1995.

DS/EN 408 (1995), 'Timber structures – Structural timber and glued laminated timber – Determination of some physical and mechanical properties', 1995.

DS/EN 26 891 (1993), 'Timber structures - Joints made with mechanical fasteners - General principles for the determination of strength and deformation characteristics', 1993.

EN 1075 (1999), 'Timber structures – Test methods – Joints made with punched metal plate fasteners', September 1999.

Eurocode 5 (1993) - ENV 1995-1-1, 'Eurocode 5 – Design of Timber Structures – Part 1-1: General Rules, General rules and rules for buildings'. CEN Brussels, 1993

Eurocode 5 (2001) - prEN 1995-1-1. Final draft of 1995-1-1, 'Eurocode 5 – Design of Timber Structures – Part 1-1: General Rules, General rules and rules for buildings'. CEN Brussels, 2001.

Foschi, R. O. (1977), 'Analysis of Wood Diaphragms and Trusses. Part II: Truss-Plate Connections', Can. J. Eng. Vol. 4, 1977.

Foschi, R. O. (1979), 'Truss Plate Modelling in the Analysis of Trusses'. Metal-Plate Wood-Truss Conference 1979, pp 88-97, 1979.

Hansen, F. T., Mortensen, N. L. & Hansen, L. P. (1990), 'Fuldskaldforsøg med trempelspær udsat for statisk og dynamisk last - nr. 1.', (in Danish) (Full-Scale Testing of Frame Trusses Subjected to Static and Dynamic Load - no. 1.), Aalborg University, ISSN 0902-7513 R9024, September 1990.

Jensen, H. & Rasmussen, H. (1993), 'Undersøgelse af tandplader i stødsamlinger' (in Danish) (Analysis of Nail Plates in Tension Splices), M. Sc.-thesis, University of Aalborg, 1993.

Jensen, J. L. (1994), ‘Dowel-Type Fastener Connections in Timber Structures subjected to Short-Term Loading’, SBI 237, Danish Building Research Institute, 1994.

Källsner, B & Kangas, J. (1991), ’Theoretical and Experimental Tension and Shear Capacity of Nail Plate Connections’, CIB-W18/24-7-1, Oxford, United Kingdom, 1991.

Karacabeyli, E., Varoglu, E., Lum, C. & Olson L. (1990), ‘Structural Performance of Punched Metal Plated Glulam Trusses’, International Timber Engineering Conference, Tokyo, 1990.

Kevarinmäki, Ari (2000), ‘Semi-rigid Behaviour of Nail Plate Joints’, Ph.D. Thesis, Helsinki University of Technology, TKK-TRT-109, 2000.

Kevarinmäki, Ari & Kangas, J. (1995), ’Nail Plate Capacity in Joint Line’, CIB-W18/28-7-8, Copenhagen, Denmark, 1995.

King, C. G. & Wheat, D. L. (1988), ‘Deflection and Member Behavior of Metal-Plate-Connected Parallel-Chord Wood Trusses’, International Conference on Timber Engineering, 1988.

Kloch, S. & Hansen, F. T. (1991), ‘Fuldskaldforsøg med trempelspær udsat for statisk og dynamisk last - nr. 3.’, (in Danish) (Full-Scale Testing of Frame Trusses Subjected to Static and Dynamic Load - no. 3.), Aalborg University, ISSN 0902-7513 R9128, August 1991.

Kloch, S. & Hansen, L. P. (1990), ‘Fuldskaldforsøg med trempelspær udsat for statisk og dynamisk last - nr. 2.’, (in Danish) (Full-Scale Testing of Frame Trusses Subjected to Static and Dynamic Load - no. 2.), Aalborg University, ISSN 0902-7513 R9025, August 1990.

Larsen, H. J. & Jensen, J. L. (2000), ‘Influence of semi-.rigidity of joints on the behaviour of timber structures’, Prog. Struct. Engng Mater., 2000.

Lau, P. W. C. (1987), ‘Factors affecting the behaviour and modelling of toothed metal-plate joints’, Canadian Journal of. Civil Engineering, 14: 1987.

Lum, C., Jones, E. & Hintz, B. (1996), ‘Design of Wood Trusses for Small Buildings’, International Wood Engineering Conference, 1996.

Lum, C. & Varoglu, E. (1988), ‘Testing and Analysis of Parallel Chord Trusses’, International Conference on Timber Engineering, 1988.

Maraghechi, K. & Itani, R. Y. (1984), ‘Influence of Truss Plate Connectors on the Analysis of Light-Frame Structures’, Wood and Fiber Science, 16(3), 1984.

Mortensen, N. L. & Kloch, S. (1992), ‘Strength and Stiffness of Knee Joints in Timber Frames’, Aalborg University, ISSN 0902-7513 R9247, December 1992.

Nielsen, J. (1996), 'Stiffness Analysis of Nail-Plate Joints Subjected to Short-Term Loads', Ph.D.-Thesis, Dept. of Building Technology and Structural Engineering, University of Aalborg, Denmark, 1996.

Nielsen, J. & Rathkjen, A. (1994), 'Laterally Loaded Nail-Plates', Dept. of Building Technology and Structural Engineering, University of Aalborg, Denmark, April 1994.

Norén, B. (1981), 'Design of Joints with Nail Plates (second edition)', CIB-W18/14-7-1, Warsaw, Poland.

Nørgaard, M. & Thomsen, K. B., 'Styrke- og stivhedsanalyse af hjørnesamlinger på trempelspær' (in Danish) (Strength and Stiffness Analysis of Knee Joints in Timber Frames), B. Sc.-thesis, University of Aalborg, 2001.

Olsson, A. & Rosenqvist, F. (1996) 'Jämförande beräkningar av nedböjningar hos trätakstolar med spilplåtförband' (in Swedish) (Comparative computation of deflections in wooden roof trusses connected with nail plates), Lund University, Division of Structural Mechanics, Report TVSM-5066, 1996.

Riberholt, H. (1982), 'Guidelines for Static Models of Trussed Rafters', CIB W-18, 15-14-1, Karlsruhe, 1982.

Riberholt, H. (1989), 'Guidelines for Design of Timber Trussed Rafters', CIB W-22, 22-14-1, Berlin, 1989.

Riley, G. & Gebremedhin, K. G. (1998), 'Axial and Rotational Stiffness Model of Metal-Plate-Connected Wood Truss Joints', 5.th World Conference on Timber Engineering, Montreux, Switzerland, 1998.

Suddarth, S. K., Pecival, D. H. & Comus, Q. B. (1981). 'Testing and Analysis of 4x2 Parallel-Chord Metal-Plate Connected Trusses'. Research Report 81-1, Building Research Council, University of Illinois, 1981.

Suddarth, S. K. & Wolfe, R. W. (1983). 'Purdue Plane Structures Analyser II – A – Computerized Wood Engineering System', General Technical Report FPL-40 U.S.D.A. Forest service, Forest Product Laboratory, Madison Wisconsin, 1983.

Triche, M. H. (1993), 'Eccentricities in Metal-Plate Connected Joints', Proceedings of Mechanical Fasteners Plenary Session at the Forest Products Research Society Annual Meeting, General Technical Report, SO-92, 1993.

Triche, M. H. & Suddarth, S. K. (1988), 'Advanced design of metal plate connector joints', Forest Products Journal, Vol. 38, No. 9, 1988.

TRÆ 31 (1995), 'Træspær. Fabriksfremstillede gitterspær og hanebåndsspær samt bjælkespær og bjælkelag' (in Danish) (Trussed rafters. Factory-made trusses, collar tie trusses, beam trusses and joist floors). ISBN 87 85108 47 2. Træbranchens Oplysningsråd, August 1995.

Typgodkännandebevis 1690/87 (2001). Spikplåtar GNT-100S (Approval for Nail plate type GNA20S), (in Swedish). Swedish Institute for Technical Approval in Construction, July 2001.

Typgodkännandebevis 5019/86 (2001). Spikplåtar GN-T150S (Nail plate type GNT150S). (in Swedish), Swedish Institute for Technical Approval in Construction, July 2001.

Urfjell, S. B. & Anneling, R. (1991), ’Provning av spikplåtar enligt ISO 8969. Ringtest mellan 5 nordiska laboratorier’ (in Swedish) (Tests with Nail Plates According to ISO 8969. Round-Robin Test with 5 Nordic Laboratories), Swedish National Testing and Research Institute, SP RAPPORT 1991:36.

Whale, L. R. J. (1995), ’Punched metal plate fastener joints’. From ‘Timber Engineering. STEP 1. Basis of design, material properties, structural components and joints’. Lecture C11 written by L. R. J. Whale, Gang Nail Systems UK.

Wolfe, Ronald W. & McCarthy, Monica (1987), ‘Assessment of Truss Plate Performance Model Applied to Southern Pine Truss Joints’, United States Department of Agriculture, Forest Products Laboratory, Research Paper FPL-RP-483.

A Test Description of Tests with Nail Plates

This chapter describes the production and storage conditions of the test specimens used to determine the properties of the nail and plate elements for the MiTek GNA20S and GNT150S nail plates. It is explained how the test equipment works and how the load is applied.

A.1 Test Material

The geometry of the GNA20S nail plate is shown in figure 3.1 on page 42. The geometry of the GNT150S nail plate is shown in figure 4.1 on page 85.

The timber is Swedish spruce of strength class K-24 (S10) with a thickness of 45 mm. The timber is visually graded at the truss plant.

The test specimens for the tests with the GNA20S nail plate were manufactured when the timber had a moisture content of 16-18% corresponding to approximately 20° and 85% relative humidity according to *EN 1075 (1999)*. However, 48 hours passed from the beginning of the production till the specimens were all done, which may have affected the moisture content in the timber. The test specimens for the tests with the GNT150S nail plate were manufactured when the timber had a moisture content of 10-14%.

After manufacturing the test specimens were kept for 3 weeks to 3 months at 20° and 65% relative humidity before testing. The test series that were in the conditioning room for 3 months were those used for determination of the anchorage properties.

The nail plates are pressed in place at a local truss plant.

In some of the series used to get the plate properties the nail plates were weakened in the joint line in order to achieve the desired failure mode. The cuts in the nail plates were made with a compass saw and it is assured that the remaining number of steel beams was counted and that they were uncut. The cuts were made symmetrically and on both sides of the specimens. Again this is not according to *EN 1075 (1999)*, but it was done to obtain the failure mode wanted. The anchorage capacities of some of the nail plates are reinforced with screws to avoid anchorage

failure. Furthermore, in some of the test series the timber is reinforced with nail plates – see figure A.1.

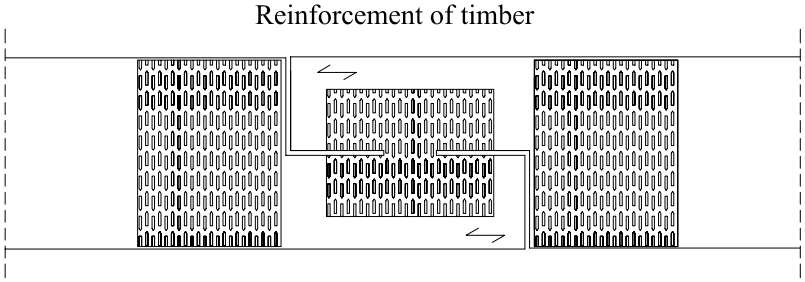

Figure A.1. Reinforcement of timber.

The density of the timber used to determine the properties for the plate element has not been measured because it is supposed only to have a small impact on the test results. The average density of the timber used to determine the properties for the nail element has been determined as 470 kg/m^3 when the moisture content was 14-18%. At the time of testing the moisture content was 9-12%.

A.2 Test Equipment

The tests were performed at the Structural Research Laboratory at Aalborg University.

A.2.1 Test Arrangement

Three different test arrangements were used:

- one for the tension test specimens where the fibre direction and the force direction are parallel
- one for the test specimens in compression
- one for the tension test specimens where the fibre direction and the force direction are not parallel.

Test arrangement for the tension tests

The tensile tests were carried out in a test set-up, where the timber is clamped at both ends between two jaws. The force is applied to the timber through friction between the jaws and the timber, see figure A.2.

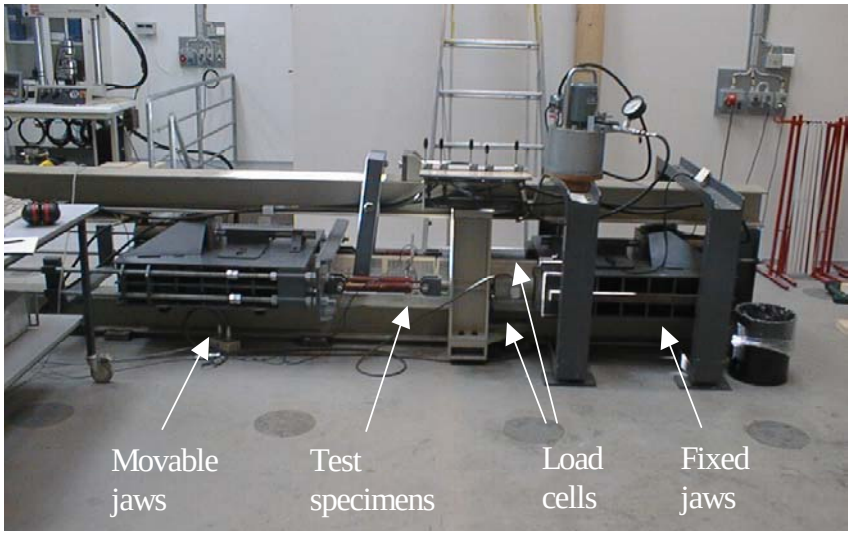

Figure A.2. Test set-up for tension tests.

By pulling in the jaws shown to the left in figure A.2 the force is applied to the test specimen. The force is measured through two load cells located near the fixed jaws.

This set-up is used to determine the plate properties of the tests, where the nail plate is subjected to tension, and to determine the nail properties for the tests where the fibre direction and the force direction are parallel.

Test arrangement for the compression tests

The compression specimens were tested in the test set-up illustrated in figure A.3.

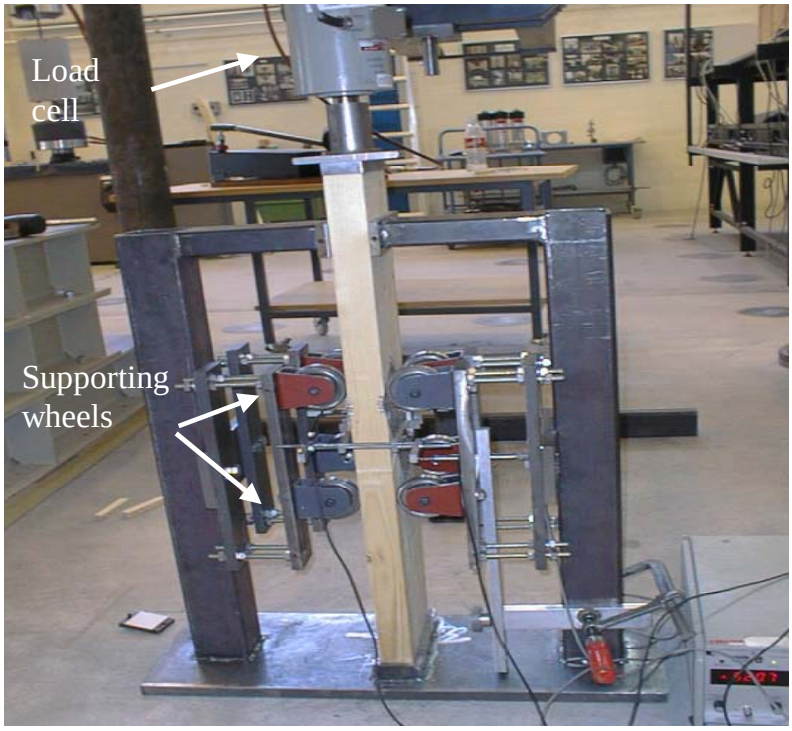

Figure A.3. Test set-up for the compression tests.

The 8 supporting wheels are adjustable and they are tightened before every test so that they prevent out-of-plane instability. At the bottom the test specimens are simply supported. This set-up is used to determine the compression properties for the plate element.

Test arrangement for the tension tests where the fibre direction is not parallel to the force direction

For determination of the anchorage capacities when the fibre direction is not parallel to the force direction the test arrangement shown in figure A.4 is used.

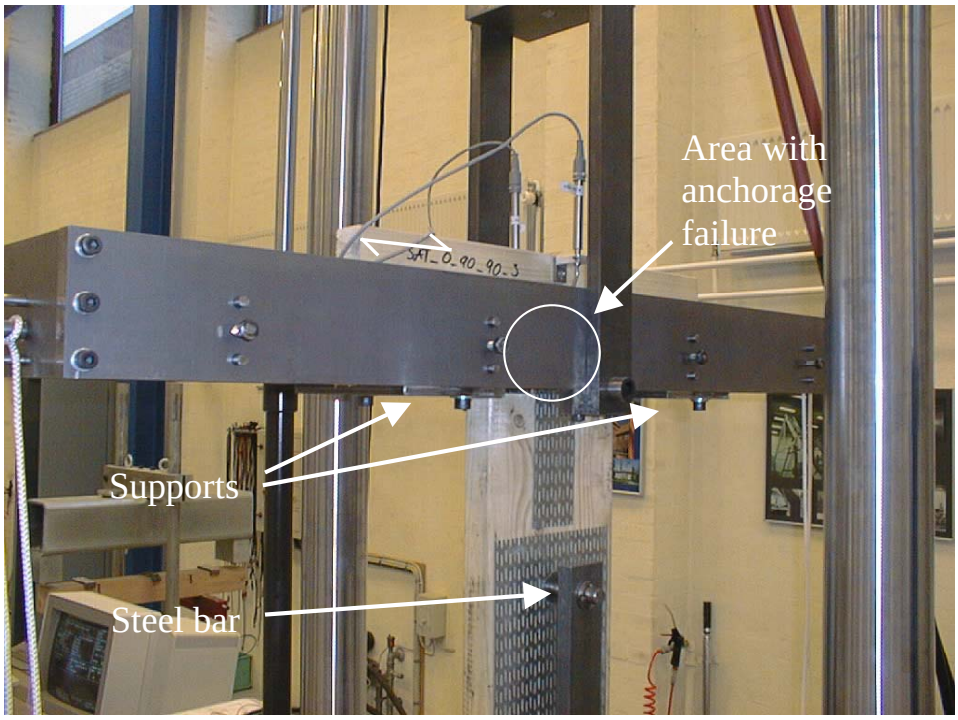

Figure A.4 Test set-up for the tension tests where the fibre direction is not parallel to the force direction.

The supports at the top are located as closely to the nail plate as possible. The load is applied to the timber via the steel bar through a hole drilled in the timber. The nail plates at the bottom are used as reinforcement to prevent the timber from splitting.

A.2.2 Application of load

The load is applied according to *DS/EN 26 891 (1993)*. When the properties of the plate element are to be determined the load is applied as shown in figure A.5 where P is the actual load and P_{est} is the estimated ultimate load.

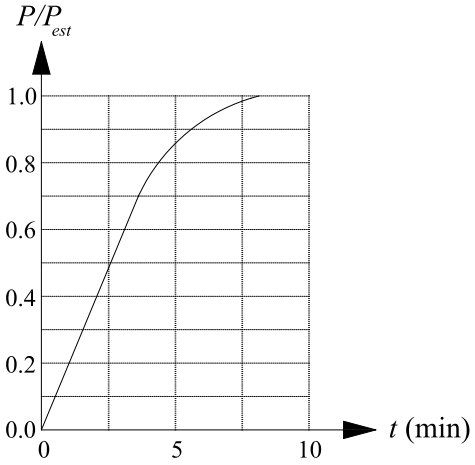

Figure A.5. Loading procedure for determination of plate values.

For determination of the anchorage values of the nail element, the load is applied as illustrated in figure A.6.

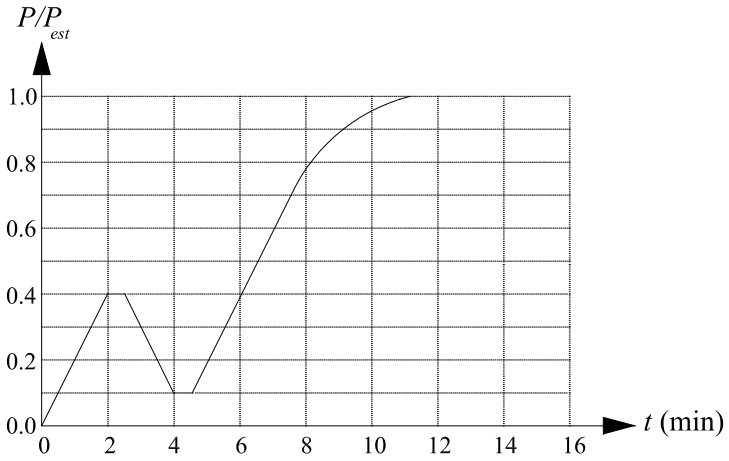

Figure A.6. Loading procedure for determination of anchorage values.

For both loading procedures the load is applied at a constant rate of $0.2P_{est}$ per minute (± 25%) if the load is below $0.7P_{est}$. If the load is above $0.7P_{est}$ a constant slip is used so that the ultimate load is reached after 3 to 5 minutes of additional testing time.

For the compression tests the load is applied via a hydraulic pump driven by hand. For the two other test set-ups the hydraulic pump is driven by a computer controlled program.

A.2.3 Displacement Measuring

Two ways of measuring the deformations are used.

Displacement Measuring Used to Determine the Properties of the Plate Element

The deformation of the nail plates over the joint line is measured by two HBM DD1 displacement transducers (± 2.0 mm) - one on each side, see figure A.7.

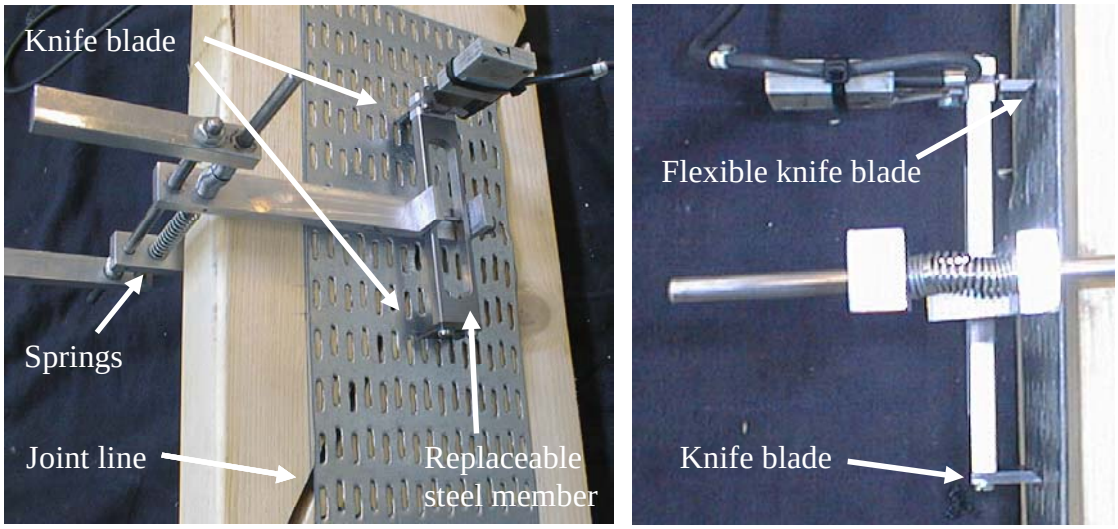

Figure A.7. Arrangement used to measure the deformation of the plate.

The springs press the four knife blades to the nail plates and ensure that the blades are fixed to the points where they are in contact with the nail plates. The displacement between the two blades on either side is measured via a strain gauge attached to the flexible knife blade.

The arrangement is always located in such a way that the measured deformation of the nail plate is parallel to the force direction. One of the knife blades on each side is stiffly connected to the steel member that connects the blades. The steel members have a length of 100 mm when the angle between the joint line and the force direction is 60° - otherwise the steel members are replaced so their length is 50 mm. It is assumed that the measured deformation is the deformation of the corresponding plate element, i.e. the nail groups on each side of the joint line act like stiff bodies.

For the six tension test series (TP_0_0_0 → TP_X_0_X → TP_150_0_150), where the joint line is parallel to the force direction, two extension steel parts are fastened to two of the blades so that the measured deformation is still the deformation of the nail plate parallel to the force direction.

For some of the tensile test specimens the failures were brittle. This destroyed one DD1 displacement transducer and after this event the tests were stopped after the plates became plastic, but before the ultimate load was reached.

The method described above to measure the deformation of the plate is found to be very precise and it is very easy to attach the transducers to the test specimen. The

measured deformations of the plate on each side of the specimen are very alike as shown in figure A.8.

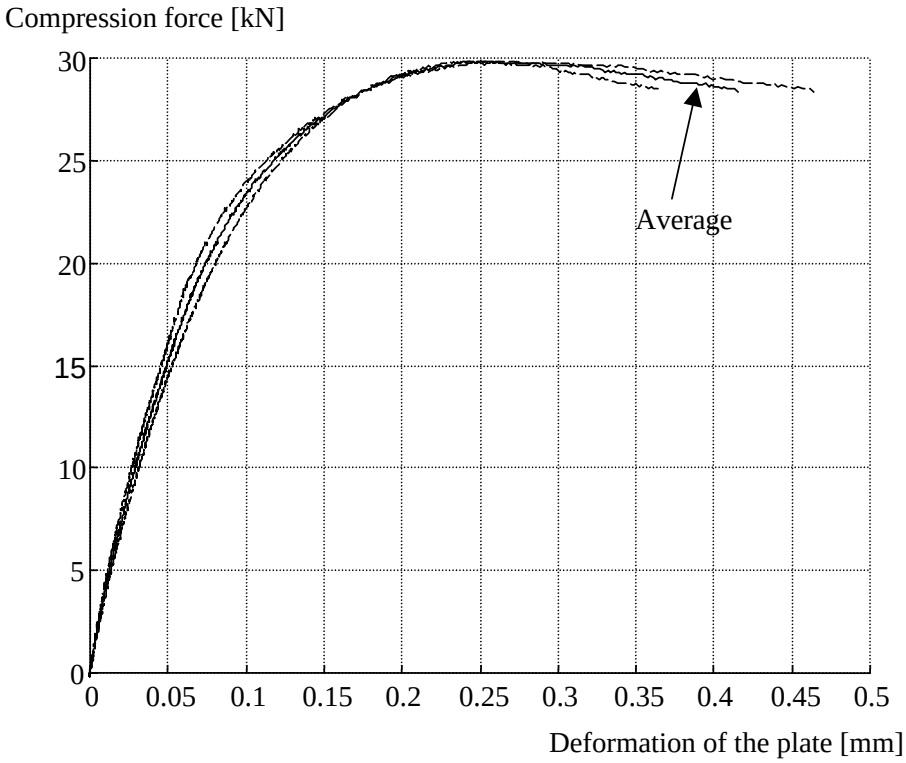

Figure A.8. Load-displacement curves for each of the two DD1 transducers (shown for the compression test series CP_210_0_120).

In some preliminary compression tests the deformation of the plate is measured as illustrated in figure A.9. The extension steel bars are attached to the displacement transducers at one end and to the nail plate at the other end (via a small mark on the surface of the nail plate). The arrangement holding the displacement transducers in place is fastened to the timber with a screw.

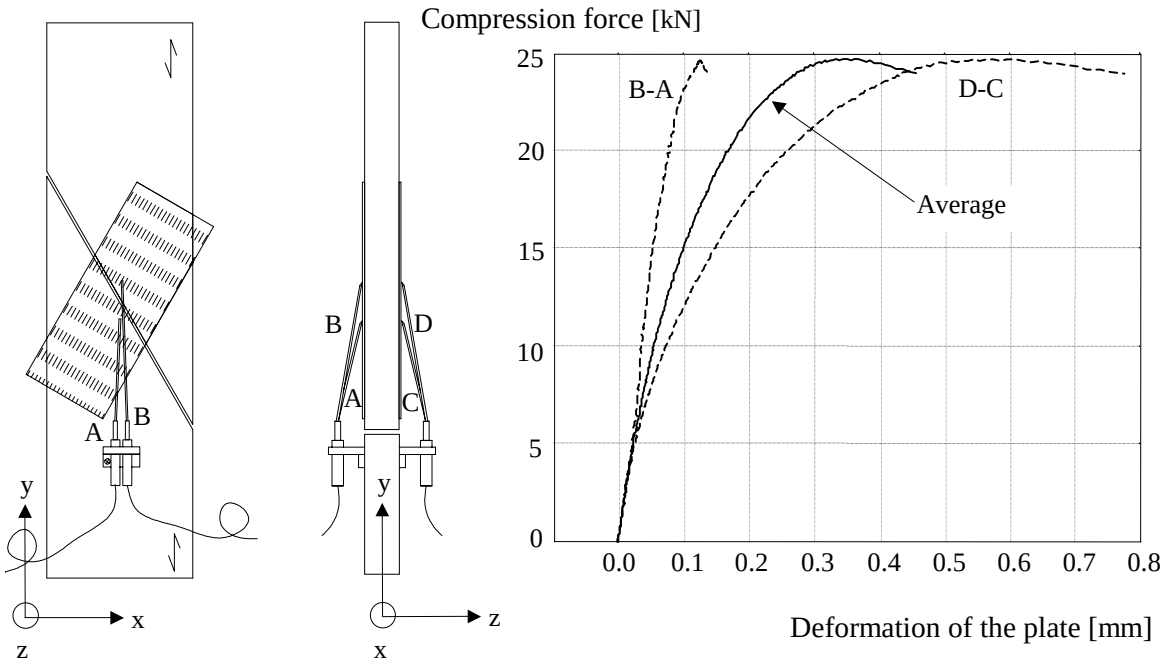

Figure A.9. One way of measuring the deformation of the plate that did not perform well. To the right the differences between the displacement transducers on each side are shown.

For some reason this method of measuring the deformation of the plate gives some results that are obviously misleading, see figure A.9 right. This may be explained by the fact that even a relatively small horizontal movement (bending) at the midpoint of the test specimen in the z-direction will result in a shortening of one of the long displacement transducers and an elongation of the other long displacement transducer. This error of measurement has a value up to 1/3 of the horizontal movement. The error is caused by the extension steel bars that form an angle with the timber. Bending around the weak axis of the timber could cause the horizontal movement that leads to the error.

The load-displacement curve in figure A.9 is not the worst case - in other cases the difference between the displacement transducers on one side of the specimen gave negative values. This means that the transducer with the short extension bar measures a displacement that is larger than that measured by the transducer with the long extension bar!

Displacement Measuring Used to Determine the Properties of the Nail Element

The displacements are measured as shown in figure A.10.

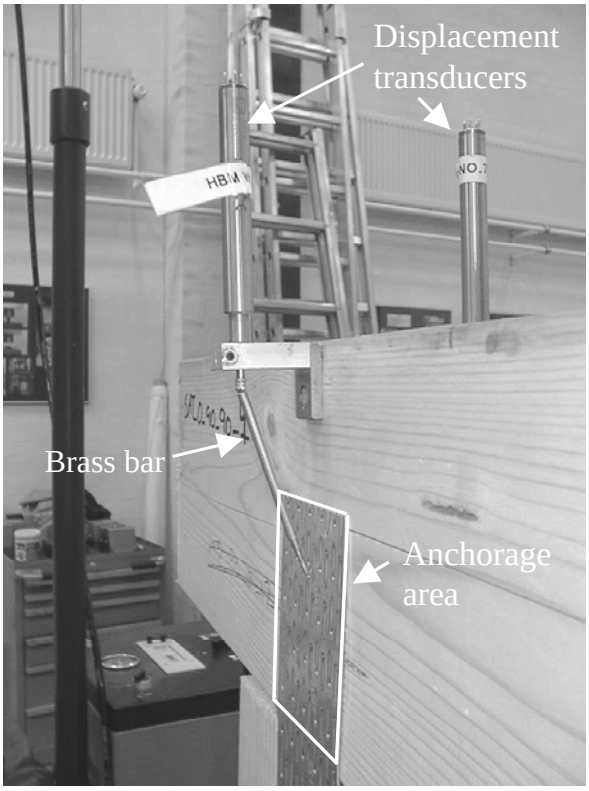

Figure A.10. Measuring method for determining the anchorage properties.

The brass bar is attached to the displacement transducer at one end and to the centre of the anchorage area at the other end. This way of measuring the displacements ensures that no deformation of the plate over the joint line is included in the measuring.

A.2.4 Data Collecting System and Handling of Test Results

The load and the displacements are measured and stored approximately twice every second.

As mentioned earlier the displacements are measured on both sides, however, the average of these displacements is used when determining the properties for the nail and plate element.

The results from the tests have not been modified or adjusted according to the actual thickness and to the actual yield stress of the nail plates as described in *EN 1075 (1999)*. Measurements of the thickness of some of the nail plates have shown that the thickness only differs very little from 1 mm. The yield stress may, however, have a greater effect on the test results and on the comparisons with TRUSSLAB calculations. The reason why the actual yield stress has not been determined is that the tested nail plates are probably produced from many different coils of steel and it would have been a huge job to get and to test steel specimens from all these coils

A.3 Conclusions

The timber is conditioned according to *EN 1075 (1999)*, but it may be discussed if the storage periods in the conditioning room were long enough to achieve the described conditions. The timber used for the tests with the GNT150S nail plate have not been stored according to *EN 1075 (1999)*, since the specimens were manufactured when the moisture content of the timber were in the range 10-14%.

For some of the specimens it has been necessary to reinforce the anchorage of the nails and to weaken the plate to achieve plate failure.

A special displacement measuring method has been used. It is easy and fast to attach the arrangement to the specimens.

The test results have not been modified according to the actual thickness and the actual yield stress of the nail plate.

Inaccurate location of the nail plate has been observed for some of the test specimens. If the inaccuracy is assumed to have a greater impact on the test results, the specimen is not tested.

Some of the plate tension tests were stopped before the ultimate load was reached in order not to damage the displacement transducers.

B Pictures from Tests with Nail Plates

In this appendix some pictures from the test series with the nail plate type GNA20S are shown. The pictures are arranged according to the three groups: tension, compression and anchorage tests.

B.1 Tension Tests

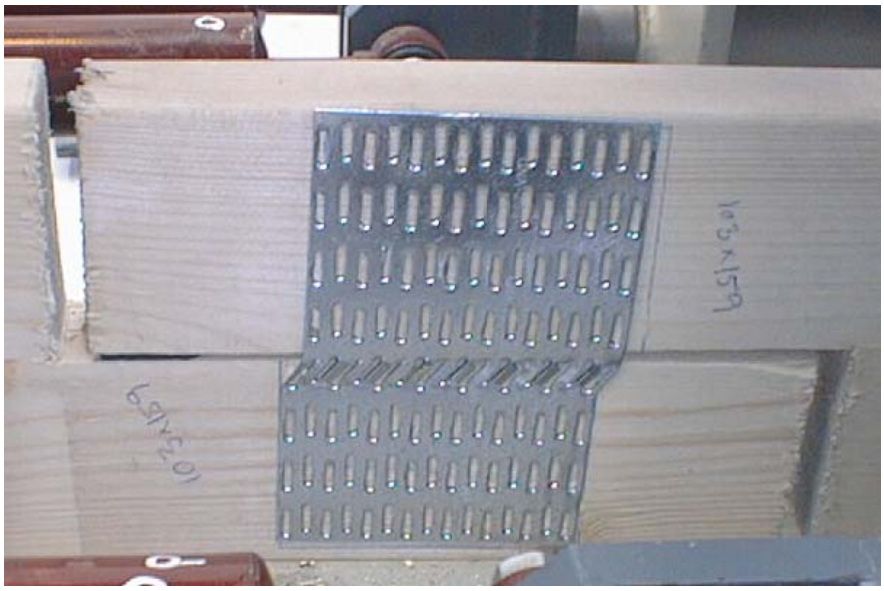

Figure B.1. Tension test series TP_90_0_90.

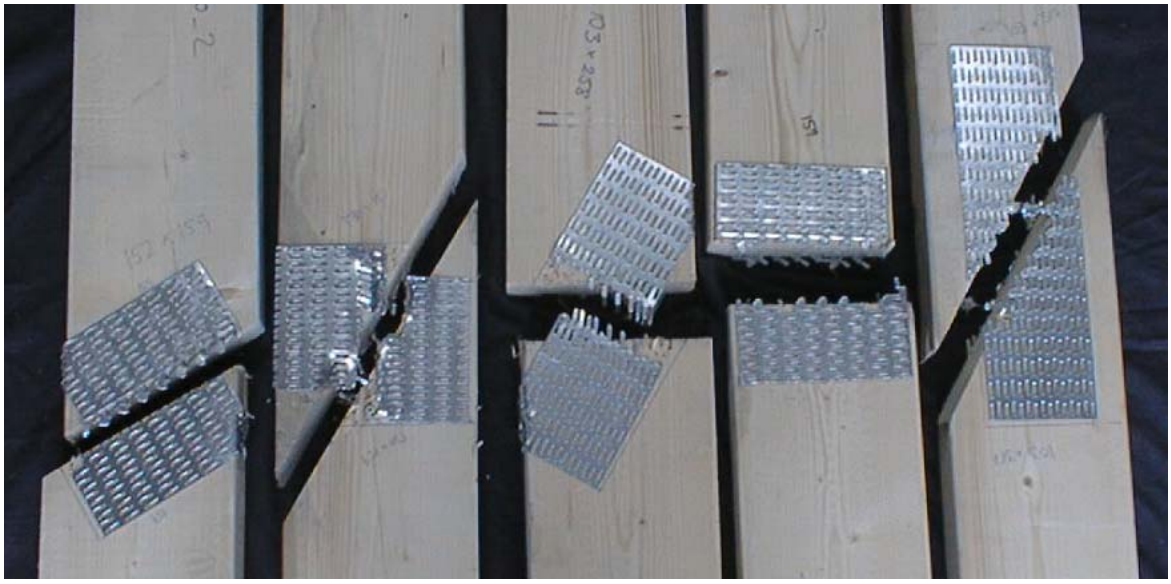

Figure B.2. Tension test series TP_120_0_180, TP_90_0_120, TP_30_0_120 and TP_90_0_180.

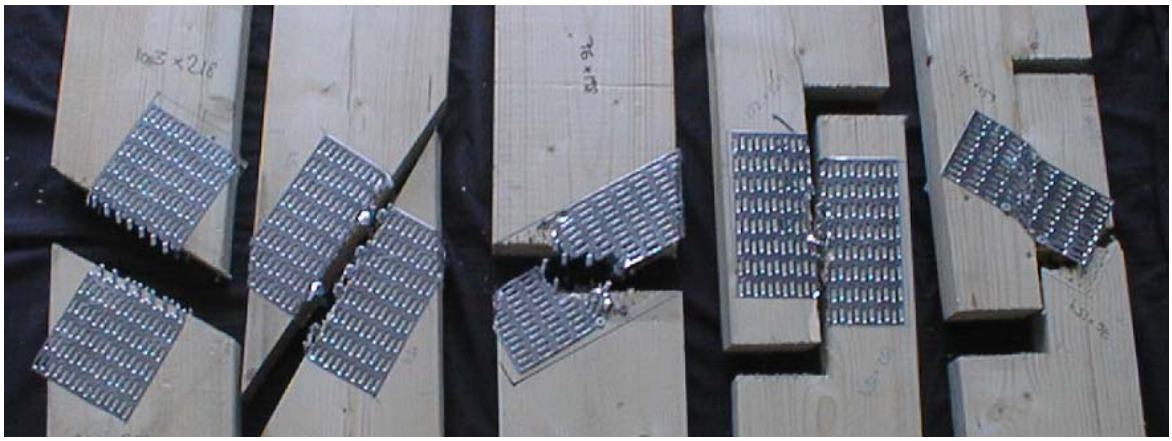

Figure B.3. Tension test series TP_30_0_90, TP_330_0_180, TP_60_0_150 and TP_60_0_60. For the series TP_60_0_60 timber failure occurred when the specimen was forced to failure. The timber failure developed after the plate had become plastic.

B.2 Compression Tests

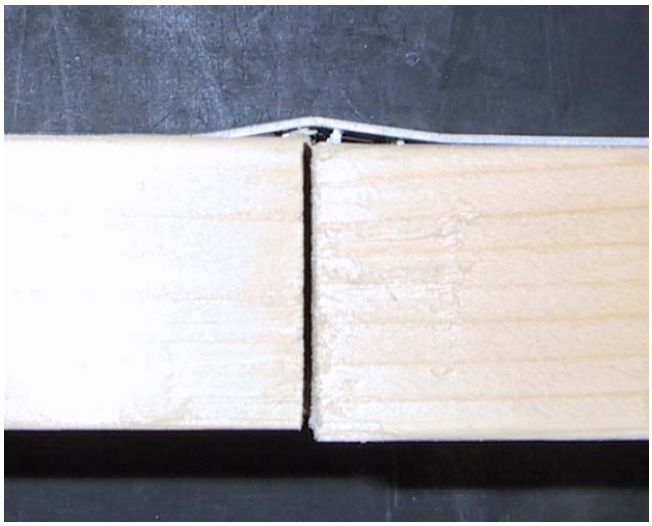

Figure B.4. Typical compression failure where the plate buckled. In some cases the buckling line did not follow the joint line.

B.3 Anchorage Tests

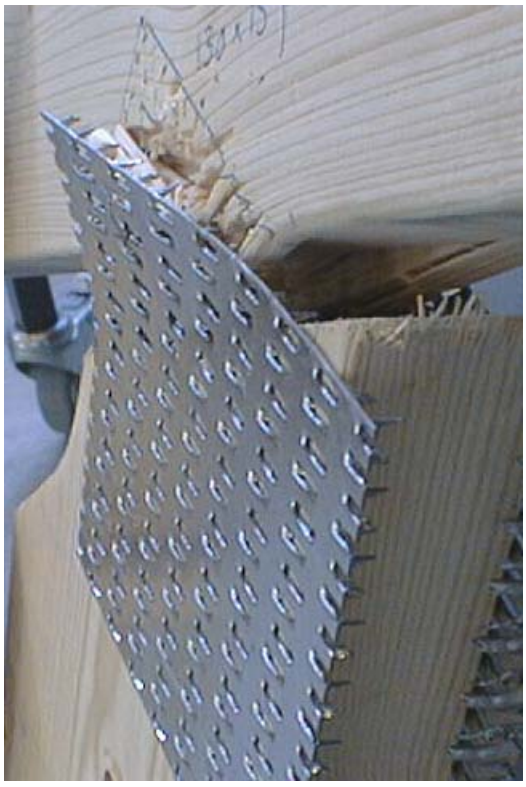

Figure B.5. Anchorage test series SA_90_60_-30.

Figure B.6. Anchorage test series SA_90_60_-30.

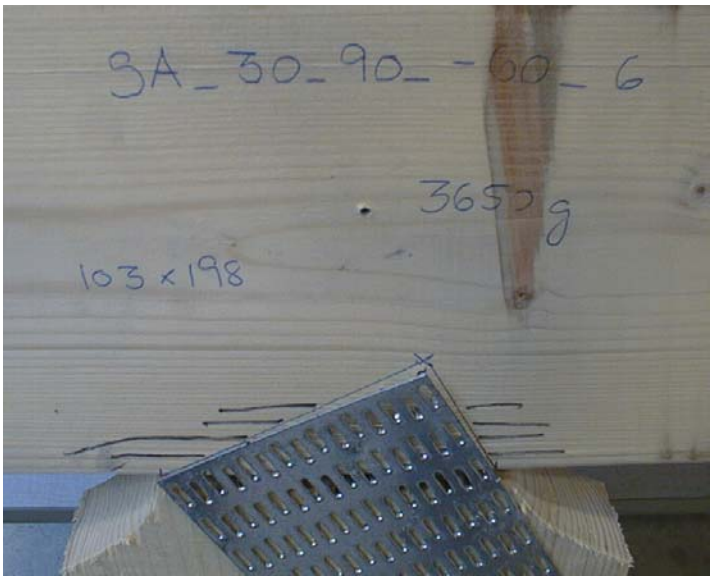

Figure B.7. Anchorage test series SA_30_90_-60.

Figure B.8. Anchorage test series SA_90_30_-60.

C Test Description of Tests with Knee Joints

Some properties of the test material used for the knee joints are determined and the test set-up is described. Furthermore, detailed drawings of the different types of knee joints are shown.

C.1 Test Material

The timber used for the knee joints is Swedish spruce of strength class K-24 (S10) with a thickness of 45 mm. The timber is visually graded at the truss plant.

The timber is supplied in two different dimensions: 45x120x2400 mm (40 beams) and 45x245x4800 mm (70 beams). After measuring the modulus of elasticity the beams are cut into parts needed for the different types of knee joints.

The density of the timber is converted to a moisture content on 12% according to *DS/EN 384 (1995)*. The corrected mean density ρ_{12} and the corrected 5-percentile $\rho_{12,k}$ are listed in table C.1 together with the corresponding values from the Danish timber code, *DS 413 (1998)*.

	120 mm beams	245 mm beams	*DS 413 (1998)*
ρ_{12}	527 kg/m^3	433 kg/m^3	420 kg/m^3
$\rho_{12,k}$	460 kg/m^3	385 kg/m^3	350 kg/m^3

Table C.1. Density of the timber beams used for the knee joints.

When comparing the values in the table it is seen that the quality for the 120 mm beams is quite high.

C.1.1 Modulus of Elasticity of the Timber Beams

The modulus of elasticity of the timber beams is determined according to *DS/EN 408 (1995)*. The modulus of elasticity is determined as the mean of two tests – one where the beam is bent up and one where the beam is bent down (both tests are made for bending around the strong axis).

When measuring the modulus of elasticity the beams had a moisture content of approximately 16% due to the fact that they were stored at 20° and 85% relative humidity and not at 20° and 65% relative humidity for time saving reasons. The values of the modulus of elasticity are used in the TRUSSLAB models and the measured value for each individual beam is therefore converted so that it corresponds to the moisture content of the beam at the time when the knee joints were tested. The calculations are performed according to *DS/EN 384 (1995)* where a 1% change of the moisture content of the timber results in a change of 2% in the modulus of elasticity.

For comparison the values are converted to a moisture content of 12% according to *DS/EN 384 (1995)*. The corrected mean density E_0 and the corrected 5-percentile $E_{0,k}$ (determined by listing all the values – not by multiplying by 0.67 as suggested in *DS/EN 384 (1995)*) are listed in the table below together with the corresponding values for from the Danish timber code, *DS 413 (1998)*.

	120 mm beams	245 mm beams	*DS 413 (1998)*
E_0	15100 MPa	10750 MPa	10500 MPa
$E_{0,k}$	11800 MPa	7900 MPa	7000 MPa

Table C.2. Modulus of elasticity - corrected to a moisture content of 12% - for the timber beams used for the knee joints.

Again the values show that the quality of the 120 mm beams is quite high.

During the cutting and the manufacturing process the timber parts are marked so that it is possible to determine the modulus of elasticity for each individual timber beam in the knee joints.

C.2 Test Equipment

The tests were performed at the Structural Research Laboratory at Aalborg University with a special test set-up.

C.2.1 Test Arrangement

A drawing of the test arrangement is shown in figure C.1.

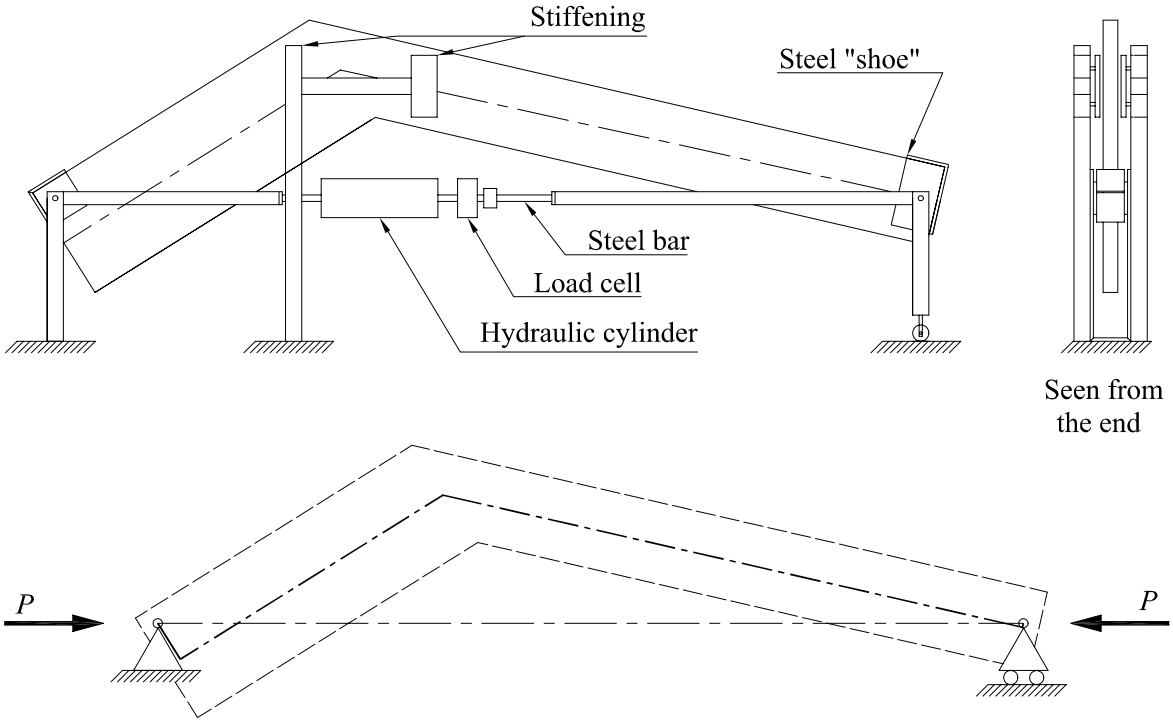

Figure C.1. Test set-up for tests with knee joints. The statical system is shown as well.

The stiffening is adjusted to fit each knee joint and it is used to ensure that the knee joints are not twisting or bending out of the plane. The ends of the stiffening are mounted with teflon.

C.2.2 Application of Load

The load is applied according to *DS/EN 26 891 (1993)* as illustrated in figure C.2.

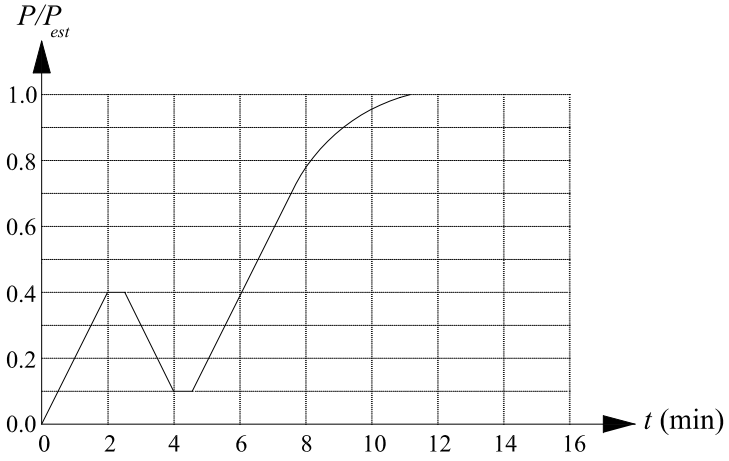

Figure C.2. Loading procedure for the knee joints.

The load is applied at a constant rate of $0.2P_{est}$ per minute (± 25%) if the load is below $0.7P_{est}$. If the load is above $0.7P_{est}$ a constant slip is used so that the

ultimate load of the knee joint is reached after 3 to 5 minutes of additional testing time.

A computer program controls the load by adjusting the movement of the load cylinder several times per second.

When the behaviour of a knee joint has become plastic or when it is estimated that the load capacity of the joint is close to failure, the displacement transducers are dismounted and the knee joint is again loaded manually until failure occurs. The ultimate load level is registered manually.

C.2.3 Displacement Measuring and Data Collection

The displacements are measured at five different locations, but only three of them are used for comparison. The locations of these three transducers are shown in figure C.3 and figure C.4.

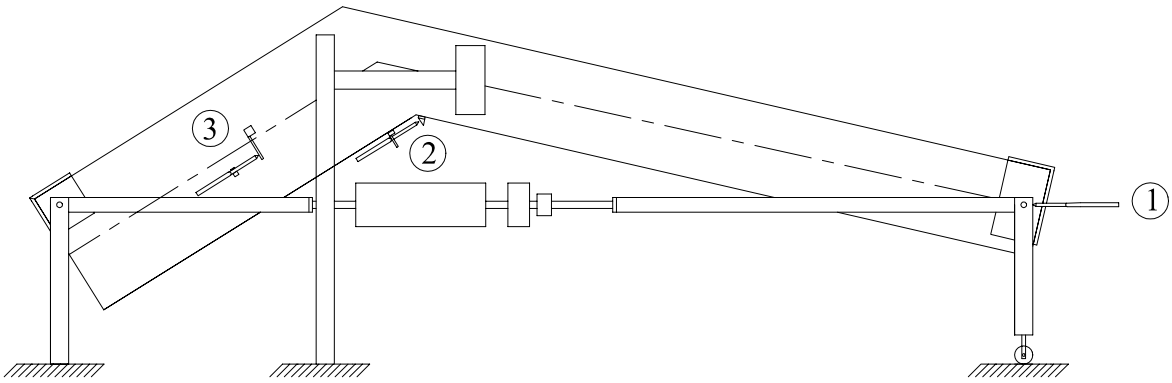

Figure C.3. Location of displacement transducers.

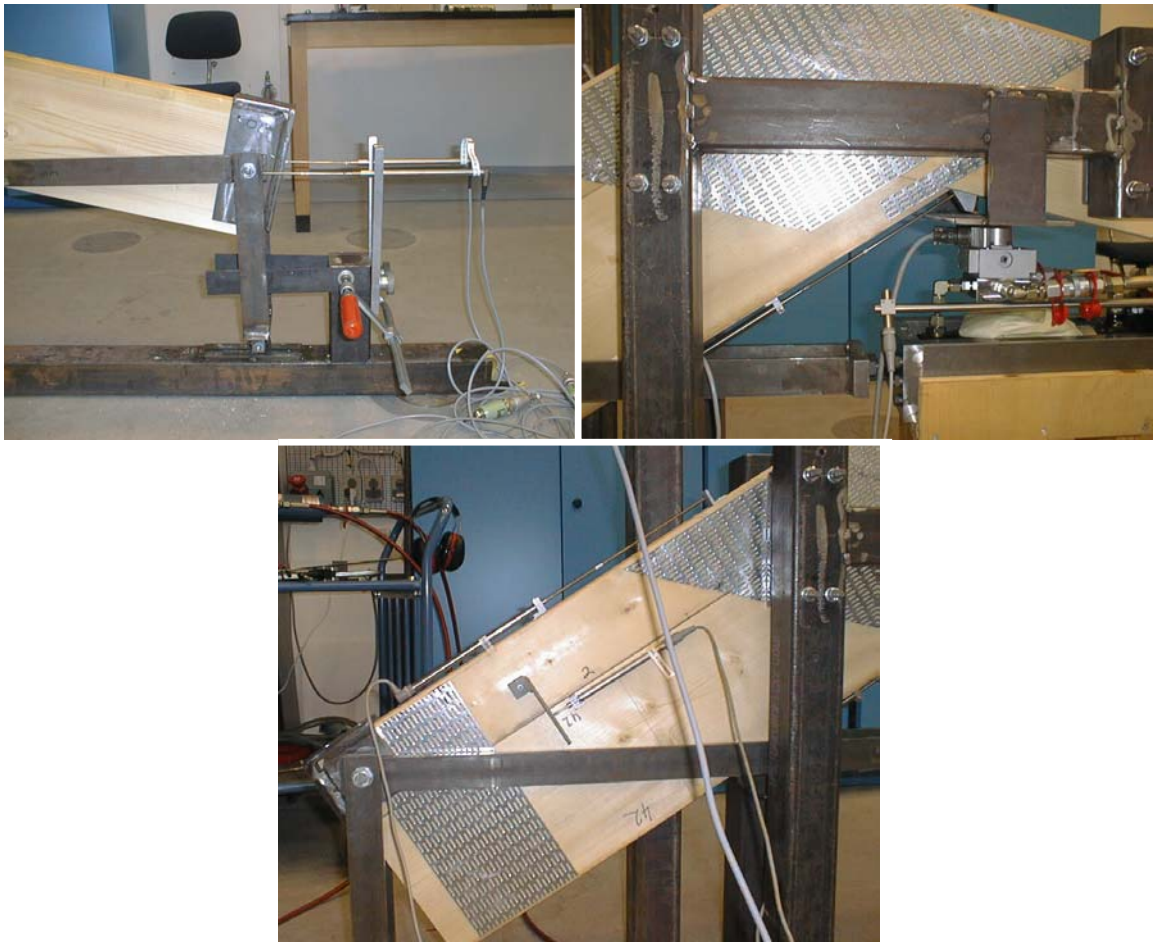

Figure C.4. Displacement transducers.

The transducers are of the type HBM1-WA with a measuring-range of ±50 mm, ±20 mm and ±10 mm at the locations 1, 2 and 3, respectively.

The load and the displacements are measured and stored approximately twice every second.

C.3 Drawings of Knee Joint Test Specimens

Dimensions are in mm and if nothing else is noted the nail plates are located 5 mm from the timber edges. Figure C.29 shows the dimensions for the specially cut nail plates.

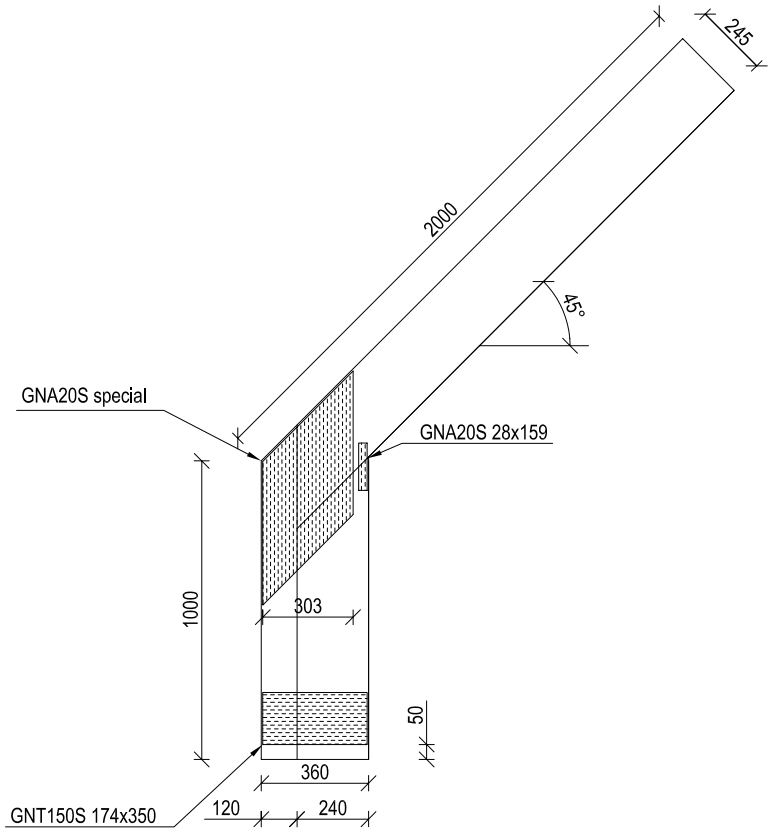

Figure C.5. Test specimens A20.

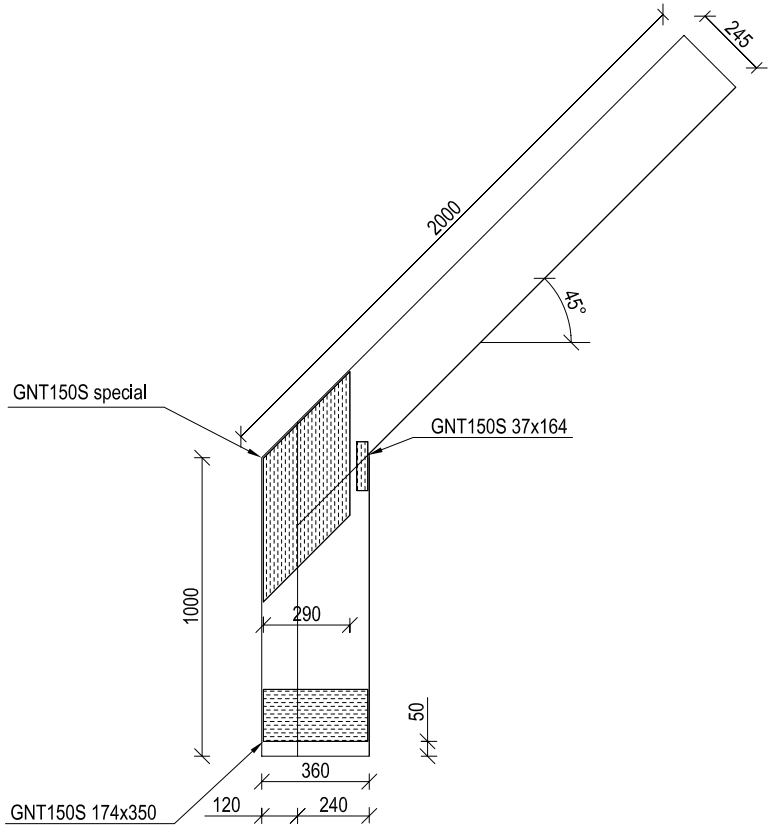

Figure C.6. Test specimens A150.

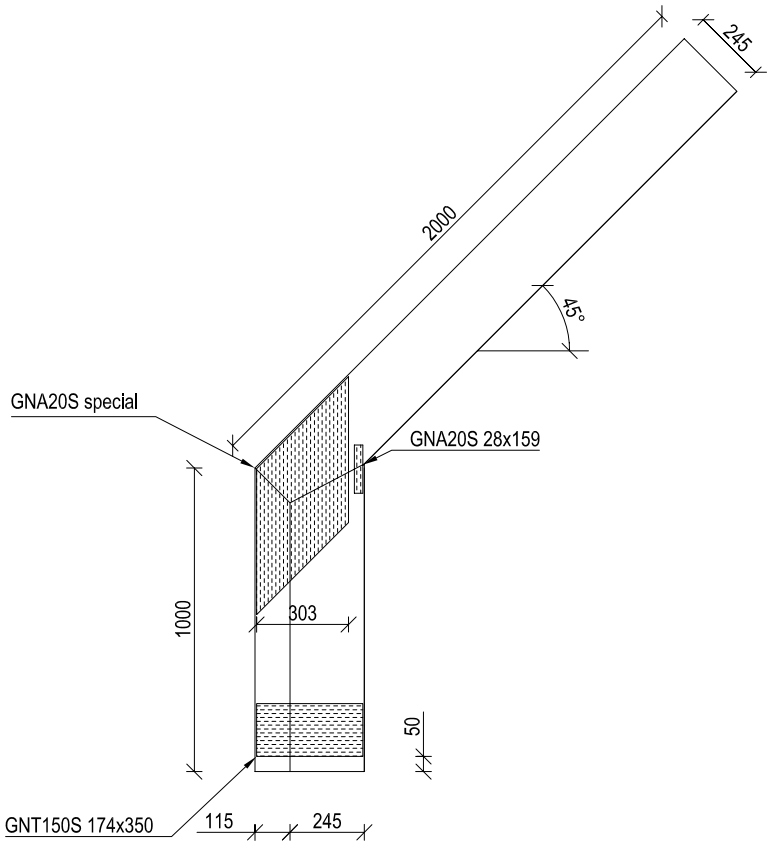

Figure C.7. Test specimens B20.

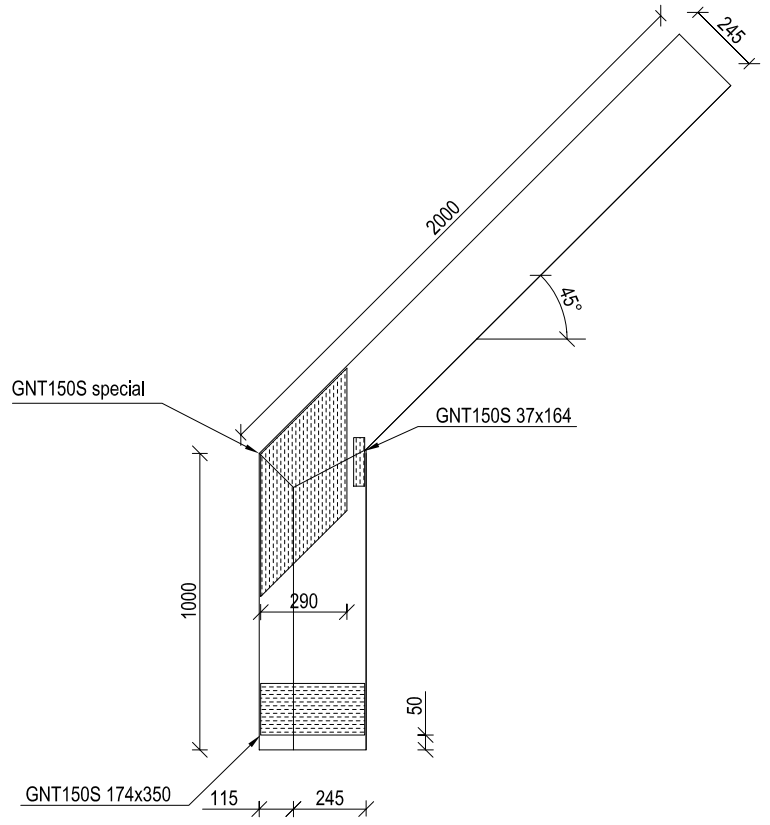

Figure C.8. Test specimens B150.

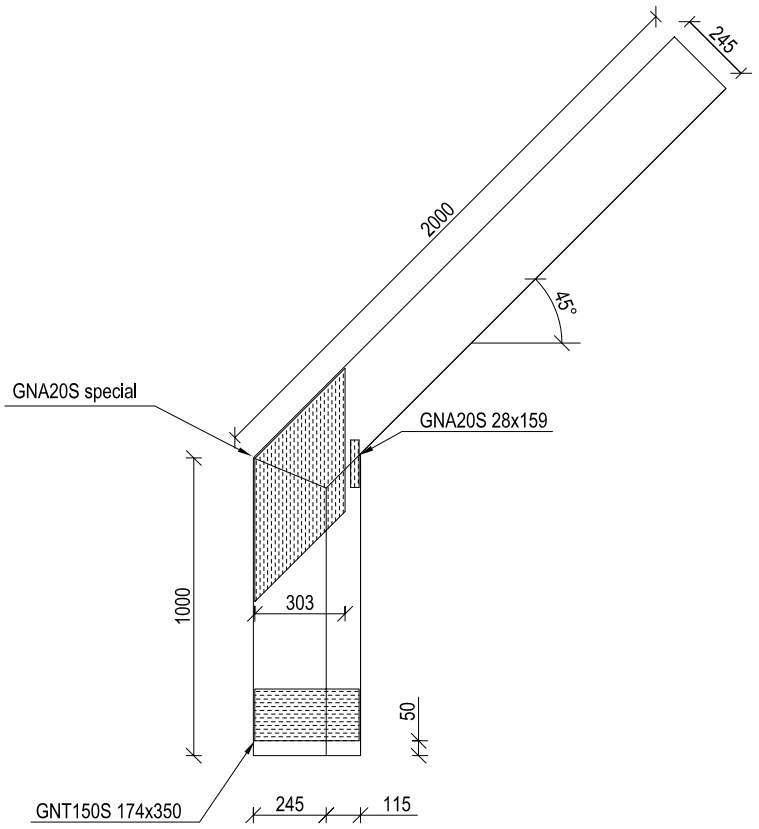

Figure C.9. Test specimens C20.

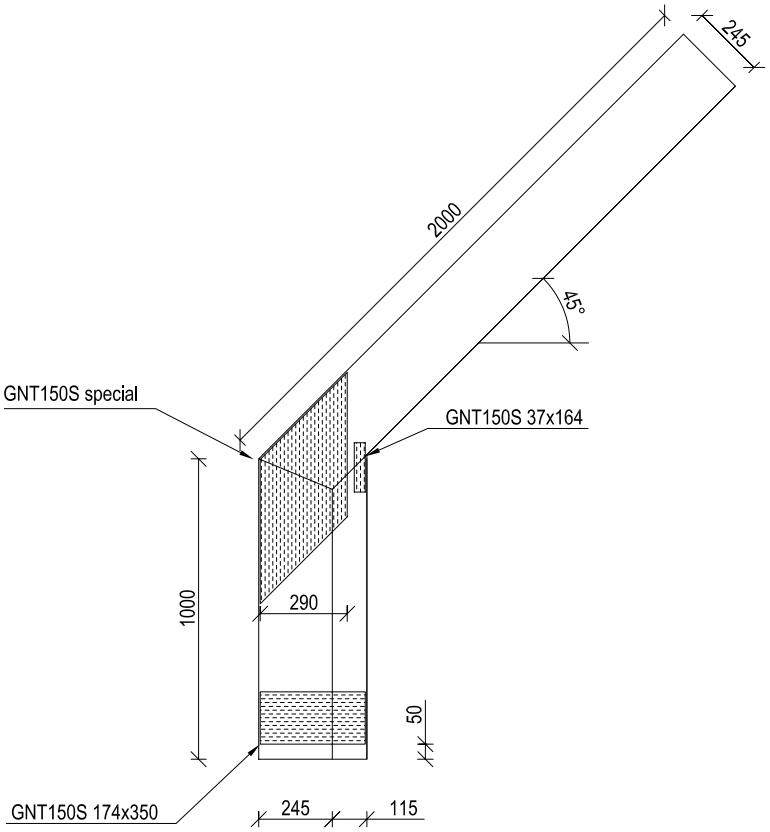

Figure C.10. Test specimens C150.

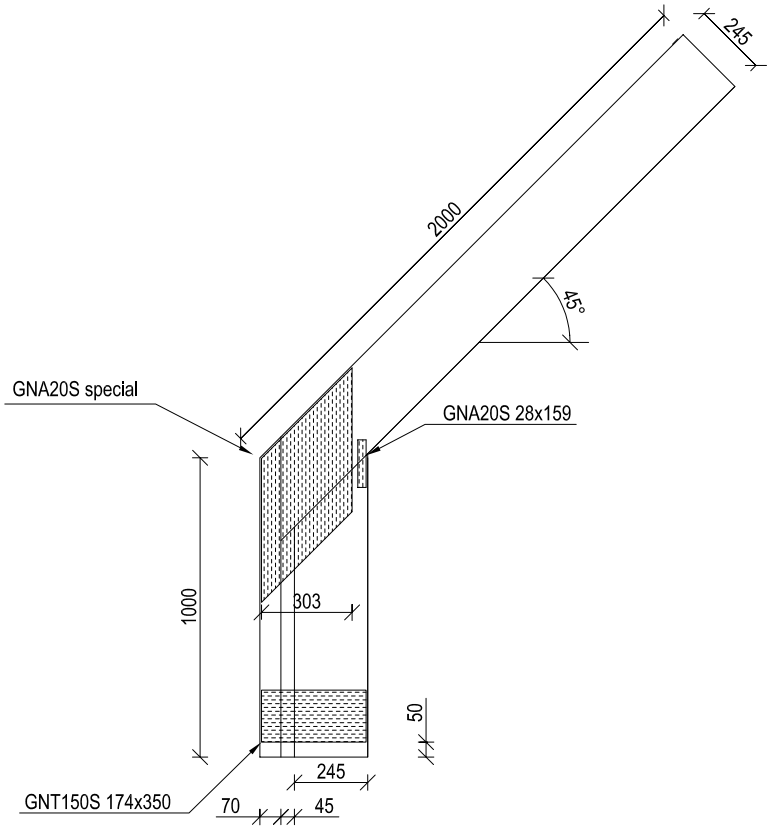

Figure C.11. Test specimens D20.

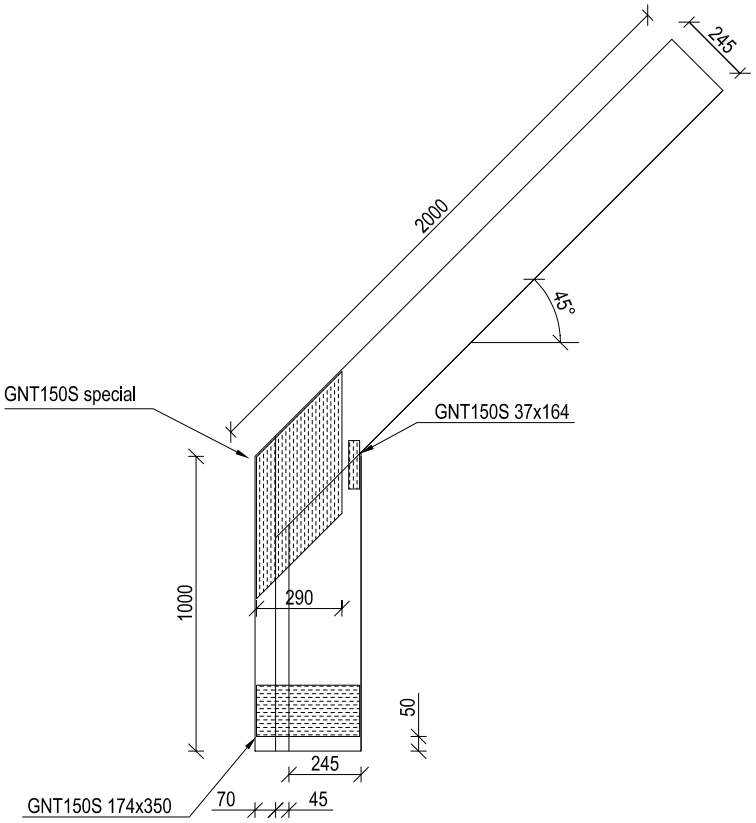

Figure C.12. Test specimens D150.

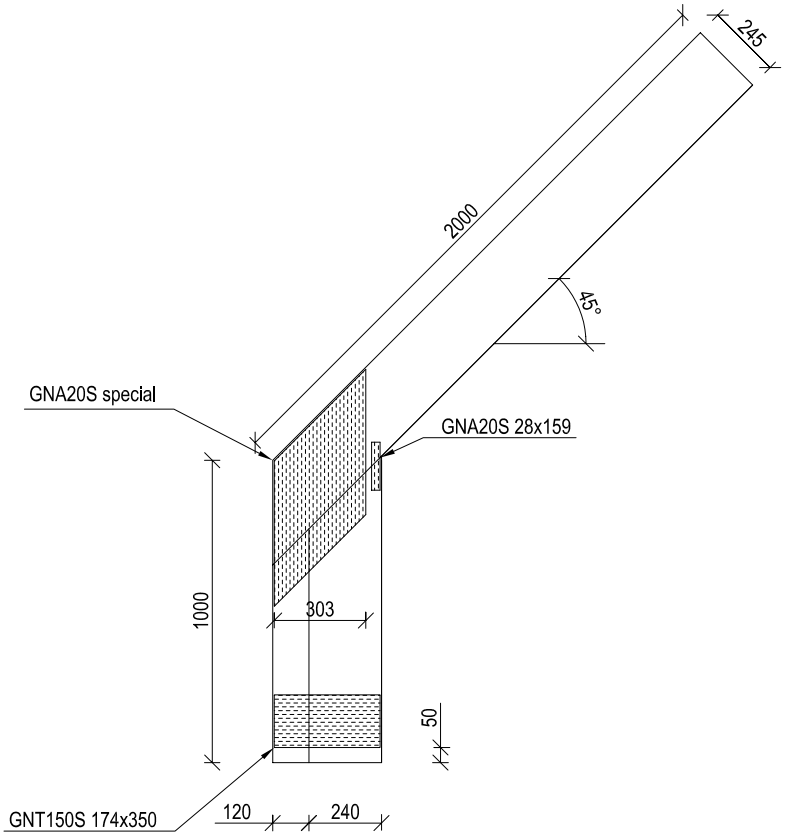

Figure C.13. Test specimens E20.

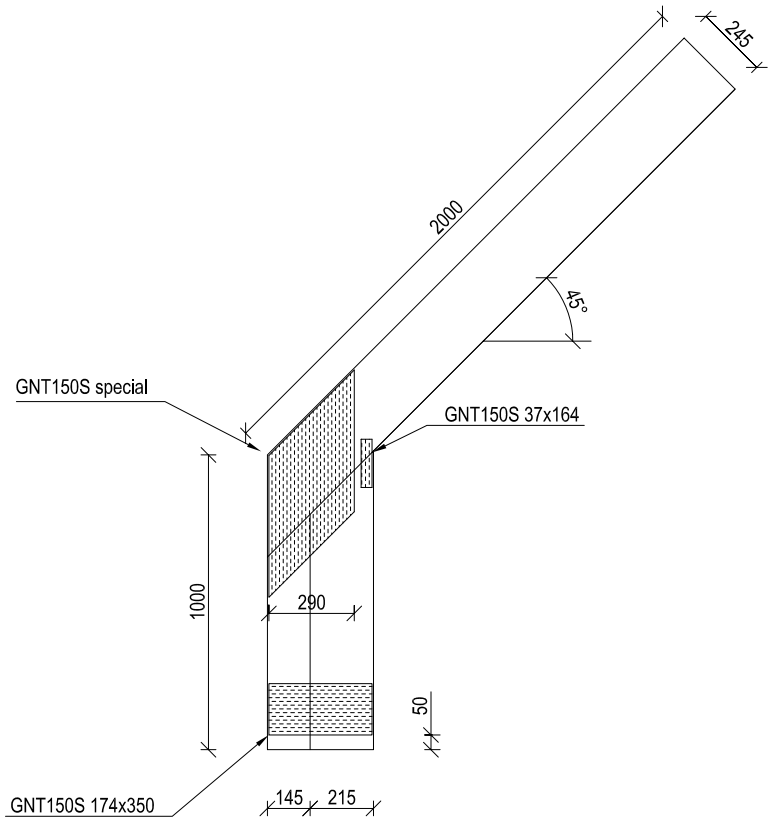

Figure C.14. Test specimens E150.

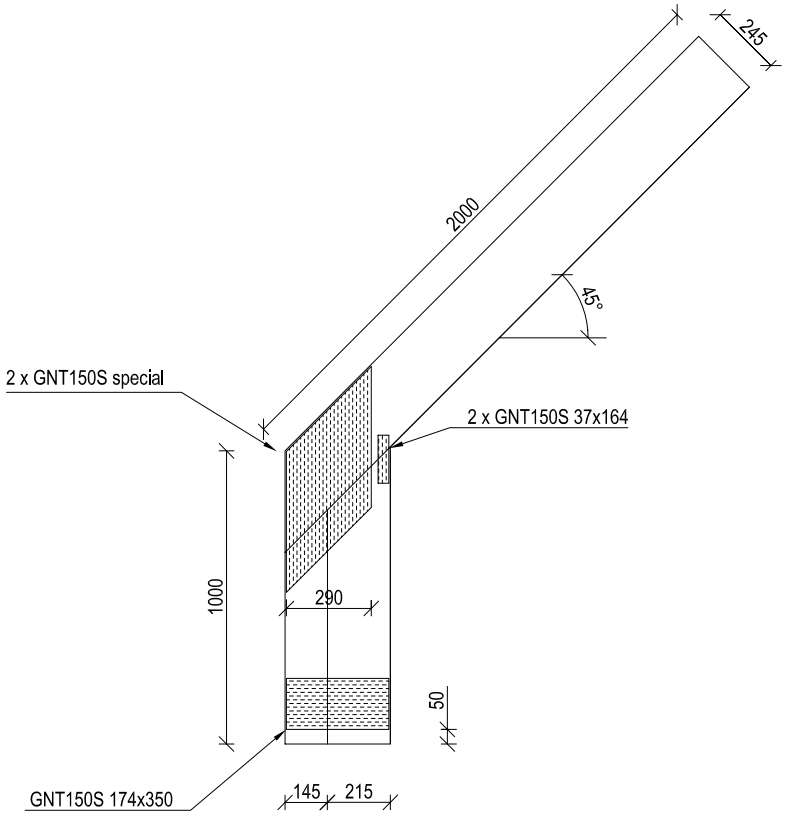

Figure C.15. Test specimens E150-2P.

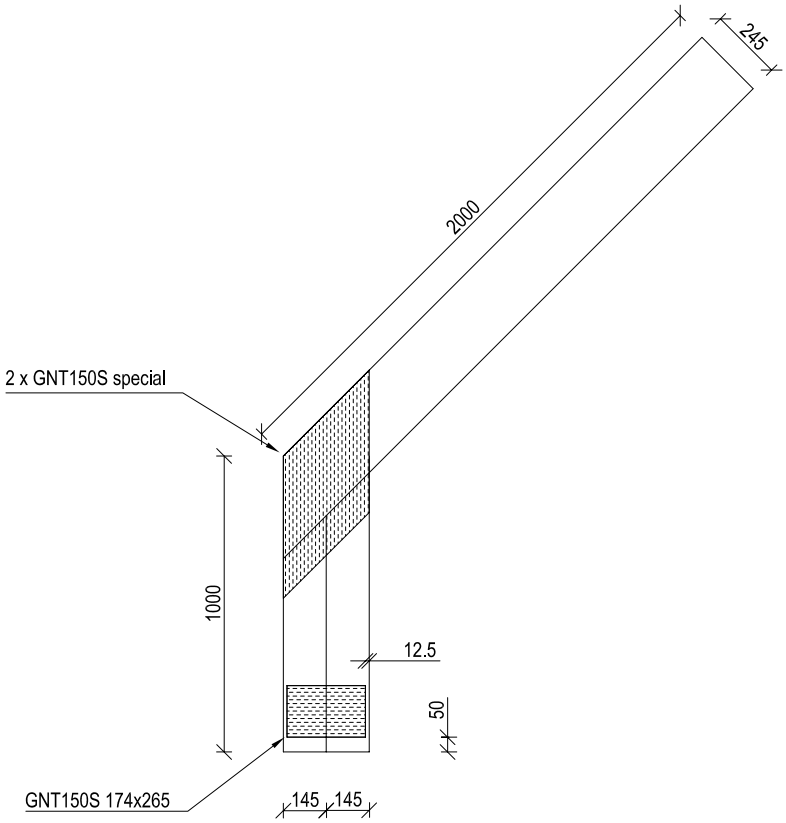

Figure C.16. Test specimens ET150-2P.

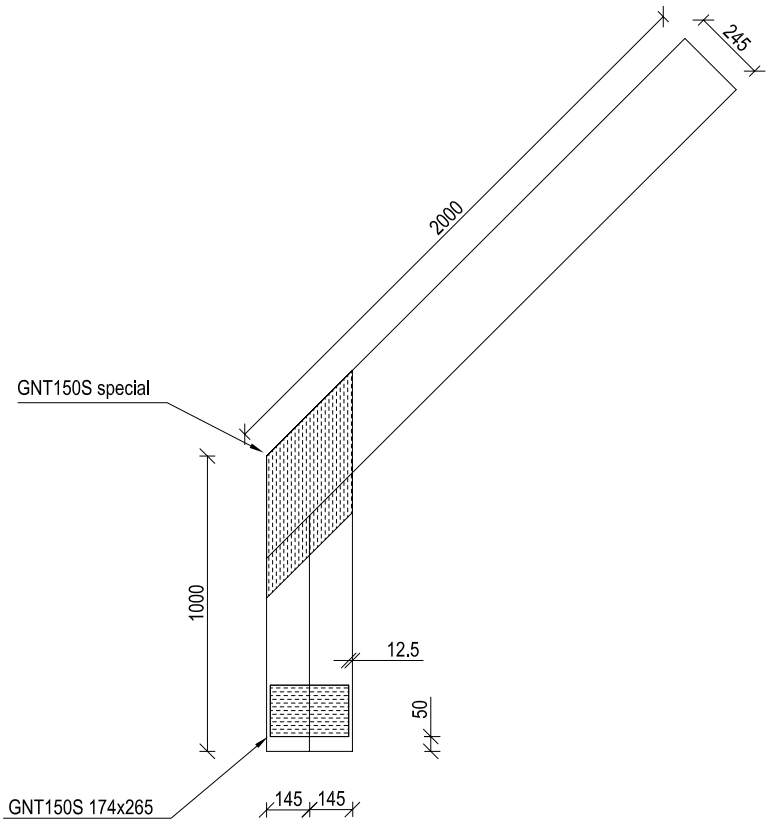

Figure C.17. Test specimens ET150.

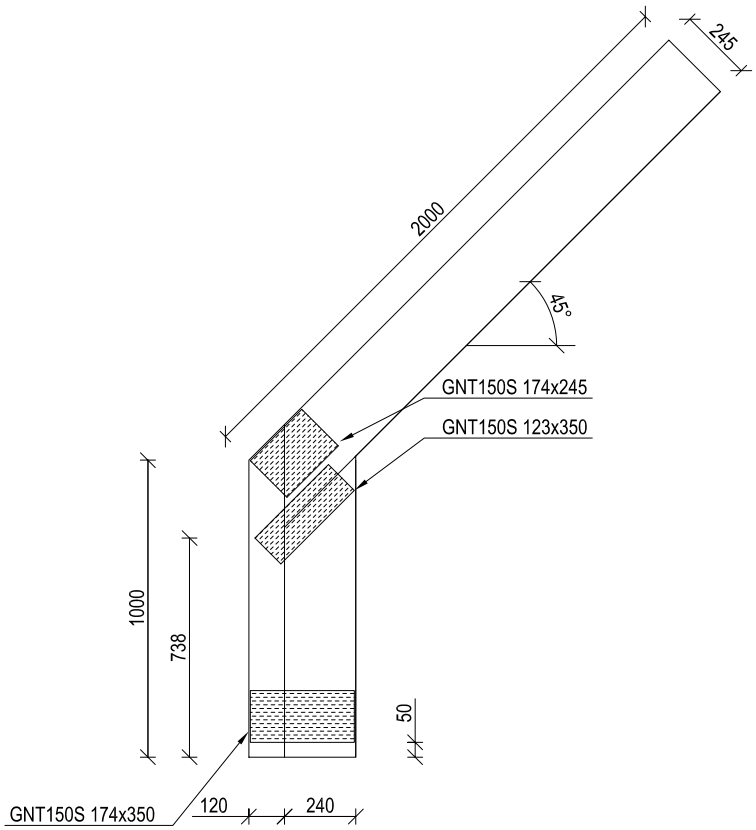

Figure C.18. Test specimens F150.

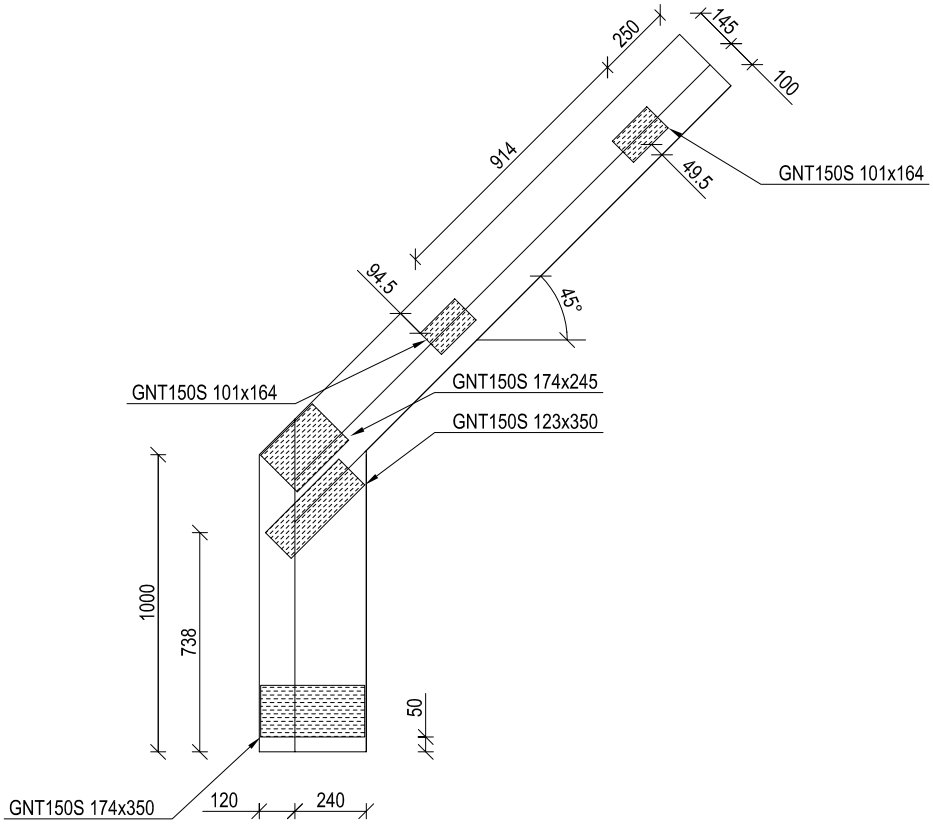

Figure C.19. Test specimens F150-2R.

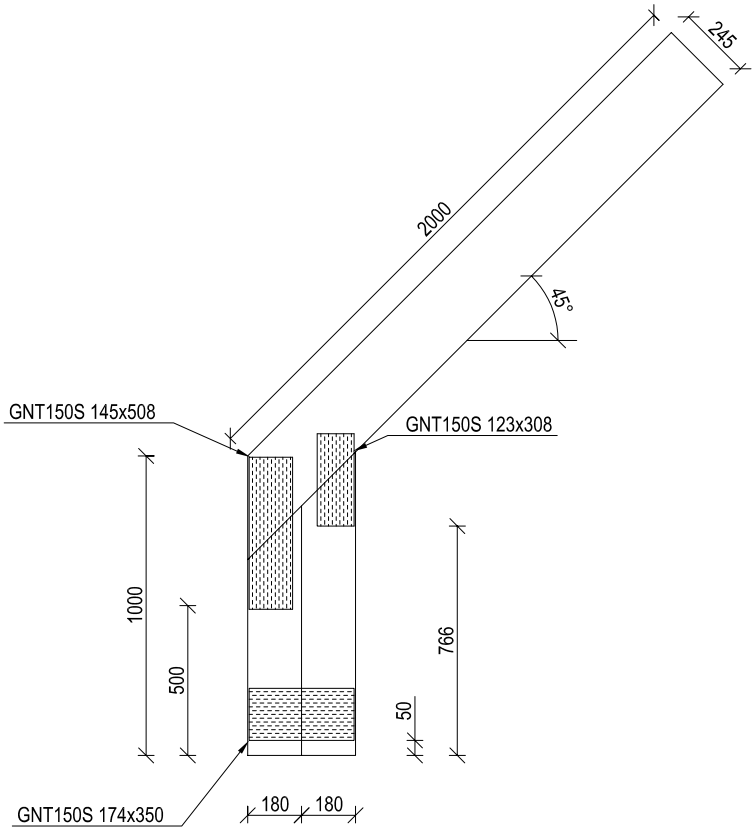

Figure C.20. Test specimens G150.

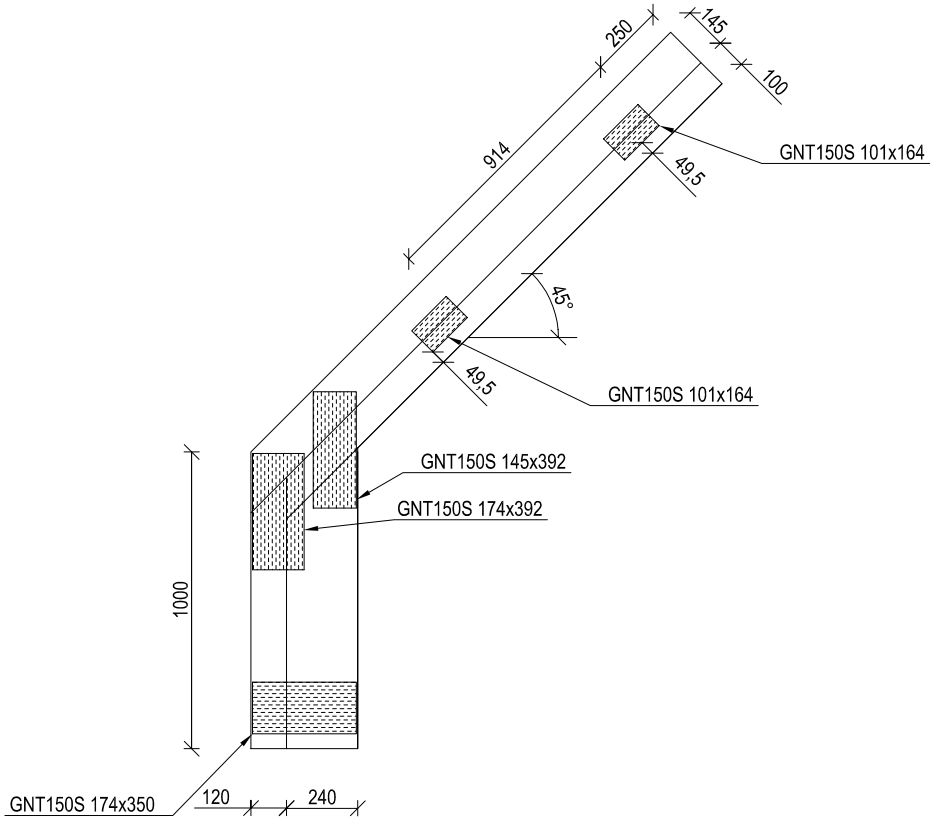

Figure C.21. Test specimens H150-2R.

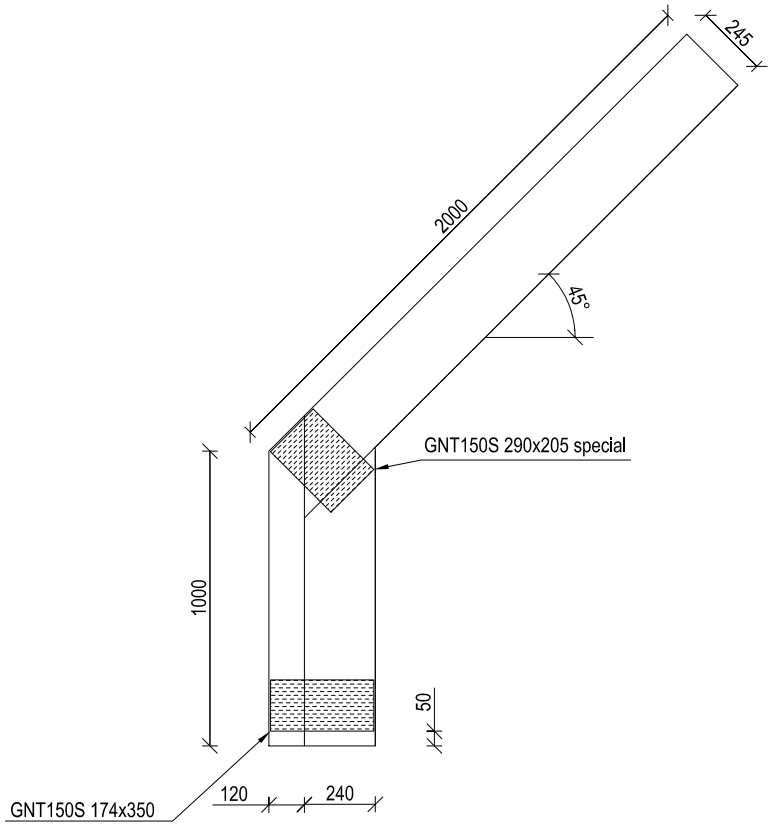

Figure C.22. Test specimens I150.

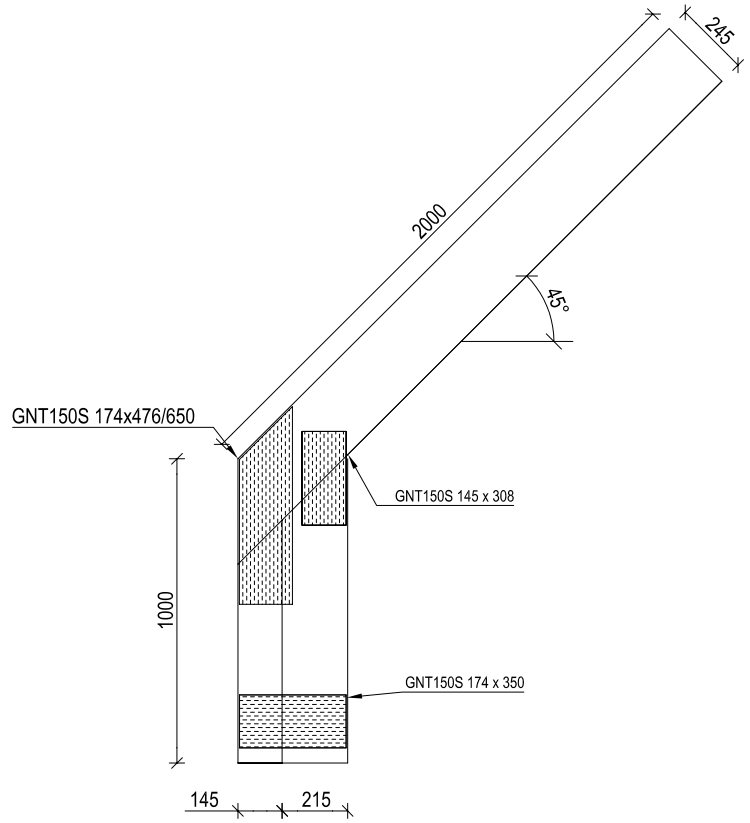

Figure C.23. Test specimens J150.

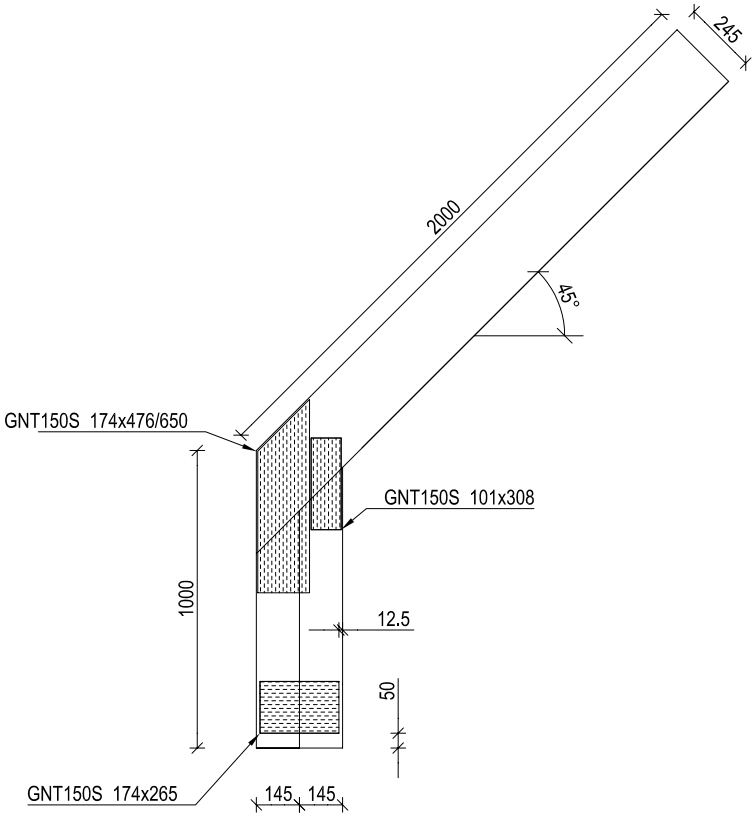

Figure C.24. Test specimens JT150.

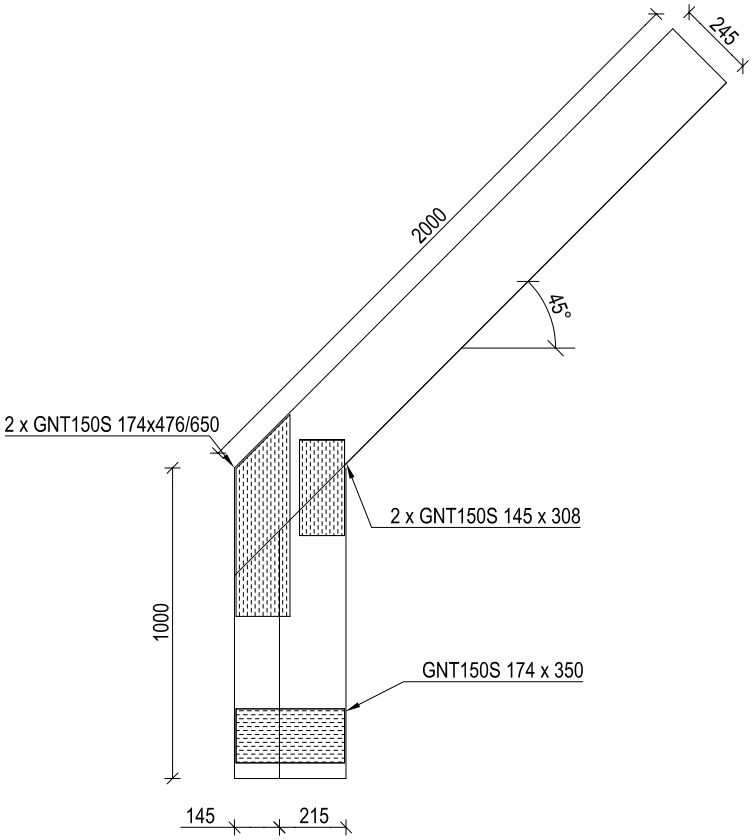

Figure C.25. Test specimens J150-2P.

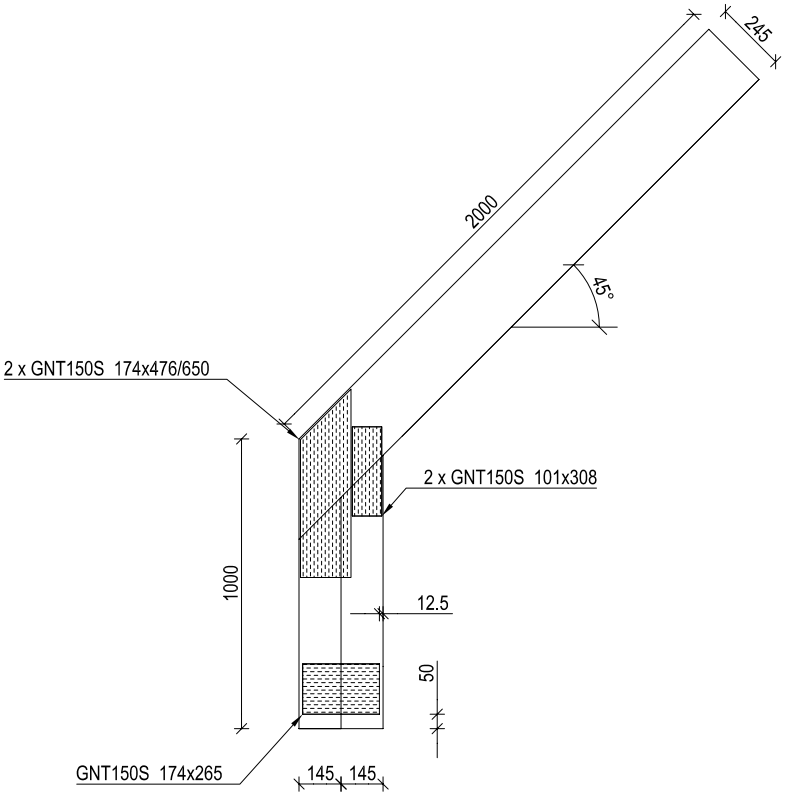

Figure C.26. Test specimens JT150-2P.

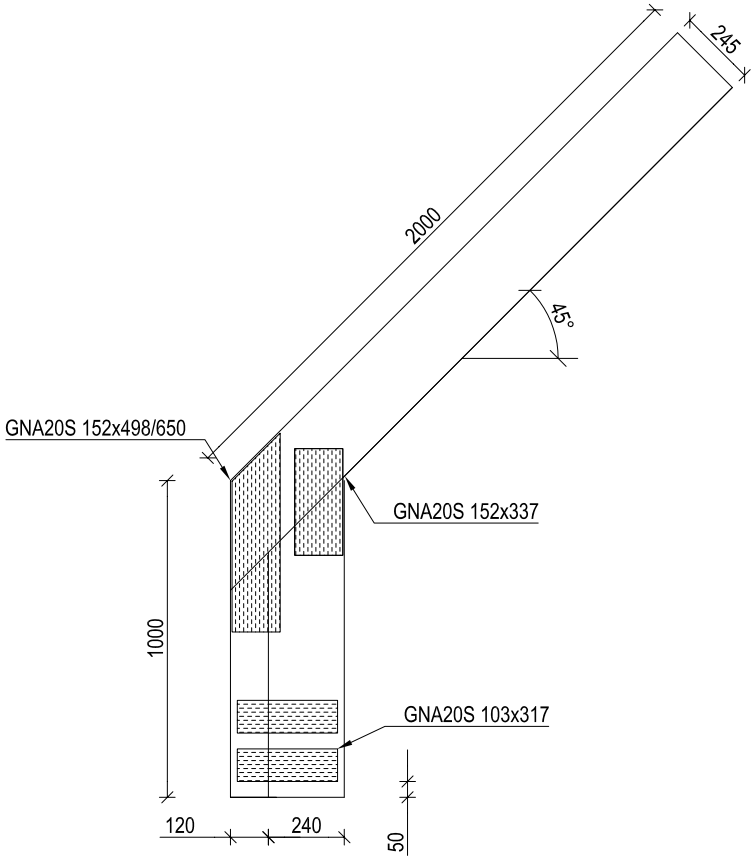

Figure C.27. Test specimens K20.

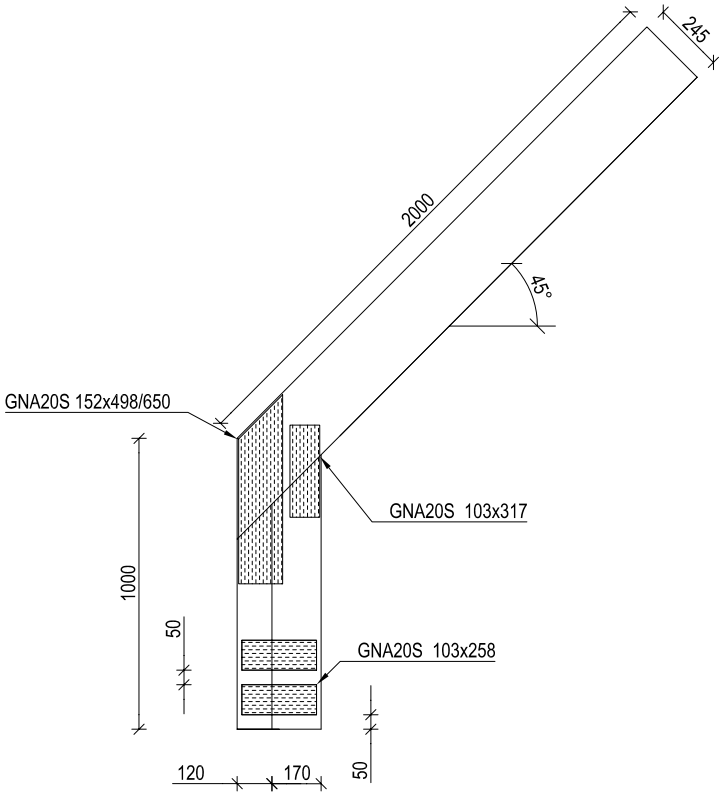

Figure C.28. Test specimens KT20.

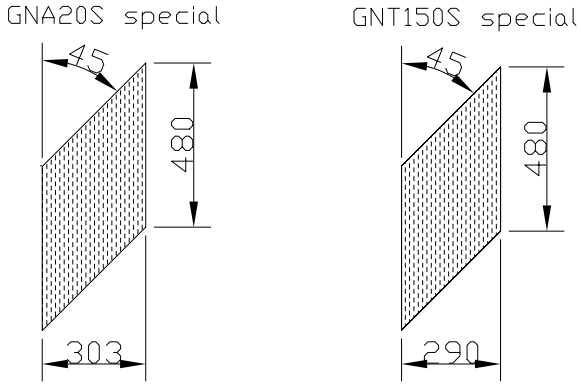

Figure C.29. Special nail plates used for the test series A20, A150, B20, B150, C20, C150, D20, D150, E20, E150, ET150, E150-2P, ET150-2P, J150, JT150, J150-2P, JT150-2P.

C.4 Conclusions

The timber is stored at 20° and 85% relative humidity before the modulus of elasticity is measured and is therefore converted to the actual moisture contents of the timber at the time when the knee joints are tested.

No errors are found in the location of the nail plates.

The stiffening arrangement is able to prevent the knee joints from twisting and bending out of the plate.

The tests are stopped before failure occurs and the displacement transducers are dismounted. After this the knee joints are tested to failure and the ultimate load is registered.

D Calculation of Knee Joints

A method to calculate the strength of the knee joint types ET150, J150, JT150, K20 and KT20 is given in this chapter. The three first-mentioned types of knee joints are considered since they are the most promising designs. The series K20 and KT20 are considered since the calculation method should also be able to predict the load capacities for these series, because they are almost identical with the series J150 and JT150, respectively (the nail plate type is different).

The calculation method is meant as a design tool for use by truss manufacturers. The load capacities predicted by the calculation method are compared with the results from the knee joint tests. The failure modes for most of the considered knee joints are splitting of the timber or bending failure in the timber. Therefore, if the calculation method predicts load capacities that do not exceed the ultimate loads determined by testing, the calculated capacities of the knee joints are considered to be on the safe side. The knowledge of splitting is not so widespread that any kind of splitting check has been implemented in the calculations.

In general it is intended to perform calculations with sectional forces achieved from a finite element model, where the knee joint is assumed to be stiff, see e.g. chapter 6. The displacements of the frame truss can also be estimated using such a finite element model. As shown in chapter 6 the differences are less than 10%, when comparing the displacements using a finite element model with semi-rigid joints to a model, where the knee joints are stiff.

To compare the calculations with the test results, the calculations in section D.1.1 are performed using the formulas for the plate and anchorage capacities in *Eurocode 5 (2001)* and mean strength values. The timber strength values are mean values as well – determined from *DS 413 (1998)*.

To give an estimate of the design moment capacity of the knee joints, the calculations in section D.1.2 are performed using the formulas for the plate and anchorage capacities in *Eurocode 5 (2001)* and design values of the strength of the nail plate. The timber strength values are design values given by *DS 413 (1998)*.

D.1 Calculation Method

In the method the leg is considered to be one single beam, even though some of the tested knee joints consist of two or three beams. This assumption requires that the legs are connected by a sufficient number of nail plates – see the suggestion in the conclusion.

The sectional forces at the middle of the joint line are considered, see figure D.1.

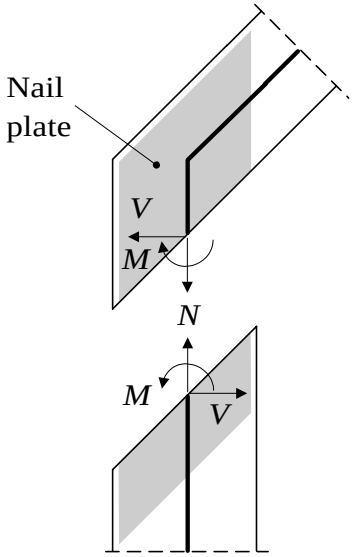

Figure D.1. Sectional forces from the finite element model.

The bending moment and the axial force are converted to the forces N_1 and N_2, see figure D.2. For the load case analysed the force N_2 is a tension force and N_1 is a compression force. The tension force N_2 and the shear force V are assumed to be transferred by the nail plates over the outer 1/3 of the width of the leg (measured horizontally) – denoted the *tension zone*. The compression force N_1 is transferred through the inner 60 mm of the joint line (measured horizontally) – denoted the *compression zone*, see figure D.2 (only the forces on the leg are shown).

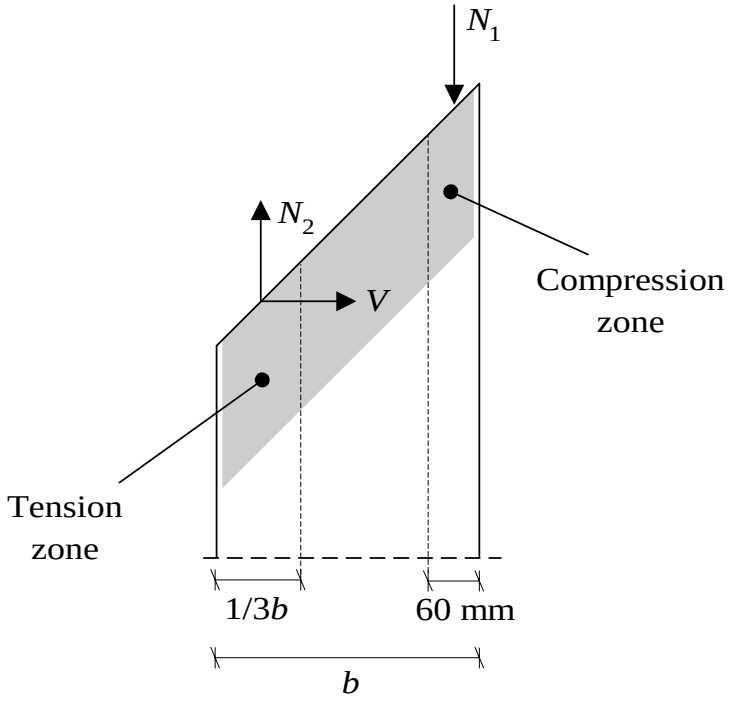

Figure D.2. Assumed force distribution in the joint line.

50% of N_1 is transferred via compression in the nail plates and 50% of N_1 is transferred via contact between the timber members.

The contact force between the timber members is converted to a force $F_{c,perp}$ perpendicular to the grain direction of the rafter and a force $F_{c,par}$ parallel to the joint line. This is shown in figure D.3. Possible stress distribution in the rafter is not taken into account. The force $F_{c,par}$ is transferred by the remaining parts of the nail plates located between the outer 1/3 of the width of the leg and the inner 60 mm – denoted the *shear zone*.

The nail plates, where 50% of the compression force N_1 is transferred, are assumed to be centrally loaded, even though the nail plates may be located 10 mm from the edge of the inner side of the leg. The anchorage areas for transferring 50% of N_1 are determined as the area of the nail plates located within 60 mm from the inner side of the leg. These areas are shown by hatched areas in figure D.3.

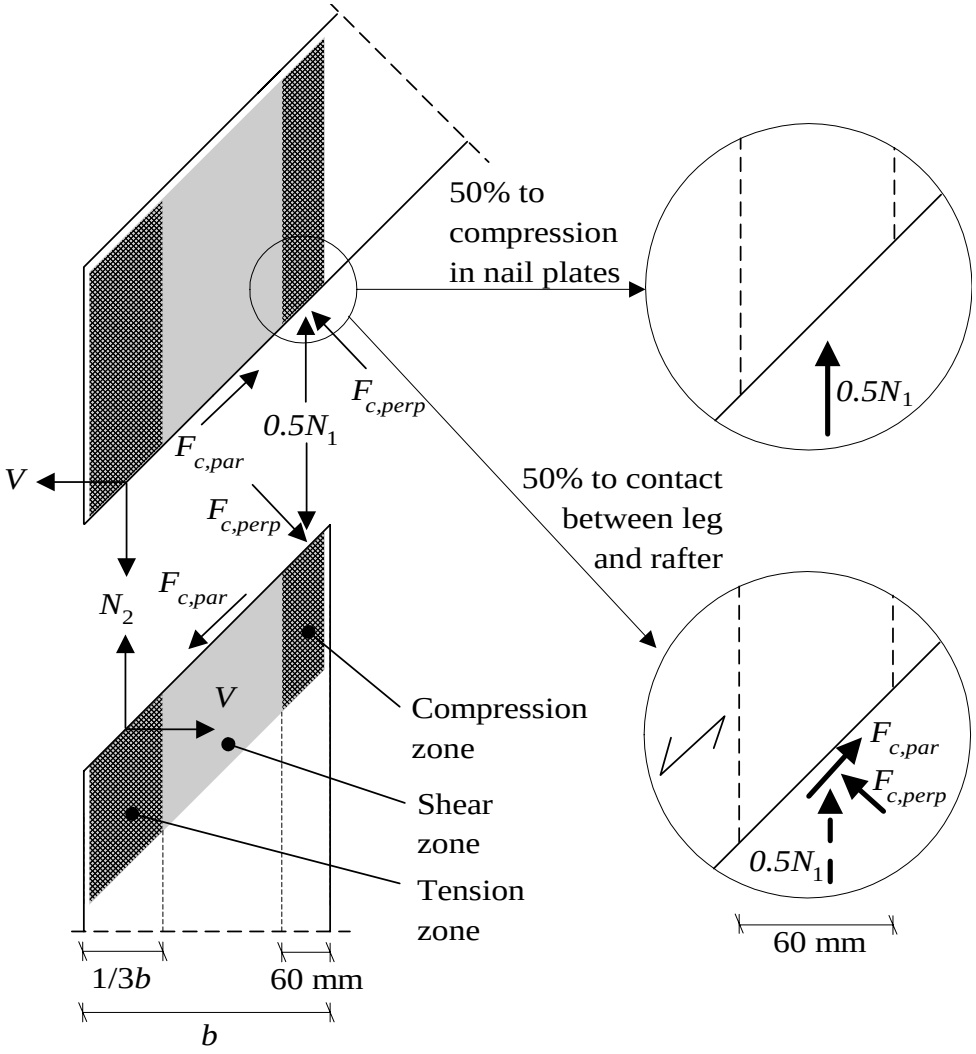

Figure D.3. The distribution of the contact forces results in an "extra" force along the joint line. At the right-hand side only the forces on the rafter are considered.

Similar to the compression zone, it is assumed that the nail plate areas located in the tension zone (shown by hatched areas) can transfer the force N_2 and the shear force V.

D.1.1 Calculation of Knee Joint Type ET150 Using Mean Values

In this section a calculation of knee joint type ET150 is performed using mean values for the strength of the timber and the nail plates. The relevant mean values are listed in table D.1.

Timber		Plate		Anchorage	
$\sigma_{c,90}$	5.0 N/mm^2	$f_{t,0}$	384 N/mm	$f_{a,0,0}$	440 N/nail
		$f_{c,0}$	239 N/mm	$f_{a,90,90}$	620 N/nail
		$f_{t,90}$	108 N/mm	Nail density	0.00672 Nails/mm^2
		$f_{c,90}$	141 N/mm	k_1	-1.22 N/nail per ^{o}
		$f_{v,0}$	111 N/mm	k_2	1.00 N/nail per ^{o}
		$f_{v,90}$	131 N/mm	α_0	90^o
		γ_0	0		
		k_v	0		

Table D.1. Mean values used in the calculations.

The mean values of the timber strength (K24) are based on the values in *DS 413 (1998)* and the strength values of the plate and anchorage capacity are based on the performed tests, see e.g. chapter 4.

The *x* and *y*-directions of the nail plate are seen in figure 3.3 on page 44.

The sectional forces at point A are given for a horizontal force on 10 kN using a finite element model of the frame section shown in figure D.4. To determine the capacity of the knee joint a factor X is introduced. This factor indicates how much the load level can be increased before the utilisation of the considered part of the joint is equal to 1.0 (if a nail plate is subjected to a tension force of 7000 N and the capacity of the nail plate in tension is 20000 N, then $X = \frac{20000\ \text{N}}{7000\ \text{N}} = 2.86$).

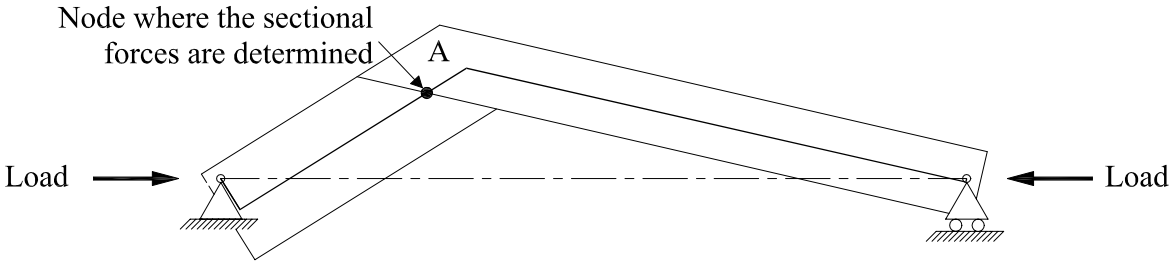

Figure D.4. Model for determination of the sectional forces at the middle of the leg.

The sectional forces are $M = -3.16\,\text{kNm}$, $N = -8.48\,\text{kN}$ and $V = -5.30\,\text{kN}$.

The geometry of the knee joint is shown in figure D.5.

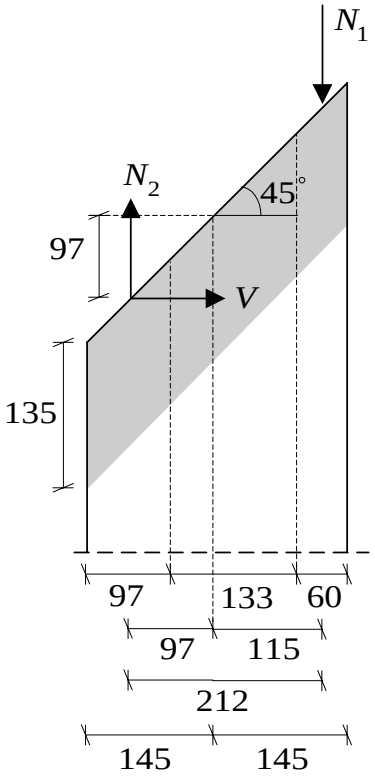

Figure D.5. Geometry of ET150. Dimensions in mm.

When taking the displacement of V into account, the bending moment M' is determined by:

$$M' = M - V \cdot 0.097\ \text{m} = \text{-}2.65\ \text{kNm} \tag{D.1}$$

N_1, N_2 and V are determined by (equivalence conditions):

$$N_1 = -\frac{M'}{0.212\ \text{m}} - N\frac{0.097\ \text{m}}{0.212\ \text{m}} = 16.38\ \text{kN} \tag{D.2}$$

$$N_2 = -\frac{M'}{0.212\ \text{m}} + N\frac{0.115\ \text{m}}{0.212\ \text{m}} = 7.90\ \text{kN} \tag{D.3}$$

$$V = -5.30\ \text{kN} \tag{D.4}$$

Compression zone:

The timber in the rafter is subjected to compression perpendicular to the grain direction, which is more critical than the situation in the leg where the compression forms an angle to the grain direction. The compression force is given by:

$$F_{c,perp} = 0.5 \cdot 16.38\ \text{kN} \cdot \sin(45^\circ) = 5.79\ \text{kN} \tag{D.5}$$

The compression stresses are given by:

$$\sigma_{c,perp} = \frac{5790\text{ N}}{\frac{60\text{ mm}}{\cos(45^\circ)} \cdot 45\text{ mm}} = 1.51\text{ N/mm}^2 \le \sigma_{c,90} = 5.0\text{ N/mm}^2 \qquad \text{(D.6)}$$

The factor X is given by:

$$\text{X} = \frac{5.0\text{ N/mm}^2}{1.51\text{ N/mm}^2} = 3.31 \qquad \text{(D.7)}$$

The compression force that must be transferred through the nail plates is $0.5 \cdot 16.38\text{ kN} = 8.19\text{ kN}$. The capacity of the two nail plates is given by:

$$R_x = \max\begin{cases} 2 \cdot f_{c,0} \cdot l \cdot \sin(\gamma) = 28680\text{ N} \\ 2 \cdot f_{v,0} \cdot l \cdot \cos(\gamma) = 13320\text{ N} \end{cases} \qquad \text{(D.8)}$$

where $l = \frac{60\text{ mm}}{\cos(45^\circ)}$ and $\gamma = 45^\circ$.

The factor X is given by:

$$\text{X} = \frac{28680\text{ N}}{8190\text{ N}} = 3.50 \qquad \text{(D.9)}$$

The anchorage capacity for the nail plate areas on the leg is less than the anchorage capacity of the nail plate areas on the rafter. The area A of the two anchorage areas on the leg is given by:

$$A = 2 \cdot 60\text{ mm} \cdot 135\text{ mm} = 16200\text{ mm}^2 \qquad \text{(D.10)}$$

The actual shear stress τ_F is given by:

$$\tau_F = \frac{8190\text{ N}}{16200\text{ mm}^2} = 0.51\text{ N/mm}^2 \qquad \text{(D.11)}$$

For the considered nail groups $\alpha = \beta = 0^\circ$ and the anchorage capacity is given by:

$$f_{a,0,0} = 440\text{ N/nail} \cdot 0.00672\text{ nails/mm}^2 = 2.95\text{ N/mm}^2 \qquad \text{(D.12)}$$

The factor X is given by:

$$\text{X} = \frac{2.95\text{ N/mm}^2}{0.51\text{ N/mm}^2} = 5.78 \qquad \text{(D.13)}$$

Tension zone:

The nail plates in the tension zone are subjected to a tension force of 7900 N in the *x*-direction and a tension force of 5300 N in the *y*-direction. The capacity of the nail plates in the tension zone is given by:

$$R_x = \max\begin{cases} 2 \cdot f_{t,0} \cdot l \cdot \sin(\gamma) = 74496 \text{ N} \\ 2 \cdot f_{v,0} \cdot l \cdot \cos(\gamma) = 21534 \text{ N} \end{cases} \quad \text{(D.14)}$$

$$R_y = \max\begin{cases} 2 \cdot f_{t,90} \cdot l \cdot \sin(\gamma) = 20952 \text{ N} \\ 2 \cdot f_{v,90} \cdot l \cdot \cos(\gamma) = 25414 \text{ N} \end{cases} \quad \text{(D.15)}$$

where $l = \frac{97 \text{ mm}}{\cos(45^\circ)}$ and $\gamma = 45^\circ$.

The factor X is determined as 4.25 from the formula:

$$\left(\frac{\text{X} \cdot 7900 \text{ N}}{R_x}\right)^2 + \left(\frac{\text{X} \cdot 5300 \text{ N}}{R_y}\right)^2 = 1.0 \quad \text{(D.16)}$$

The anchorage capacity for the nail plate areas on the leg is less than the anchorage capacity of the nail plate areas on the rafter – even though the value of $f_{a,\alpha,\beta}$ is smaller on the rafter. The two nail groups are subjected to the force and moment shown in figure D.6.

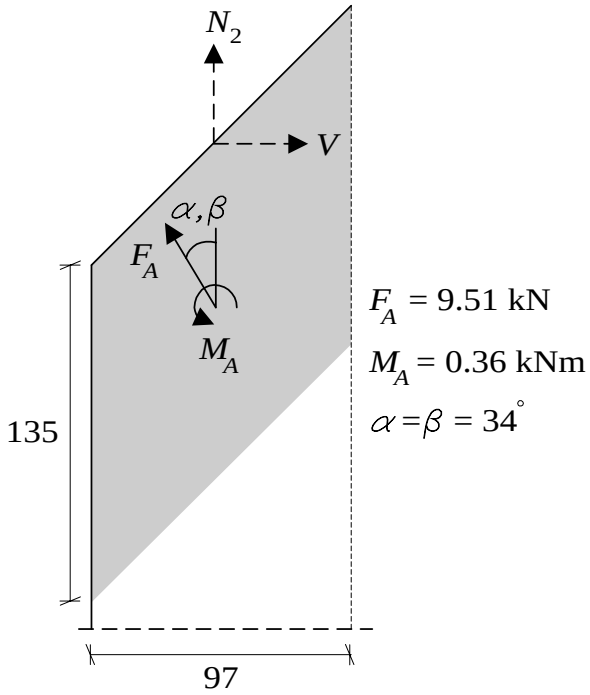

Figure D.6. Loads on anchorage areas in the tension zone.

The area A of the two anchorage areas on the leg is given by:

$$A = 2 \cdot 97 \text{ mm} \cdot 135 \text{ mm} = 26190 \text{ mm}^2 \quad \text{(D.17)}$$

The plastic rotational section modulus for the two nail plate areas is determined by the approximation (from Eurocode 5 (2001)):

$$W_p = 2 \cdot \frac{A\sqrt{\left(\frac{A}{h}\right)^2 + h^2}}{4} = 1.088 \cdot 10^6 \text{ mm}^3 \qquad \text{(D.18)}$$

where h (97 mm) is the maximum height of the anchorage area perpendicular to the longest side, and the area A is given by half of the value given in formula (D.17).

The anchorage capacity $f_{a,34,34}$ is determined as 3.80 N/mm^2. The actual stresses are given by:

$$\tau_F = \frac{F_A}{A} = 0.36 \text{ N/mm}^2 \qquad \text{(D.19)}$$

$$\tau_M = \frac{M_A}{W_p} = 0.33 \text{ N/mm}^2 \qquad \text{(D.20)}$$

The factor X is determined to 6.94.

Shear zone:
The force $F_{c,par} = 5.79 \text{ kN}$ is transferred through the shear zone. The load is transformed into a compression force of 4.09 kN in the *x*-direction of the nail plate and a tension force of 4.09 kN in the *y*-direction. The length of the joint line measured horizontally is 133 mm.

The capacities of the nail plate are given by:

$$R_x = \max\begin{cases} 2 \cdot f_{c,0} \cdot l \cdot \sin(\gamma) = 63574 \text{ N} \\ 2 \cdot f_{v,0} \cdot l \cdot \cos(\gamma) = 29526 \text{ N} \end{cases} \qquad \text{(D.21)}$$

$$R_y = \max\begin{cases} 2 \cdot f_{t,90} \cdot l \cdot \sin(\gamma) = 28728 \text{ N} \\ 2 \cdot f_{v,90} \cdot l \cdot \cos(\gamma) = 34846 \text{ N} \end{cases} \qquad \text{(D.22)}$$

where $l = \frac{133 \text{ mm}}{\cos(45^\circ)}$ and $\gamma = 45^\circ$.

The factor X is determined as 7.46.

For the anchorage capacity of the nail groups the factor X is determined as 15.10.

Summary:
According to the calculations above, the capacity of the knee joint type ET150 is dominated by compression in the rafter perpendicular to the grain direction. The factor X is determined as 3.31, which corresponds to the following capacity of the joint (with mean values of the strength parameters):

$M = -10.5 \text{ kNm}$ $\quad$ $N = -28.1 \text{ kN}$ $\quad$ $V = -17.5 \text{ kN}$

The maximum horizontal load that can be applied is 33.1 kN, see figure D.4.

D.1.2 Calculation of Knee Joint Type ET150 Using Design Values

To give an estimate of the design capacity of knee joint type ET150 the calculations in section D.1.1 are repeated with design values of the strength properties.

The calculations are based on normal safety class, K24 timber quality and the load is assumed to be a snow load. The design values for the timber strength are from *DS 413 (1998).*

There are no Danish approvals of the GNT150S and the GNA20S nail plates that can be used with the expressions in Eurocode 5 (2001). Therefore, the strength values used for the nail plate are composed of values from the Danish Approval – see *Boligministeriet, Bygge- og boligstyrelsen, MK-Godkendelse, (1996),* the Swedish Approval – see *Typgodkännandebevis 5019/86 (2001)* and from the test results in chapter 4. The partial safety factors are taken from the Danish steel code *DS 412 (1998)* and the Danish timber code *DS 413 (1998)*. The partial safety factor for the plate values is determined as 1.43 and the partial safety factor for the anchorage capacity is determined as 1.64. The design values are listed in table D.2.

Timber		Plate		Anchorage	
$\sigma_{c,90,d}$	1.71 N/mm^2	$f_{t,0,d}$ *)	303 N/mm	$f_{a,0,0,d}$ *)	204 N/nail
		$f_{c,0,d}$ +)	129 N/mm	$f_{a,90,90,d}$ *)	132 N/nail
		$f_{t,90,d}$ *)	91 N/mm	Nail density	0.00672 Nails/mm^2
		$f_{c,90,d}$ +)	112 N/mm	k_1 o)	-1.22 N/nail per ^{o}
		$f_{v,0,d}$ *)	91 N/mm	k_2 o)	1.00 N/nail per ^{o}
		$f_{v,90,d}$ *)	103 N/mm	α_0 o)	90^o
		γ_0 o)	0		
		k_v o)	0		

*Table D.2. Design values used in the calculations. The values from the Danish approval are indicated by *), the values from the Swedish approval are indicated by +) and the values from the tests in chapter 4 are indicated by o).*

It should be noted that there are inconsistencies in the values in table D.2 – e.g. the values of k_1, k_2 and α_0 are determined by the tests in chapter 4, whereas the values of $f_{a,0,0,d}$ and $f_{a,90,90,d}$ are from the Danish approval. They should have

been determined from the same tests, however, such tests have not yet been performed.

From calculations it is concluded that compression perpendicular to the rafter is the controlling part. The factor X is determined as 1.13, which corresponds to the following capacity of the joint (with design values of the strength parameters):

$$M_d = -3.6\ \text{kNm} \qquad N_d = -9.6\ \text{kN} \qquad V_d = -6.0\ \text{kN}$$

The design values listed above correspond to sectional forces at the middle of the joint line between the leg and the rafter. Normally the truss producers only use nail plates in knee joints with a design value of the bending moment less than 2.5 kNm. However, this value corresponds to the node in the finite element model, where the beam element of the leg intersects the beam element of the rafter. When taking this into account the values listed above correspond to:

$$M_d = -4.6\ \text{kNm} \qquad N_d = -9.6\ \text{kN} \qquad V_d = -6.0\ \text{kN}$$

at the intersection between the beam element of the leg and the beam element of the rafter.

Since compression perpendicular to the grain direction of the rafter is the dominating part of the knee joint the inconsistencies in some of the strength values of the nail plate become more insignificant.

D.2 Results from Calculations Versus Test Results

The results from the calculations of the different types of knee joints versus the test results are listed in table D.3. The results are presented as the maximum value of the horizontal load, see figure D.4. Results from the two series E20 and E150 are not shown in the table, because the calculation model is not suitable for these types of knee joints. This is caused by the assumption in the calculations that the nail plates in the compression zone must transfer 50% of the compression force. However, the nail plates in the compression zone for the test series E20 and E150 are too small and their capacities are low.

Knee joint type	Test results	Calculation results (using mean strength values)	Calculation results (using design strength values)
ET150	41 kN	33.1 kN	11.3 kN
J150	42 kN	42.4 kN	14.5 kN
JT150	35 kN	33.1 kN	11.3 kN
K20	37 kN	27.3 kN	13.3 kN
KT20	27 kN	21.2 kN	10.2 kN

Table D.3. Results from calculations versus test results.

For the series ET150, J150 and JT150 the controlling part of the joints is compression perpendicular to the grain direction of the rafter. The series K20 and KT20 are dominated by the capacity of the nail plates in the compression zone.

D.3 Conclusions

The aim of this section is to give a calculation method to predict the strength of knee joints. Some comments on the calculation method are given:

- The method requires sufficient deformation capacity in the nail plates to achieve the assumed force distributions. It is assumed that the deformation capacity is sufficient for nail plates.
- The extensions of the tension and compression zones (1/3*b* and 60 mm, respectively) are chosen, since these values result in joint capacities relatively close to the capacities determined by testing.
- To ensure high stiffness, stress distribution in the rafter is not considered (in the compression zone). The capacity of the compression zone is assumed to be reached when the stresses (calculated on the surface of the rafter) reach a certain level. If the stresses were calculated at the centre of the rafter assuming a distribution of the stresses, then this would cause that larger compression forces can be transferred. It will, however, also result in larger deformations before the ultimate load level would be reached.
- Even though the calculation method does not utilise the nail plates fully the sizes of the nail plates should not be decreased, because it will decrease the stiffness of the knee joints – see the suggested design of a knee joint later in this section.
- Friction forces between timber members are not taken into account.

- In the calculation method both the nail plate and the timber members are used to transfer the force in the compression zone The compression zone is given a fixed width of 60 mm. Furthermore, stress distribution in the rafter is not taken into account. These things ensure that the transferred compression force is kept under a certain limit, which reduces the risk of splitting in the leg near the inner corner. Moreover, the requirement that the nail plate must transfer 50% of the compression force ensures higher stiffness since the joint capacity is assumed to be reached when the plate starts buckling.

When comparing the results from the calculation method with the test results for the knee joint types ET150, J150 and JT150, see table D.3, it is found that the calculation methods predict load capacities of the joints that are up to 20% lower than the test results, which is on the safe side. For the joint types K20 and KT20 the calculation predicts load capacities, that are up to 27% lower than those found by testing. The calculation method predicts lower capacities for the K-series compared with the J-series due to the fact that the GNA20S nail plate starts buckling in the compression zone at a lower load level than the GNT150S nail plate, which is also observed during testing.

From the results of the calculation using design values it is found that the design moment capacity for e.g. joint type ET150 is 4.6 kNm. This is an increase of 84% compared to the value of 2.5 kNm that is the limit for some truss manufactures for producing frame trusses with knee joints made with nail plates.

A suggestion for a knee joint is shown in figure D.7.

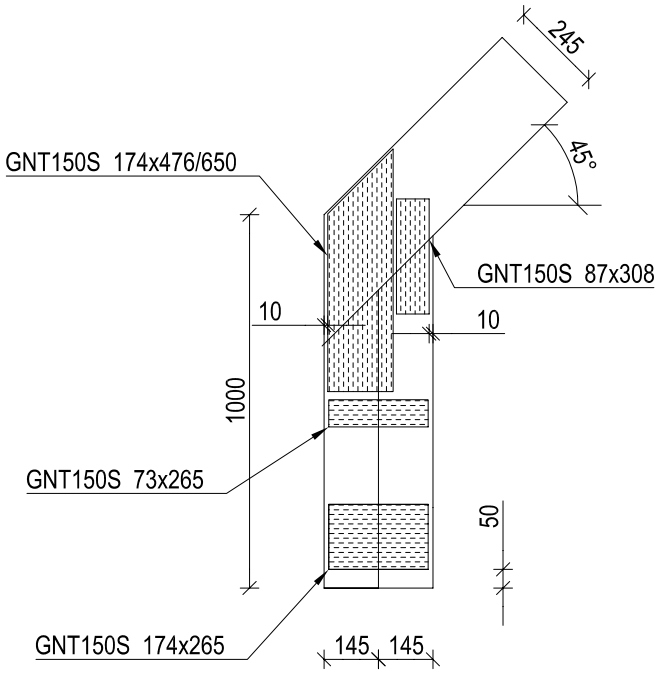

Figure D.7. Suggestions for stiff and strong knee joints. Dimensions in mm.

The nail plates are located 10 mm from the inner and outer sides of the leg to prevent timber cracks during production. The outer nail plates must be located close to the top of the rafter to prevent splitting in the rafter. The timber members in the contact zone should be produced and assembled with high precision to ensure timber contact. To minimize the risk of splitting in the leg and to ensure that the two timber beams act as one beam, extra nail plates are used in the leg.

The nail plates connecting the rafter and the legs can be replaced by two large nail plates (as knee joint type ET150).

In the calculation method it is assumed that the inner part of the knee joint is subjected to compression and the outer part to tension. If the opposite situation occurs it is suggested to switch the extension of the zones so the outer compression zone becomes 60 mm wide and the inner tension is given a width of 1/3*b*. However, this situation is rarely seen in Denmark.

It should also be noted that if the rafter is extended with an overhang it increases the capacity of the knee joint, since this reduces the risk of splitting in the rafter.

The calculation method is only tested for a limited number of knee joints and only one load configuration is considered. The sectional forces used in this chapter are determined from a section of the frame truss. In the considered load configuration the values of the axial force and the shear force are, however, larger than the corresponding values considering a full frame truss, see table 6.3 on page 165. Full-scale tests with different geometry of the knee joints and different geometry of the frame truss should be performed and the test results should be compared with the calculation method. Also, different load configurations should be considered.